AD-A094 751 NIELSEN ENGINEERING AND RESEARCH INC MOUNTAIN VIEW CA F/G 1/1
EXPERIMENTAL AND THEORETICAL STUDY OF FLOW FIELDS AND STORE FOR--ETC(U)
SEP 80 F K GOODWIN, J N NIELSEN N60530-79-C-0169
UNCLASSIFIED NEAR-TR-222 NWC-TP-6210 NL

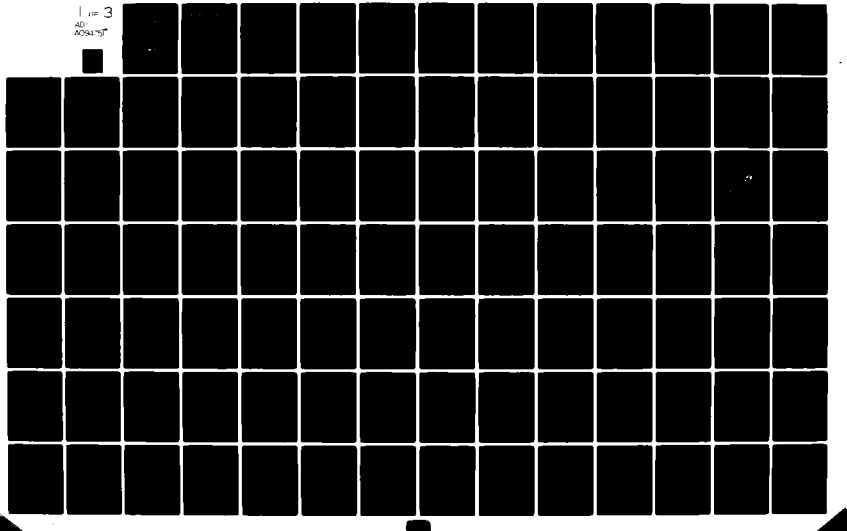

NWC TP 6210

(12) LEVEL II

Experimental and Theoretical Study of Flow Fields and Store Forces in Close Proximity to a Triple Ejection Rack at Transonic Speeds

by
Frederick K. Goodwin
and Jack N. Nielsen
Nielsen Engineering & Research, Inc.

SEPTEMBER 1980

NAVAL WEAPONS CENTER
CHINA LAKE, CALIFORNIA 93555

Naval Weapons Center
AN ACTIVITY OF THE NAVAL MATERIAL COMMAND

FOREWORD

A previous exploratory development program had compared aerodynamic loads for a Mk 83 store installed on a triple ejector rack (TER) on an F-4 aircraft. As reported (NWC TP 6026), loads predicted using a widely accepted state-of-the-art code did not agree with wind tunnel and flight test data. The wind tunnel tests and analyses conducted under the current Launch Dynamics program identify causes of the poor predictions and recommend changes to the code. This work was accomplished during the period June 1979 to June 1980; the wind tunnel tests were conducted during November 1979.

The effort reported herein was conducted by Nielsen Engineering and Research, Inc., under contract N60530-79-C-0169 to the Naval Weapons Center (NWC), China Lake, California. This effort was supported by the Naval Air Systems Command (NAVAIR) under the Strike Warfare Weaponry Technology Block Program (AirTask A03W03P2/008B/0F32-300-000). This airtask provides for continued exploratory development in the air superiority and air-to-surface mission areas. Mr. W. C. Volz, AIR-320C, was the cognizant NAVAIR Technology Administrator.

Mr. R. E. Smith was the NWC contract Technical Coordinator and has reviewed this report for technical accuracy. Wind tunnel test time was provided by the Flight Dynamics Laboratory, Wright-Patterson Air Force Base under the direction of Mr. Calvin Dyer.

Approved by
C. L. SCHANIEL, *Head*
Ordnance Systems Department
29 August 1980

Under authority of
W. B. HAFF
Capt., U.S. Navy
Commander

Released for publication by
R. M. HILLYER
Technical Director

NWC Technical Publication 6210

Published by . . . . . Technical Information Department
Collation . . . . . Cover, 122 leaves
First printing . . . . . 115 unnumbered copies

UNCLASSIFIED

SECURITY CLASSIFICATION OF THIS PAGE *(When Data Entered)*

REPORT DOCUMENTATION PAGE		READ INSTRUCTIONS BEFORE COMPLETING FORM
1. REPORT NUMBER NWC TP 6210	2. GOVT ACCESSION NO. AD-A094 751	3. RECIPIENT'S CATALOG NUMBER
4. TITLE *(and Subtitle)* EXPERIMENTAL AND THEORETICAL STUDY OF FLOW FIELDS AND STORE FORCES IN CLOSE PROXIMITY TO A TRIPLE EJECTION RACK AT TRANSONIC SPEEDS		5. TYPE OF REPORT & PERIOD COVERED Final Report June 1979-June 1980
		6. PERFORMING ORG. REPORT NUMBER NEAR TR-222
7. AUTHOR(s) Frederick K. Goodwin Jack N. Nielsen		8. CONTRACT OR GRANT NUMBER(s) N60530-79-C-0169
9. PERFORMING ORGANIZATION NAME AND ADDRESS Nielsen Engineering and Research, Inc. 510 Clyde Avenue Mountain View, CA 94043		10. PROGRAM ELEMENT, PROJECT, TASK AREA & WORK UNIT NUMBERS AirTask A03W03P2/008B/0F32-300-000
11. CONTROLLING OFFICE NAME AND ADDRESS Naval Weapons Center China Lake, CA 93555		12. REPORT DATE September 1980
		13. NUMBER OF PAGES 242
14. MONITORING AGENCY NAME & ADDRESS *(if different from Controlling Office)*		15. SECURITY CLASS. *(of this report)* UNCLASSIFIED
		15a. DECLASSIFICATION/DOWNGRADING SCHEDULE

16. DISTRIBUTION STATEMENT *(of this Report)*

Approved for public release; distribution unlimited.

17. DISTRIBUTION STATEMENT *(of the abstract entered in Block 20, if different from Report)*

18. SUPPLEMENTARY NOTES

19. KEY WORDS *(Continue on reverse side if necessary and identify by block number)*

Wind Tunnel	TER Rack
Aerodynamics	Store Separation
Loads (Captive)	Store Trajectory
F4	Mathematical Model
Store (Captive)	

20. ABSTRACT *(Continue on reverse side if necessary and identify by block number)*

See reverse side of this form.

DD FORM 1 JAN 73 1473 EDITION OF 1 NOV 65 IS OBSOLETE
S/N 0102 LF 014 6601

UNCLASSIFIED

SECURITY CLASSIFICATION OF THIS PAGE *(When Data Entered)*

(U) *Experimental and Theoretical Study of Flow Fields and Store Forces in Close Proximity to a Triple Ejection Rack at Transonic Speeds*, by Frederick K. Goodwin and Jack N. Nielsen, Nielsen Engineering and Research, Inc. China Lake, CA, Naval Weapons Center, September 1980, 242 pp. (NWC TP 6210, publication UNCLASSIFIED.)

(U) A combined experimental-theoretical investigation has been made to study the flow fields and store loads in the proximity of a triple ejection rack mounted on an inboard wing pylon of an F-4C airplane. The experimental investigation, made in the 4-Foot Transonic Wind Tunnel at AEDC, included attached load measurements on models of a Mark-83 bomb with and without fins, as well as load measurements on a sting-mounted (CTS) model of the bottom store in the proximity of the rack. In addition, flow-field measurements were made in the proximity of the TER. Systematic data were taken in an airplane build-up sequence including additions of the wing pylon, rack, one shoulder store and two shoulder stores from M_∞ = 0.6 to 0.95. Strong interference effects were found within less than one store diameter of the rack which greatly affected the values of the attached loads.

(U) Systematic comparisons were made between experimental and the predictions of a store separation computer program for induced flow fields and store loads due to addition of the pylon, rack, and shoulder stores. For the effects of the rack and shoulder stores improvements are required in the computer program to obtain better load predictions for the store near the attached position. Specific suggestions on how to effect these improvements are made.

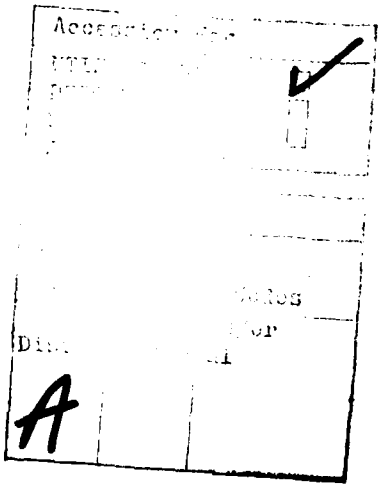

CONTENTS

Figures (Contd.):

Figures (Contd.):

Figures (Contd.):

INTRODUCTION

Recently the AFFDL/Nielsen subsonic store separation program, Reference 1, has been used to make predictions for comparisons with flight and wind-tunnel captive store loads on a MK-83 bomb on an F-4C aircraft. The bomb was mounted on the bottom station of a triple ejection rack (TER) with dummy bombs mounted on the two shoulder stations. The comparisons are presented in Reference 2 and indicate that deficiencies may exist in the TER model in the computer program.

The work documented in this report had two main objectives. The first was to provide a data base which could be used to determine where deficiencies in the computer program exist. The second objective was to attempt to identify the deficiencies by making comparisons of computer program results with the data.

The test program was conducted in the 4-Foot Transonic Wind Tunnel (4T) of the Propulsion Wind Tunnel Facility (PWT) at the Arnold Engineering Development Center (AEDC). The testing period was November 12 through November 21, 1979. Reference 3 is the AEDC document describing the test

program. The test program was jointly sponsored by the Naval Weapons Center (NWC) and the Air Force Flight Dynamics Laboratory (AFFDL/FGC).

During the test program, force and moment data were obtained using both captive trajectory system (CTS) and bracket supported store models. Flow-field data were obtained using a 20° half-angle conical probe. The testing was performed at Mach numbers from 0.6 to 0.95 and at angles of attack up to 16°. For all types of testing the F-4C parent aircraft configuration was built up component by component in order to isolate interference effects. The data obtained during the program have been recorded on magnetic tape and FORTRAN programs have been written for use in retrieving the data. The tapes and programs are available upon request from Mr. R. E. Smith, Code 3243, Naval Weapons Center, China Lake, CA 93555.

The next section of this report will expand further on the purpose and scope of the test program, describe the test apparatus, and present the test conditions. This will be followed by a series of sub-sections, each one devoted to describing a specific type of data. Information is presented which will allow the user to determine the AEDC "run" number for the data in which he is interested. These numbers are used in conjunction with the magnetic tapes and computer programs to retrieve the data. Instructions for doing this are presented and the computer output is described.

The section of this report following the discussion of the experimental program presents a discussion of the experimental results. The compatibility of the captive or

attached loads with the grid loads is discussed. Then phenomena exhibited by the data during the parent aircraft build-up sequence are discussed under the headings

(a) Attached loads
(b) Grid loads
(c) Flow fields

The next section of the report presents comparisons between the experimental data and predictions made using the computer program of Reference 1. This section will try to determine limitations of the computer program by comparisons with the significant effects found experimentally as discussed in the previous section. The data and theory comparisons will be used to determine ways of improving the program.

The last section of the report will present specific recommendations for computer program modifications which should improve the accuracy of the program.

WIND-TUNNEL TEST PROGRAM

PURPOSE AND SCOPE OF THE TEST PROGRAM

The purpose of the test program was to provide a systematic set of data which could be used in evaluating and improving the capability of the computer program of Reference 1 to predict the aerodynamic forces and moments acting on stores carried in a TER configuration. The

capability of calculating store forces and moments with the store in the carriage position is of interest as well as the capability in the detached position. For this reason force and moment tests were performed using both bracket supported and CTS supported force models. In order to calculate analytically the forces and moments acting on a store, the aircraft induced flow field in which the store is immersed must be predicted. Flow-field survey data were taken to provide information on the aircraft induced flow field.

The scope of the program was to obtain these three types of data for a range of Mach numbers, 0.6 to 0.95; angles of attack, -4° to 16°; and parent aircraft configurations. The parent aircraft used was the F-4C. It was selected because of the work documented in Reference 2 which initiated this investigation. The parent aircraft was built up component by component from a clean F-4C to an F-4C with wing pylons, fuselage pylon, TER on the inboard wing pylon, and stores on the shoulder locations of the TER. The store used in the present tests was the Mk-83 bomb used in the work of Reference 2. The component by component build up was performed so that the effect of each component could be determined. For example, the F-4C with inboard left wing pylon and TER was tested with and without Mk-83 stores on the shoulder locations. Differences in the data show the effects of the shoulder stores on the flow field and the bottom store forces and moments.

TEST APPARATUS

Wind Tunnel

The Aerodynamic Wind Tunnel (4T) is a closed-loop, continuous flow, variable-density tunnel in which the Mach number can be varied from 0.1 to 1.3 and can be set at discrete Mach numbers of 1.6 and 2.0 by placing nozzle inserts over the permanent sonic nozzle. The nominal range of the stagnation pressure is from 400 to 3,400 pounds per square foot, absolute. The test section is 4 feet square and 12.5 feet long with perforated, variable porosity (0.5 to 10 percent open) walls. It is completely enclosed in a plenum chamber from which the air can be evacuated, allowing part of the tunnel airflow to be removed through the perforated walls of the test section. A more complete description of the test facility may be found in Reference 4.

Model Support Systems

For this test, two separate and independent support systems were used. The aircraft model was installed inverted in the test section and was supported by an offset sting attached to the main pitch sector. For captive loads testing, the store model was mounted on a balance fastened to the bottom station of the TER on the aircraft model. For grid aerodynamic loads and flow-field testing the store model or the flow-field probe was mounted on the captive trajectory support (CTS). The aircraft model was removed when obtaining free-stream data, and the CTS was moved upward and downstream in the tunnel during the captive loads phase to

minimize interference. Isometric drawings of typical captive loads, grid survey, and flow-field testing installations are shown in Figure 1 of Reference 3 along with block diagrams of the computer control loops. A schematic showing the test section details and the location of the models in the tunnel when using the CTS is shown in Figure 2 of that reference. A further description of the CTS rig can be found in Reference 4.

Parent Aircraft Model Components and Stores

The basic details of the five-percent (1/20th) scale model of the F-4C are shown in Figure 1. The model is geometrically similar to the full-scale aircraft except that the part aft of the engine exhausts has been removed to minimize CTS interference. This removal does not influence the results of this test program. The F-4C model has flow-through engine inlets with subsonic and supersonic exhaust chokes. The subsonic chokes were used during the test program. During part of the captive loads phase of the test program a total pressure rake, containing 13 total pressure orifices, was mounted just aft of the right-side engine exhaust choke. The interior surface of the choke itself was instrumented with six static pressure orifices. These pressure measurements were made in order that a calculation of the ratio of the inlet velocity relative to the free-stream velocity could be made. This velocity ratio influences the input data to the computer program of Reference 1. Details and dimensions of the total pressure rake and the static pressure instrumentation of the exhaust choke are shown in Figure 6 of Reference 3.

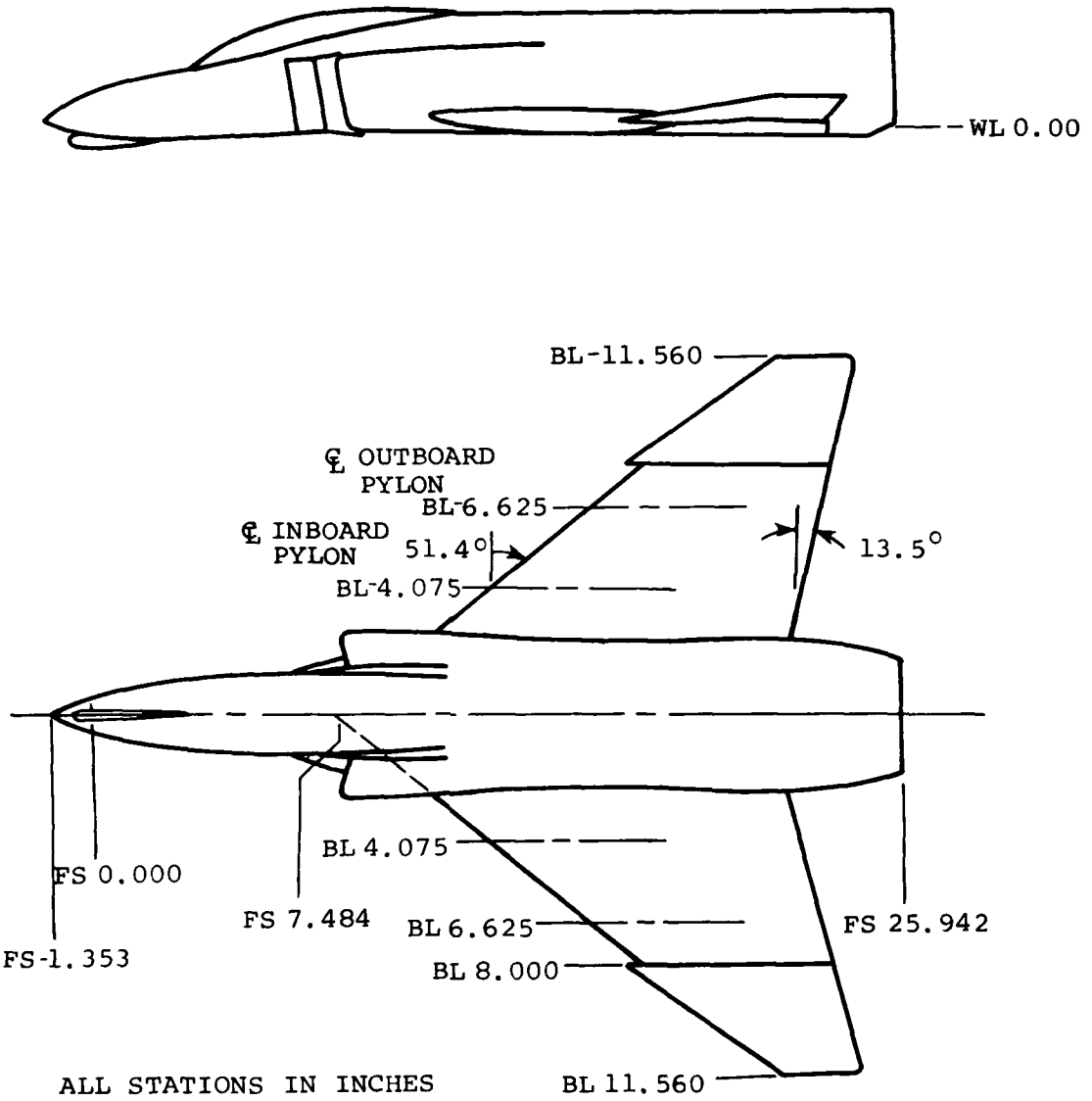

FIGURE 1. Five-Percent Scale Model of the F-4C Aircraft.

Details of the F-4C pylons are shown in Figure 2. For most tests only the left wing inboard pylon was used. All testing was done under the left wing. Pylons were not installed on the right wing for any of the tests.

The triple ejector rack (TER) used in the test program is shown in Figure 3. The TER was used in conjunction with the left-wing inboard pylon. This rack model simulates sway-braces and ventilating passages.

The stores which were used are shown in Figure 4. They are models of the Mk-83 bomb. Figure 4(a) shows the actual bomb shape and Figure 4(b) shows a model which was modified for CTS sting support. Models with identical body shapes but without tail fins were also used. The dummy stores used on the shoulder locations of the TER were the shape shown in Figure 4(a). Both finned and unfinned models were used. Four force models were used during the captive force and moment tests. Tests were performed with both configurations shown in Figure 4 with and without tail fins.

TEST CONDITIONS

The Mach number range used in the test program was 0.6 to 0.95. All testing was performed at a nominal Reynolds number per foot of 3.5×10^6. The store angle of attack was varied from -4° to 16°. Since the store is oriented on the TER one degree nose down relative to the aircraft reference waterline (aircraft angle of attack is measured relative to this line), the aircraft angle of attack varied from -3° to 17°. Nominal values of other tunnel parameters are listed

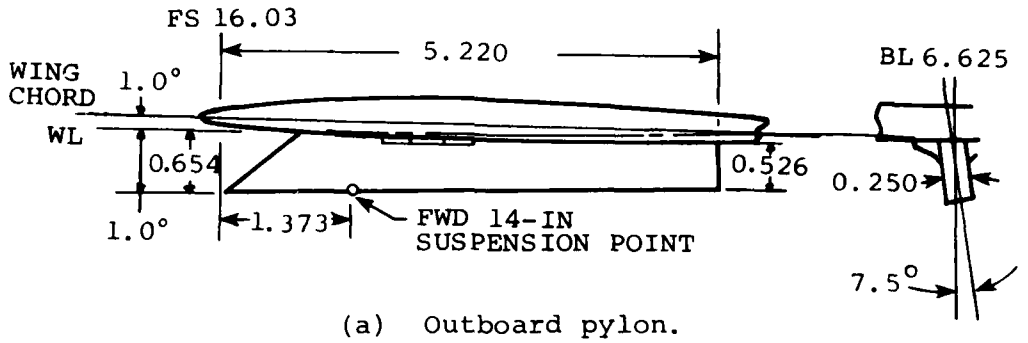

(a) Outboard pylon.

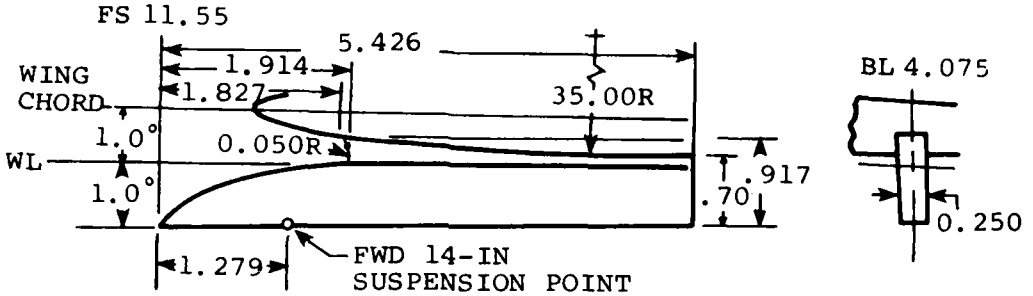

(b) Inboard pylon.

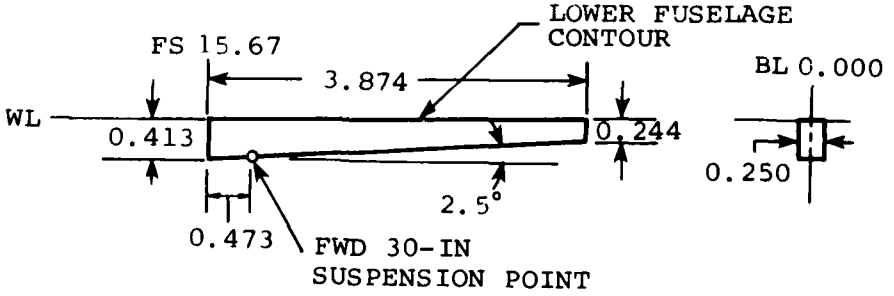

ALL DIMENSIONS IN INCHES

(c) Center pylon.

FIGURE 2. Details of the Models of the F-4C Pylons.

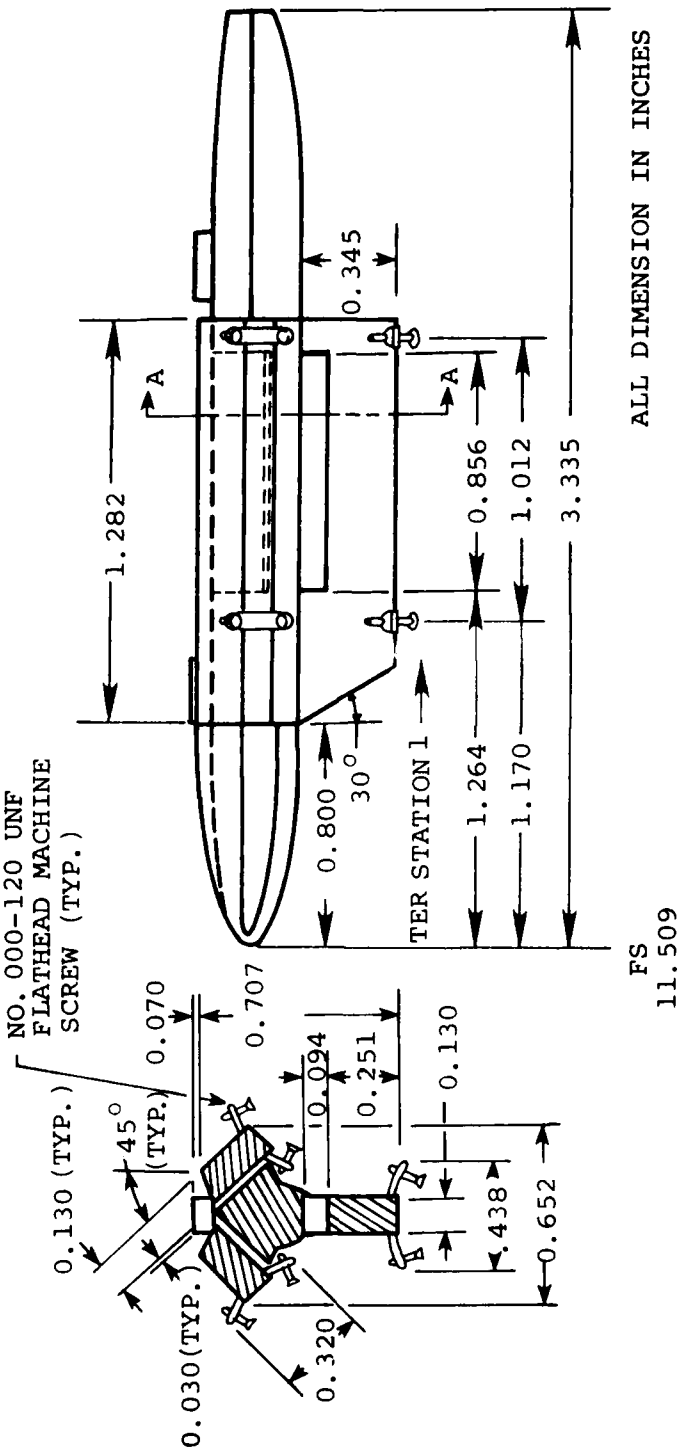

FIGURE 3. Details of the Model of the Triple Ejector Rack.

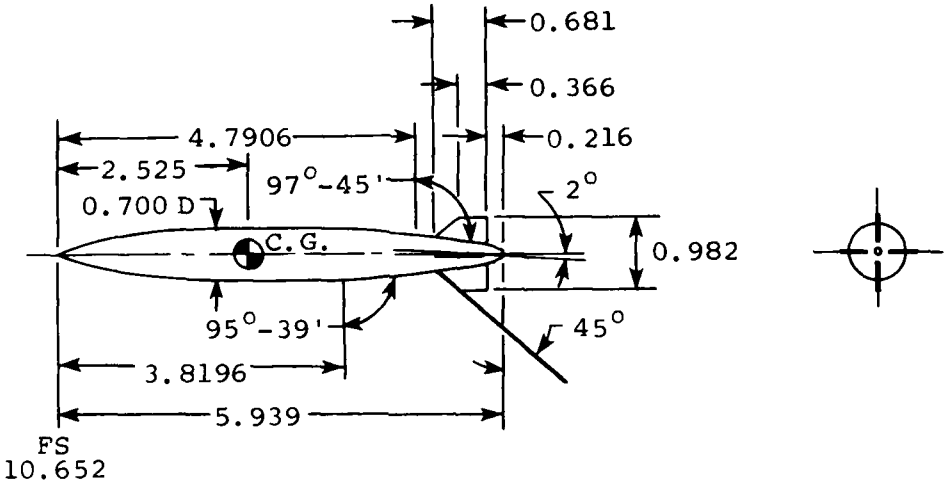

(a) Actual configuration.

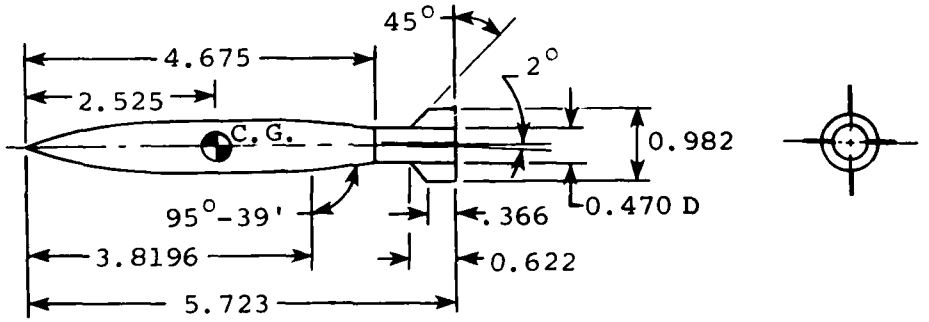

ALL DIMENSIONS IN INCHES

(b) Configuration modified for sting support.

FIGURE 4. Mk-83 Bomb Models.

in the following table as a function of the Mach numbers used during the tests.

TABLE 1. Nominal Test Conditions.

M_∞	p_{t_∞} psfa	q_∞ psf	T_{t_∞} °R	R_{e_∞} ft^{-1}
0.6	2186	432	549.6	3.5×10^6
0.7	1975	489	↓	↓
0.8	1835	539		
0.9	1741	584		
0.95	1708	604		

PARENT AIRCRAFT CONFIGURATIONS

Eight parent aircraft configurations were used during the test program. They are listed in Table 2. The first column lists the eight numbers. These numbers will be used in the next sections of this report which describe the tests. The remaining eight columns list model components which could be attached to the parent F-4C. These components are

$P_{\text{℄}}$ fuselage centerline pylon

P_I left-wing inboard pylon

P_O left-wing outboard pylon

TABLE 2. Parent Aircraft Configurations.

CONFIG. NO.*	$P_{\mathcal{L}}$	P_I	P_O	T	$(S_2)_U$	$(S_3)_U$	$(S_2)_F$	$(S_3)_F$
1								
2		X						
3		X		X				
4		X		X	X			
5		X		X	X	X		
6		X		X			X	X
7	X	X	X	X			X	X
8		X		X			X	

*Configuration composed of basic F-4C model with addition of components indicated in line across table.

T	TER attached to left-wing inboard pylon
$(S_2)_U$	unfinned dummy store attached to outboard shoulder station on TER
$(S_3)_U$	unfinned dummy store attached to inboard shoulder station on TER
$(S_2)_F$	finned dummy store attached to outboard shoulder station on TER with fins vertical and horizontal
$(S_3)_F$	finned dummy store attached to inboard shoulder station on TER with fins vertical and horizontal

The dummy store numbering system is shown in Figure 5. A check in a box opposite a configuration number in Table 2 indicates this model component was attached to the clean F-4C.

CAPTIVE FORCE AND MOMENT TESTS

The captive force and moment phase of the test program consisted of taking six-component force and moment data on four different Mk-83 bomb models. The two store shapes shown in Figure 4 were used with and without tail fins. The test installation is shown in Figure 6. A strain-gage balance was installed internally in the store. It was supported by a bracket protruding from the TER. The balance leads were run through the TER, pylon, and F-4C. All testing was done with the force model mounted on the bottom

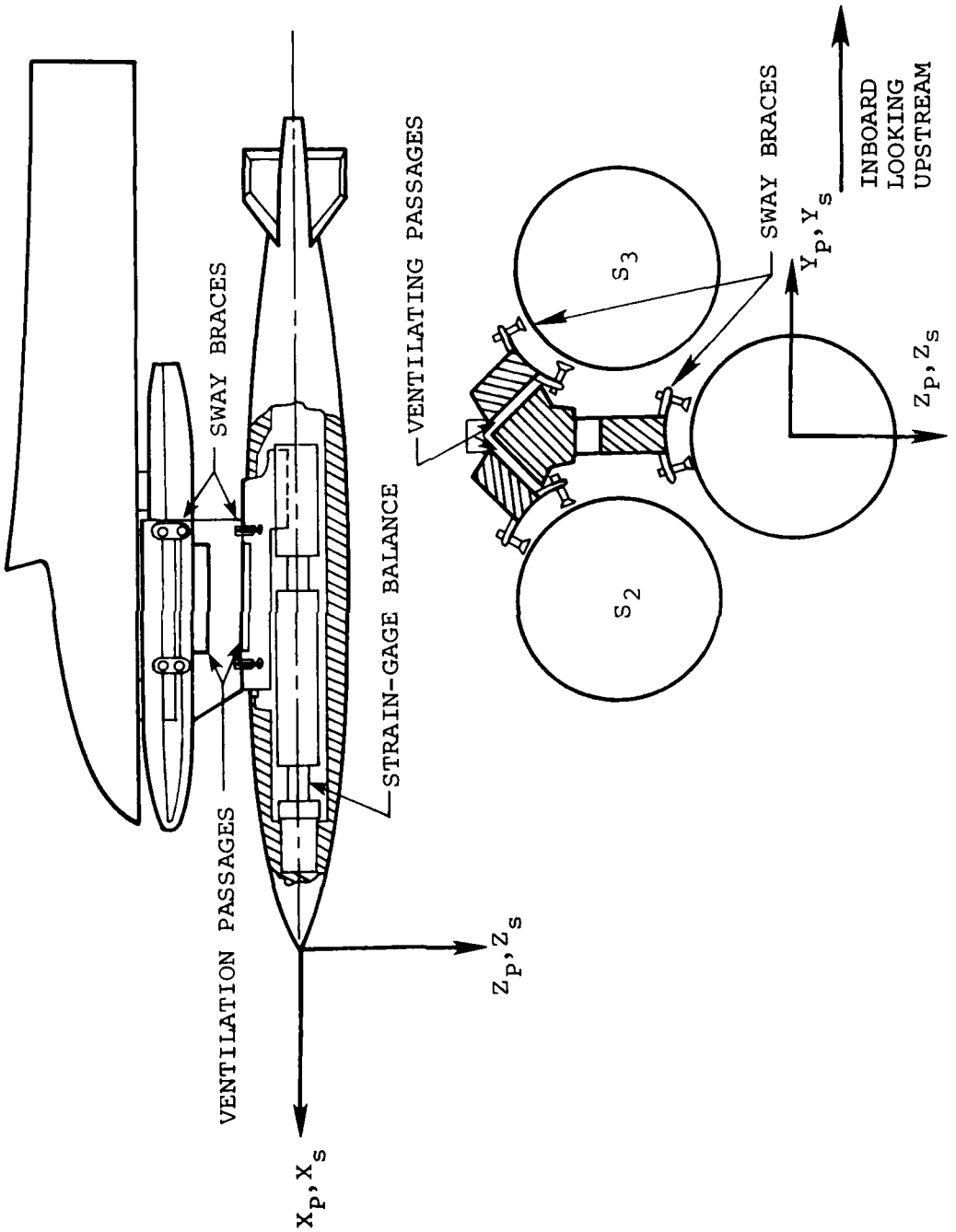

FIGURE 5. Coordinate Systems and Dummy Store Numbering System.

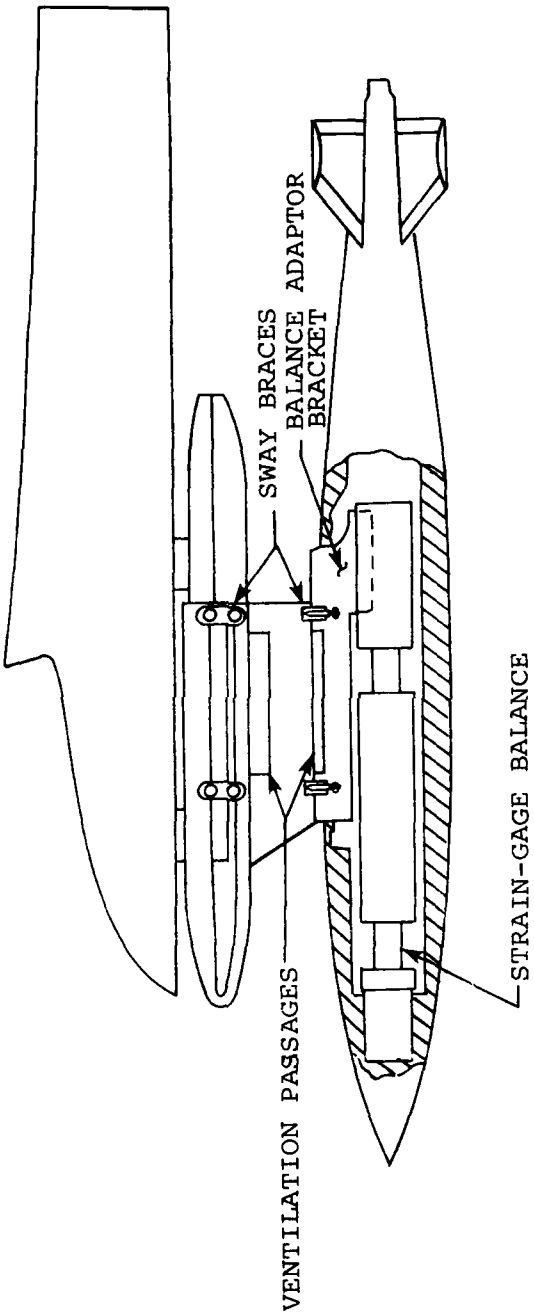

FIGURE 6. Captive Loads Store, Balance and TER Assembly.

station of the TER. The finned stores were always attached to the balance with the fins rolled 45° from the vertical and horizontal.

The captive aerodynamic loads data were obtained at aircraft angles of attack from -3° to 17°, store angles of attack from -4° to 16°, at zero degrees sideslip angle. All angle of attack polars were run automaticaly utilizing online computer facilities to calculate the control commands to set the aircraft model attitude.

The force and moment data for the store were reduced to coefficient form using the standard 4T data reduction programs. The forces and moments are in the store body axis system with the moments taken about the store center of gravity location shown in Figure 4. Positive senses of the forces and moments and the store body axis system are shown in Figure 7. During the present tests the fins were rolled 45° from the orientation shown in the figure. The estimated aerodynamic coefficient uncertainties are listed in Table 3. They are taken from Reference 3.

TABLE 3. Aerodynamic Coefficient Uncertainties.

M_∞	C_N	C_Y	C_A	C_m	C_n	C_ℓ
0.60	±0.03	±0.03	±0.04	±0.04	±0.03	±0.01
0.70	±0.02	±0.02	±0.04	±0.04	±0.02	±0.01
0.80	±0.02	±0.02	±0.03	±0.03	±0.02	±0.01
0.90	±0.02	±0.02	±0.03	±0.03	±0.02	±0.01
0.95	+0.02	+0.02	+0.03	±0.03	±0.02	±0.01

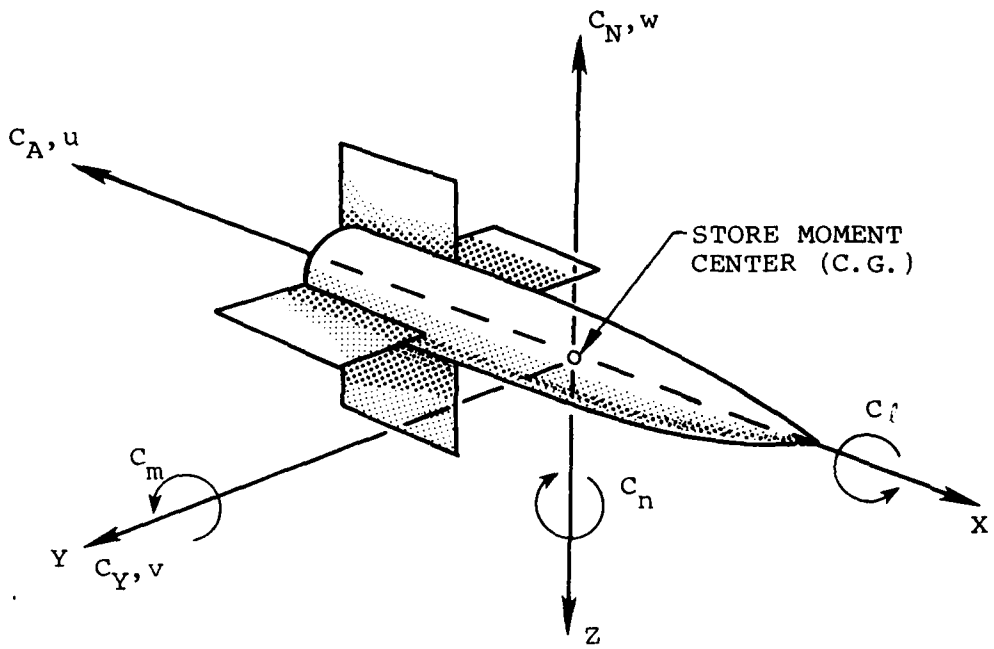

FIGURE 7. Axis System for Store Showing Positive Sense of Axes, Forces and Moments, and Velocities.

During the first part of the captive loads phase the 13 pressures measured by the total pressure rake just aft of the right-side engine exhaust choke and the six static pressures measured inside the choke were recorded. These pressures were used to calculate the engine duct exit Mach number, exit mass flow rate, capture ratio (exit mass flow rate divided by theoretical (reference) inlet mass flow rate), and exit velocity divided by free-stream velocity. The following procedure was used to calculate these quantities. The average static pressure, $\bar{p}$, was calculated as was the average total pressure, $\bar{p}_t$. The ratio $\bar{p}/\bar{p}_t$ was determined. If this ratio was greater than 0.5283, the exit flow was subsonic and the exit Mach number was calculated from

$$M_e = \left\{ 5 \left[\left(\frac{\bar{p}_t}{\bar{p}} \right)^{2/7} - 1 \right] \right\}^{1/2} \tag{1}$$

For all tests performed during this test program the flow was subsonic although provision was made in the data reduction program to handle supersonic exit flows, $\bar{p}/\bar{p}_t < 0.5283$.

With the exit Mach number, M_e, determined, the exit mass flow is calculated,

$$\dot{m}_e = \bar{p}_t M_e A_e (1 + 0.2M_e^2)^{-3} \left(\frac{0.8843}{T_{t_\infty}} \right)^{1/2} \tag{2}$$

the capture ratio is calculated,

$$c_R = \dot{m}_e \Big/ \left[p_{t_\infty} M_\infty A_i (1 + 0.2M_\infty^2)^{-3} \left(\frac{0.8843}{T_{t_\infty}} \right)^{1/2} \right] \tag{3}$$

as is the ratio of exit velocity to free-stream velocity.

$$\frac{V_e}{V_\infty} = \frac{M_e}{M_\infty} \left(\frac{1 + 0.2M_\infty^2}{1 + 0.2M_e^2} \right)^{1/2} \tag{4}$$

In Equation (2) the cross sectional area of the duct exit, A_e, used was 7.4662×10^{-3} square feet, model scale. The inlet area, A_i, appears in Equation (3). In the data reduction a value of 1.705×10^{-2} square feet, model scale, was used. This value was provided to AEDC by McDonald Douglas and is the value they use. The cross-sectional area of the inlet opening on the wind-tunnel model was 1.1×10^{-2} square feet, model scale.

Summary of Tests

The captive loads tests are summarized in Table 4. Column 1 lists the parent aircraft configuration number from Table 2. Column 2 lists the store force and moment model

TABLE 4. Captive Force and Moment Tests.

CONFIG. NO.	FORCE MODEL	M_∞	α_s INITIAL DEG.	α_s FINAL DEG.	$\Delta\alpha_s$ DEG.	AEDC RUN NO.
3	S_{AF}	0.6	-4	16	2	86
↓	↓	0.8	↓	↓	↓	87
↓	↓	0.95	↓	↓	↓	88
4	↓	0.6	↓	↓	↓	81
↓	↓	0.8	↓	↓	↓	82
↓	↓	0.95	↓	↓	↓	83
5	↓	0.6	↓	↓	↓	77
5	↓	0.95	↓	↓	↓	78
8	↓	0.6	↓	↓	↓	91
↓	↓	0.8	↓	↓	↓	92
↓	↓	0.95	↓	↓	↓	93
6	↓	0.6	↓	↓	↓	97,104+,174*
↓	↓	0.7	↓	↓	↓	98,105+,170*
↓	↓	0.8	↓	↓	↓	99,106+,171*
↓	↓	0.9	↓	↓	↓	100,107+,172*
↓	↓	0.95	↓	↓	↓	101,108+,173*
↓	S_{AU}	0.6	↓	↓	↓	111
↓	↓	0.95	↓	↓	↓	112
5	↓	0.6	↓	↓	↓	129
5	↓	0.95	↓	↓	↓	130
3	↓	0.6	↓	↓	↓	121,126*
↓	↓	0.95	↓	↓	↓	122,125*
↓	S_{MF}	0.6	↓	↓	↓	141
↓	↓	0.8	↓	↓	↓	142
↓	↓	0.95	↓	↓	↓	143
5	↓	0.6	↓	↓	↓	136
5	↓	0.95	↓	↓	↓	137
6	↓	0.6	↓	↓	↓	146
↓	↓	0.8	↓	↓	↓	147
↓	↓	0.95	↓	↓	↓	148

See footnote at end of table.

TABLE 4. (Contd.)

CONFIG. NO.	FORCE MODEL	M_∞	α_s INITIAL DEG.	α_s FINAL DEG.	$\Delta\alpha_s$ DEG.	AEDC RUN NO.
6	S_{MU}	0.6	-4	16	2	153
6	↓	0.95	↓	↓	↓	154
5	↓	0.6	↓	↓	↓	164
5	↓	0.95	↓	↓	↓	165
3	↓	0.6	↓	↓	↓	160
3	↓	0.95	↓	↓	↓	161

+Repeat with total pressure rake aft of right engine exhaust removed.

*Repeat with pressure rake removed and hole in TER station no. 1 pylon filled.

attached to the parent aircraft at TER station no. 1. The store model designations are

S_{AF}	Mk-83 actual configuration force model with tail fins (see Figure 4(a))
S_{AU}	same as S_{AF} but without tail fins
S_{MF}	Mk-83 modified configuration force model with tail fins (see Figure 4(b))
S_{MU}	same as S_{MF} but without tail fins

The third column lists the free-stream Mach number, M_∞, and the next three columns list the initial store angle of attack, the final store angle of attack, and the increment in angle of attack. The parent aircraft angle of attack, measured relative to waterline, WL, zero shown in Figure 1 is one degree greater than the store angle of attack.

The last column lists the AEDC run number for the data obtained for that particular configuration and Mach number. This column provides input data for the data retrieval computer program.

Some explanation of the two footnotes on the table is required. During run numbers 86 through 101, the total pressure rake just aft of the right-side engine exhaust was present. The runs marked with the superscript + were made with the rake removed to determine the effect of the rake on the store forces and moments. The rake was found not to effect the forces and moments. It was also determined as the testing progressed that for runs 86 through

122 a small screw hole in the leading edge of the TER station number 1 pylon was not filled with putty or wax. It was filled and the runs with the superscript * were made to determine the effect. It was found that the differences in the forces and moments with and without the hole filled were within the data uncertainties listed in Table 3.

Use of Data Retrieval Computer Program

The captive loads force and moment data are all written on the first file of a magnetic tape. The second file on the tape contains the CTS or grid force and moment data to be described in the next section of this report. A computer program has been written which allows the captive loads data for run numbers listed in Table 4 to be retrieved from the tape and tabulated. To retrieve these data the force and moment data tape must be positioned at the beginning of the first file.

A listing of the computer program is presented in Appendix A. The first card of input is in a 3A4 format and contains the word "CAPTIVE" beginning in column 1. This is used to compare with a header on the tape to assure that the correct tape is mounted and that it is positioned at the correct file. The second input card in an I5 format specifies the number of run numbers of data to be retrieved. The specific run numbers from Table 4 are input on the next cards, eight to a card in 8F10.0 format. The run numbers can be in any order. The computer program sorts them into numerical sequence before searching the tape.

Description of Tabulated Data

There is one page of output for each run number of data. A sample is shown in Figure 8. The first line of output identifies the type of data, in this case captive loads; the AEDC report number documenting this test (Reference 3); and the ARO project number and test number. The next two lines list the run number, parent aircraft configuration, and store model. The following four lines of output list the free-stream test conditions. The remainder of the page tabulates the data obtained. When the last four columns are equal to 0.000, the total pressure rake just aft of the right-side engine exhaust was not used.

The nomenclature used in the tabulated output is contained in the following list.

ALPHA PAR	angle of attack of the parent aircraft, deg.
ALPHA STORE	angle of attack of the store, deg.
BETA STORE	sideslip angle of the store, positive nose to the right, deg.
CAT	store axial-force coefficient uncorrected for base pressure, axial force/(Q S)
CLL	store rolling-moment coefficient, rolling moment/(Q S L)
CLM	store pitching-moment coefficient, pitching moment/(Q S L)

CAPTIVE LOADS DATA   AEDC-TSR-79-[illegible]   ARO PROJECT NUMBER P41C-F0 (TEST TC-623)

RUN NO. 82   PARENT CONFIGURATION F-4C,PI,T,TS,[illegible]   STORE [illegible]

***** FREE-STREAM CONDITIONS *****

MACH NO	PT PSFA	TT DEG(R)	P PSFA	T DEG(R)	V FT/SEC	Q PSF	RE/FT FT(-1)
0.799	1838.7	551.9	1206.4	449.4	865.9	539.9	3.449E+06

***** MODEL DATA *****

ALPHA PAR DEG	ALPHA STORE DEG	BETA STORE DEG	CN	CY	CAT	CLM	CLN	CLL	NCP DIAMS	YCP DIAMS	MNE	MDOTN LBM/SEC	CR	VR
-3.01	-4.23	0.02	0.269	0.078	0.302	-1.600	-0.165	0.006	-5.944	-2.132	0.746	0.286	0.419	0.941
-0.97	-2.14	-0.02	0.162	-0.113	0.296	-1.198	0.144	0.017	-7.402	-1.183	0.745	0.286	0.419	0.937
1.04	-0.10	-0.04	0.112	-0.254	0.284	-1.020	0.292	0.037	-9.067	-1.127	0.743	0.285	0.419	0.937
2.86	1.73	-0.07	0.064	-0.386	0.279	-0.941	0.436	0.046	-13.972	-1.128	0.744	0.286	0.418	0.938
5.09	3.98	-0.09	0.007	-0.543	0.268	-0.724	0.627	0.056	*******	-1.155	0.741	0.284	0.415	0.932
7.05	5.96	-0.13	-0.041	-0.701	0.259	-0.614	0.891	0.063	15.017	-1.268	0.734	0.280	0.411	0.926
9.05	7.97	-0.17	-0.088	-0.879	0.257	-0.521	1.201	0.065	5.419	-1.366	0.737	0.281	0.413	0.929
11.05	9.99	-0.20	[illegible]	-1.045	0.252	-0.439	1.454	0.062	3.533	-1.396	0.750	0.286	0.418	0.945
13.09	12.03	-0.23	-0.144	-1.181	0.250	-0.399	1.699	0.058	2.762	-1.438	0.758	0.288	0.420	0.954
14.87	13.81	-0.26	-0.147	-1.306	0.251	[illegible]	1.904	0.052	2.663	-1.461	0.767	0.289	0.422	0.963
16.89	15.83	-0.29	-0.134	-1.436	0.257	-0.422	2.108	0.043	3.155	-1.465	0.800	0.293	0.427	0.998

FIGURE 8. Sample of Captive Loads Data Tabulation.

CLN	store yawing-moment coefficient, yawing moment/(Q S L)
CN	store normal-force coefficient, normal force/(Q S)
CR	capture ratio calculated using Equation (3)
CY	store side-force coefficient, side force/(Q S)
L	reference length used in computing moment coefficients, 0.7 inch model scale
MACH NO	free-stream Mach number
MDOTN	duct exit mass-flow rate calculated using Equation (2), lbm/sec
MNE	duct exit Mach number
NCP	normal-force center-of-pressure location, CLM/CN; store diameters, L, from the center of gravity, positive ahead
P	free-stream static pressure, psfa
PT	free-stream total pressure, psfa
Q	free-stream dynamic pressure, psf
RE/FT	free-stream Reynolds number per foot, ft^{-1}

S	reference area used in computing force and moment coefficients, 0.385 square inches model scale
T	free-stream static temperature, ^{o}R
TT	free-stream total temperature, ^{o}R
V	free-stream velocity, ft/sec
VR	ratio of engine exit velocity to free-stream velocity calculated using Equation (4)
YCP	side-force center-of-pressure location, CLN/CY; store diameters, L, from the center of gravity, positive ahead

GRID FORCE AND MOMENT TESTS

The grid force and moment phase of the test program consisted of taking six-component force and moment data on two different Mk-83 bomb models. The store shape shown in Figure 4(b) was used with and without tail fins. A sketch of the test installation is shown in Figure 9. The parent aircraft is mounted on the main pitch sector and the store is mounted on an internal balance. A sting protruding from the base of the store attaches the store and balance to the CTS. The finned store was always attached to the balance with the fins rolled 45^{o} from the vertical and horizontal. This is the zero degree, $\phi_s = 0^{o}$, roll orientation of the store.

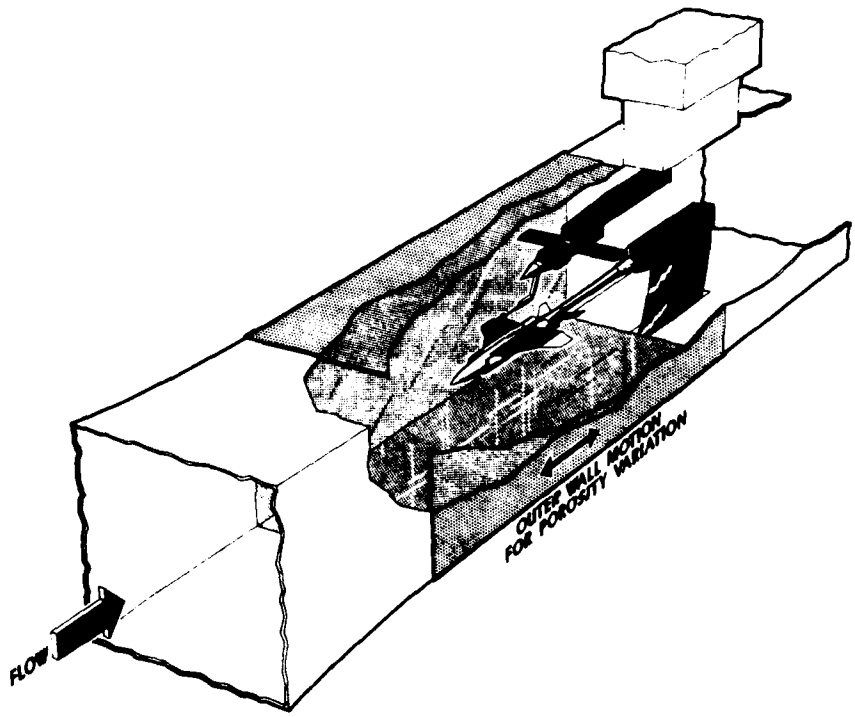

FIGURE 9. Sketch of Grid Force and Moment Phase Test Installation.

Grid force and moment data were obtained at aircraft angles of attack from 1^{o} to 17^{o}, store angles of attack from 0^{o} to 16^{o}, at zero degrees sideslip angle. Testing was accomplished by placing the aircraft at a particular angle of attack. The store was then placed as close as possible to the carriage position at TER station number 1. Data were taken at a series of points as the store was moved away from this position parallel to itself.

Free-stream data were obtained on each of the two stores, alone. For these tests the parent aircraft model was removed and data were taken for store angles of attack from -4^{o} to 16^{o}. Data were obtained on the finned store through a roll angle range of 0^{o} to 90^{o} in 22.5^{o} increments.

The force and moment data for the store were reduced to coefficient form using the standard 4T data reduction programs. The forces and moments are in the store body axis system and the moments are taken about the store center of gravity location shown in Figure 4. Positive senses of the forces and moments are shown in Figure 7. As the store was rolled during the free-stream tests, the store X,Y,Z coordinate system rolled with the store. The aerodynamic coefficient uncertainties are listed in Table 3. They are taken from Reference 3.

Summary of Tests

The store free-stream tests are summarized in Table 5. Column 1 lists the store force model. The store model designations are

TABLE 5. Store Free-Stream Force and Moment Tests.

FORCE MODEL	M_∞	ϕ_s DEG.	α_s INITIAL DEG.	α_s FINAL DEG.	$\Delta\alpha_s$ DEG.	AEDC RUN NO.
S_{MF}	0.6	0.0	-4	16	2	12
		22.5				13
		45.0				14
		67.5				15
		90.0				16
	0.7	0.0				17
		22.5				18
		45.0				19
		67.5				20
		90.0				21
	0.8	0.0				22
		22.5				23
		45.0				24
		67.5				25
		90.0				26
	0.9	0.0				27
		22.5				28
		45.0				29
		67.5				30
		90.0				31
	0.95	0.0				32
		22.5				33
		45.0				34
		67.5				35
		90.0				36
S_{MU}	0.6	0.0				40
	0.7					41
	0.8					42
	0.9					43
	0.95					44

S_{MF} Mk-83 modified configuration force model with tail fins (see Figure 4(b))

S_{MU} same as S_{MF} but without tail fins

The second column gives the free-stream Mach number, M_∞, and the third column the store roll angle, ϕ_s. Positive roll is clockwise when viewed from the rear. The next three columns list the initial store angle of attack, the final store angle of attack, and the increment in angle of attack. The last column presents the AEDC run number for the data obtained for that particular Mach number, roll angle combination. This column provides input data for the data retrieval computer program.

Table 6 summarizes the grid force and moment tests with a parent aircraft present. Column 1 lists the parent aircraft configuration number from Table 2. Column 2 indicates which of the two force models was mounted on the balance. The free-stream Mach number, M_∞, is listed in column 3 and the store angle of attack, α_s, in column 4. The parent aircraft angle of attack measured with respect to waterline, WL, zero shown in Figure 1 is one degree greater than the store angle of attack. The fifth column indicates which Z_s/D schedule was used for that particular run. D is the store maximum diameter, 0.7 inch model scale. The origin of the X_s, Y_s, Z_s coordinate system is shown in Figure 5 and is located at the tip of the store nose when the store is in the carriage position on the bottom station of the TER. The two Z_s/D schedules are shown in the last two columns of the first page of Table 6. The value of $Z_s/D = 0.0$ could not be obtained since this would result in the store's touching the

TABLE 6. Grid Force and Moment Tests.

CONFIG. NO.	FORCE MODEL	M_∞	α_s DEG.	Z_s/D SCHD.	AEDC RUN NO.	Z_s/D SCHDS. ZA	ZB
1	S_{MF}	0.6	0	ZA	343	0.0	0.0
			4		344	.4	.1
			8		345	.8	.2
			12		346	1.2	.3
			16		347	1.6	.4
		0.95	0		352	2.0	.6
			4		351	2.4	.8
			8		350	2.8	1.0
			12		349	3.2	1.2
			16		348	3.6	1.4
2		0.6	0		338	4.0	1.6
			4		339	4.4	2.0
			8		340	4.8	2.4
3		0.6	0	ZB	300	5.2	2.8
			4		301	5.6	3.2
			8		302	6.0	3.6
			12		303		4.0
			16		304		4.4
		0.8	0		310		4.8
			4		309		5.2
			8		308		5.6
			12		307		6.0
			16		306		
		0.95	0		311		
			4		312		
			8		313		
			12		314		
			16		315		
6		0.6	0		249,327*		
			4		250		
			8		251		
			12		254		
			16		255		
		0.7	0		258,328*		
			4		257		
			8		256		
		0.8	0		260,329*		
			4		261		
			8		262		

See footnote at end of table.

TABLE 6. (Contd.)

CONFIG. NO.	FORCE MODEL	M_∞	α_s DEG.	Z_s/D SCHD.	AEDC RUN NO.	Z_s/D SCHDS. ZA ZB
6	S_{MF}	0.8	12	ZB	263	(see 1st page of table)
			16		264	
		0.9	0		279,331*	
			4		274	
			8		265	
		0.95	0		280,334*	
			4		275	
			8		276	
			12		277	
			16		278	
8		0.6	0		283	
			4		284	
			8		285	
		0.8	0		292	
			4		287	
			8		286	
		0.95	0		294	
			4		295	
			8		296	
5		0.6	0		319	
			4		320	
			8		321	
		0.95	0		324	
			4		323	
			8		322	
	S_{MU}	0.6	0		219	
			4		220	
			8		221	
		0.95	0		229	
			4		225	
			8		224	
6		0.6	0		240	
			4		241	
			8		242	

See footnote at end of table.

TABLE 6. (Contd.)

CONFIG. NO.	FORCE MODEL	M_∞	α_s DEG.	Z_s/D SCHD.	AEDC RUN NO.	Z_s/D SCHDS. ZA ZB
6	S_{MU}	0.95	0	ZB	245	(see 1st page of table)
↓	↓	↓	4	↓	244	
			8		243	
3		0.6	0		232	
		↓	4		233	
			8		234	
		0.95	0		237	
		↓	4		236	
			8		235	

*Repeat with TER station number 1 sway braces removed.

parent aircraft. The first value of Z_s/D was usually between 0.05 and 0.10.

Column 6 of Table 6 lists the AEDC run number for the data obtained for that particular parent aircraft configuration, Mach number, and angle of attack. This column provides input data for the data retrieval computer program.

Use of Data Retrieval Computer Program

The grid force and moment data are all written on the second file of a magnetic tape. The first file on the tape contains the captive loads data which were previously described. A computer program has been written which allows the grid data for run numbers listed in Tables 5 and 6 to be retrieved from the tape and tabulated. To retrieve these data the force and moment data tape must be positioned at the beginning of the second file.

A listing of the computer program is presented in Appendix B. The first card of input is in a 3A4 format and contains the word "GRID" beginning in column 1. This is used to compare with a header on the tape to assure that the correct tape is mounted and that it is positioned at the correct file. The second input card in an I5 format specifies the number of run numbers of data to be retrieved. The specific run numbers from Tables 5 and 6 are input on the next cards, eight to a card in 8F10.0 format. The run numbers can be in any order. The computer program sorts them into numerical sequence before searching the tape.

Description of Tabulated Data

There is one page of output for each run number of data. A sample is shown in Figure 10. The first line of output identifies the type of data, in this case grid force data; the AEDC report number documenting this test (Reference 3); and the ARO project number and test number. The next two lines list the run number, parent aircraft configuration, and store model. The following four lines of output list the free-stream test conditions. The remainder of the page tabulates the data obtained.

The nomenclature used in the tabulated output is contained in the following list.

ALPHA PAR	angle of attack of the parent aircraft, deg.
ALPHA STORE	angle of attack of the store, deg.
BETA STORE	sideslip angle of the store, positive nose to the right, deg.
CAT	store axial-force coefficient uncorrected for base pressure, axial force/(Q S)
CLL	store rolling-moment coefficient, rolling moment/(Q S L)
CLM	store pitching-moment coefficient, pitching moment/(Q S L)
CN	store normal-force coefficient, normal force/(Q S)

GRID FORCE DATA AEDC-TSR-79-P79 ARO PROJECT NUMBER P41C-F0 (TEST TC-623)
RUN NO. PARENT CONFIGURATION STORE
219 F-4C+PT+T+(52)D+(53)D MK-33+MD

***** FREE-STREAM CONDITIONS *****

MACH NO	PT PSFA	TT DEG(R)	P PSFA	T DEG(R)	V FT/SEC	Q PSF	RE/FT FT(-1)
0.599	2131.7	560.3	1672.2	504.2	659.6	420.4	3.49*10**6

***** MODEL DATA *****

ALPHA PAR DEG	ALPHA STORE DEG	BETA STORE DEG	THA STORE DEG	PHI STORE DEG	XP IN	YP IN	ZP/D	CN	CY	CAT	CLM	CLN	CLL	NCP DIAMS	YCP DIAMS
1.00	-0.00	0.05	-0.00	-0.07	-0.01	-0.03	0.07	0.511	-0.117	0.206	-1.110	-0.360	0.007	-2.170	3.070
1.00	-0.00	0.03	-0.00	-0.04	-0.00	-0.03	0.10	0.507	-0.115	0.208	-1.101	-0.358	0.004	-2.172	3.103
1.00	0.00	0.02	0.00	-0.14	-0.01	-0.03	0.20	0.423	-0.073	0.195	-0.865	-0.293	0.006	-2.044	4.019
1.00	0.01	0.02	0.01	-0.14	-0.01	-0.02	0.30	0.373	-0.057	0.186	-0.742	-0.270	0.005	-1.991	4.762
1.00	0.00	0.02	0.00	-0.07	-0.00	-0.02	0.40	0.332	-0.047	0.178	-0.655	-0.260	0.003	-1.973	5.574
1.00	0.00	0.01	0.00	-0.11	-0.00	-0.02	0.60	0.270	-0.029	0.163	-0.525	-0.251	0.005	-1.947	8.654
1.00	0.00	0.02	0.00	-0.14	-0.00	-0.02	0.79	0.222	-0.026	0.159	-0.446	-0.236	0.002	-2.009	9.126
1.00	0.00	0.02	0.00	-0.18	-0.00	-0.02	1.01	0.188	-0.023	0.152	-0.380	-0.219	0.003	-2.021	9.547
1.00	-0.01	0.02	-0.01	-0.14	-0.00	-0.02	1.21	0.165	-0.022	0.150	-0.340	-0.203	0.003	-2.058	9.430
1.00	-0.01	0.02	-0.01	-0.14	-0.01	-0.02	1.41	0.144	-0.023	0.145	-0.302	-0.191	0.005	-2.098	8.478
1.00	-0.00	0.01	-0.00	-0.14	-0.00	-0.01	1.61	0.128	-0.021	0.142	-0.274	-0.180	0.004	-2.140	8.522
1.00	-0.01	0.02	-0.01	-0.14	-0.00	-0.02	2.01	0.105	-0.020	0.142	-0.233	-0.166	0.005	-2.220	8.449
1.00	-0.01	0.02	-0.01	-0.11	-0.00	-0.02	2.38	0.089	-0.020	0.140	-0.200	-0.153	0.005	-2.238	7.806
1.00	-0.01	0.02	-0.01	-0.07	-0.00	-0.02	2.79	0.077	-0.017	0.139	-0.177	-0.143	0.004	-2.313	8.546
1.00	-0.00	0.02	-0.00	-0.11	-0.00	-0.02	3.18	0.069	-0.018	0.135	-0.156	-0.131	0.002	-2.244	7.365
1.00	-0.00	0.01	-0.00	-0.11	-0.01	-0.02	3.59	0.061	-0.016	0.132	-0.139	-0.123	0.004	-2.261	7.449
1.00	-0.01	0.01	-0.01	-0.11	-0.00	-0.01	3.99	0.056	-0.015	0.132	-0.123	-0.117	0.004	-2.207	7.741
1.00	-0.01	0.01	-0.01	-0.11	-0.00	-0.02	4.39	0.052	-0.015	0.135	-0.113	-0.111	0.005	-2.187	7.387
1.00	-0.01	0.01	-0.01	-0.07	-0.00	-0.01	4.79	0.047	-0.015	0.131	-0.100	-0.105	0.005	-2.103	7.045
1.00	-0.01	0.01	-0.01	-0.07	-0.00	-0.01	5.19	0.046	-0.015	0.128	-0.089	-0.100	0.004	-1.930	6.700
1.00	-0.00	0.01	-0.00	-0.11	-0.00	-0.02	5.59	0.045	-0.014	0.128	-0.084	-0.094	0.004	-1.873	6.913
1.00	-0.01	0.01	-0.01	-0.11	-0.00	-0.01	6.00	0.045	-0.013	0.125	-0.075	-0.088	0.005	-1.682	6.510

FIGURE 10. Sample of Grid Force and Moment Data Tabulation.

CY	store side-force coefficient, side force/(Q S)
DPHI	store roll angle, positive clockwise looking upstream, deg.
DTHA	store total angle of attack, angle between store longitudinal axis and the free-stream velocity vector, deg.
L	reference length used in computing moment coefficients, 0.7 inch model scale
MACH NO	free-stream Mach number
NCP	normal-force center-of-pressure location, CLM/CN; store diameters, L, from the center of gravity, positive ahead
P	free-stream static pressure, psfa
PT	free-stream total pressure, psfa
Q	free-stream dynamic pressure, psf
RE/FT	free-stream Reynolds number per foot, ft^{-1}
S	reference area used in computing force and moment coefficients, 0.385 square inches model scale
T	free-stream static temperature, ^{o}R
TT	free-stream total temperature, ^{o}R

V	free-stream velocity, ft/sec
XP	X_s-coordinate of the store nose in the X_s, Y_s, Z_s coordinate system of Figure 5, in.
YCP	side-force center-of-pressure location, CLN/CY; store diameters, L, from the center of gravity, positive ahead
YP	Y_s-coordinate of the store nose in the X_s, Y_s, Z_s coordinate system of Figure 5, in.
ZP/D	Z_s-coordinate of the store nose divided by the store maximum diameter (0.7 in) in the X_s, Y_s, Z_s coordinate system of Figure 5

FLOW-FIELD SURVEY TESTS

The flow-field survey phase of the test program consisted of measuring the flow field in the region beneath the parent aircraft which the bottom store on the TER would occupy in and near the carriage position. Details of the 20 degree half-angle conically tipped probe used during the tests are shown in Figure 11. The test installation is similar to that shown in Figure 9 for the grid force and moment tests except that the probe is mounted on the CTS rather than the balance and force model. The probe has four equally spaced static pressure orifices on the cone surface and a total pressure orifice at the cone apex.

Flow-field data were taken at aircraft angles of attack from 1° to 17°. The probe angle of attack was kept the same

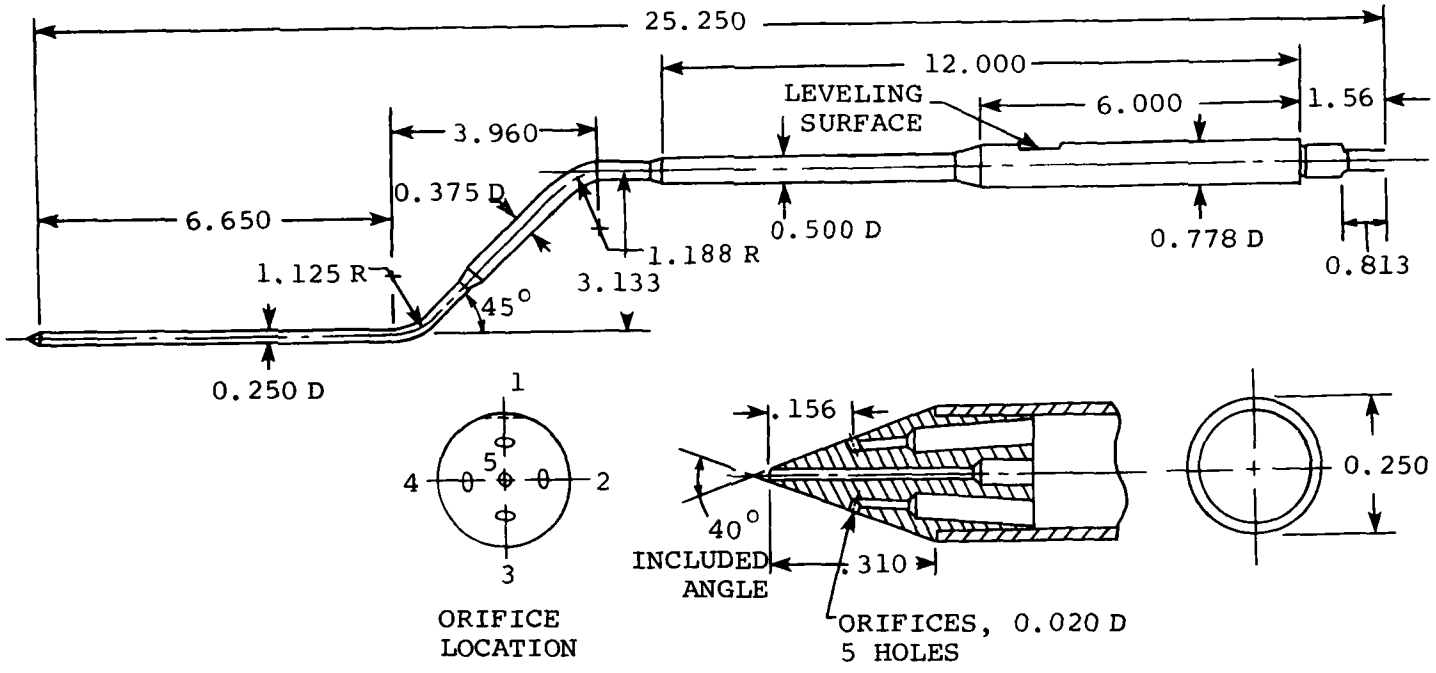

FIGURE 11. Details of Flow-Field Probe.

as the bottom store on the TER, that is, one degree less than the parent aircraft. The origin of the probe coordinate system is the X_p, Y_p, Z_p system shown in Figure 5. The probe longitudinal axis and the X_p axis are parallel.

Data were obtained by making axial traverses at a series of Y_p, Z_p positions. These locations are shown in the following sketch by the crosses.

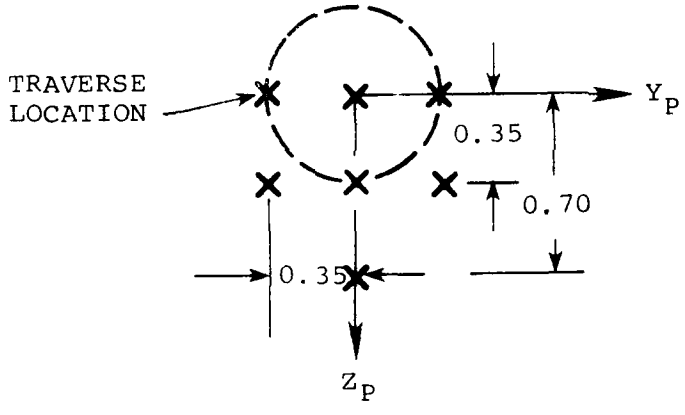

The dashed circle represents the Mk-83 bomb in the carriage position on the TER. The X_p range for most of the traverses was from X_p = -0.15 inch to X_p = -5.85 inches, approximately the length of the Mk-83 model. For two of the traverses, Y_p = 0.0 and Z_p = 0.0 and 0.70, the range was extended to -8.85 inches.

Standard 4T data reduction programs were used to calculate the local velocity components and flow angles. These programs used the five probe pressures and probe calibration data. At the beginning of this phase of the testing, sufficient probe calibration data were taken to verify the validity of the previous calibrations. The estimated accuracy in the calculated local angles of attack and sideslip, from Reference 3, is $\pm 0.25^{\circ}$.

Summary of Tests

The flow-field survey tests are summarized in Table 7. Column 1 lists the parent aircraft configuration number from Table 2. The free-stream Mach number, M_{∞}, is in column 2 and the probe angle of attack, α_p, in column 3. The fourth column indicates the X_p schedule which was used for the traverse. These two schedules are shown at the bottom of each page of the table. The probe angle of attack listed in the third column is one degree less than the parent aircraft angle of attack, measured with respect to waterline, WL, zero shown in Figure 1.

The remainder of Table 7 lists the AEDC run numbers for the data obtained for a particular parent aircraft configuration, Mach number, probe angle of attack, and probe position. The X_p, Y_p, Z_p coordinate system origin is shown in Figure 5. Blanks in the table indicate that no data were taken. The run numbers provide input data for the data retrieval computer program.

TABLE 7. Flow-Field Survey Tests.

CONFIG. NO.	M_∞	α_P DEG.	X_P SCHD.	AEDC RUN NO.						
				Y_P = 0.0 in.			Y_P = 0.35 in.		Y_P = -0.35 in.	
				Z_P=0	Z_P=0.35	Z_P=0.70	Z_P=0	Z_P=0.35	Z_P=0	Z_P=0.35
1	0.6	0	A	956		958				
		0	B		957					
		4	A	959		961				
		4	B		960					
		8	A	962		964				
		8	B		963					
		12	A	965		967				
		12	B		966					
		16	A	968		970				
		16	B		969					
	0.95	0	A	985		987				
		0	B		986					
		4	A	973		975				
		4	B		974					
		8	A	976		978				
		8	B		977					
		12	A	979		981				
		12	B		980					
		16	A	982		984				
		16	B		983					
2	0.6	0	A	939		941				
		0	B		940		942		943	
		4	A	944		946				
		4	B		945		947		948	
		8	A	949		951				
		8	B		950		952		953	
3		0	A	771		773				
		0	B		772		774	775	776	777
		4	A	778		780				
		4	B		779		781	782	783	784

X_P SCHDS.:

	INITIAL X_P, IN.	FINAL X_P, IN.	ΔX_P, IN.
A	-0.15	-8.85	-0.30
B	-0.15	-5.85	-0.30

TABLE 7. (Contd.)

CONFIG. NO.	M_∞	α_p DEG.	X_p SCHD.	AEDC RUN NO.						
				Y_p = 0.0 in.			Y_p = 0.35 in.		Y_p = -0.35 in.	
				Z_p=0	Z_p=0.35	Z_p=0.70	Z_p=0	Z_p=0.35	Z_p=0	Z_p=0.35
3	0.6	8	A	785		787				
		8	B		786		788	789	790	791
		12	A	792		794				
		12	B		793		795	796	797	798
		16	A	799		801				
		16	B		800		802	803	804	805
	0.8	0	A	806		808				
		0	B		807		809	810	811	812
		4	A	820		822				
		4	B		821		823	824	825	826
		8	A	827		829				
		8	B		828		830	831	832	833
		12	A	835		837				
		12	B		836		838	839	840	841
		16	A	842		844				
		16	B		843		845	846	847	848
	0.95	0	A	849		851				
		0	B		850		852	853	854	855
		4	A	856		858				
		4	B		857		859	860	861	862
		8	A	863		865				
		8	B		864		866	867	868	869
		12	A	870		872				
		12	B		871		873	874	875	876
		16	A	877		879				
		16	B		878		880	881	882	883
4	0.6	0	A	886		888				
		0	B		887		889	890	891	892
		4	A	893		895				
		4	B		894		896	897	898	899

X_p SCHDS.:

	INITIAL X_p, IN.	FINAL X_p, IN.	ΔX_p, IN.
A	-0.15	-8.85	-0.30
B	-0.15	-5.85	-0.30

TABLE 7. (Contd.)

CONFIG. NO.	M_∞	α_p DEG.	X_p SCHD.	AEDC RUN NO.						
				Y_p = 0.0 in.			Y_p = 0.35 in.		Y_p = -0.35 in.	
				Z_p=0	Z_p=0.35	Z_p=0.70	Z_p=0	Z_p=0.35	Z_p=0	Z_p=0.35
4	0.6	8	A	900		902				
4		8	B		901		903	904	905	906
5		0	A	913		915				
		0	B		914		916	917	918	919
		4	A	920		923				
		4	B		921		924	925	926	927
		8	A	928		930				
		8	B		929		931	932	933	934
6		0	A	597		599				
		0	B		598		600	601	602	603
		4	A	604		606				
		4	B		605		607	608	610	611
		8	A	612		615				
		8	B		614		616	617	619	620
		12	A	621		623				
		12	B		622		624	625	626	627
		16	A	663		665				
		16	B		664		666	667	668	669
	0.8	0	A	670		672				
		0	B		671		673	674	675	676
		4	A	677		679				
		4	B		678		680	681	682	683
		8	A	684		686				
		8	B		685		687	688	689	690
		12	A	691		693				
		12	B		692		694	695	696	697
		16	A	698		700				
		16	B		699		701	702	703	704
	0.95	0	A	706		708				
	0.95	0	B		707		709	710	711	712

X_p SCHDS.:

	INITIAL X_p, IN.	FINAL X_p, IN.	ΔX_p, IN.
A	-0.15	-8.85	-0.30
B	-0.15	-5.85	-0.30

TABLE 7. (Contd.)

CONFIG. NO.	M_∞	α_P DEG.	X_P SCHD.	AEDC RUN NO.						
				Y_P = 0.0 in.			Y_P = 0.35 in.		Y_P = -0.35 in.	
				Z_P=0	Z_P=0.35	Z_P=0.70	Z_P=0	Z_P=0.35	Z_P=0	Z_P=0.35
6	0.95	4	A	713		715				
		4	B		714		716	717	718	719
		8	A	720		724				
		8	B		721		725	726	727	728
		12	A	729		731				
		12	B		730		732	733	734	735
		16	A	736		738				
		16	B		737		739	740	741	742
7	0.6	0	A	569		571				
		0	B		570		572	573	574	575
		4	A	576		578				
		4	B		577		579	580	582	583
		8	A	584		587				
		8	B		586		588	589	591	593
8		0	A	745		747				
		0	B		746		748	749	750	751
		4	A	752		754				
		4	B		753		755	756	757	759
		8	A	760		762				
		8	B		761		763	764	765	767

X_P SCHDS.:

	INITIAL X_P, IN.	FINAL X_P, IN.	ΔX_P, IN.
A	-0.15	-8.85	-0.30
B	-0.15	-5.85	-0.30

Use of Data Retrieval Computer Program

The flow-field data are all contained in one file on a magnetic tape. A computer program has been written which allows the flow-field data for run numbers listed in Table 7 to be retrieved from the tape and tabulated. A listing of the computer program is presented in Appendix C. The first card of input is in a 3A4 format and contains the word "FLOW" beginning in column 1. This is used to compare with a header on the tape to assure that the correct tape is mounted. The second input card in an I5 format specifies the number of run numbers of data, $\leq$ 100, to be retrieved. The specific run numbers from Table 7 are input on the next cards, eight to a card in 8F10.0 format. The run numbers can be in any order. The computer program sorts them into numerical sequence before searching the tape.

Description of Tabulated Data

There is one page of output for each run number of data. A sample is shown in Figure 12. The first line of output identifies the type of data, in this case flow field; the AEDC report number documenting this test (Reference 3); and the ARO project number and test number. The next two lines list the run number and parent aircraft configuration. The following four lines of output list the free-stream test conditions. The next four lines show the angles of attack of the parent aircraft and the probe. The remainder of the page tabulates the probe position, in the coordinate system of Figure 5, and the quantities calculated from the probe measurements.

FLOW-FIELD SURVEY DATA   AEDC-TSR-79-P79   ARO PROJECT NUMBER P41C-F0 (TEST TC-623)

RUN NO.	PARENT CONFIGURATION
571	F-4C,PCL,PT,T,(-2)F,(-3)F,P0

***** FREE-STREAM CONDITIONS *****

MACH NO	PT PSFA	TT DEG(R)	P PSFA	T DEG(R)	V FT/SEC	Q PSF	RE/FT FT(-1)
0.600	2210.7	553.3	1733.6	516.2	667.9	436.5	3.51*10**6

ALPHA PAR DEG	ALPHA PRORF DEG
1.00	0.0

***** FLOW FIELD DATA *****

XP IN	YP IN	ZP IN	ALP DEG	SIG DEG	ALPT DEG	PHI DEG	VX/V	VY/V	VZ/V	VL/V	ML	QL/Q	PTP/PT
-0.15	-0.01	0.70	-2.96	-1.10	3.15	200.28	0.992	-0.019	-0.051	0.993	0.595	0.989	1.000
-0.45	-0.01	0.70	-3.27	-1.11	3.44	198.72	0.995	-0.019	-0.057	0.996	0.597	0.994	1.000
-0.75	-0.01	0.70	-3.42	-1.15	3.59	198.51	0.999	-0.020	-0.060	1.001	0.602	1.001	0.999
-1.05	-0.01	0.70	-3.46	-1.18	3.63	198.76	1.009	-0.021	-0.061	1.011	0.608	1.018	1.000
-1.35	-0.01	0.70	-3.32	-1.16	3.50	199.26	1.018	-0.021	-0.059	1.020	0.613	1.033	1.000
-1.65	-0.01	0.70	-3.01	-1.15	3.21	200.84	1.030	-0.021	-0.054	1.032	0.619	1.053	1.001
-1.95	-0.01	0.70	-2.52	-1.15	2.76	204.51	1.037	-0.021	-0.046	1.038	0.624	1.062	1.000
-2.25	-0.01	0.70	-1.99	-1.14	2.28	209.80	1.043	-0.021	-0.036	1.043	0.629	1.072	1.000
-2.55	-0.01	0.70	-1.52	-1.11	1.88	216.23	1.044	-0.020	-0.028	1.045	0.629	1.074	1.000
-2.85	-0.01	0.71	-1.06	-1.09	1.51	225.82	1.046	-0.020	-0.019	1.046	0.630	1.077	1.000
-3.15	-0.01	0.70	-0.58	-1.07	1.22	241.52	1.046	-0.020	-0.011	1.046	0.629	1.077	1.001
-3.45	-0.01	0.70	-0.15	-1.03	1.04	261.80	1.043	-0.019	-0.003	1.043	0.628	1.071	1.000
-3.75	-0.01	0.71	0.19	-1.00	1.02	280.81	1.040	-0.018	0.003	1.040	0.625	1.066	1.000
-4.05	-0.01	0.70	0.41	-0.97	1.05	292.66	1.032	-0.018	0.007	1.033	0.623	1.053	0.999
-4.34	-0.01	0.70	0.52	-0.97	1.10	298.26	1.030	-0.017	0.009	1.030	0.620	1.050	1.000
-4.65	-0.01	0.70	0.56	-0.93	1.09	301.11	1.026	-0.017	0.010	1.026	0.616	1.043	1.000
-4.95	-0.01	0.70	0.54	-0.90	1.05	301.09	1.023	-0.016	0.010	1.023	0.614	1.038	1.000
-5.25	-0.01	0.70	0.48	-0.87	0.99	299.14	1.019	-0.015	0.009	1.019	0.615	1.032	1.000
-5.55	-0.01	0.70	0.46	-0.81	0.93	299.24	1.019	-0.014	0.008	1.020	0.613	1.034	1.001
-5.85	-0.01	0.71	0.39	-0.78	0.87	296.32	1.015	-0.014	0.007	1.015	0.612	1.025	1.000
-6.14	-0.01	0.70	0.31	-0.75	0.81	292.19	1.018	-0.013	0.005	1.018	0.610	1.030	1.001
-6.44	-0.01	0.70	0.25	-0.72	0.76	288.86	1.017	-0.013	0.004	1.017	0.611	1.027	0.999
-6.75	-0.01	0.70	0.26	-0.66	0.71	291.31	1.019	-0.012	0.005	1.019	0.612	1.030	1.000
-7.05	-0.01	0.70	0.26	-0.63	0.68	292.73	1.020	-0.011	0.005	1.020	0.614	1.033	1.000
-7.35	-0.02	0.70	0.33	-0.62	0.70	298.28	1.023	-0.011	0.006	1.023	0.615	1.038	1.000
-7.64	-0.01	0.70	0.42	-0.59	0.72	305.39	1.024	-0.011	0.008	1.024	0.615	1.040	1.000
-7.95	-0.01	0.70	0.51	-0.57	0.76	311.73	1.025	-0.010	0.009	1.025	0.616	1.041	1.000
-8.25	-0.01	0.70	0.58	-0.56	0.80	316.19	1.024	-0.010	0.010	1.024	0.616	1.039	1.000
-8.55	-0.02	0.70	0.65	-0.54	0.85	320.49	1.023	-0.010	0.012	1.023	0.616	1.038	1.000
-8.85	-0.01	0.70	0.71	-0.55	0.90	321.98	1.023	-0.010	0.013	1.023	0.615	1.038	1.000

FIGURE 12. Sample of Flow-Field Survey Data Tabulation.

The nomenclature used in the tabulated output is contained in the following list.

ALP	local angle of attack as seen by the probe; angle between the velocity component in the X_p, Z_p plane and that in the X_p direction, deg.; positive for positive VZ
ALPHA PAR	angle of attack of the parent aircraft, deg.
ALPHA PROBE	angle of attack of the probe, deg.
ALPT	total angle of attack as seen by the probe, angle between probe longitudinal axis and the local total velocity vector, deg.
MACH NO	free-stream Mach number
ML	local Mach number in the flow field
P	free-stream static pressure, psfa
PHI	angle between the velocity component in the probe Y_p, Z_p plane and the negative Z_p axis, deg.; positive clockwise viewed from the rear
PT	free-stream total pressure, psfa
PTP/PT	ratio of local total pressure to free-stream total pressure
Q	free-stream dynamic pressure, psf

OL/Q	ratio of local dynamic pressure to free-stream dynamic pressure
RE/FT	free-stream Reynolds number per foot, ft^{-1}
SIG	local sidewash angle as seen by the probe; angle between the velocity component in the X_p, Y_p plane and that in the negative X_p direction, deg.; positive for positive VY
T	free-stream static temperature, ^{o}R
TT	free-stream total temperature, ^{o}R
V	free-stream velocity, ft/sec
VL/V	total local velocity divided by the free-stream velocity
VX/V	local X_p velocity component, positive in the negative X_p direction, divided by the free-stream velocity
VY/V	local Y_p velocity component, positive in the positive Y_p direction, divided by the free-stream velocity
VZ/V	local Z_p velocity component, positive in the negative Z_p direction, divided by the free-stream velocity

XP — position of the probe static pressure orifices in the X_p direction in the X_p, Y_p, Z_p coordinate system of Figure 5, in.

YP — position of the probe longitudinal axis in the Y_p direction in the X_p, Y_p, Z_p coordinate system of Figure 5, in.

ZP — position of the probe longitudinal axis in the Z_p direction in the X_p, Y_p, Z_p coordinate system of Figure 5, in.

DISCUSSION OF ATTACHED LOADS

INTRODUCTORY REMARKS

A significant problem in store loads is whether a sting-supported store will yield the attached store loads (forces and moments) as it approaches the attached-store position as close as possible under practical testing conditions without making contact with the rack. In fact, the nature of the interference forces on the store for small gaps between store and rack is not well understood. The purpose of this and the next section is to elucidate the nature of these loads as revealed by the present measurements.

Our knowledge of the loads on a store in close proximity to the attached position is not extensive, but light has been shed on this subject by the tests of Dix in Reference 5. The tests were of Mk-83 bombs on a TER rack mounted on a

model of an F-4C airplane and included both attached loads and loads on a sting-supported bomb. His results are presented for $\alpha_s = 0^\circ$ and do not include parent aircraft component build-up results. For the bottom store, the shoulder stores were present; for the shoulder store, the opposite shoulder store was present. His data show that the captive loads cannot be obtained by extrapolating CTS data to zero Z/D in general. For some coefficients (CLM, CA, CLN), such extrapolation was better than for others (CN, CY). Large changes occurred for Z/D < 0.2 which could not be measured with the CTS system because of limitation in accuracy of positioning the store.

In this investigation a more extensive investigation was made of the problem, and the effects of angle of attack and configuration build-up were measured. Also flow-field data in the vicinity of the attached bottom store position were taken.

Before discussing the load measurements, we will show the relationship between the attached and grid loads.

RELATIONSHIP BETWEEN ATTACHED AND GRID LOADS

Stores S_{MF} and S_{MU} are the ones tested both on the attached-loads balance and the CTS sting supported balance. Data for store S_{MF} in combination with configuration 3 of Table 2 (F4-C, inboard pylon, TER) are shown in Figure 13. In Figure 13(a) the normal-force coefficient is shown versus Z_p/D for five angles of attack at $M_\infty = 0.6$. The sting data extend down to $Z_p/D = .07$. There is a large change in CN in the range

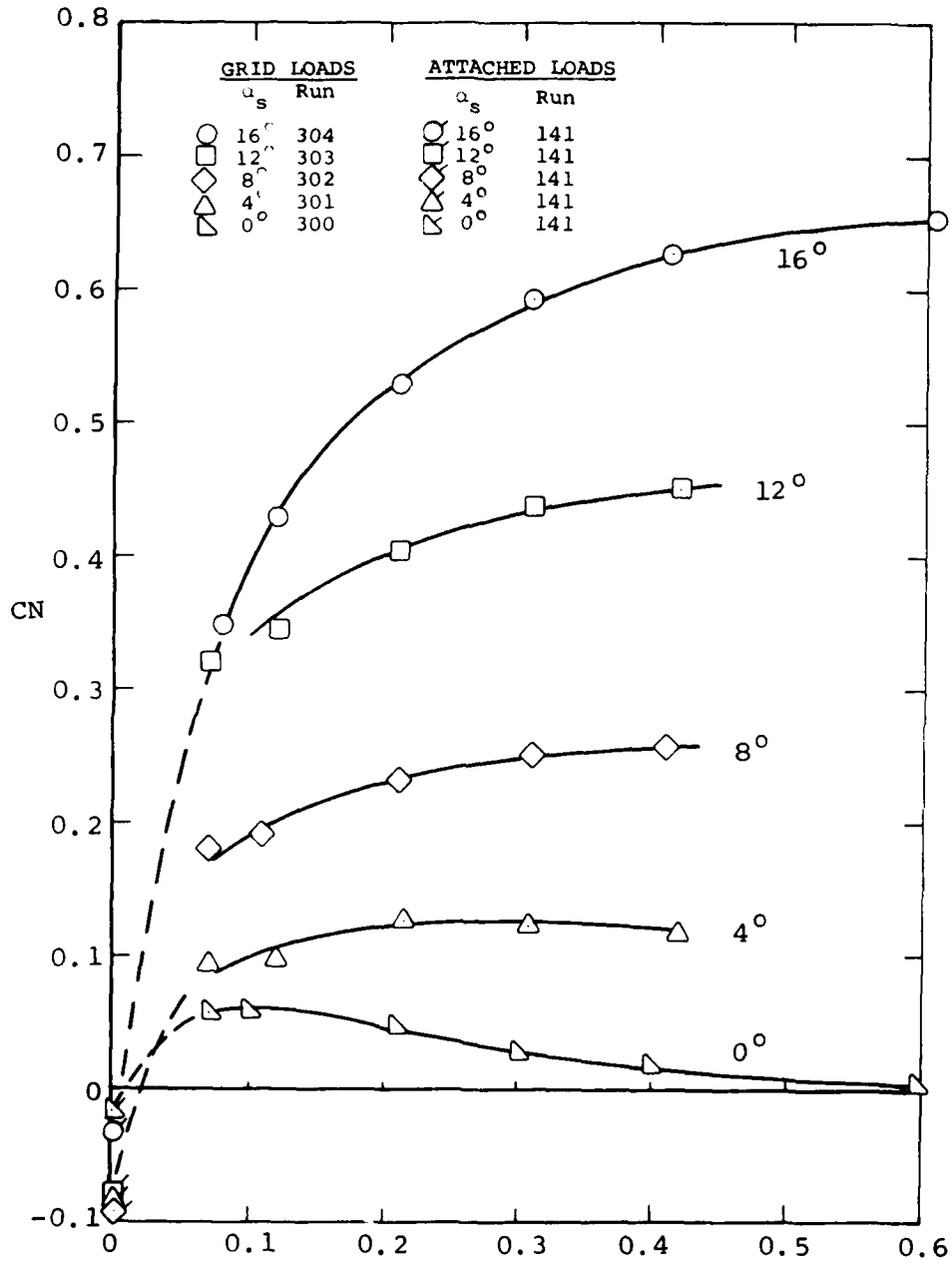

(a) Normal-force coefficient.

FIGURE 13. Comparison of Attached and Grid Loads for Store S_{MF} in Combination with Configuration 3 at $M_\infty = 0.6$.

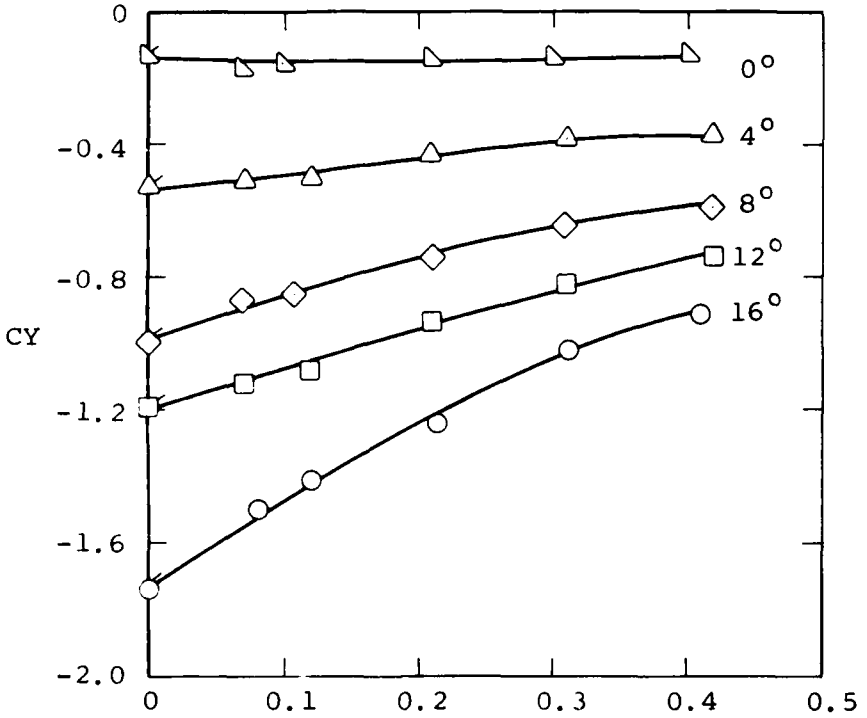

(b) Side-force coefficient.

FIGURE 13. Continued.

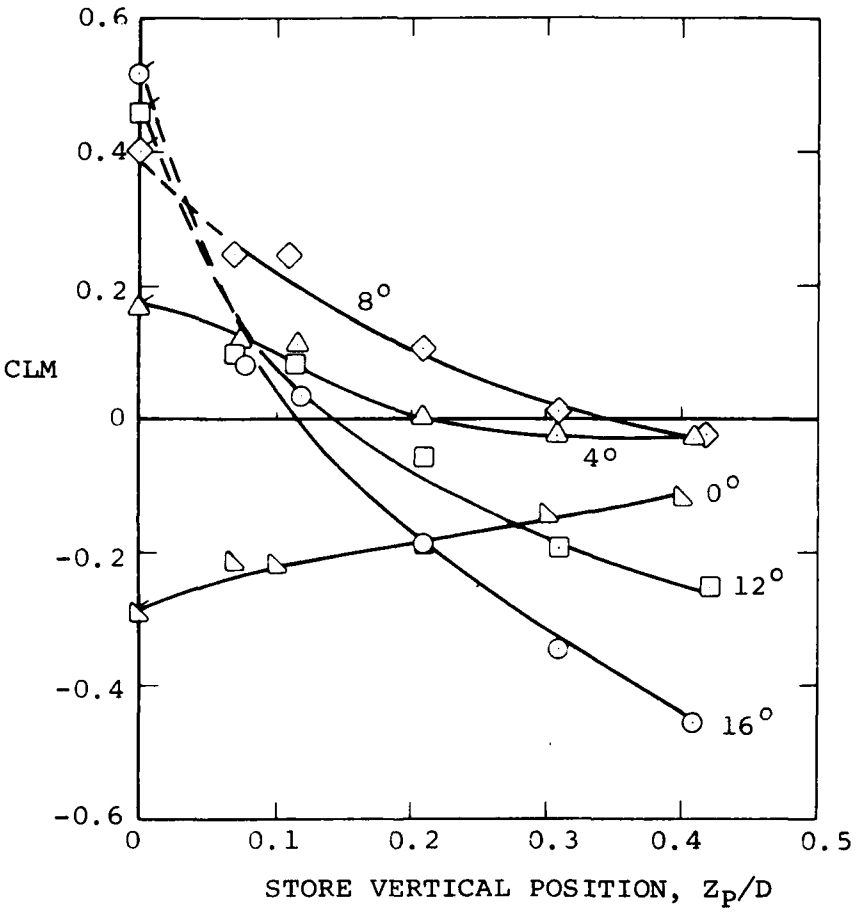

(c) Pitching-moment coefficient.

FIGURE 13. Continued.

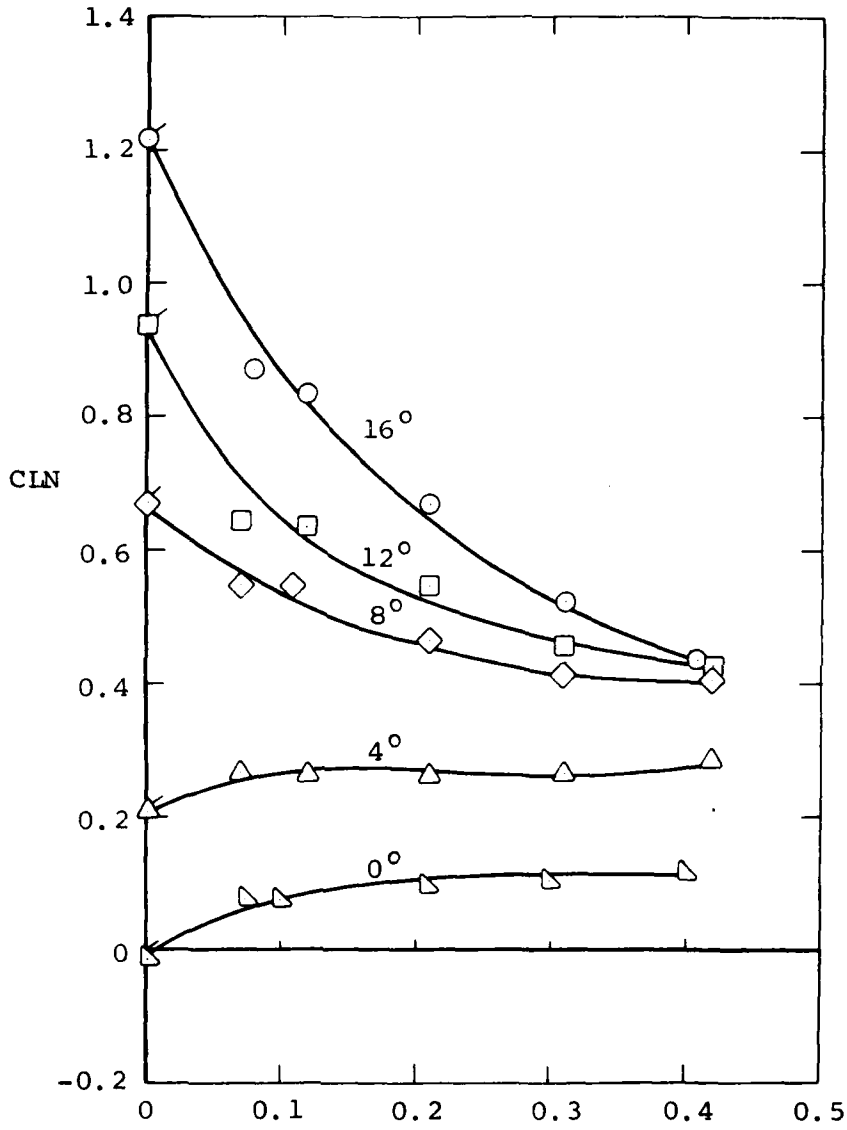

(d) Yawing-moment coefficient.

FIGURE 13. Continued.

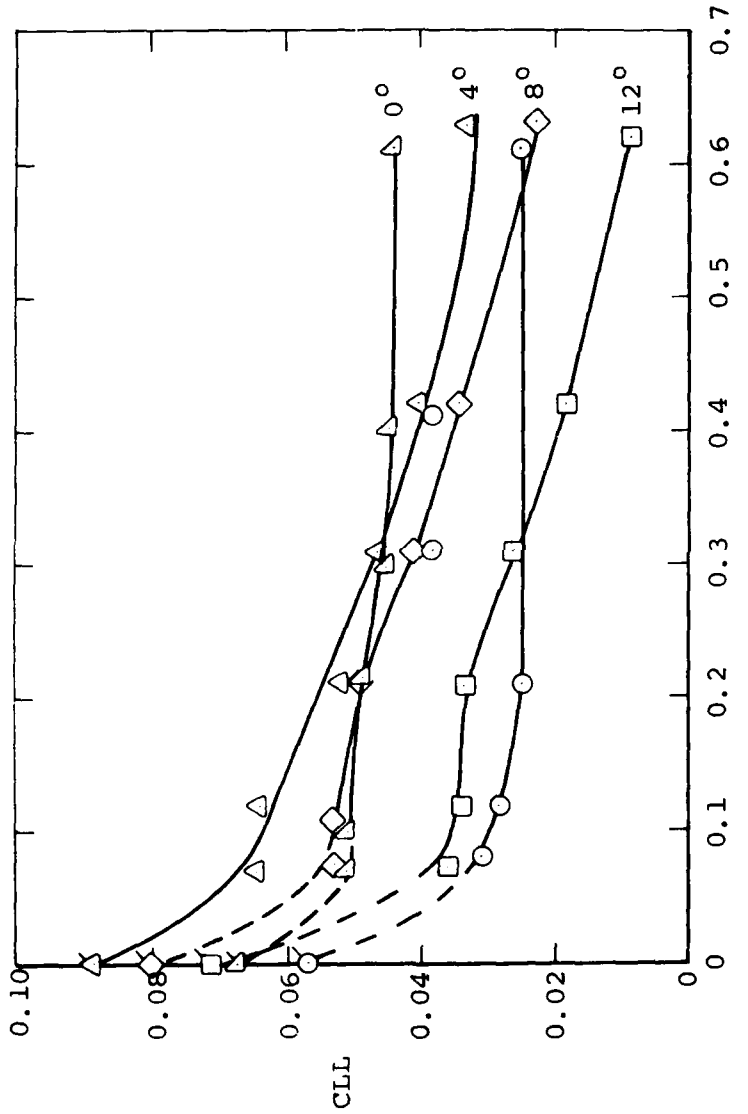

(e) Rolling-moment coefficient.

FIGURE 13. Concluded.

$0 < Z_p/D < .07$ as indicated by the attached-store data which cannot be reproduced by extrapolating the sting results to zero gap. This range of Z_p/D, representing only 0.05 in. model scale, produces surprisingly large interference forces which increase with angle of attack.

Examination of the other parts of Figure 13 for the other coefficients shows that, with the possible exception of side-force coefficient, extrapolation of the sting data to $Z_p = 0$ is not accurate. The question naturally arises whether the attached loads are accurately measured. Subsequent data will verify their repeatability. It is our belief based on the overall consistency of the data as well as the results of Dix that the attached loads are valid.

The question arises whether the above phenomena are also valid at high Mach numbers. Curves similar to those of Figure 13 are presented in Figure 14 for store S_{MU} in combination with configuration 3 at $M_\infty = 0.95$. The same general behavior is seen as previously. In Figure 15, the normal-force coefficients are shown for three Mach numbers for store S_{MF} in combination with configuration 3. These effects of Mach number on the behavior for $Z_p/D < .07$ are small. It appears that both the sting and attached load data are repeatable, and that the strong interference is not Mach number dependent.

There are adequate data to illustrate a number of effects on the way the loads of the attached bottom store vary with angle of attack. The effects of the following variables on these attached store loads will now be illustrated.

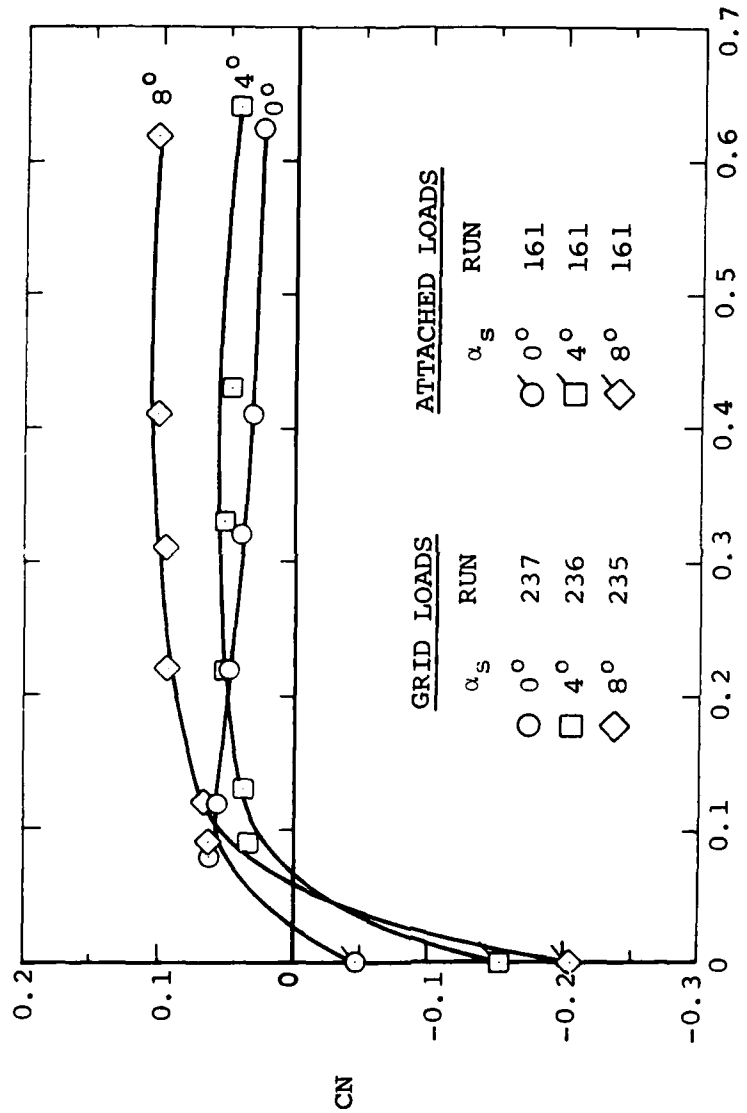

(a) Normal-force coefficient.

FIGURE 14. Comparison of Attached and Grid Loads for Store S_{MU} in Combination with Configuration 3 at $M_\infty = 0.95$.

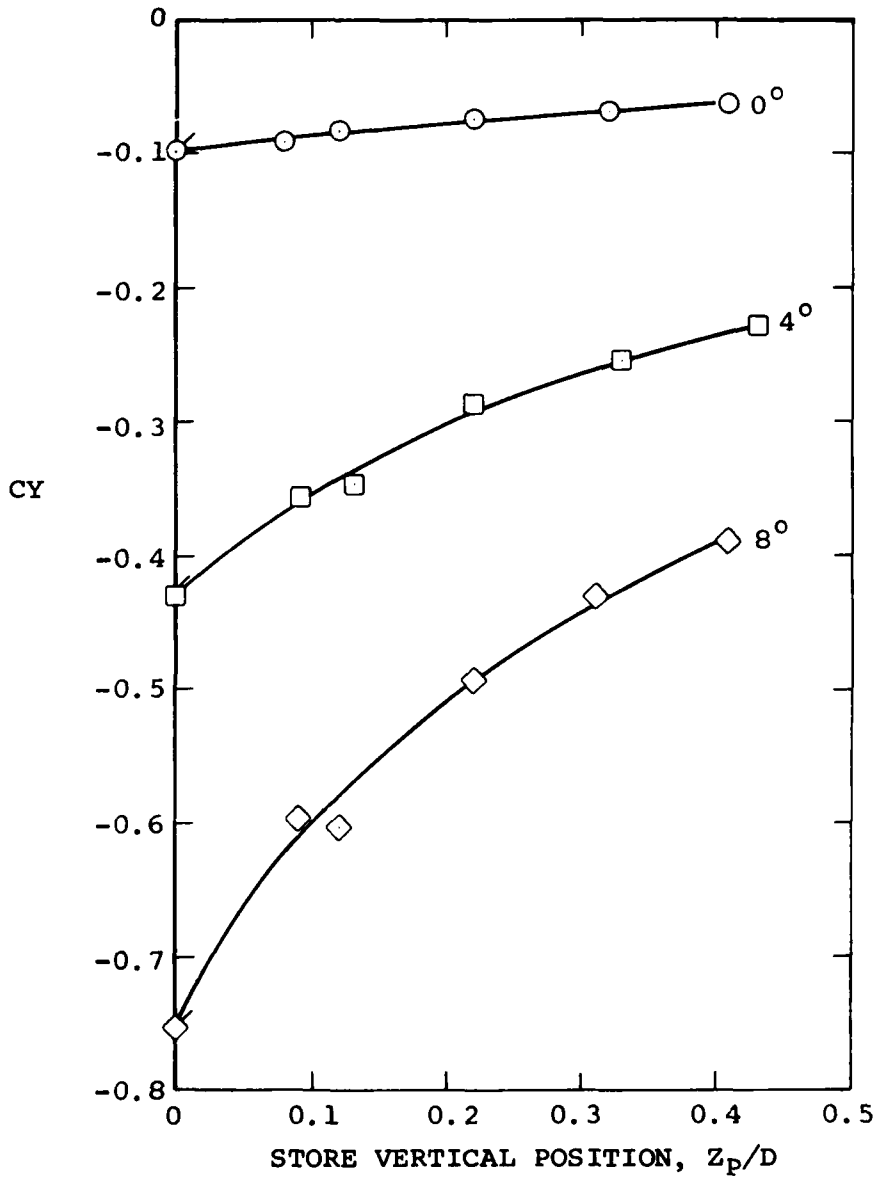

(b) Side-force coefficient.

FIGURE 14. Continued.

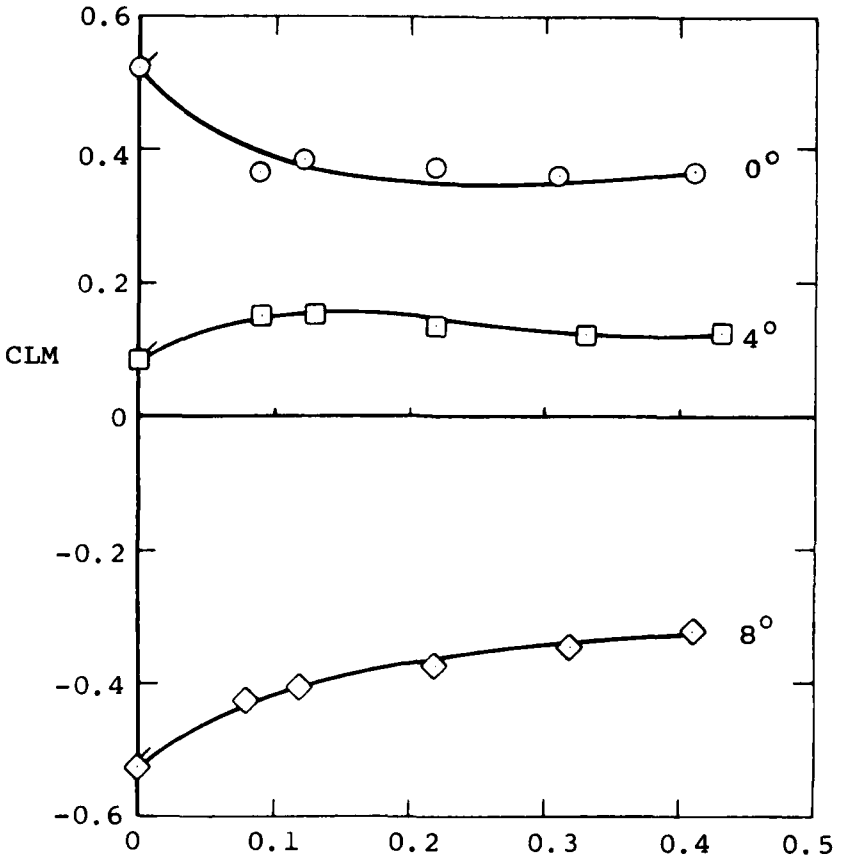

(c) Pitching-moment coefficient.

FIGURE 14. Continued.

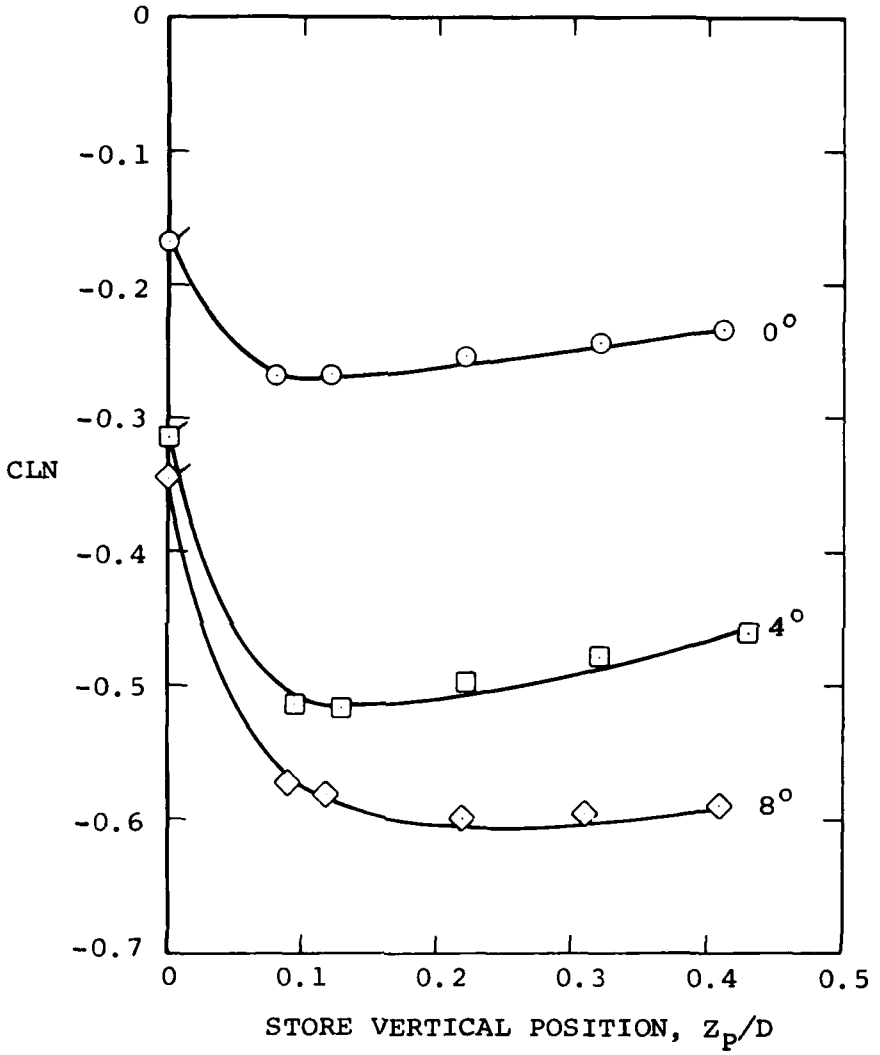

(d) Yawing-moment coefficient.

FIGURE 14. Concluded.

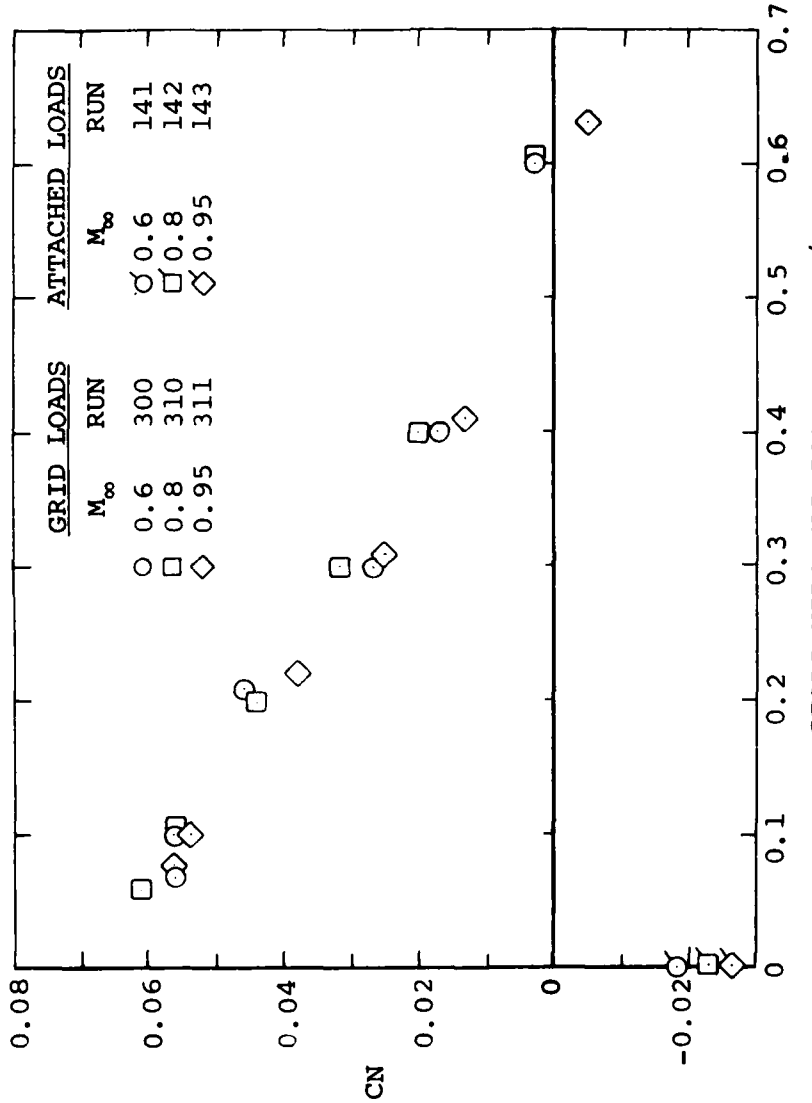

(a) $\alpha_s = 0°$.

FIGURE 15. Effect of Mach Number on Attached and Grid Loads for Store S_{MF} in Combination with Configuration 3.

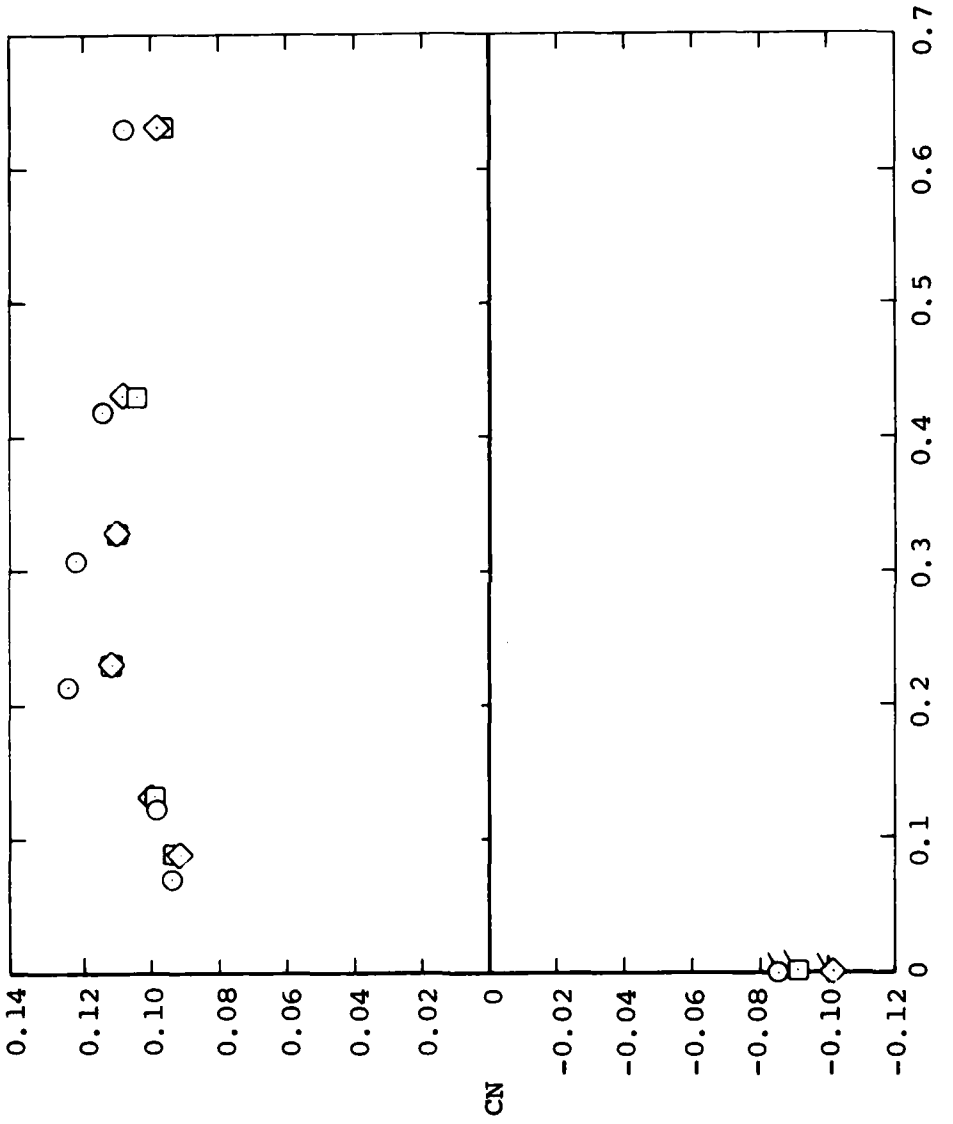

(b) $\alpha_s = 4^\circ$.

FIGURE 15. Concluded.

(a) Configuration (other than bottom store)
(b) Mach number
(c) Effect of adding fins to shoulder stores
(d) Effect of number of shoulder stores
(e) Effect of bottom store configuration

EFFECT OF CONFIGURATION

Attached store loads (forces and moments) were measured on four different bottom store configurations for configurations 3, 4, 5, 6, and 8. The variations of loads for store S_{AF} at $M_\infty = 0.6$ with angle of attack are shown in Figure 16 for the above five configurations. Figure 16(a) shows that at angles of attack between -4° and $+8^\circ$, configuration 3 yields the least normal force (positive upward). Configurations 4 and 8, which only have one shoulder store, yield more normal force; and configurations 5 and 6, with two shoulder stores, yield the largest normal forces. What is of particular interest is that the addition of fins to the shoulder stores has a small effect on normal force. Also at angles of attack above 8°, the effects of configuration differences are much less than at lower angles of attack.

The side-force variation with α_s shown in Figure 16(b) shows that the side force is relatively insensitive to configuration especially for angles of attack less than 8°. Positive side force is directed towards the fuselage from the left-wing inboard pylon.

Pitching-moment coefficients shown in Figure 16(c) are generally nose down. For angles of attack less than about

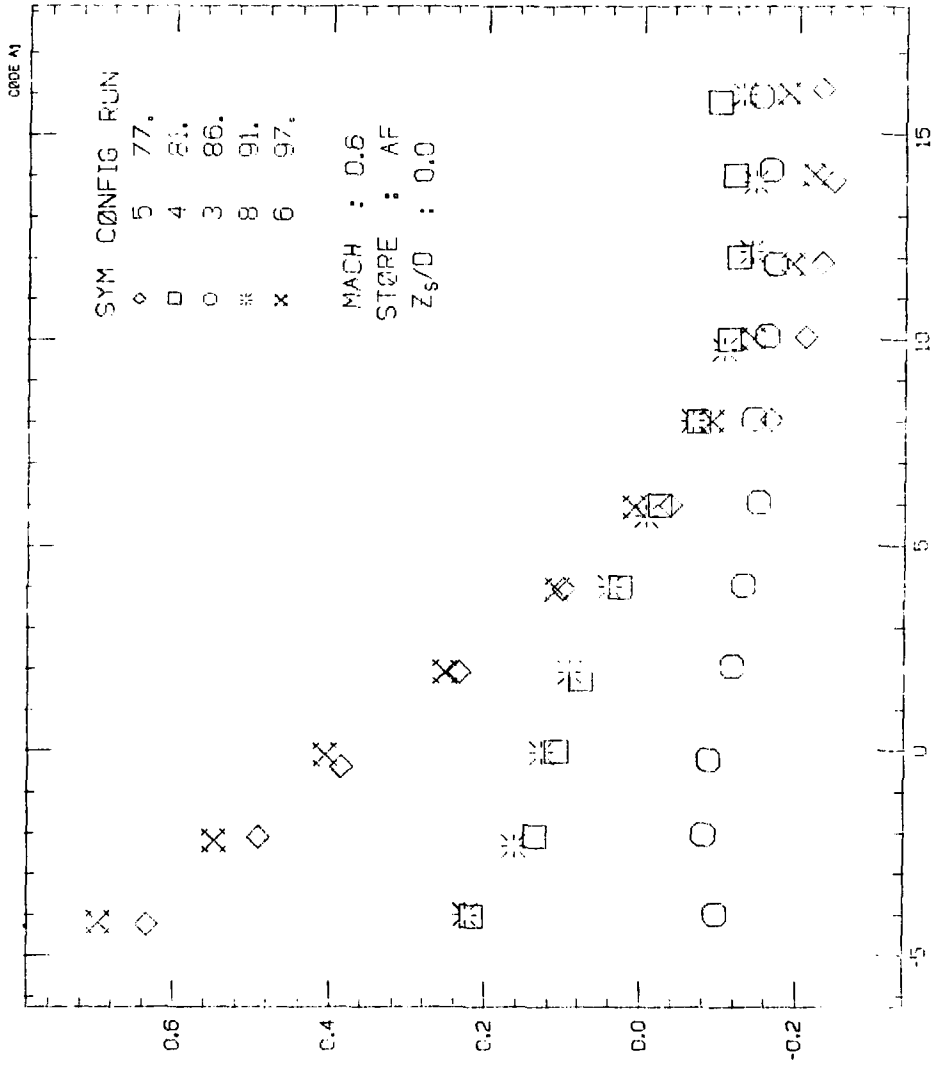

(a) Normal-force coefficient.

FIGURE 16.- Effect of Airplane Configuration on Attached Loads of Bottom Store SAF at M_∞ = 0.6.

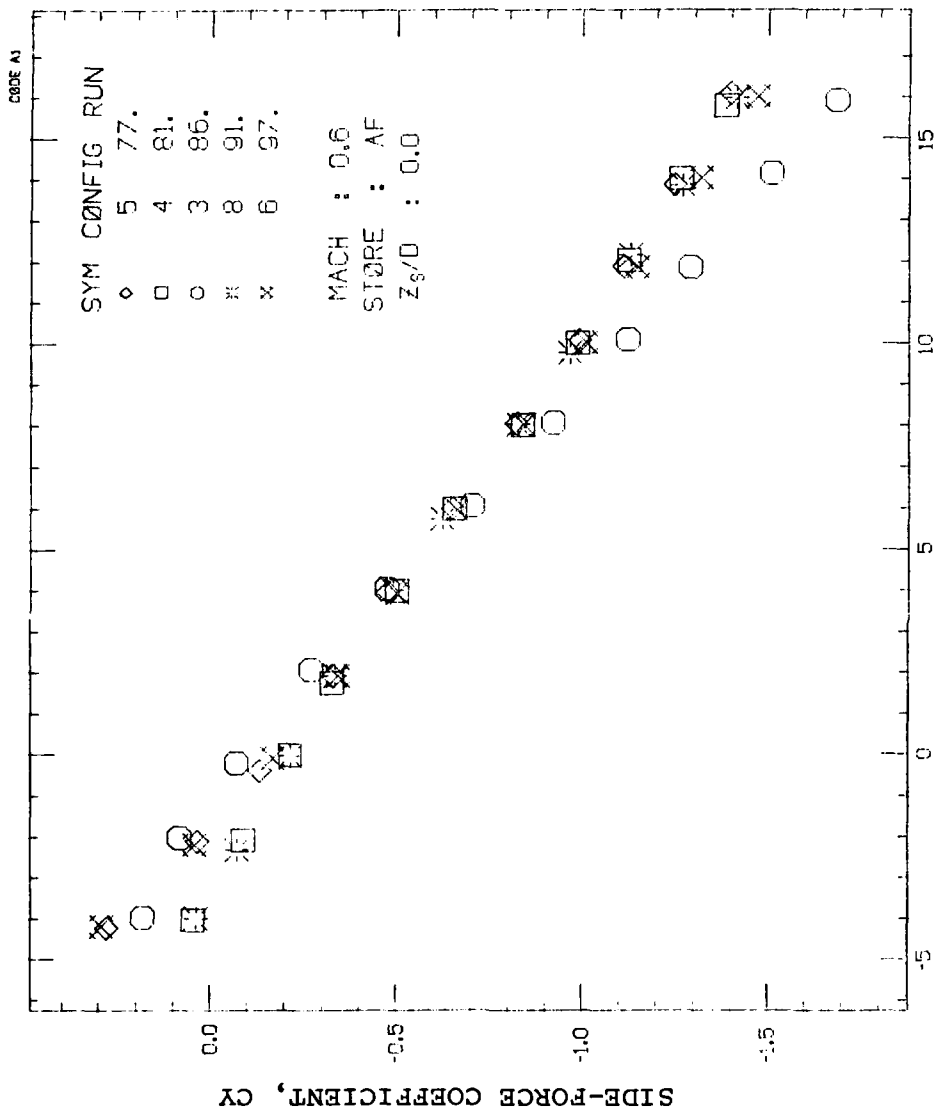

(b) Side-force coefficient.

FIGURE 16. Continued.

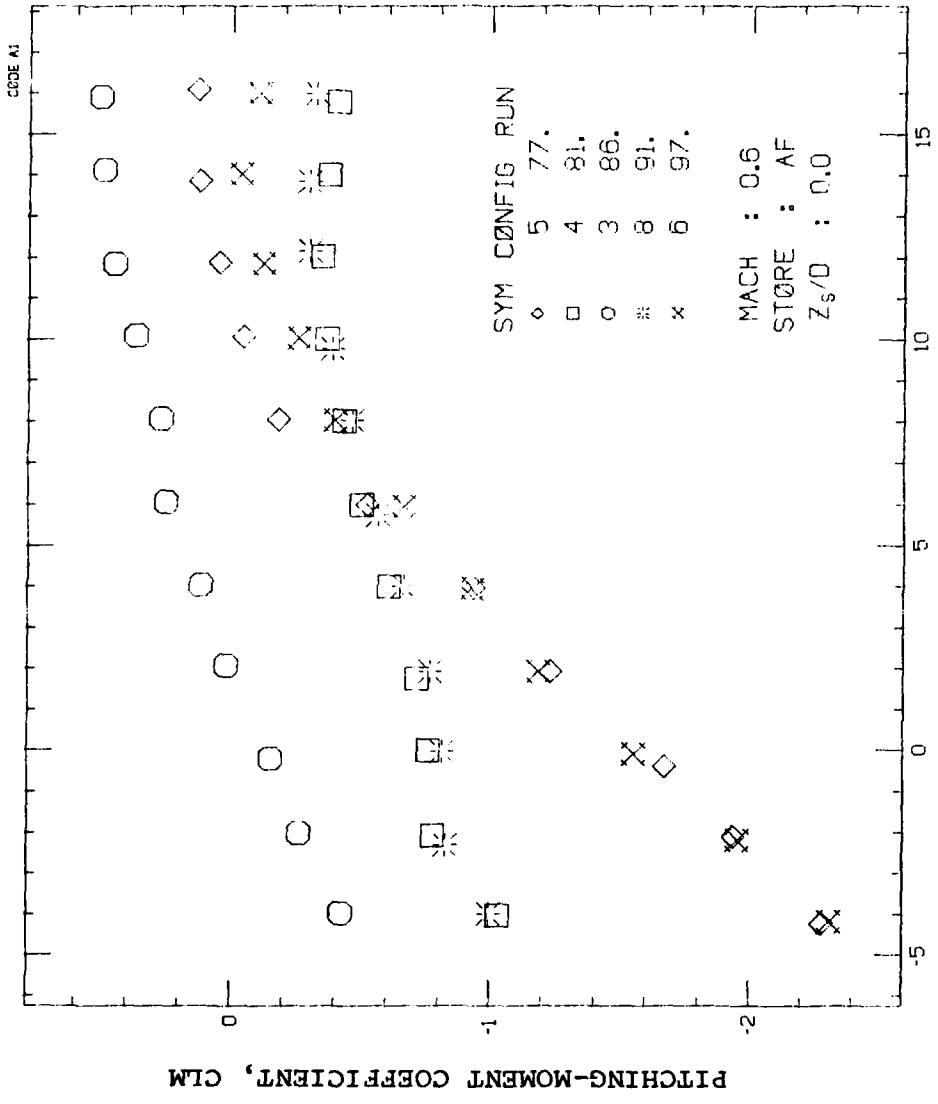

(c) Pitching-moment coefficient.

FIGURE 16. Continued.

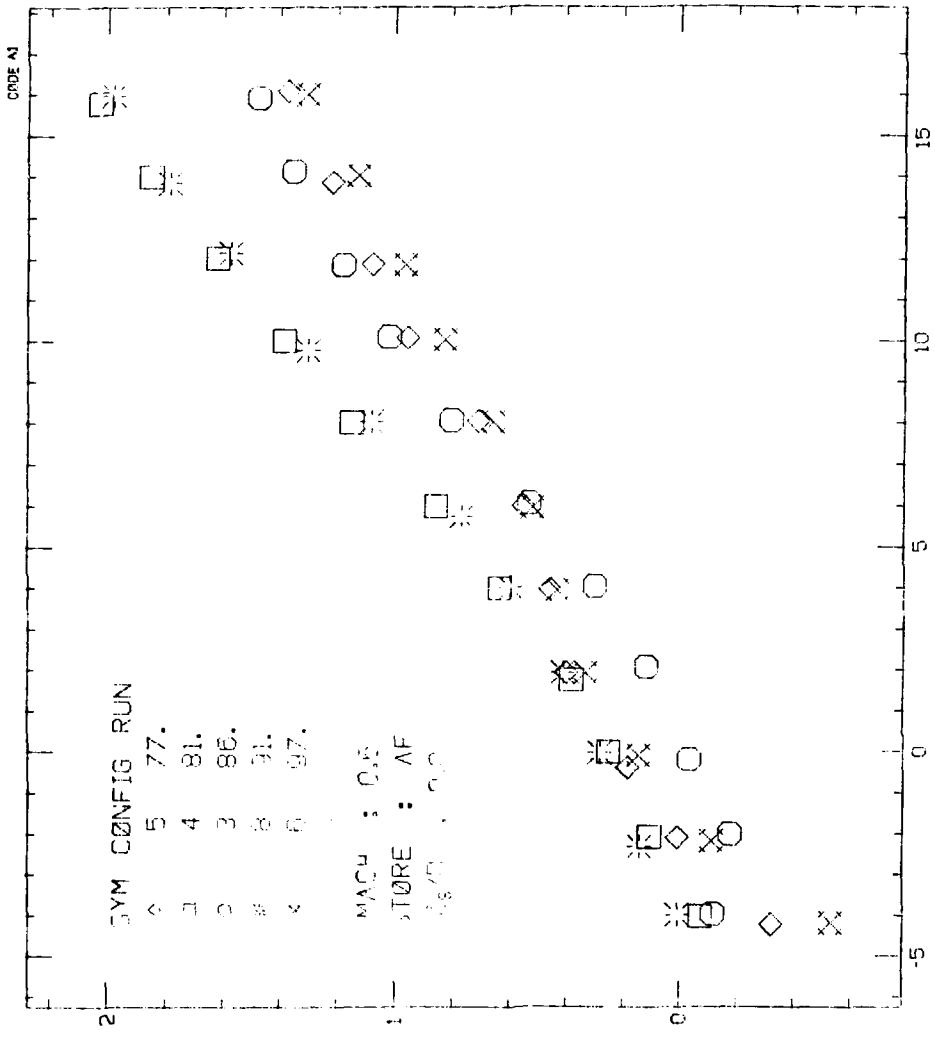

(d) Yawing-moment coefficient.

FIGURE 16. Continued.

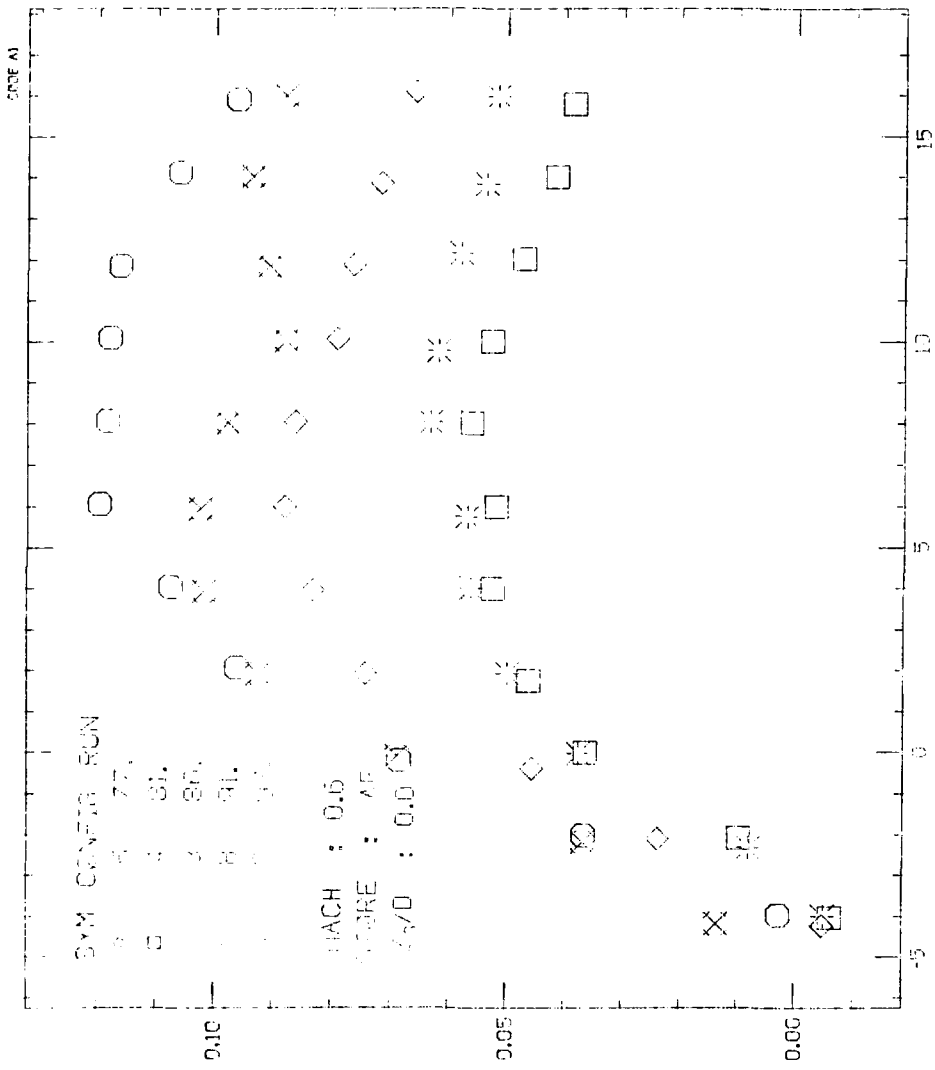

(e) Rolling-moment coefficient.

FIGURE 16. Concluded.

6^{o}, the effect of configuration on the magnitude of the pitching-moment coefficient is similar to its effect on normal force. However in the range above 6^{o} to 8^{o}, configurations 5 and 6 have smaller pitching moments than configurations 4 and 8. Again adding fins to the shoulder stores causes negligible effect.

The yawing-moment coefficient is slightly nonlinear with α_s from -4^{o} to 16^{o} and is positive. There are significant differences due to configuration changes, but the addition of fins to the shoulder store has a negligible effect.

The rolling-moment coefficients in Figure 16(e) are positive, nonlinear, and have maxima around 6^{o} to 8^{o}. The configuration effects are significant. The addition of the fins to the shoulder stores causes a significant effect in the higher angle range.

The same kind of data as Figure 16 for $M_\infty = 0.95$ show the same general qualitative effects.

EFFECT OF MACH NUMBER

A set of curves for the loads on S_{AF} for configuration 6 at $M_\infty = 0.6$, 0.7, 0.8, 0.9 and 0.95 in Figure 17 shows that Mach number has its largest effect on normal force. Mach number effects on the rest of the coefficients are not large.

(a) Normal-force coefficient.

FIGURE 17. Effect of Mach Number on the Attached Loads of Bottom Store S_{AF} for Configuration 6.

(b) Side-force coefficient.

FIGURE 17.- Continued.

(c) Pitching-moment coefficient.

FIGURE 17. Continued.

YAWING-MOMENT COEFFICIENT, CLN

STORE ANGLE-OF-ATTACK, α_s, DEG

(d) Yawing-moment coefficient.

FIGURE 17. Continued.

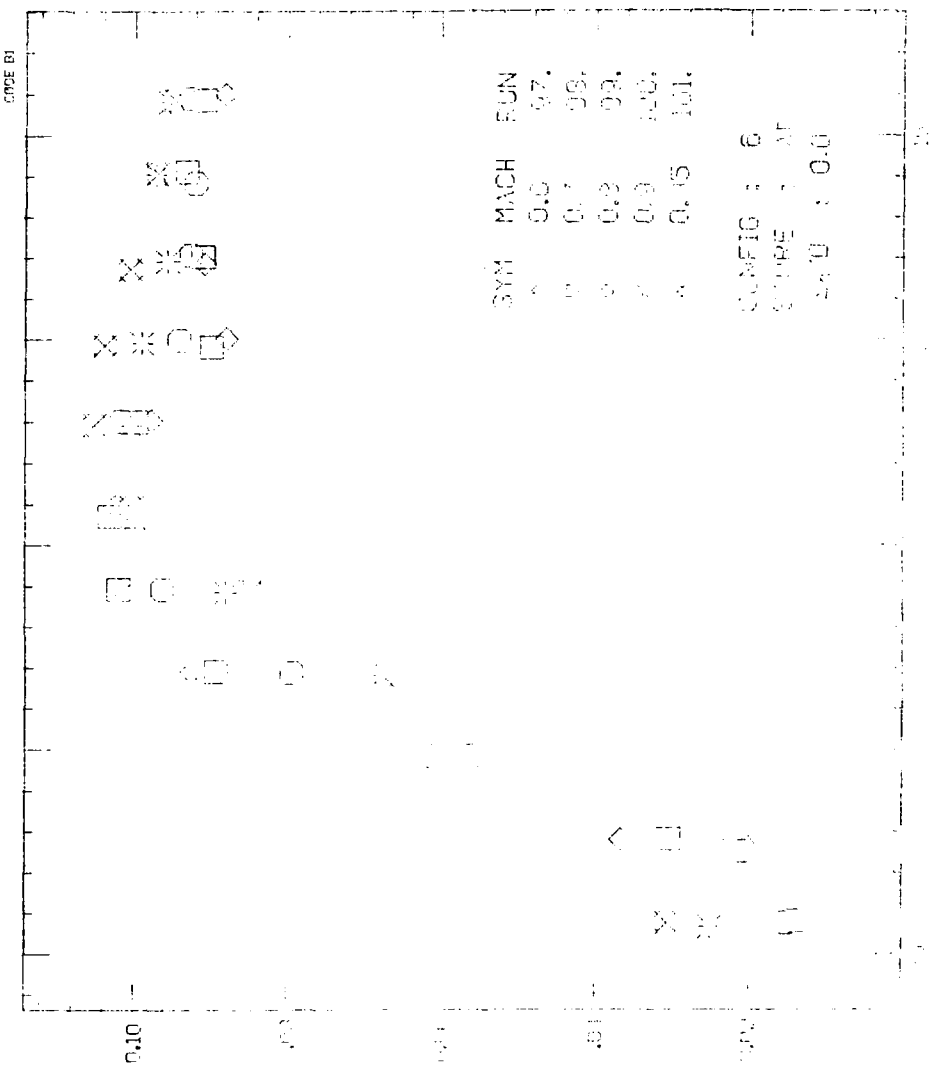

STORE ANGLE-OF-ATTACK, α_s, DEG

(e) Rolling-moment coefficient.

FIGURE 17. Concluded.

EFFECT OF ADDING FINS TO SHOULDER STORES

The effect of adding fins to the shoulder stores on the bottom store loads is seen by comparing results for configurations 4 and 8 or configurations 5 and 6 (latter case corresponding to flight). The loads on store S_{AF} are shown in Figure 18 for $M_\infty = 0.6$ for configurations 5 and 6. The data show negligible effect of adding the fins to the stores except for rolling-moment coefficient and for pitching-moment coefficient at high angle of attack. At $M_\infty = 0.95$ the same kind of results show negligible effect of adding fins to the shoulder stores except on CN and CLN at negative angles of attack, and on rolling moment.

EFFECT OF NUMBER OF SHOULDER STORES

By comparing store loads for configurations 4 and 5 or 6 and 8, the effect of the number of shoulder stores on the bottom store loads can be determined. Figure 19 presents the loads on S_{AF} at $M_\infty = 0.6$ for configurations 4 and 5. The addition of a second shoulder store has the effect of increasing normal-force coefficient at low angles of attack and decreasing it at high angles of attack with corresponding changes in the pitching-moment coefficient. While the addition of the second shoulder store has a small effect on side-force coefficient except at negative angle of attack, it does have a significant effect on yawing-moment coefficient. Rolling-moment coefficient is also changed.

At $M_\infty = 0.95$ the data exhibit the same qualitative effects as at $M_\infty = 0.6$.

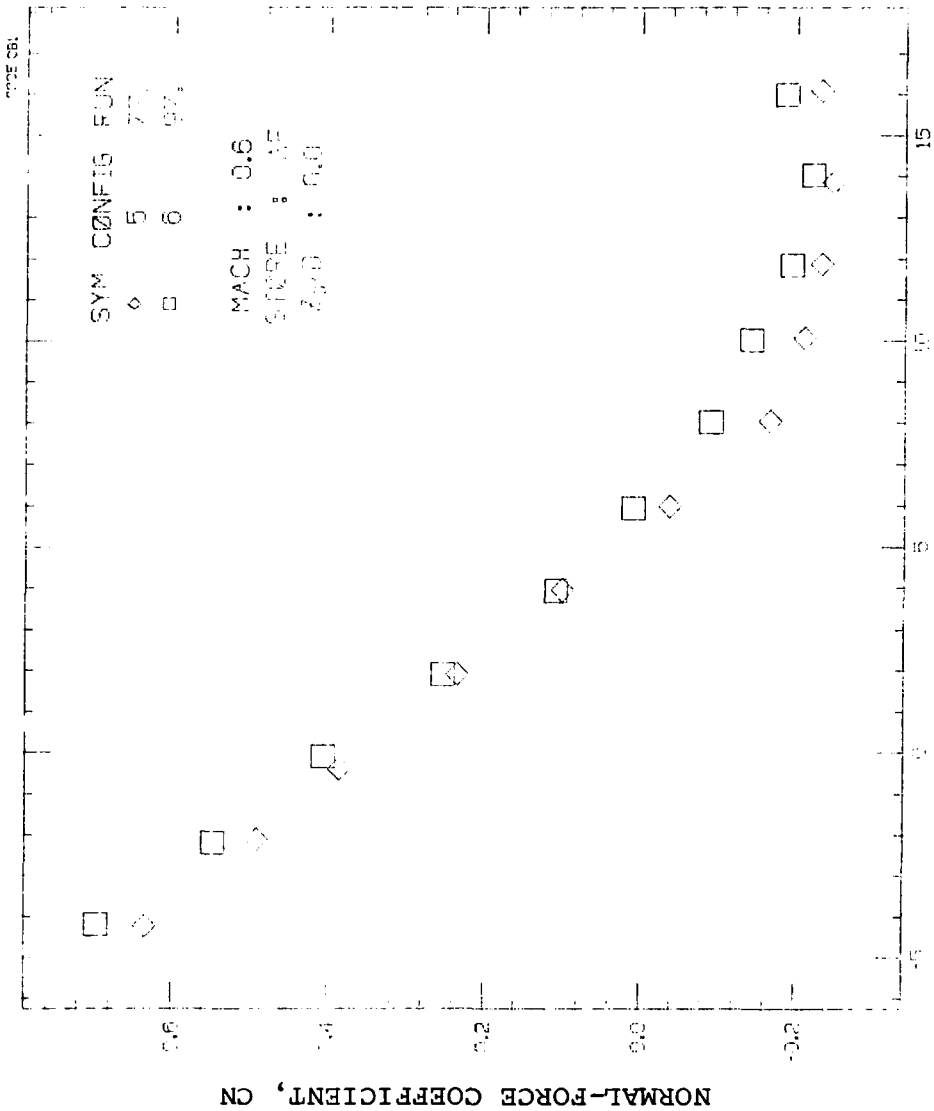

FIGURE 18. Effect of Adding Fins to Shoulder Stores on Attached Loads of Bottom Store S_{AF} at $M_\infty = 0.6$.
(a) Normal-force coefficient.

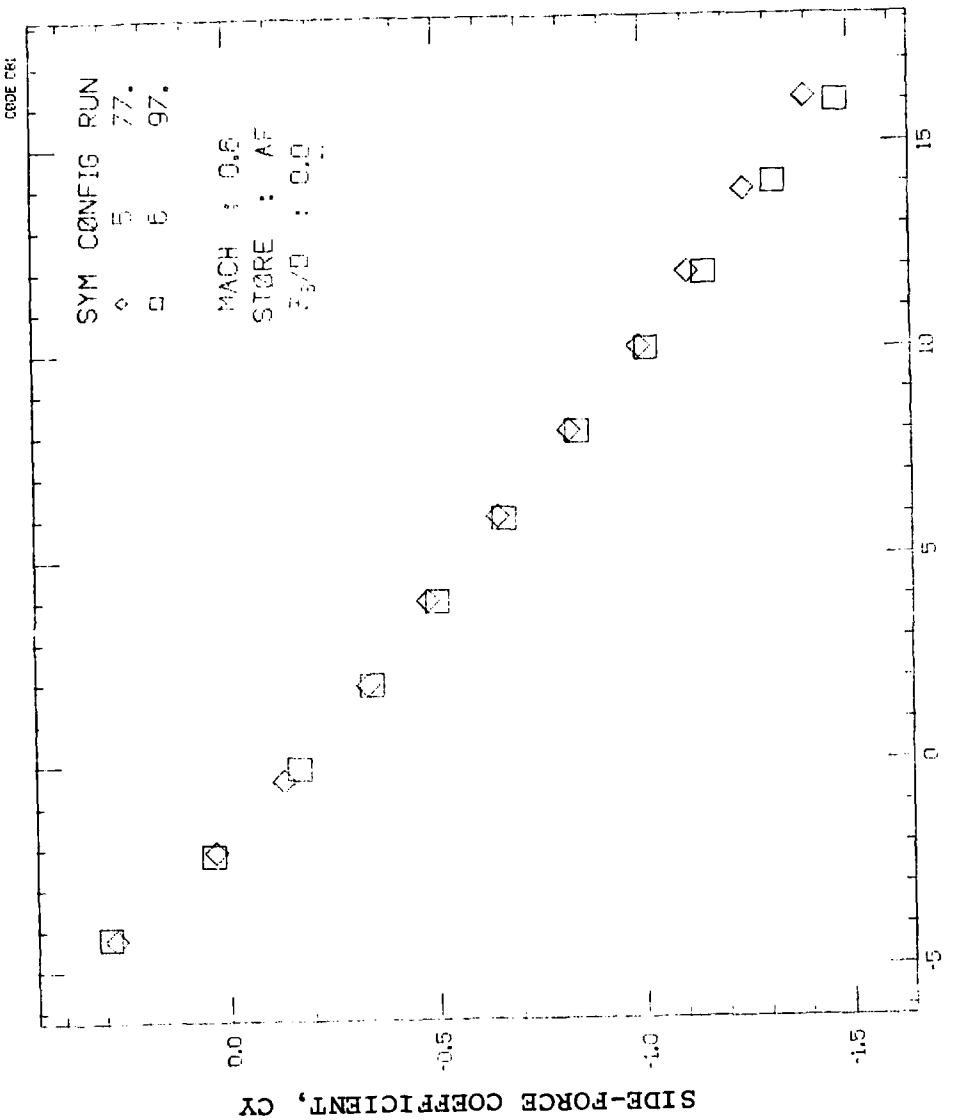

(b) Side-force coefficient.

FIGURE 18. Continued.

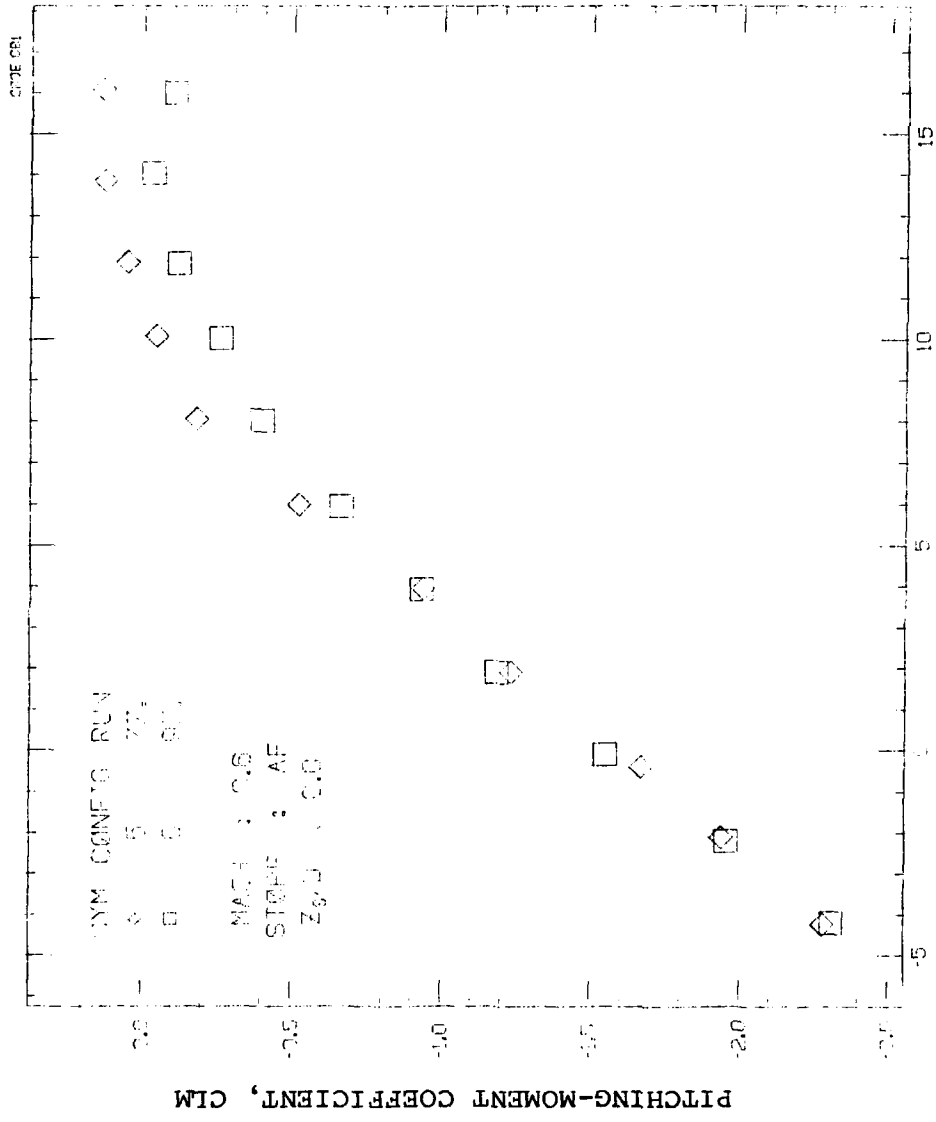

(c) Pitching-moment coefficient.

FIGURE 18. Continued.

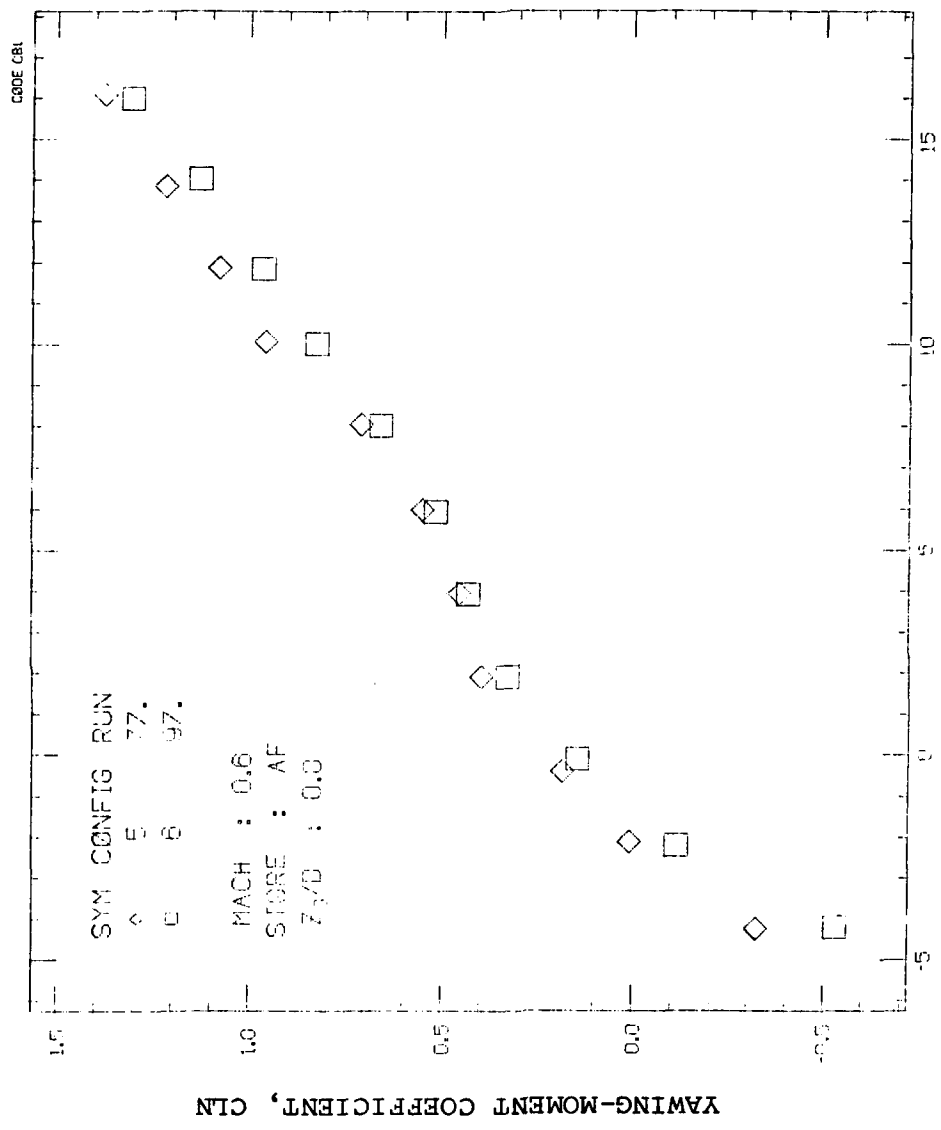

(d) Yawing-moment coefficient.

FIGURE 18. Continued.

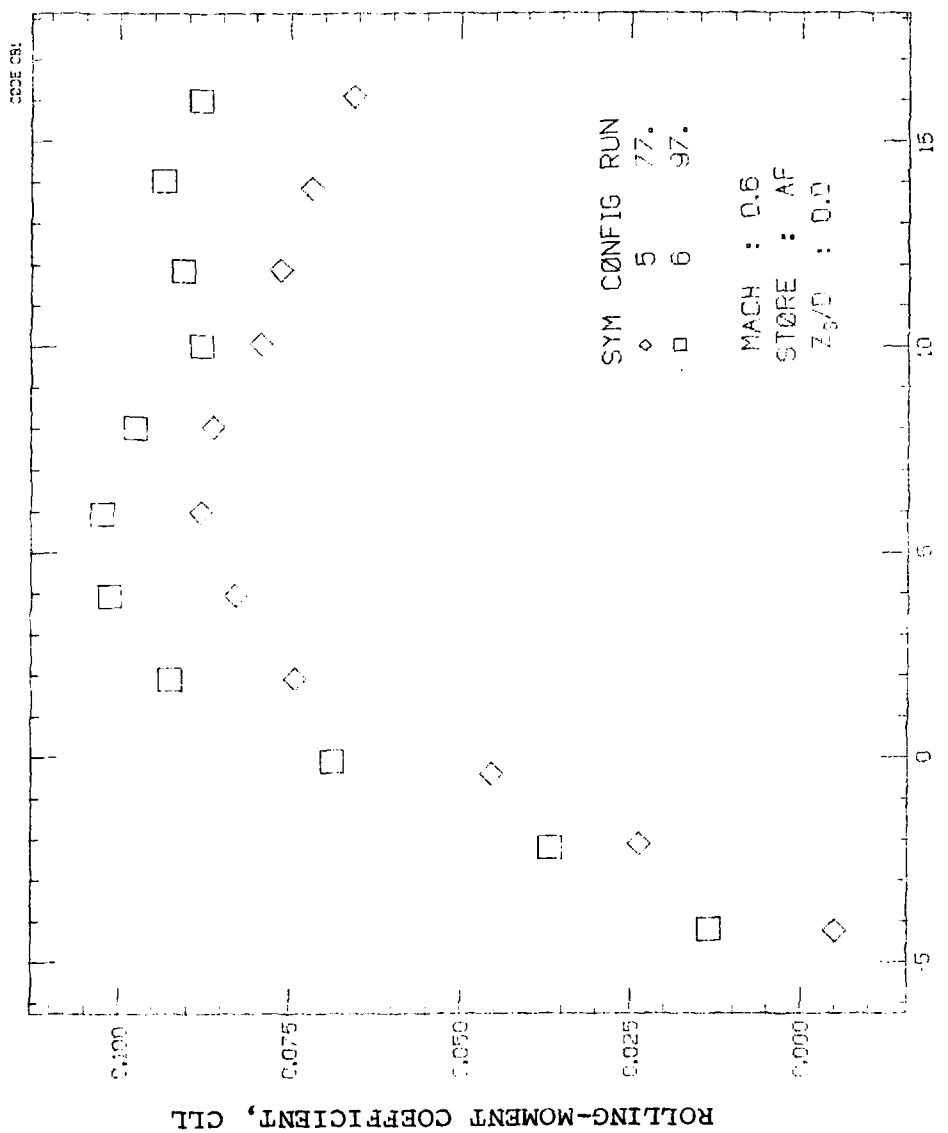

(e) Rolling-moment coefficient.

FIGURE 18. Concluded.

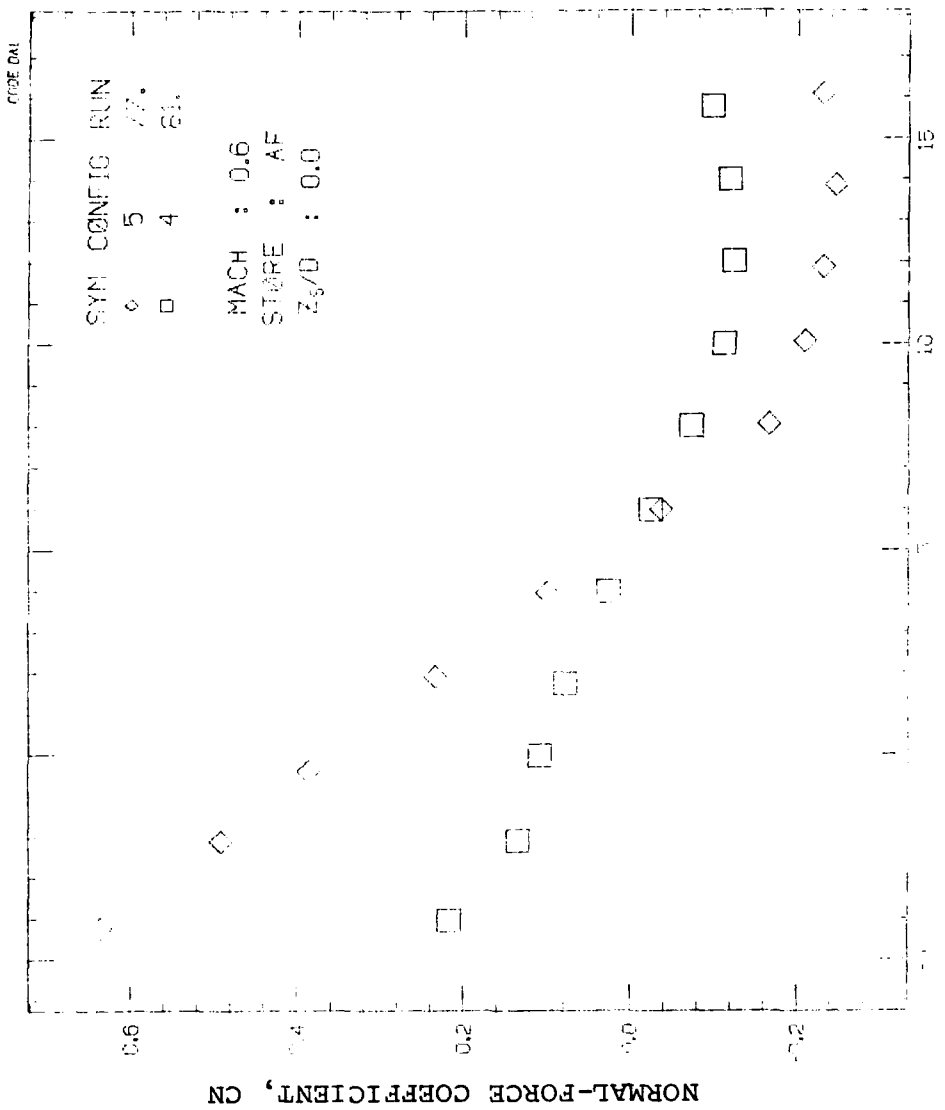

(a) Normal-force coefficient.

FIGURE 19. Effect of Number of Shoulder Stores on the Attached Loads of the Bottom Store S_{AF} at M_∞ = 0.6.

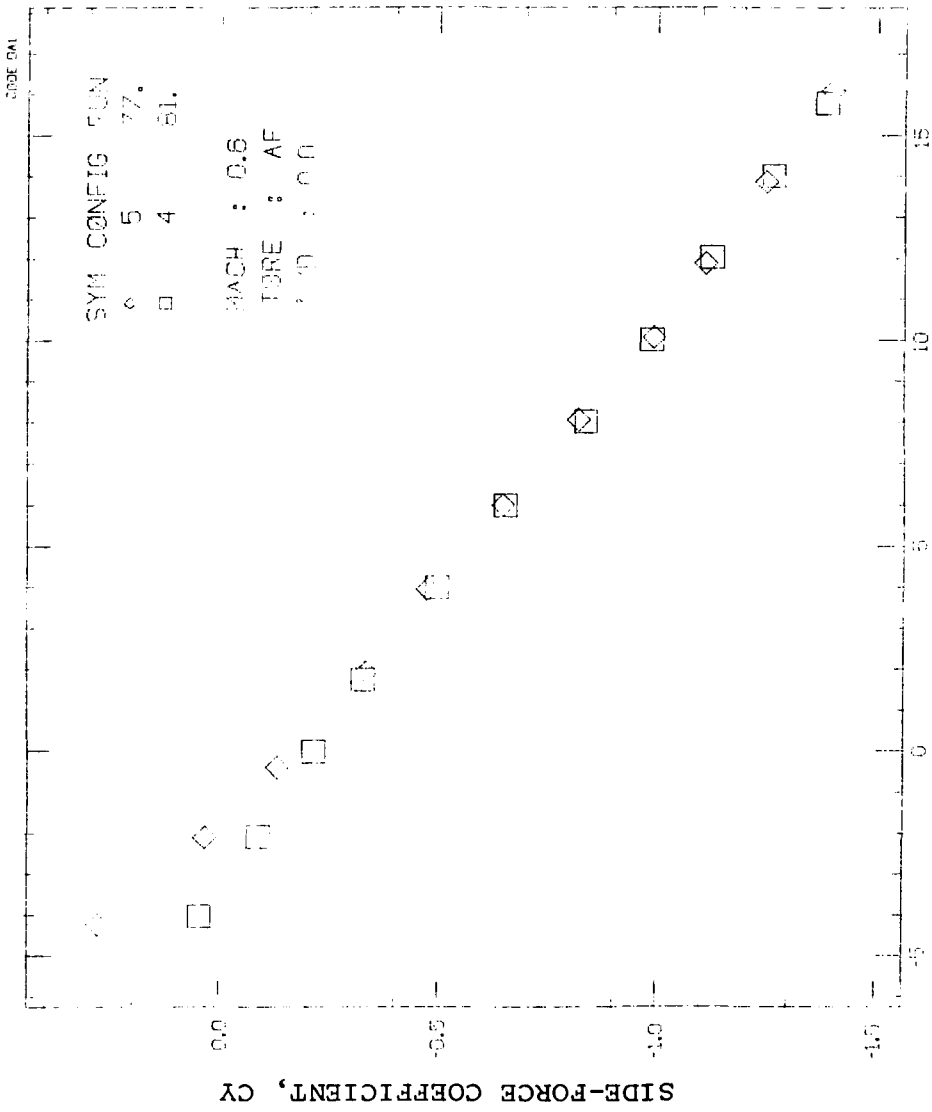

(b) Side-force coefficient.

FIGURE 19. Continued.

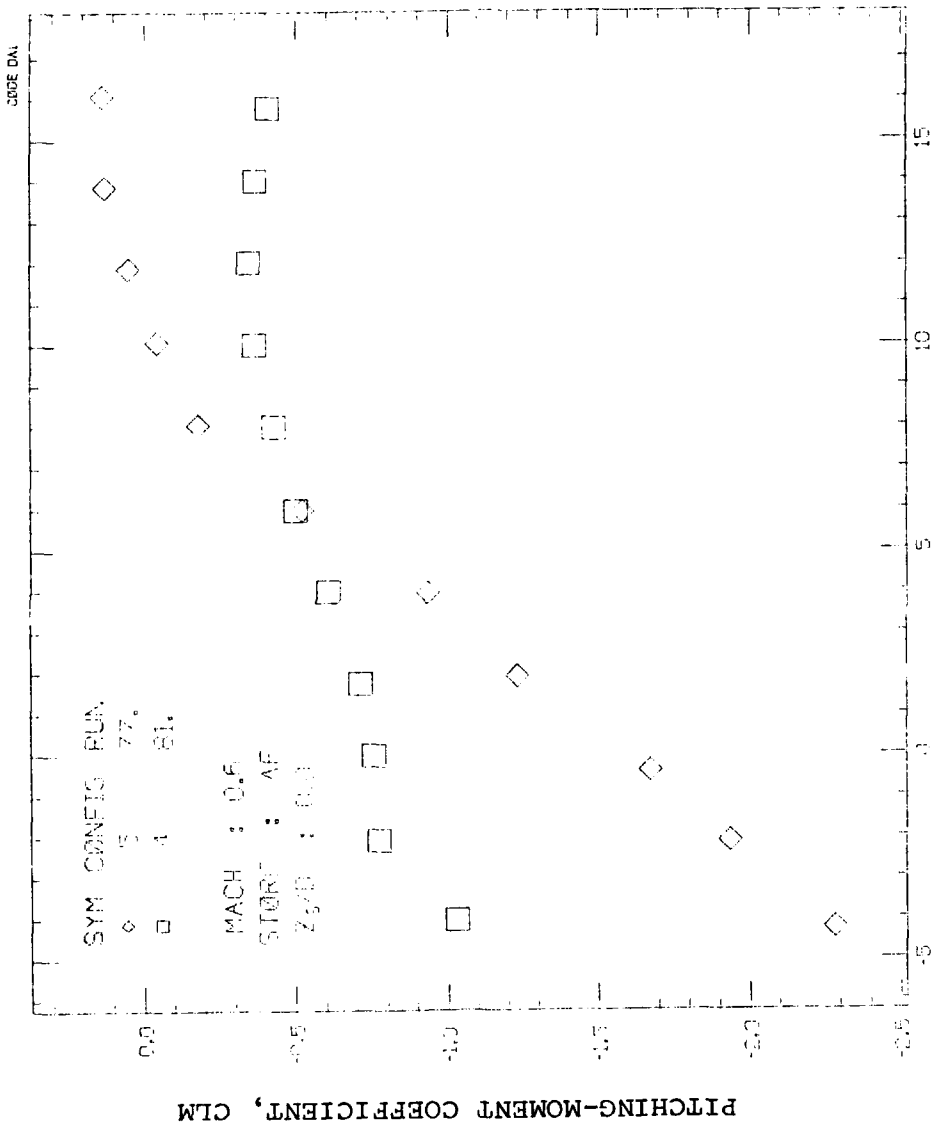

(c) Pitching-moment coefficient.

FIGURE 19. Continued.

AD-A094 751 NIELSEN ENGINEERING AND RESEARCH INC MOUNTAIN VIEW CA F/G 1/1
EXPERIMENTAL AND THEORETICAL STUDY OF FLOW FIELDS AND STORE FOR--ETC(U)
SEP 80 F K GOODWIN, J N NIELSEN N60530-79-C-0169
UNCLASSIFIED NEAR-TR-222 NWC-TP-6210 NL

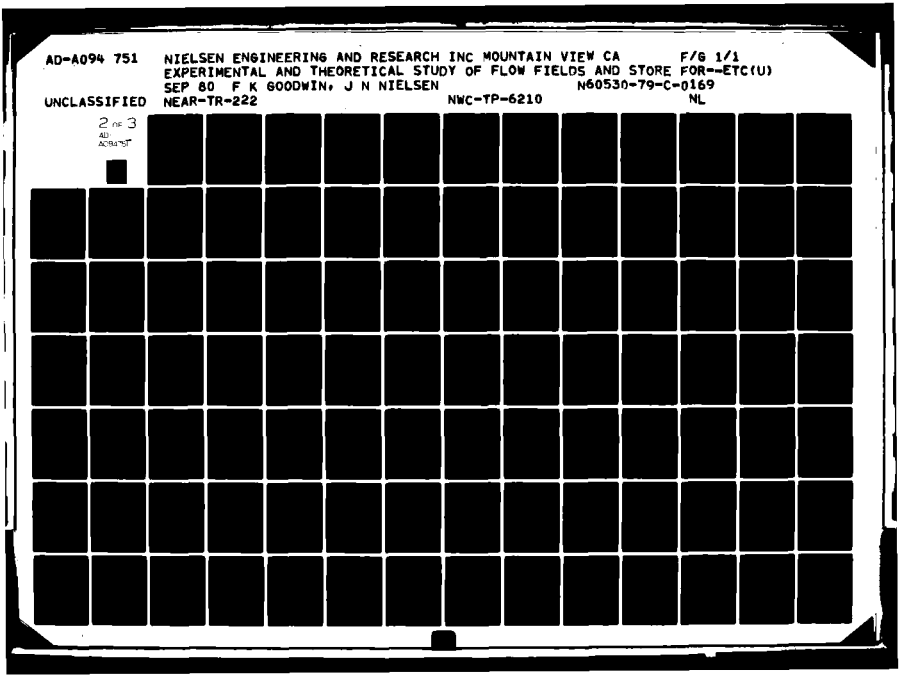

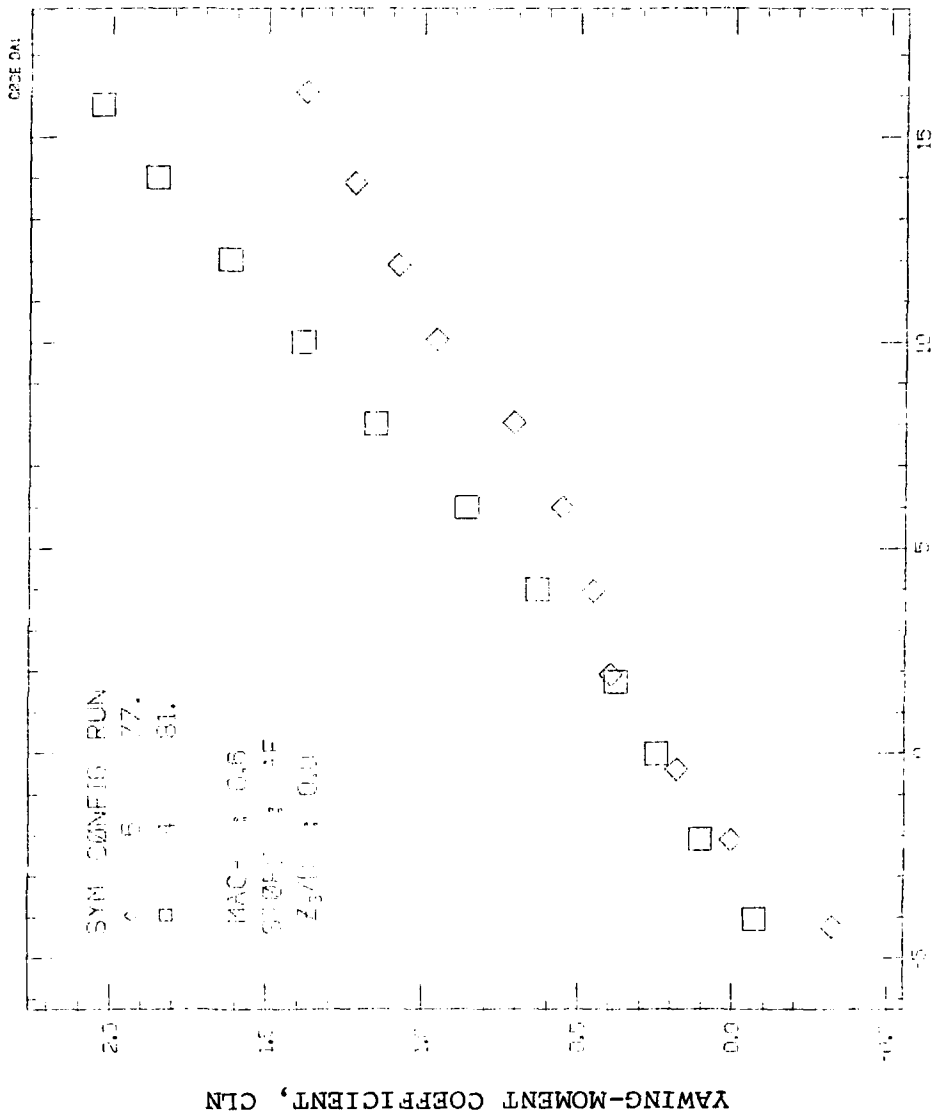

(d) Yawing-moment coefficient.

FIGURE 19. Continued.

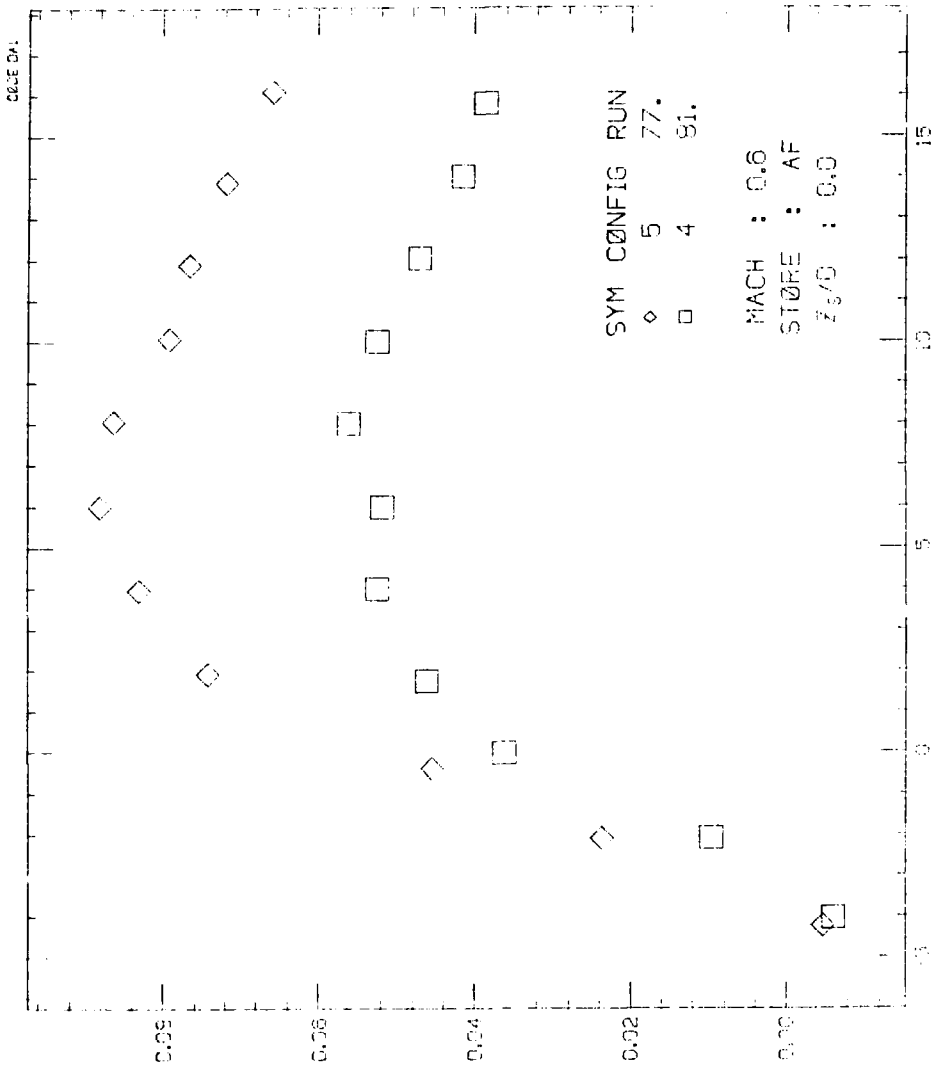

(e) Rolling-moment coefficient.

FIGURE 19. Concluded.

EFFECT OF BOTTOM STORE CONFIGURATION

It is of interest to know how the four stores tested, S_{AF}, S_{AU}, S_{MF}, and S_{MU}, vary in their attached loads. Such results for $M_\infty = 0.6$ are shown in Figure 20 for the stores attached to configuration 6. The stores are all different with respect to normal-force and pitching-moment characteristics. With regard to side-force and yawing-moment coefficients, the finned stores are nearly the same and the unfinned stores are also nearly the same. Significant difference exist between the finned stores with regard to rolling-moment coefficient. The measured rolling moments for the unfinned stores are an indication of the accuracy of the measurements.

DISCUSSION OF GRID LOADS

CONFIGURATION EFFECTS AT $\alpha_s = 0^\circ$

The grid loads on the bottom store as it moves downward from close proximity to the rack are influenced by angle of attack, configuration, Mach number, addition of fins to the shoulder stores, and the number of shoulder stores. Figure 21 shows the loads on store S_{MF} at $M_\infty = 0.6$ as influenced by configuration and store vertical position. Only the first 1.25 diameter of store vertical position are shown.

Examination of the normal-force results shows the least normal force for configuration 2 with a small positive

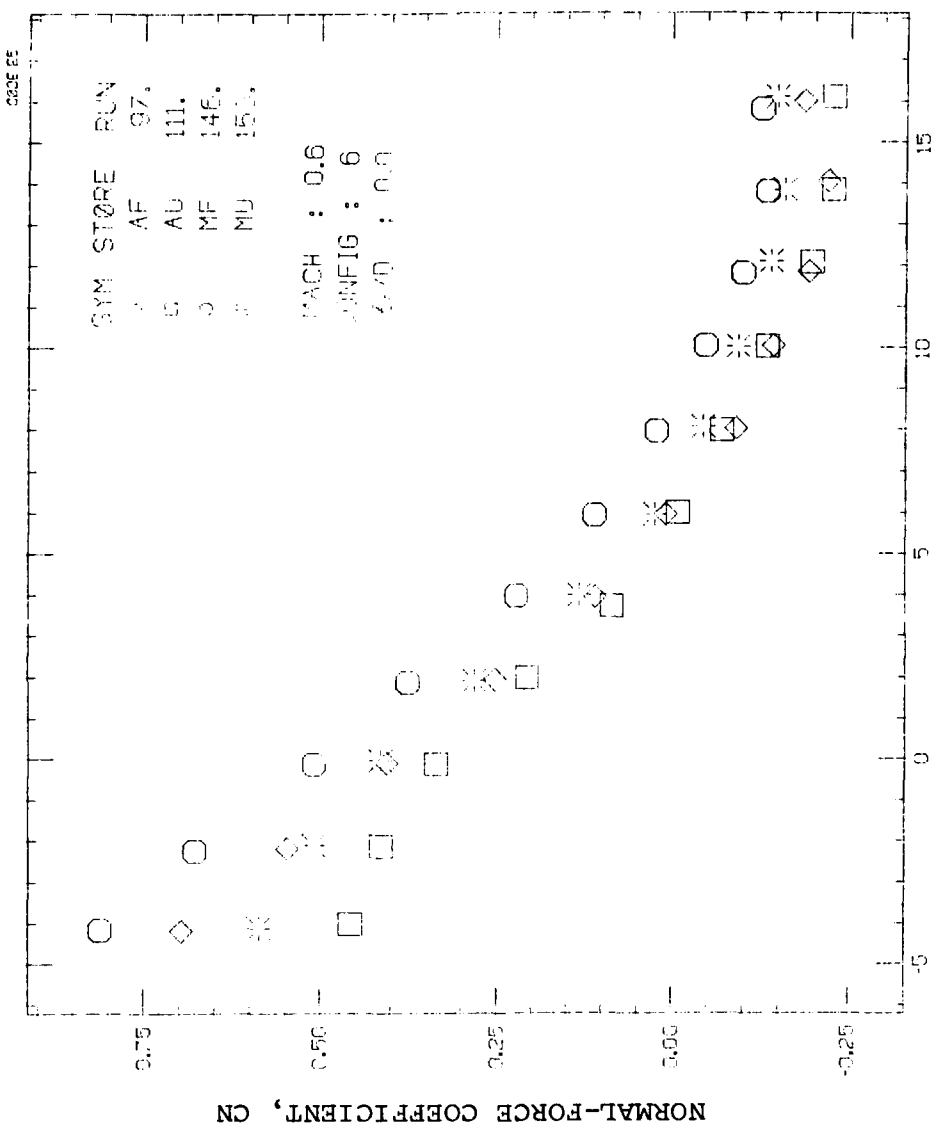

(a) Normal-force coefficient.

FIGURE 20. Dependence of Attached Loads of Bottom Store on Its Configuration for Airplane Configuration 6 at M_∞ = 0.6.

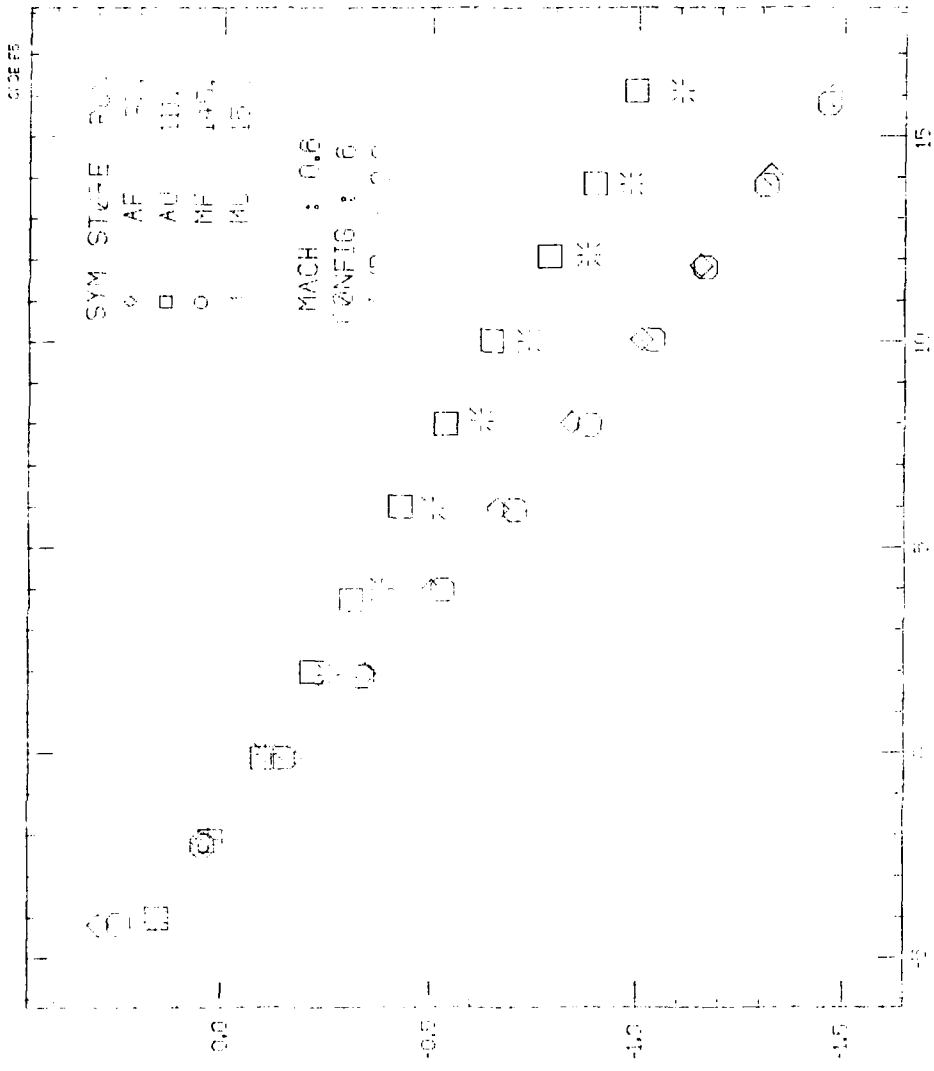

(b) Side-force coefficient.

FIGURE 20. Continued.

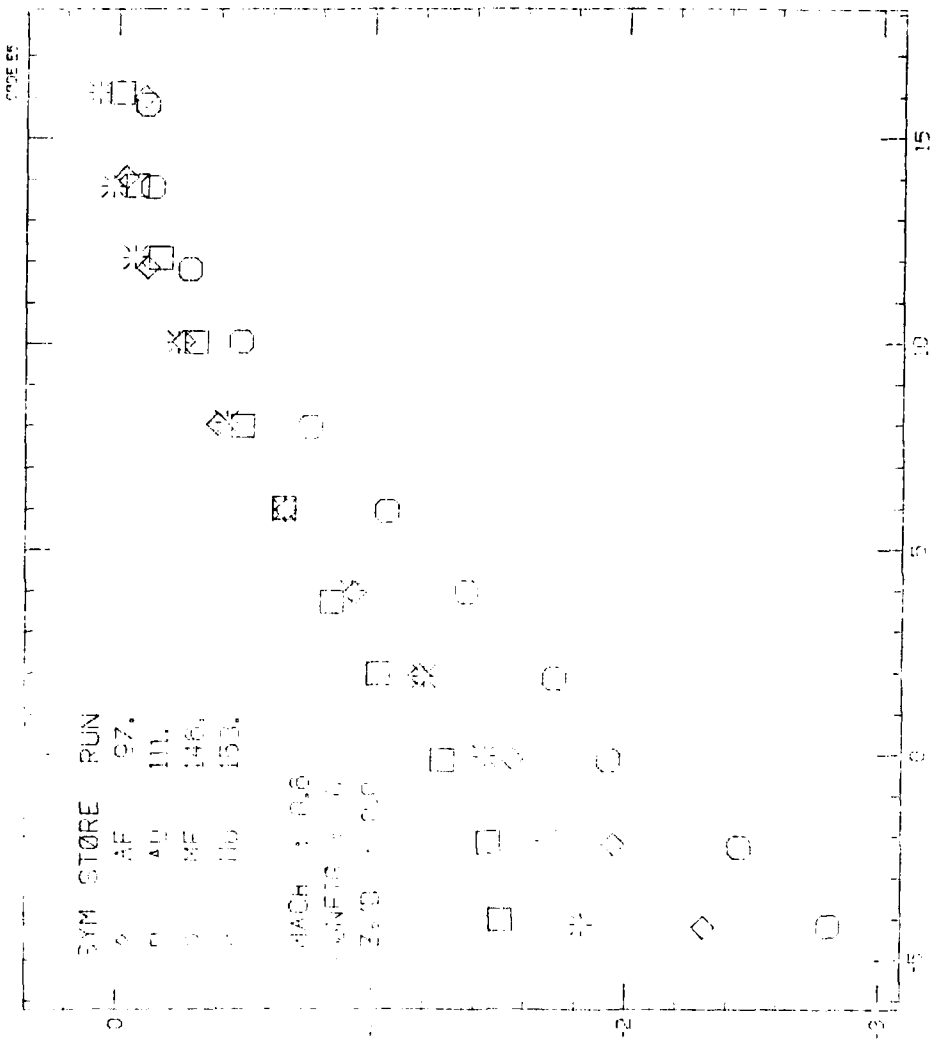

(c) Pitching-moment coefficient.

FIGURE 20. Continued.

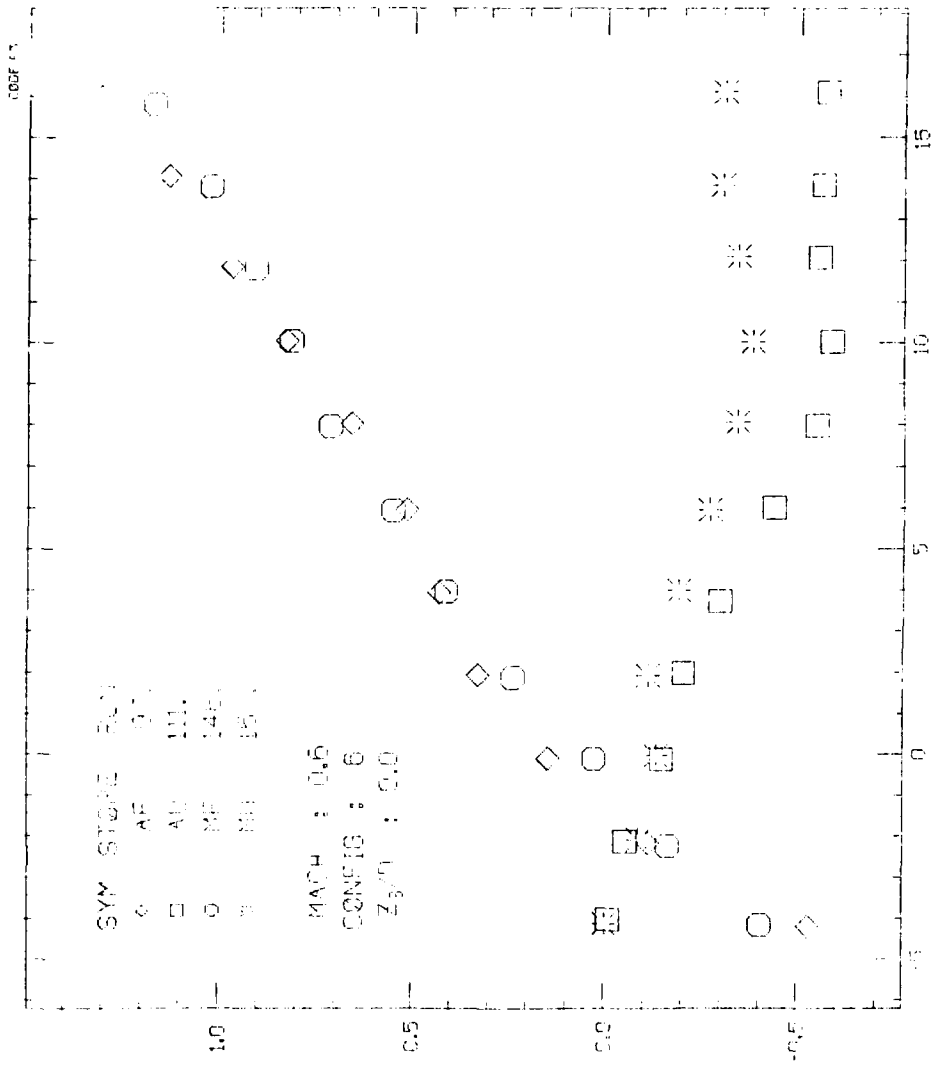

(d) Yawing-moment coefficient.

FIGURE 20. Continued.

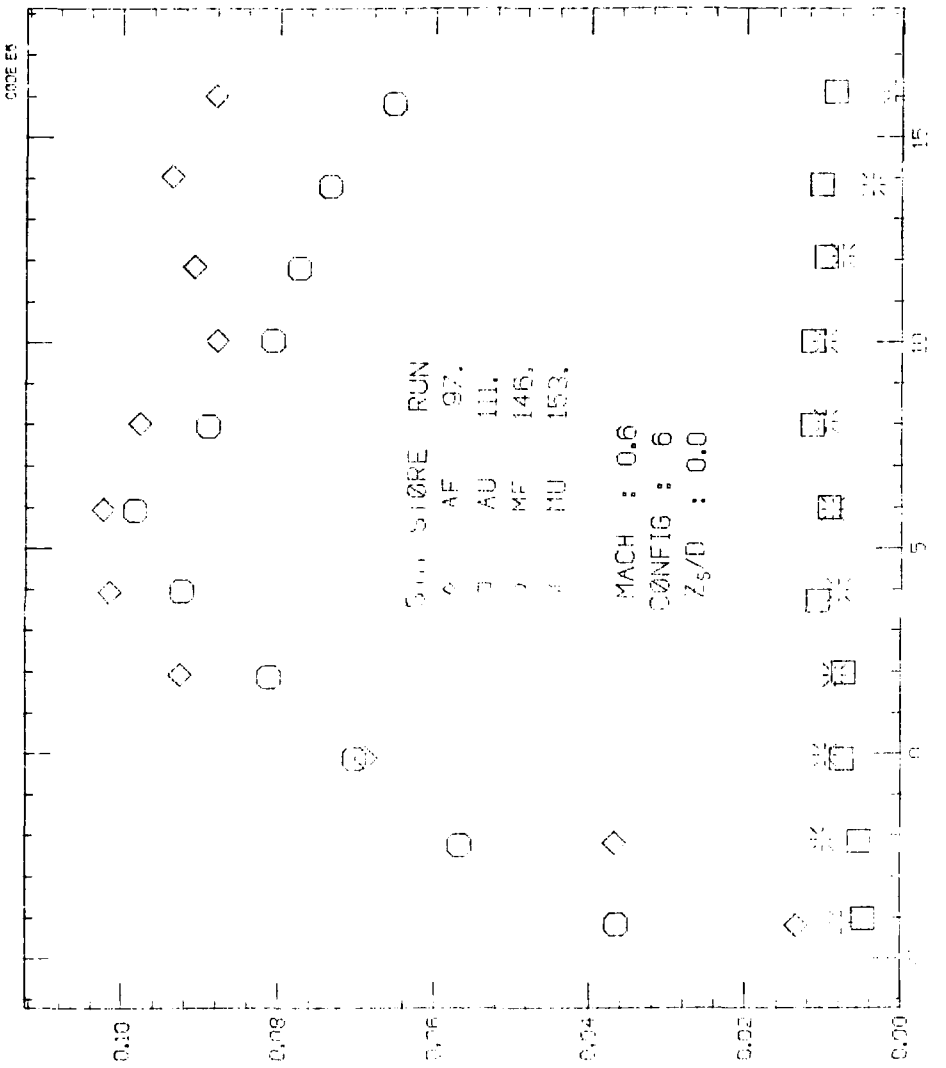

(e) Rolling-moment coefficient.

FIGURE 20. Concluded.

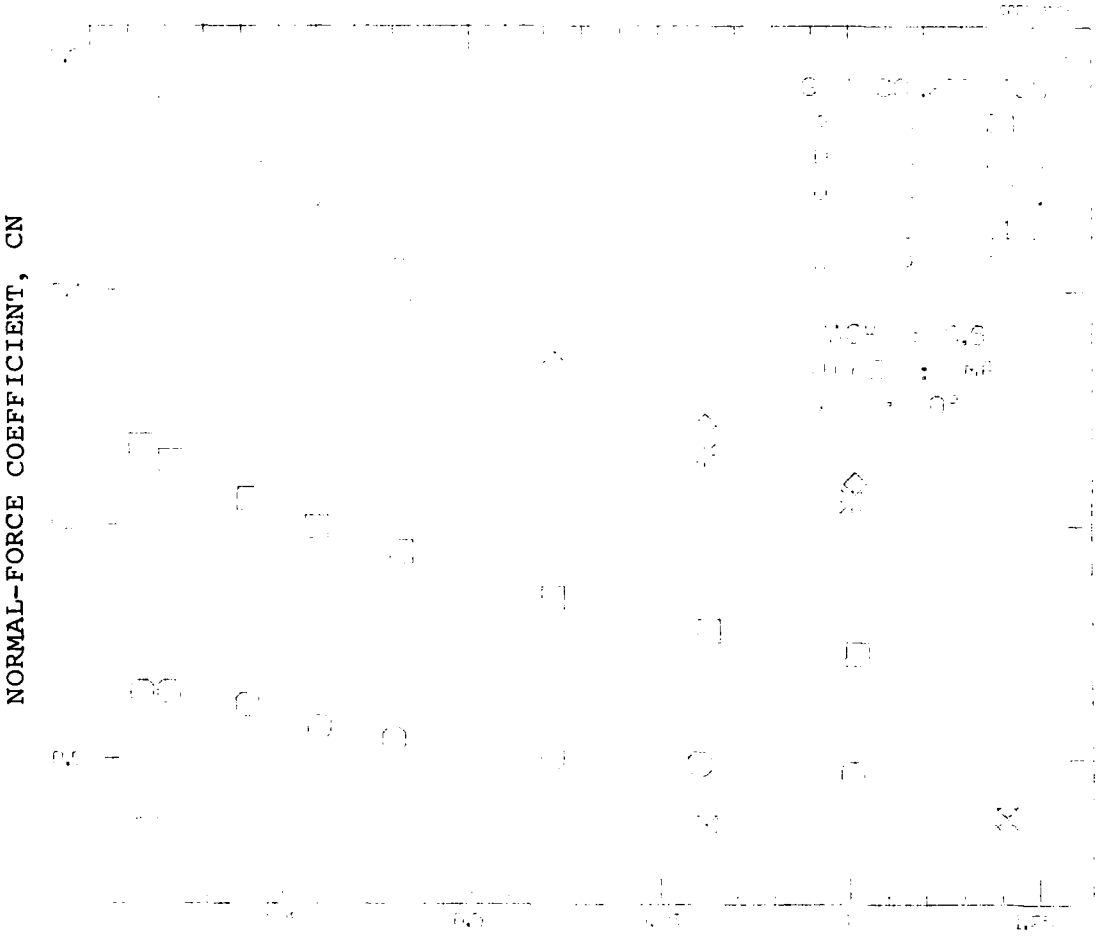

(a) Normal-force coefficient.

FIGURE 21. Grid Loads on Store S_{MF} as Influenced by Airplane Configuration; $M_\infty = 0.6$, $\alpha_s = 0^o$.

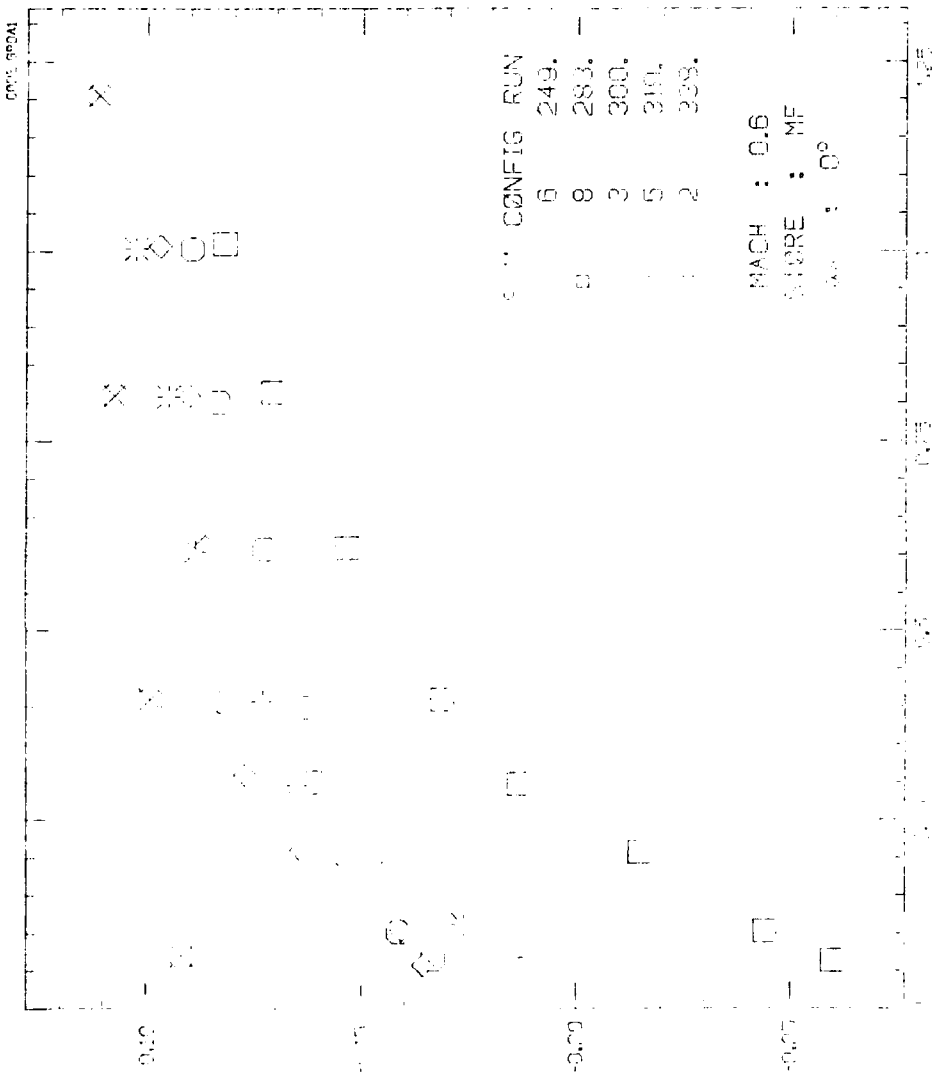

STORE VERTICAL POSITION, Z_p/D

(b) Side-force coefficient.

FIGURE 21. Continued.

(c) Pitching-moment coefficient.

FIGURE 21. Continued.

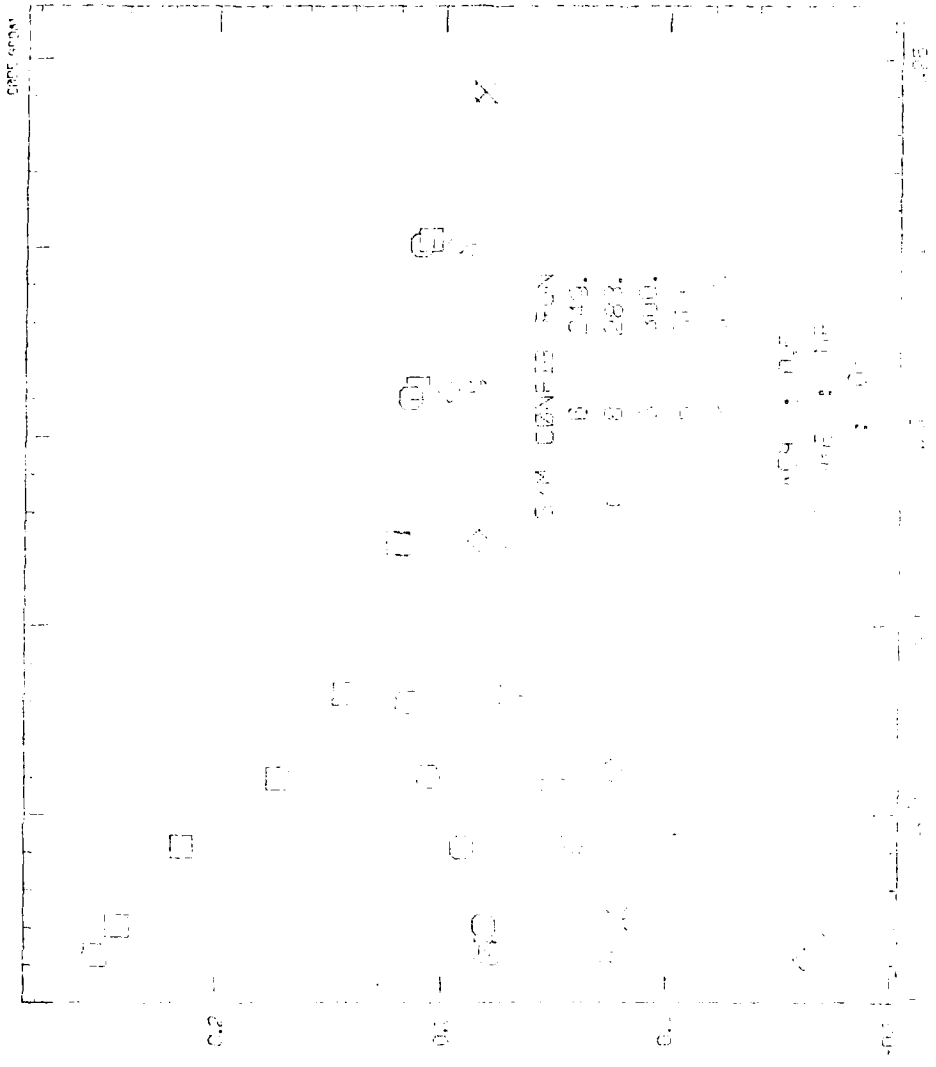

STORE VERTICAL POSITION, Z_p/D

(d) Yawing-moment coefficient.

FIGURE 21. Continued.

(e) Rolling-moment coefficient.

FIGURE 21. Concluded.

increment due to addition of the TER. Addition of one shoulder store contributes positive increments about twice those due to the TER. Addition of the other shoulder store adds an even larger positive increment to the normal force. Addition of the fins to the shoulder stores adds further small positive increments in normal force. We conclude that the addition of the shoulder stores are most important, followed by the addition of the TER, and finally the addition of the fins to the shoulder stores.

The side-force results in Figure 21(b) show that the largest effects of configuration occur at small Z_p/D. The effect of adding the second shoulder store is to almost cancel the increment due to adding the first. The effect of adding fins to the shoulder stores is again fairly small.

The pitching-moment results show the same qualitative effects as the normal-force results. The yawing-moment results show large configuration effects at small Z_p/D (on an expanded scale) and small effects at large Z_p/D. The store alone has a rolling-moment coefficient of .037 at $\alpha_s = 0^o$ because of fin cant. Additional rolling moments of about the same magnitude can be developed at small Z_p/D because of configurational differences. At these small values of Z_p/D increments in CLL as large as 0.01 can be developed by the addition of fins to the shoulder stores. The store alone has rolling-moment coefficients in the range of .026-.037 at $\phi_s = 0^o$ and .026-.040 at $\phi_s = 22.5^o$ for $0^o \leq \alpha_s \leq 8^o$ principally by virtue of the cant of the tail fins. (Note that $\phi_s = 0^o$ corresponds to the X tail roll orientation.)

CONFIGURATION EFFECTS AT $\alpha_s = 8^o$

Figure 22 shows the same kind of data as in Figure 21 except for $\alpha_s = 8^o$ instead of $\alpha_s = 0^o$. The results of Figure 22(a) show that the normal-force coefficient increases as the bottom store moves away from the rack rather than remains constant or decreases as at $\alpha_s = 0^o$. Also the addition of the outboard shoulder store to configuration 3 now reduces the normal force rather than increases it. The effect of adding the fins to the shoulder store affects the bottom store normal force only for small values of Z_p/D.

The side-force coefficients of Figure 22(b) are much higher than those of Figure 22(a), and the effects of configuration changes are generally much less. There is not much qualitative difference in the pitching-moment coefficient behavior at $\alpha_s = 8^o$, Figure 22(c), from that at $\alpha_s = 0^o$. For the yawing-moment coefficient, lower values prevail at $\alpha_s = 8^o$, Figure 22(d), than at $\alpha_s = 0^o$, with some qualitative differences in behavior. The peak rolling-moment coefficients at $\alpha_s = 8^o$ do not exceed those at $\alpha_s = 0^o$ by much.

With regard to the effect of adding fins to the shoulder stores on the results, compare configurations 5 and 6 in Figure 22. Adding the fins generally causes a small but significant effect at small values of Z_p/D. The effect is usually much smaller than that due to adding the shoulder stores to the rack.

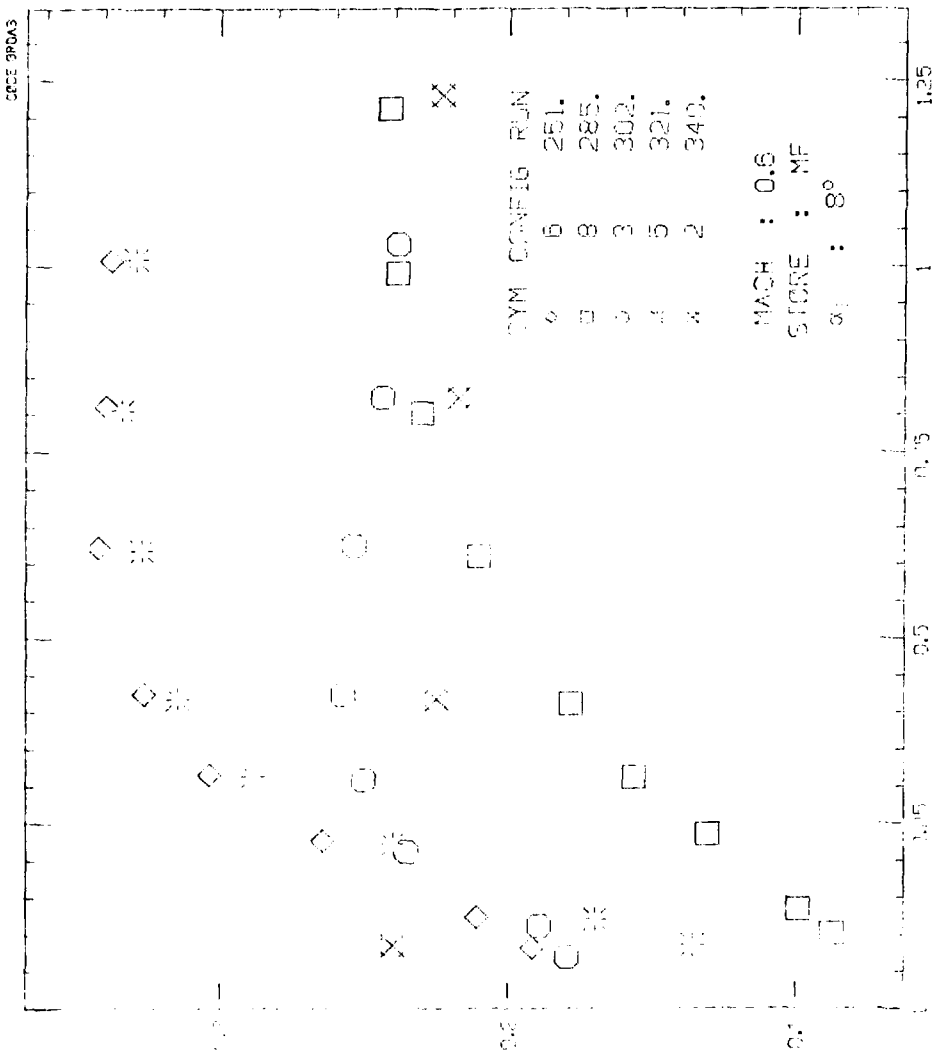

(a) Normal-force coefficient.

FIGURE 22. Grid Loads on Store SMF as Influenced by Airplane Configuration; $M_\infty = 0.6$, $\alpha_s = 8^o$.

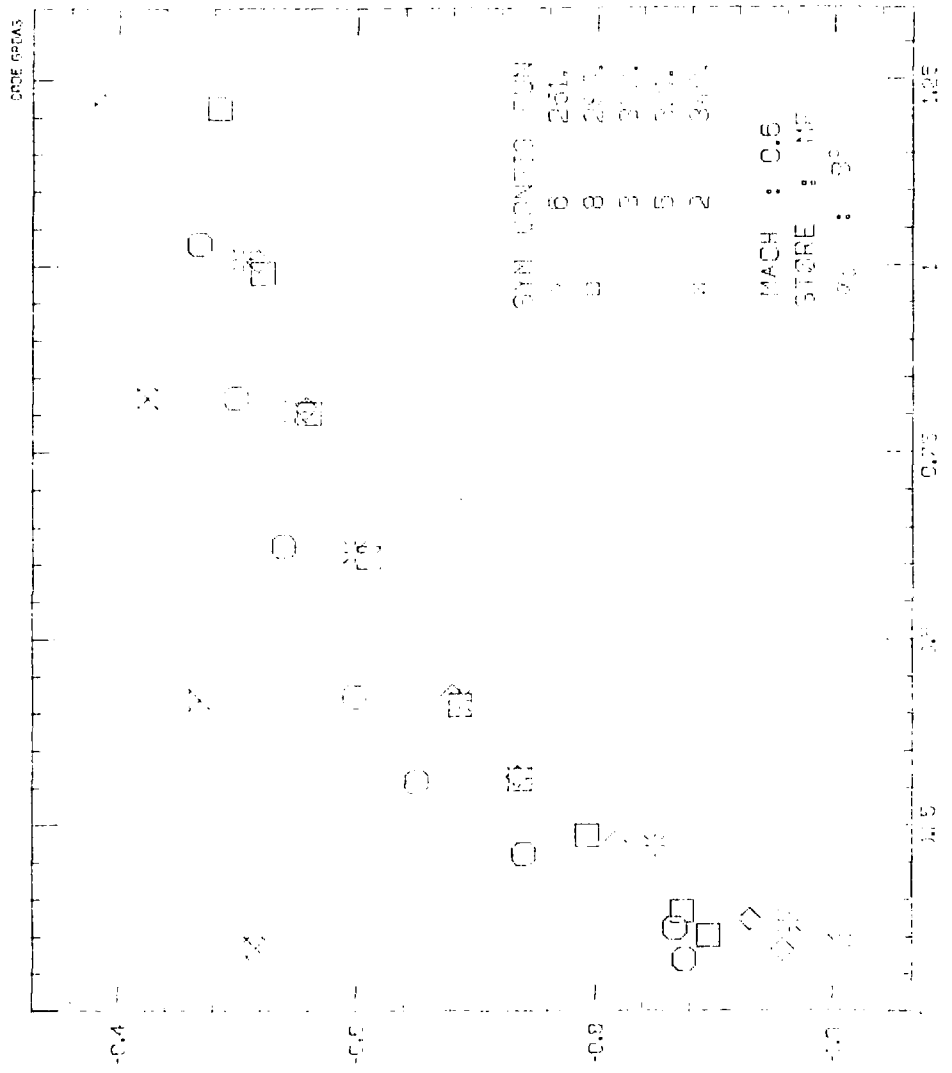

(b) Side-force Coefficient.

FIGURE 22. Continued.

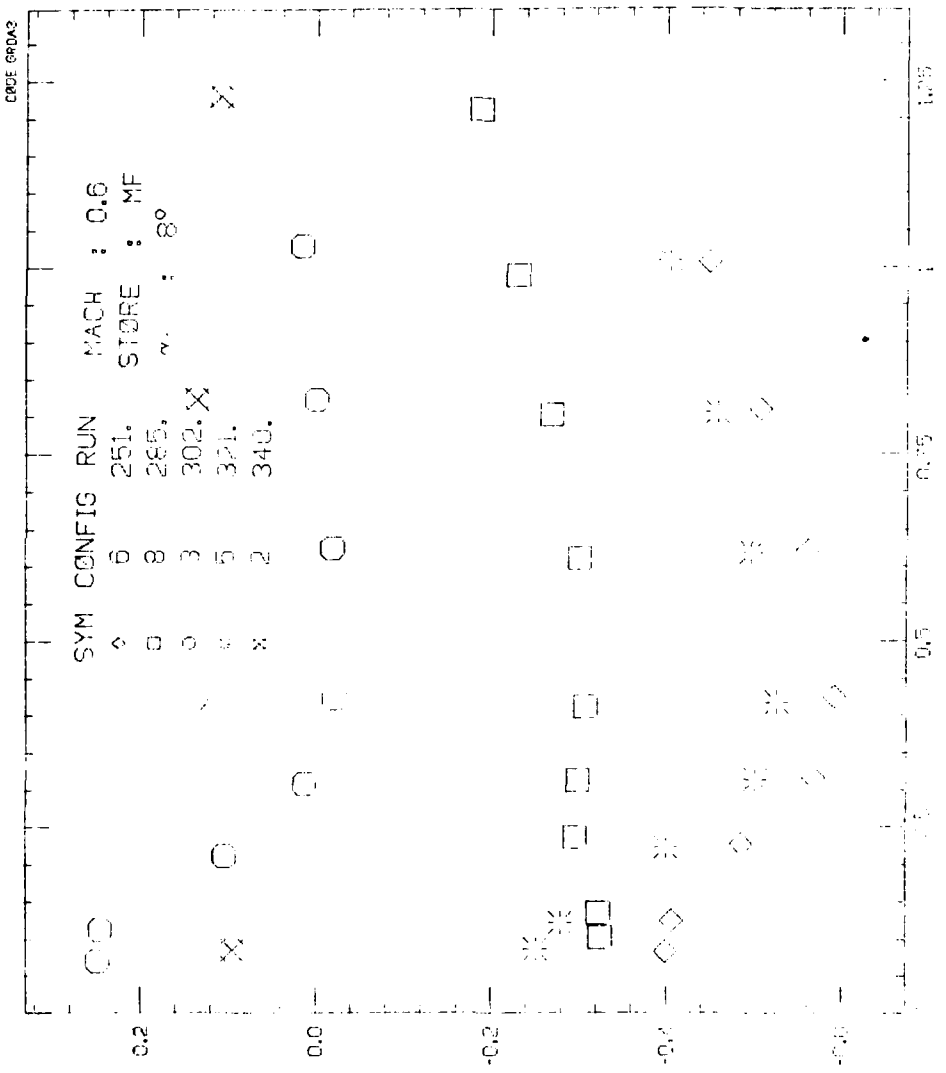

(c) Pitching-moment coefficient.

FIGURE 22. Continued.

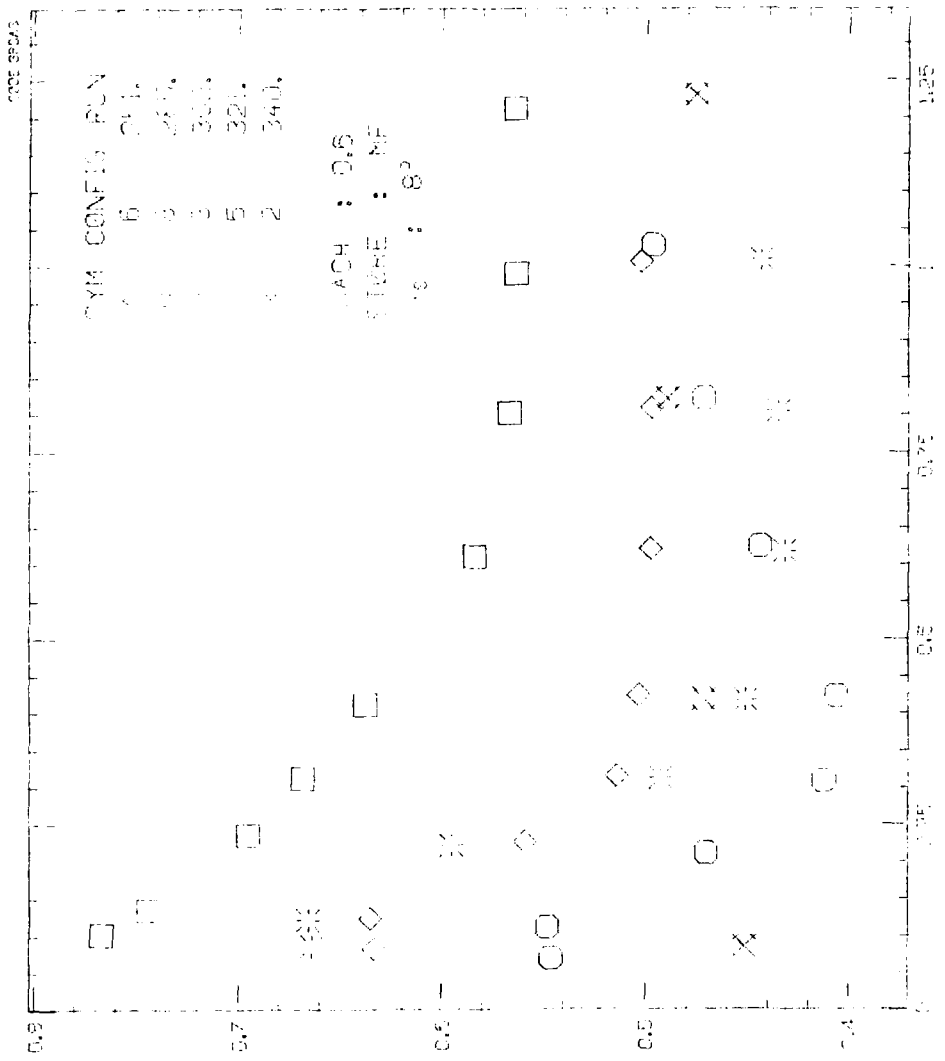

YAWING-MOMENT COEFFICIENT, CLN

STORE VERTICAL POSITION, Z_p/D

(d) Yawing-moment coefficient.

FIGURE 22. Continued.

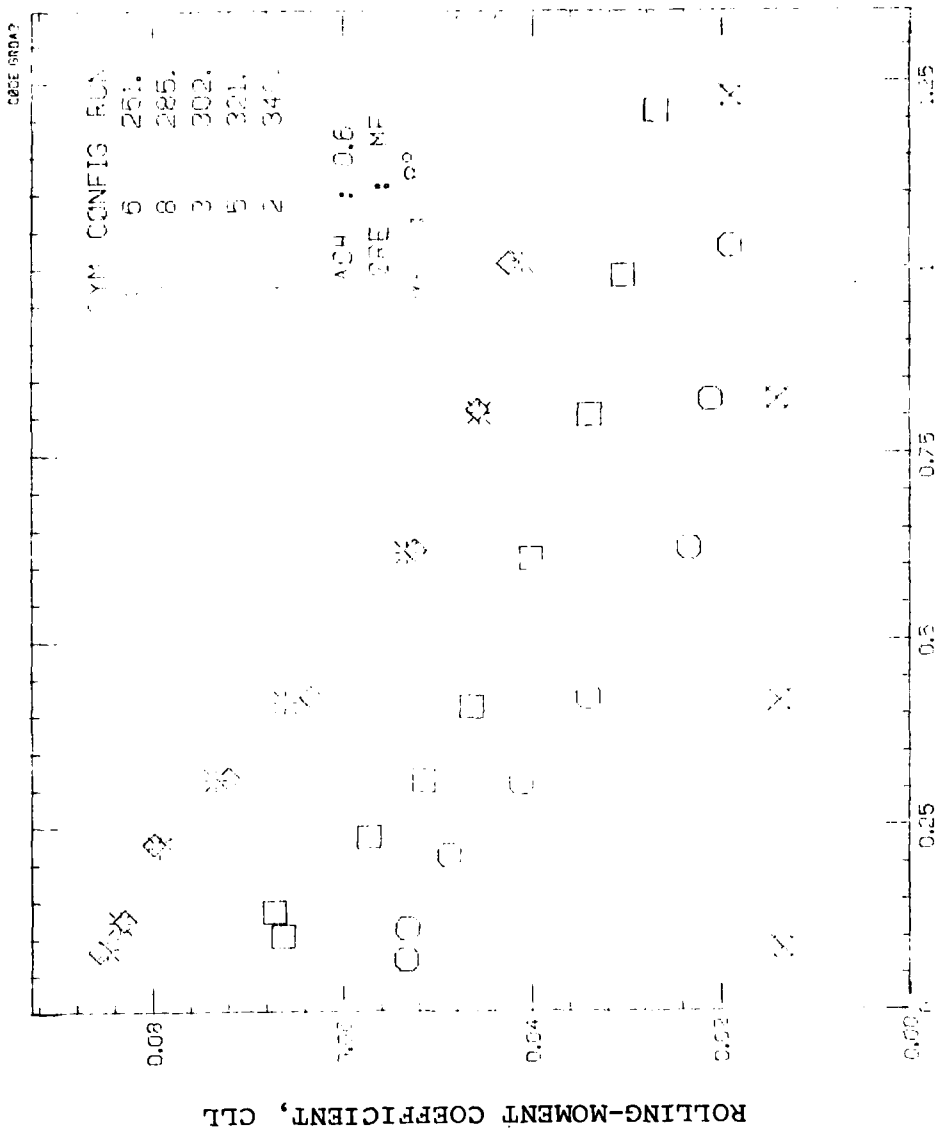

(e) Rolling-moment coefficient.

FIGURE 22. Concluded.

EFFECT OF MACH NUMBER

The effects of Mach number on the grid loads of bottom store S_{MF} are shown in Figure 23 for configuration 6 at $\alpha_s = 0^o$. The effects of Mach number on normal-force coefficient are not large for $M_\infty = 0.6$-0.8, for the entire range of Z_p/D. At low values of this parameter, the spread between the $M_\infty = 0.6$ and 0.95 data becomes fairly significant. This result also is true of the attached load data seen in Figure 17(a) for the same test conditions but for store S_{AF}.

The side-force results of Figure 23(b) show small effects of Mach number for all values of Z_p/D, when the expanded scale on the figure is taken into consideration. The pitching-moment results of Figure 23(c) show a systematic effect of Mach number. The data on yawing moment show little effect of Mach number at high values of Z_p/D, but at low values the data for $M_\infty = 0.6$, 0.7, and 0.8 form one trend and those for 0.9 and 0.95 another trend. The rolling moment data all show the same trend with Z_p/D with secondary variations due to M_∞.

It is of interest to contrast the effect of Mach number on the loads at $\alpha_s = 8^o$ shown in Figure 24 with those at $\alpha_s = 0^o$ shown in Figure 23. The effects of M_∞ at $\alpha_s = 8^o$ on normal-force coefficient are about the same magnitude as they are at $\alpha_s = 0^o$. The effects of Mach number on side-force coefficient at $\alpha_s = 8^o$ are proportionally about the same as at $\alpha_s = 0^o$, but the increments are much larger since the side-force coefficients are much larger.

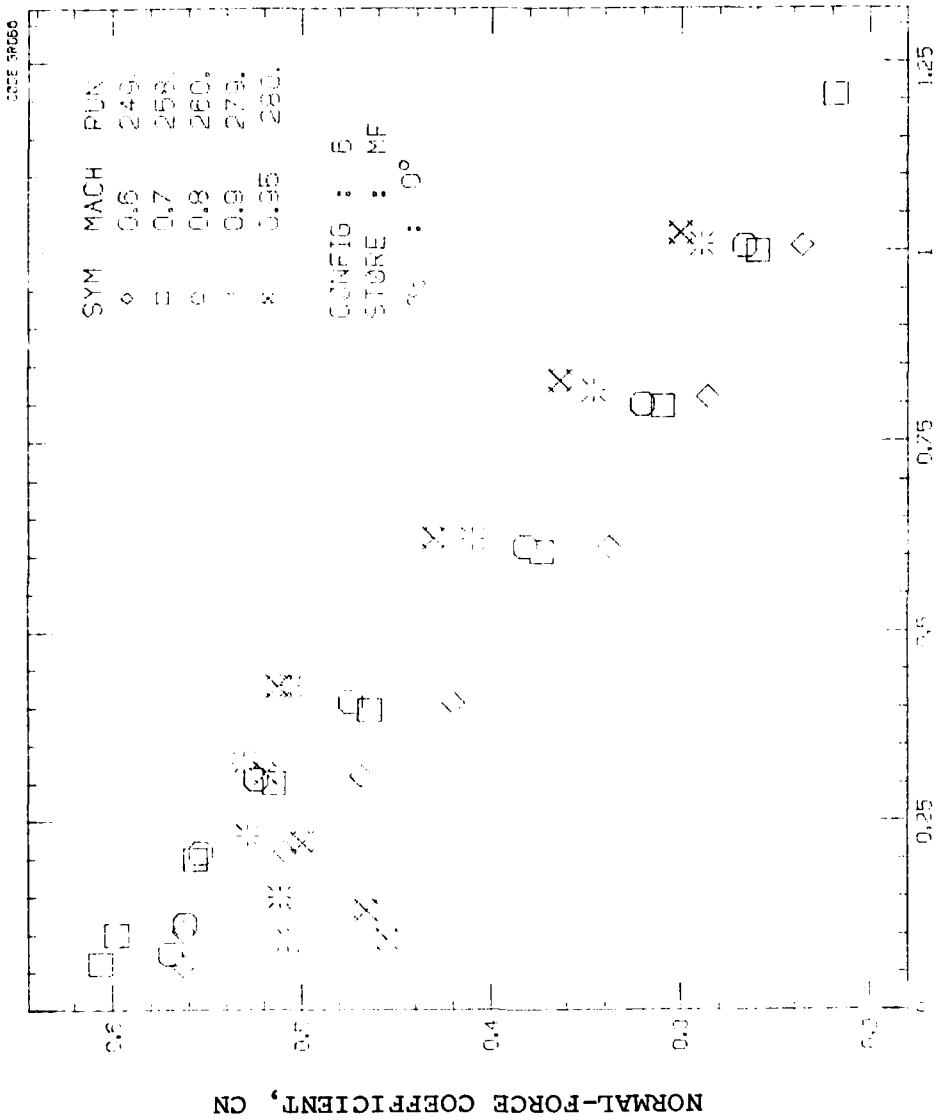

FIGURE 23. Grid Loads on Store S_{MF} as Influenced by Mach Number; Configuration 6, $\alpha_s = 0^0$.

(a) Normal-force coefficient.

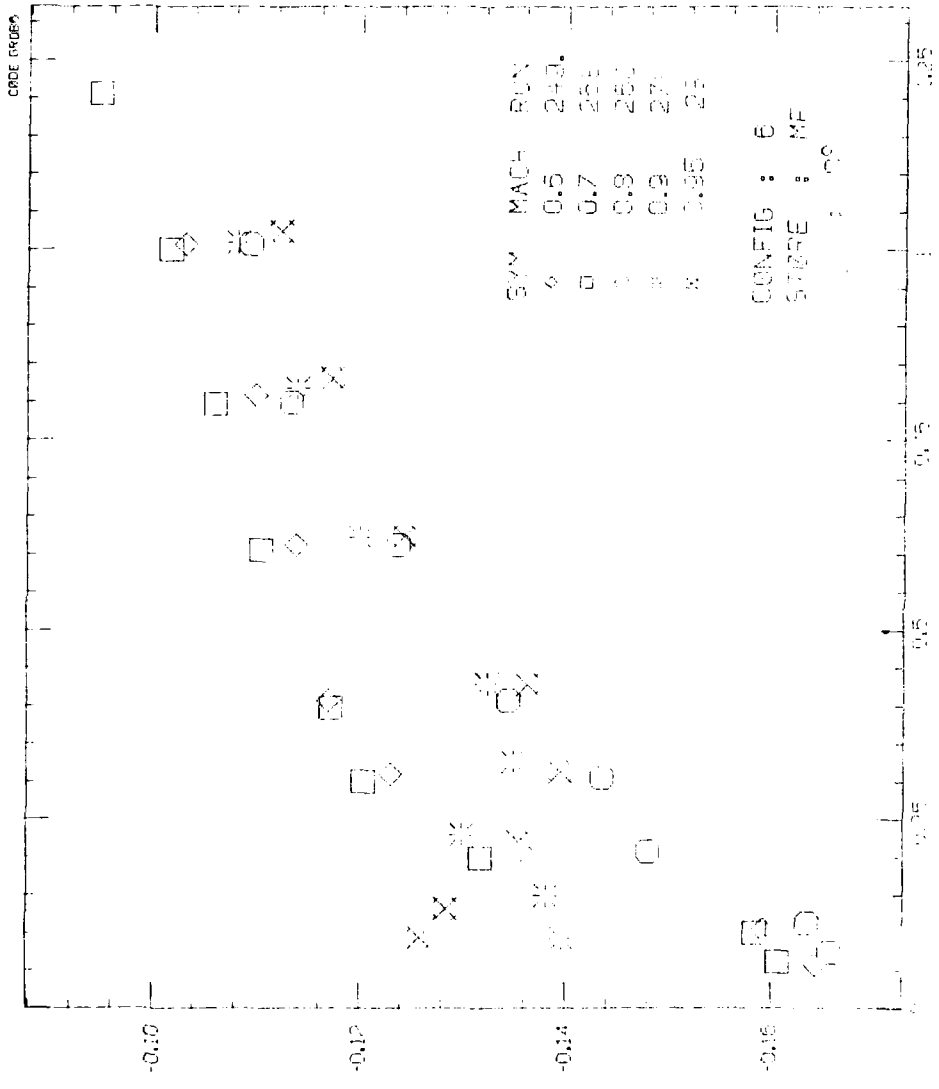

(b) Side-force coefficient.

FIGURE 23. Continued.

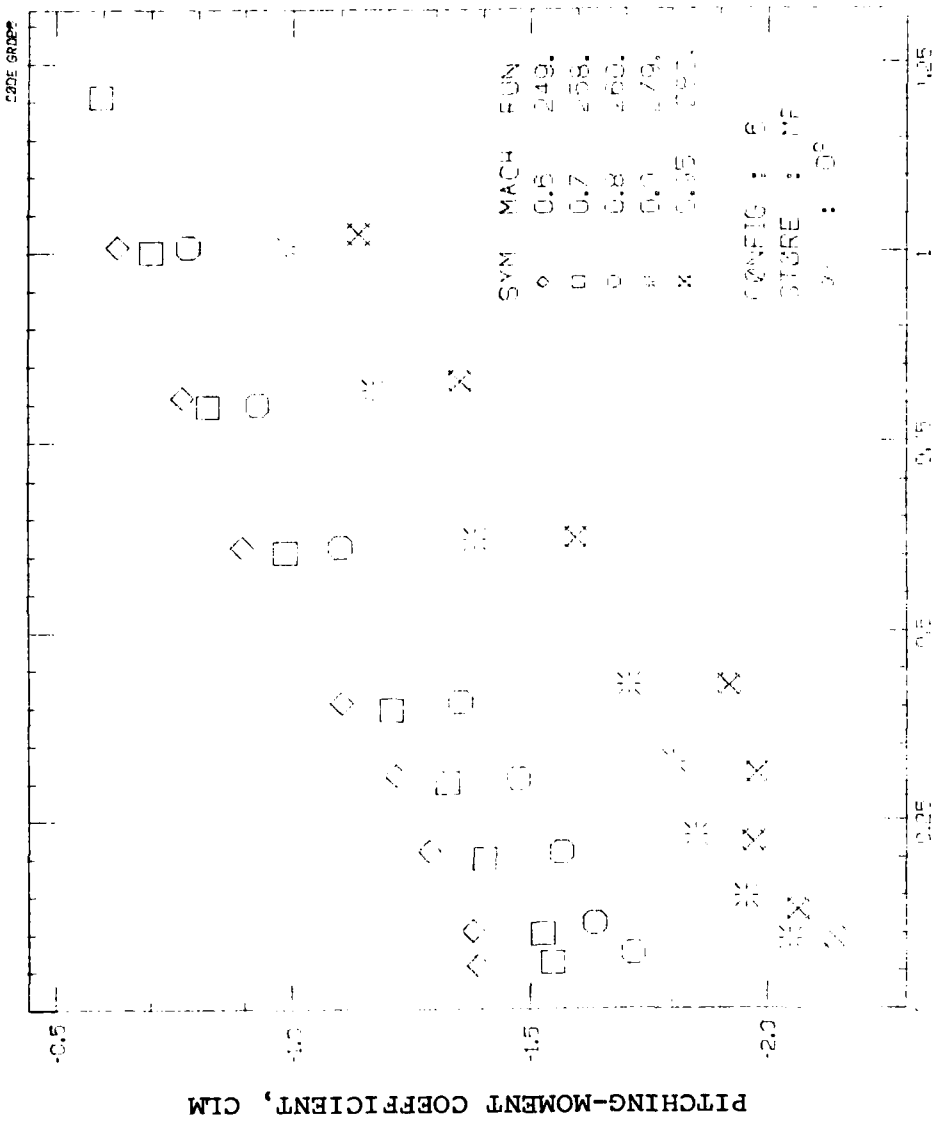

(c) Pitching-moment coefficient.

FIGURE 23. Continued.

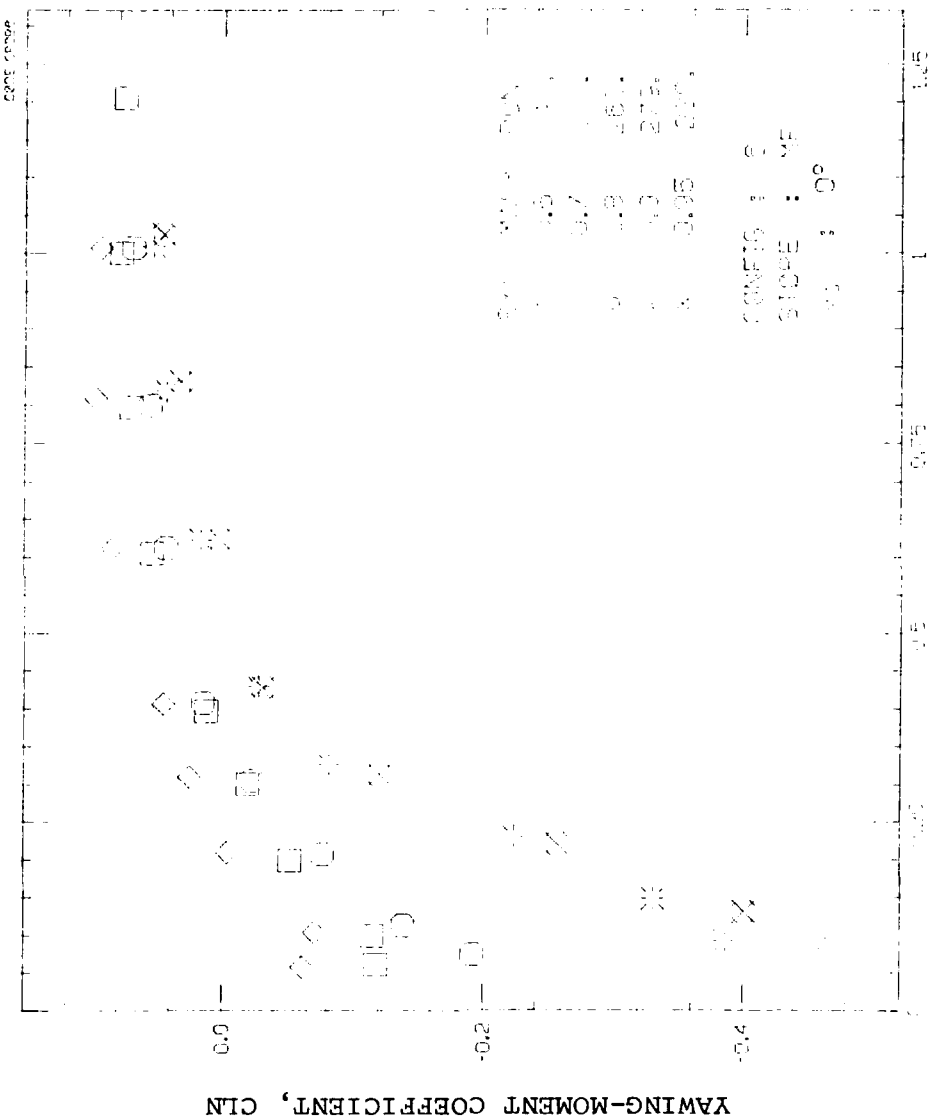

(d) Yawing-moment coefficient.

FIGURE 23. Continued.

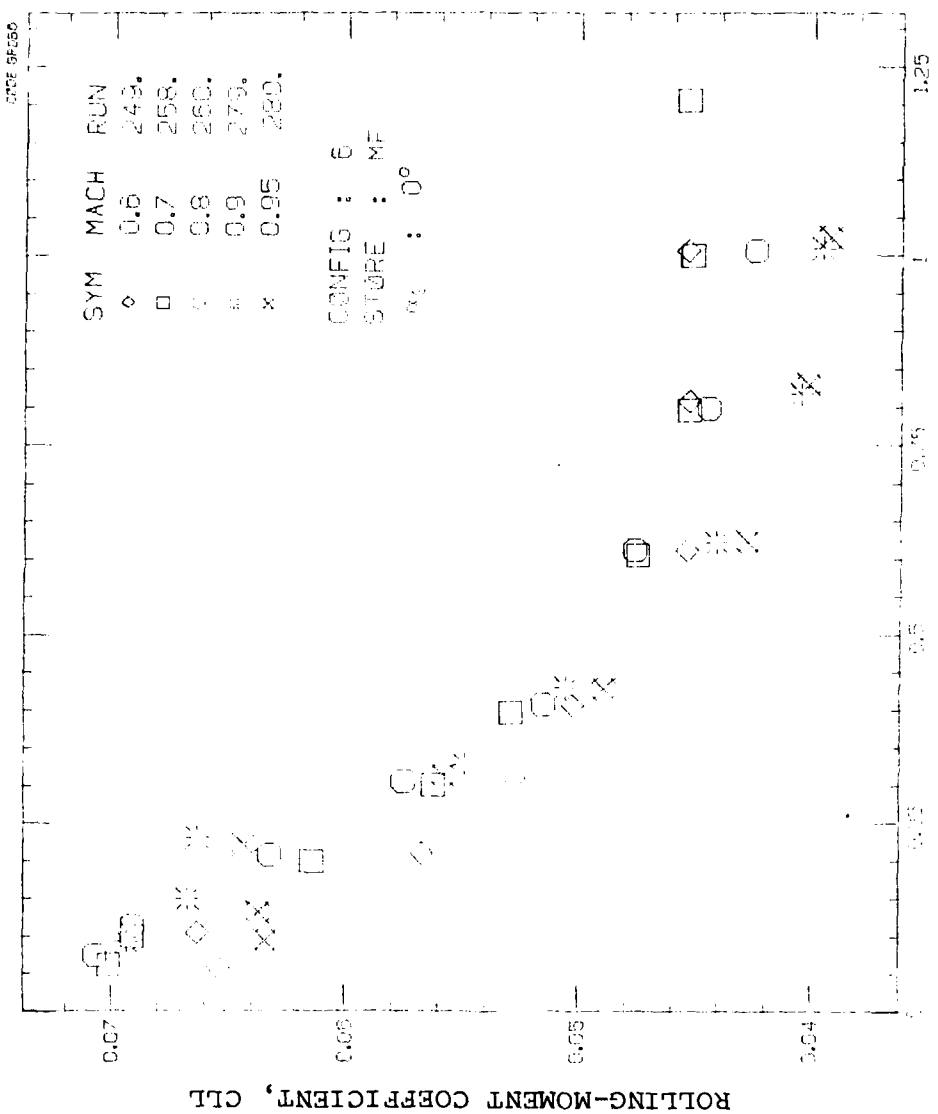

ROLLING-MOMENT COEFFICIENT, CLL

STORE VERTICAL POSITION, Z_p/D

(e) Rolling-moment coefficient.

FIGURE 23. Concluded.

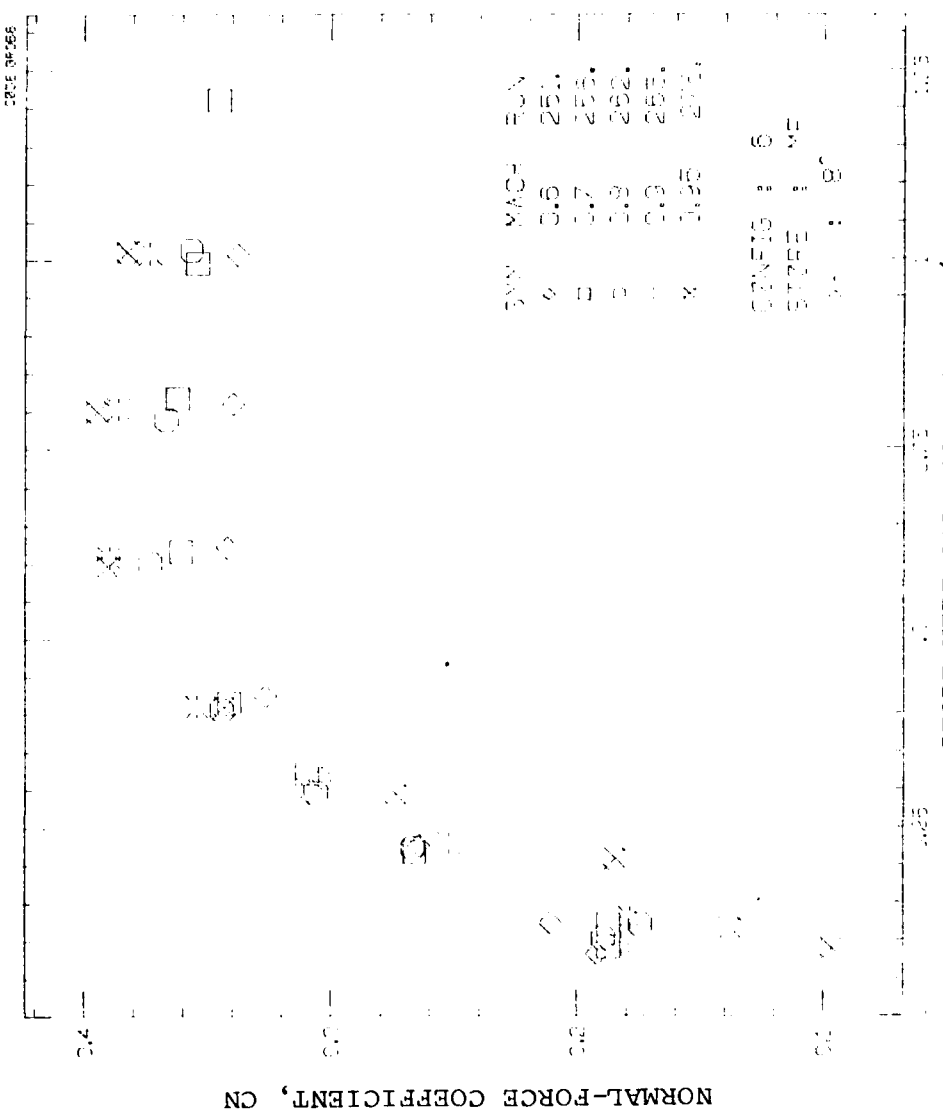

FIGURE 24. Grid Loads for Store S_{MF} as Influenced by Mach Number; Configuration 6, $\alpha_s = 8^{\circ}$.

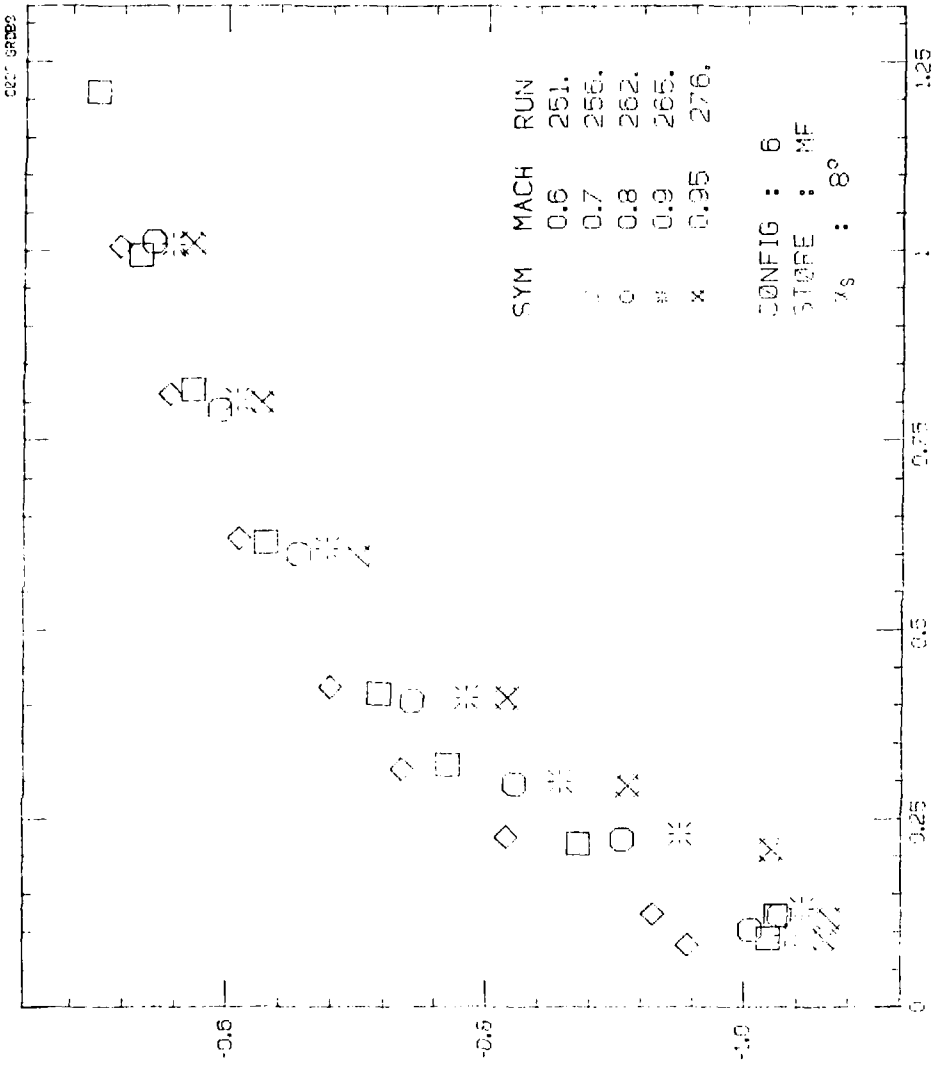

(b) Side-force coefficient.

FIGURE 24. Continued.

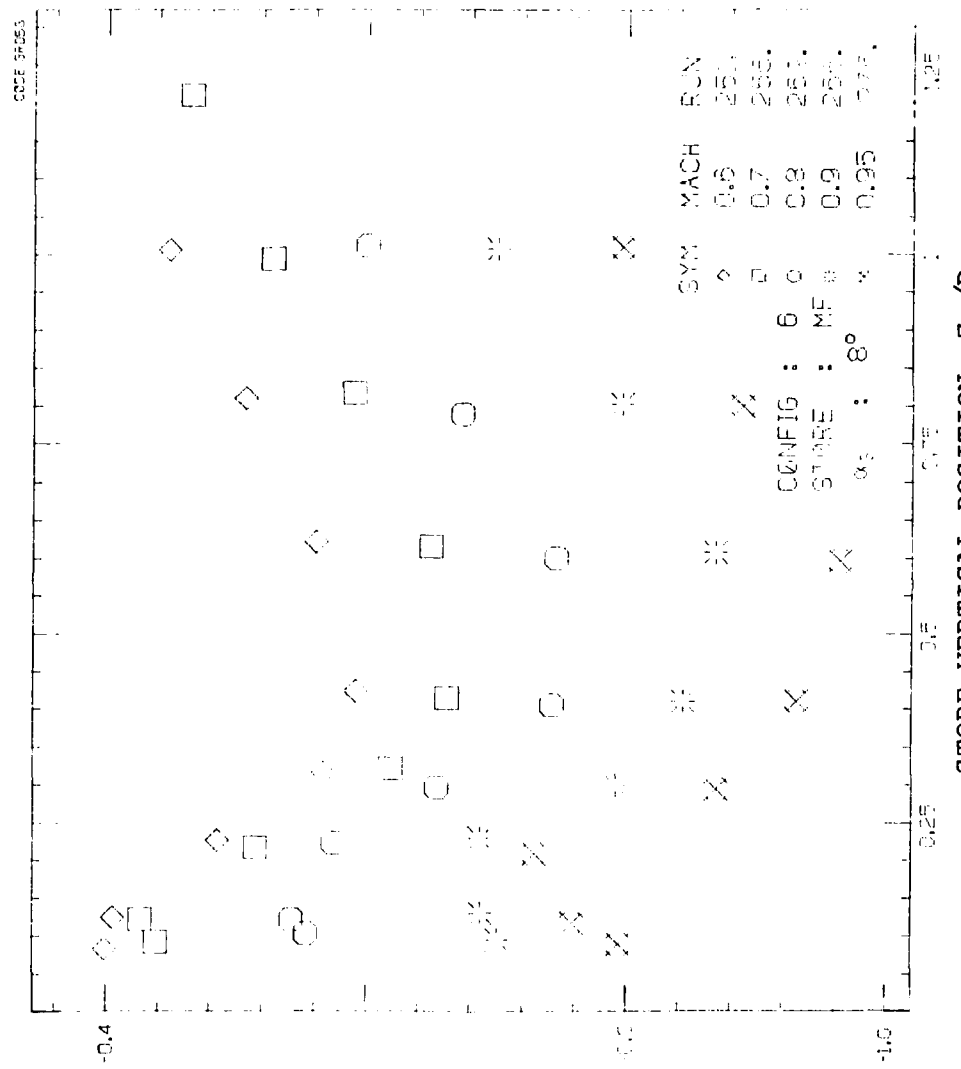

STORE VERTICAL POSITION, Z_P/D

(c) Pitching-moment coefficient.

FIGURE 24. Continued.

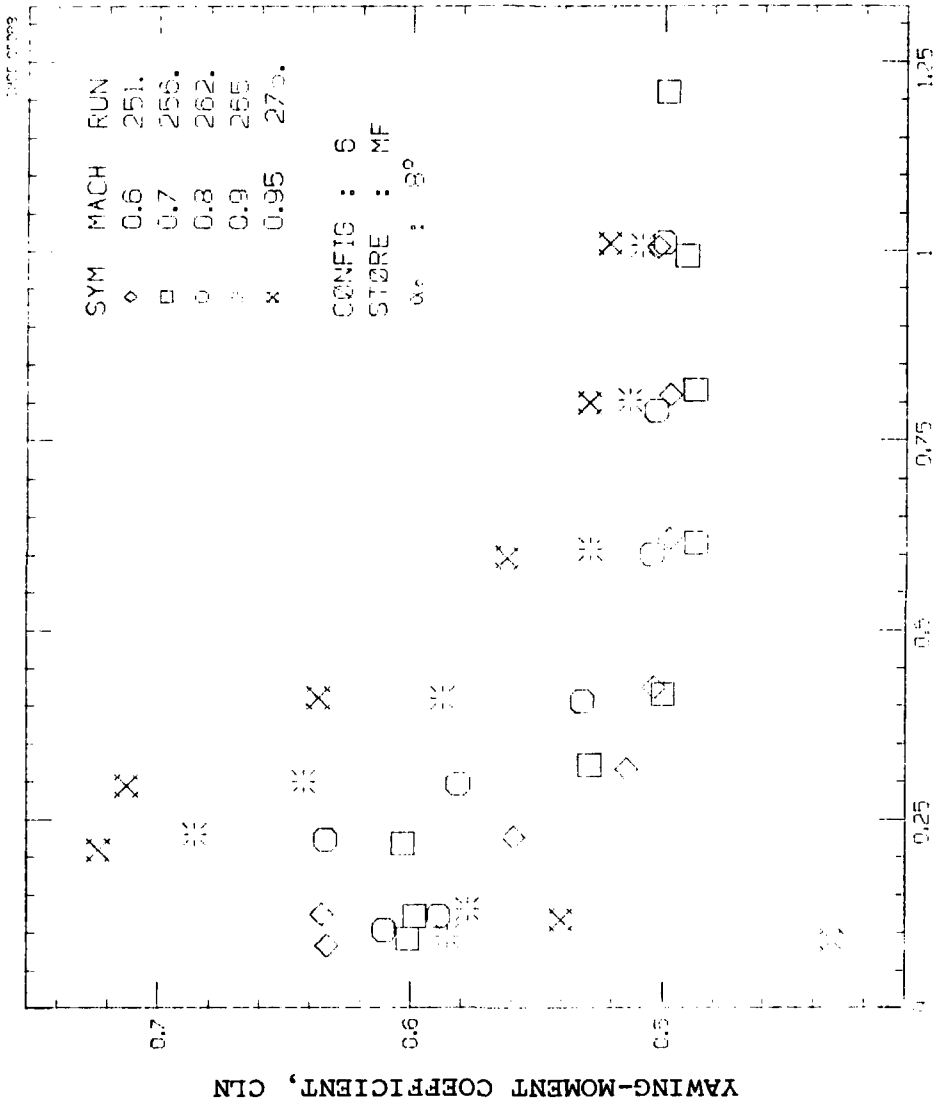

(d) Yawing-moment coefficient.

FIGURE 24. Continued.

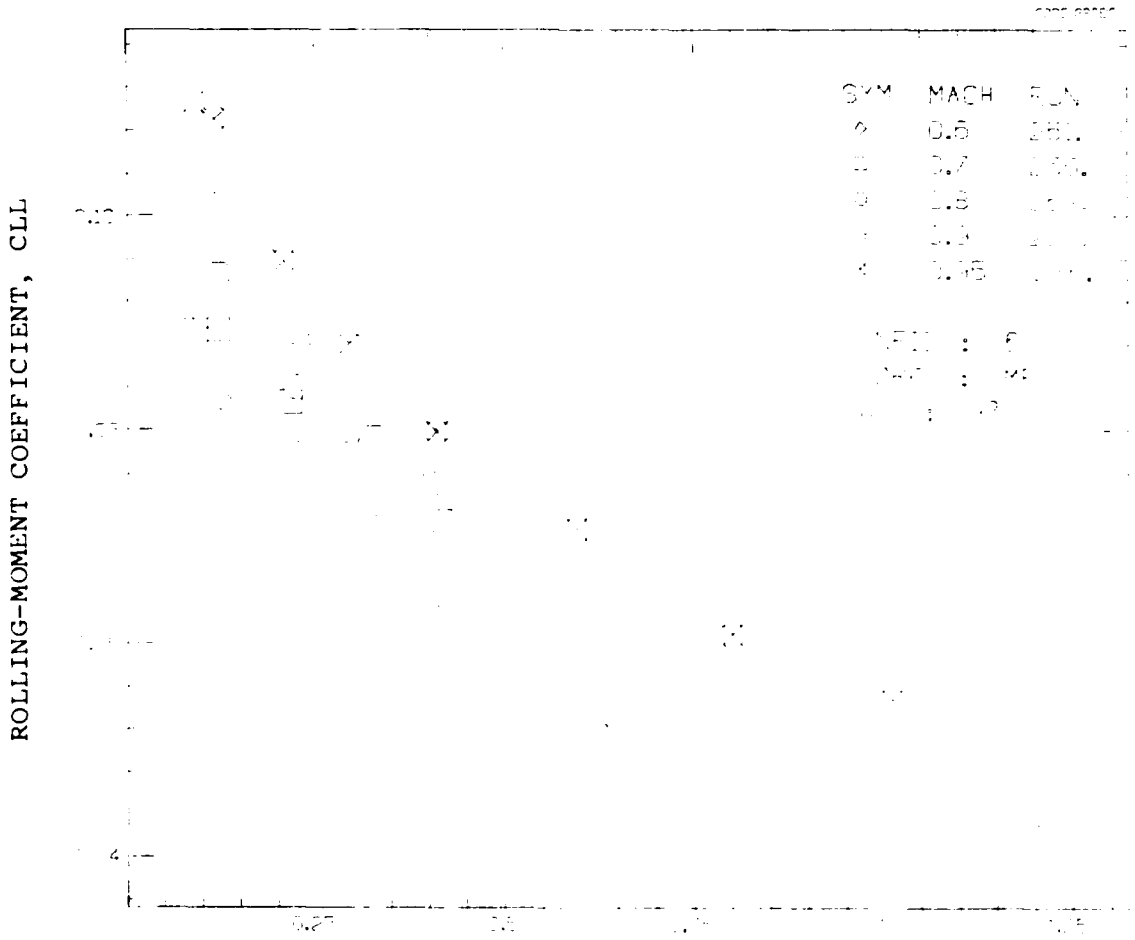

(e) Rolling-moment coefficient.

FIGURE 24. Concluded.

A systematic effect of M_∞ on the pitching-moment coefficient is manifest at $\alpha_s = 8^o$ just as at $\alpha_s = 0^o$ but the qualitative effect of Z_p/D is different in the two cases. The yawing-moment qualitative variation with Z_p/D is quite different at $\alpha_s = 8^o$ than at $\alpha_s = 0^o$. The effects of M_∞ on the data are least for $M_\infty = 0.6$-0.8 and larger for $M_\infty = 0.8$-0.95. As at $\alpha_s = 0^o$, the trend of rolling-moment coefficient with Z_p/D at $\alpha_s = 8^o$ dominates the behavior with a secondary effect of M_∞ superimposed on the Z_p/D trend.

EFFECT OF ADDING FINS TO SHOULDER STORES

It is a complication to model the shoulder store fins in the computer program. It is therefore of interest to see what is lost in accuracy by not doing so. A measure of the inaccuracies incurred can be obtained by comparing the loads on the bottom store at identical positions in configurations 5 and 6. These data for S_{MF} at $\alpha_s = 0^o$ are shown in Figure 25 for $M_\infty = 0.6$. The fin effects on normal-force coefficient are a maximum of about 10 percent at small Z_p/D. The maximum fin effect on side force coefficient is about .02, also at very low Z_p/D. There is about a maximum 10 percent effect on pitching-moment coefficient. The yawing-moment coefficients are quite small being both negative and positive. An error of about 0.1 in the coefficient occurs at very low values of Z_p/D. At low Z_p/D the rolling-moment coefficient difference is about 0.01.

It is of interest to look at other cases to see the effect of adding the fins to the shoulder stores as

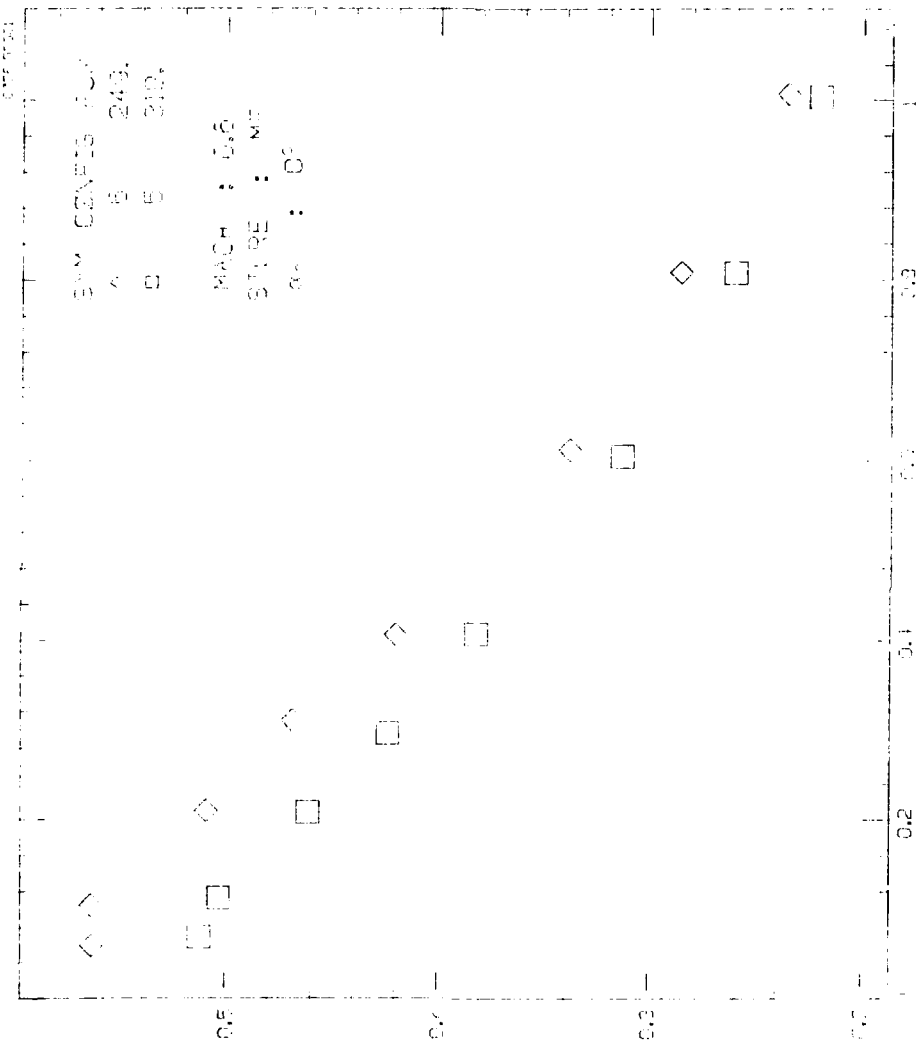

(a) Normal-force coefficient.

FIGURE 25. Grid Loads on Store S_{MF} as Influenced by Addition of Fins to Shoulder Stores; $M_\infty = 0.6$, $\alpha_s = 0^0$.

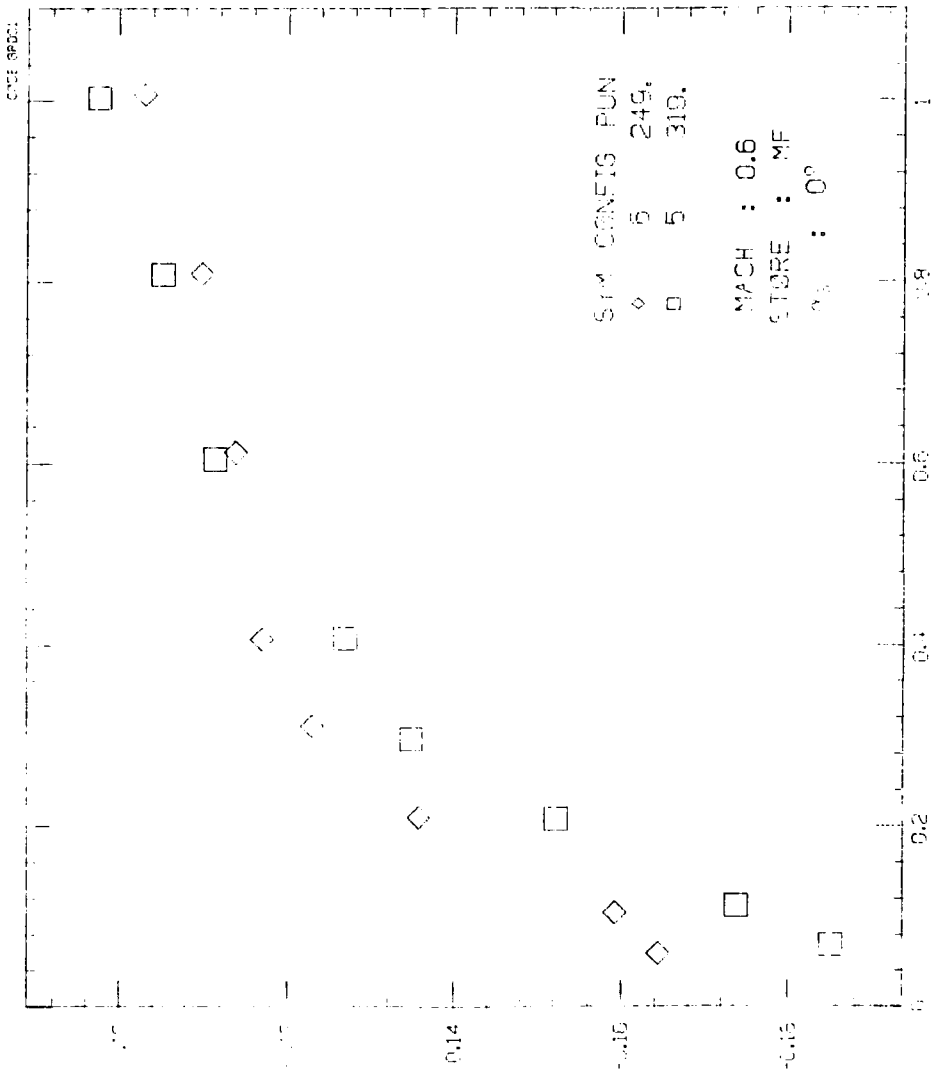

(b) Side-force coefficient.

FIGURE 25. Continued.

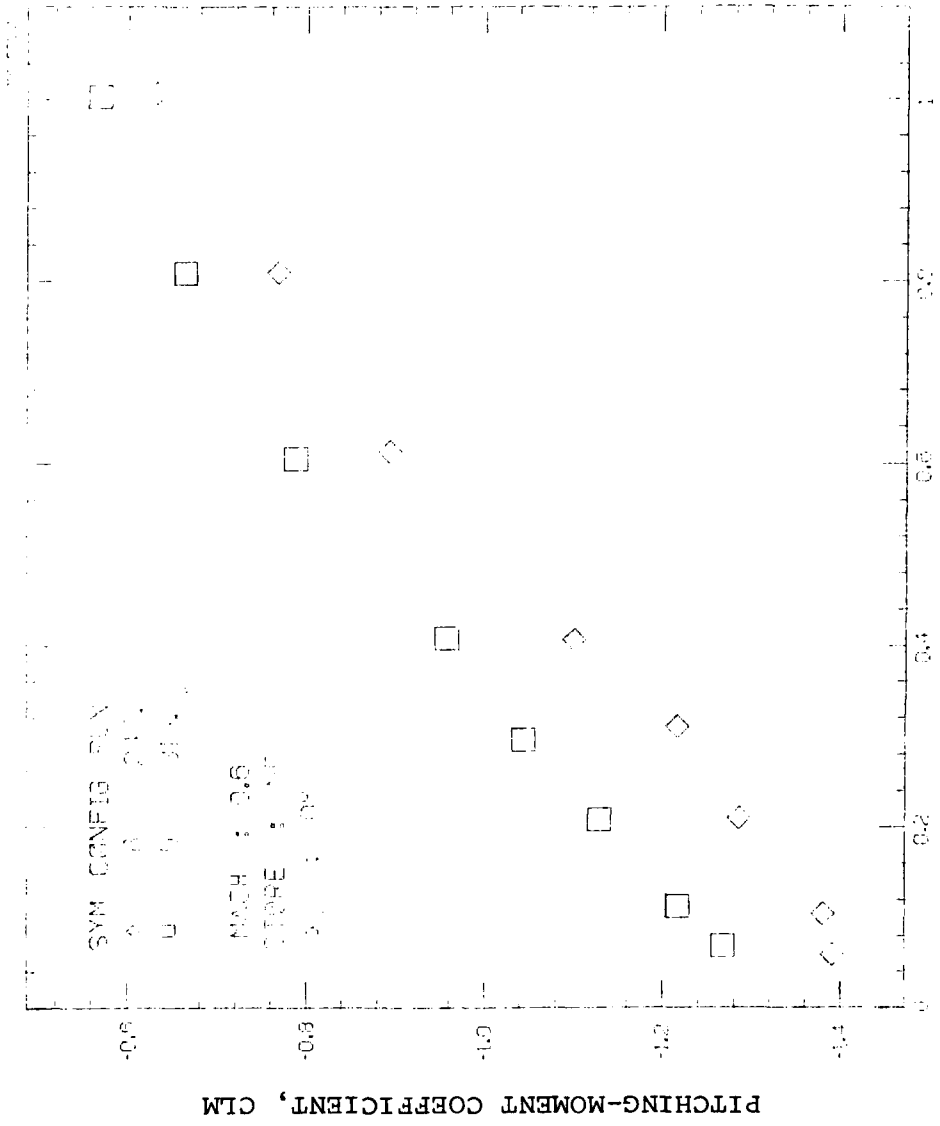

(c) Pitching-moment coefficient.

FIGURE 25. Continued.

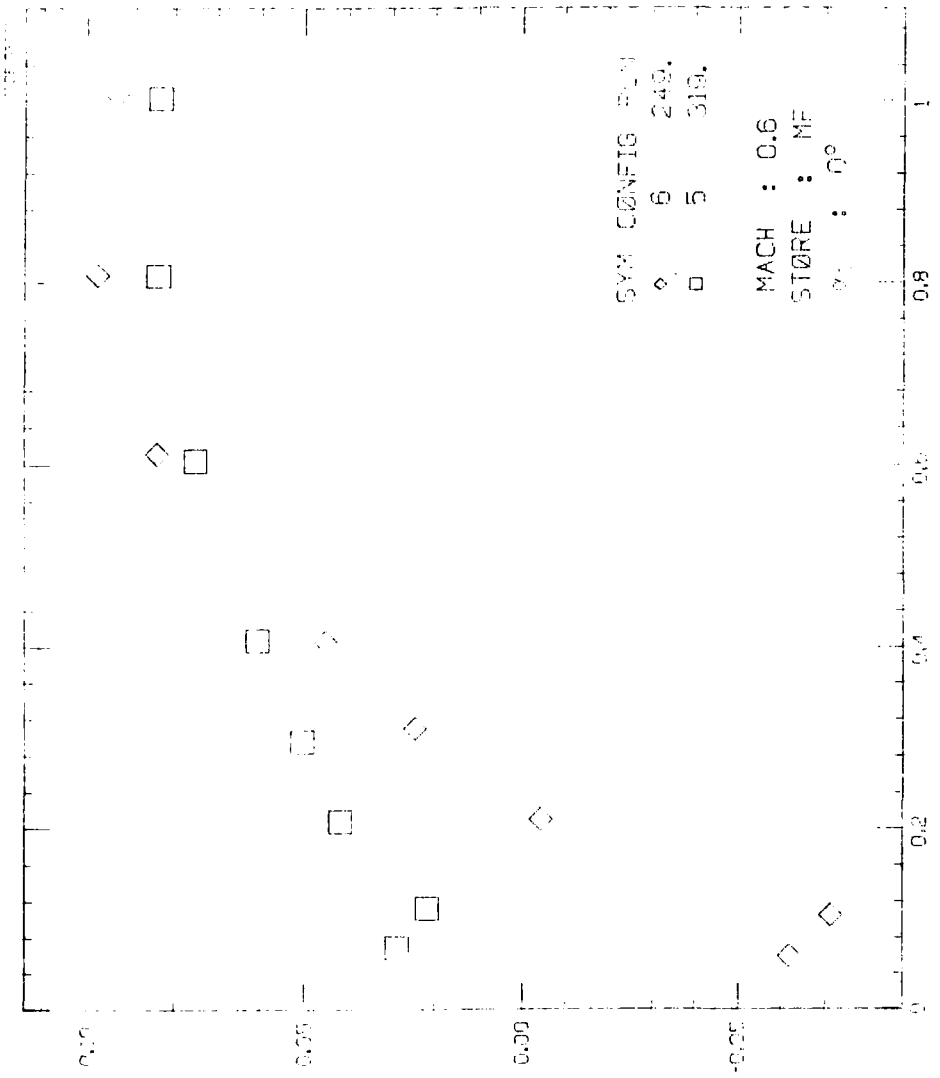

(d) Yawing-moment coefficient.

FIGURE 25. Continued.

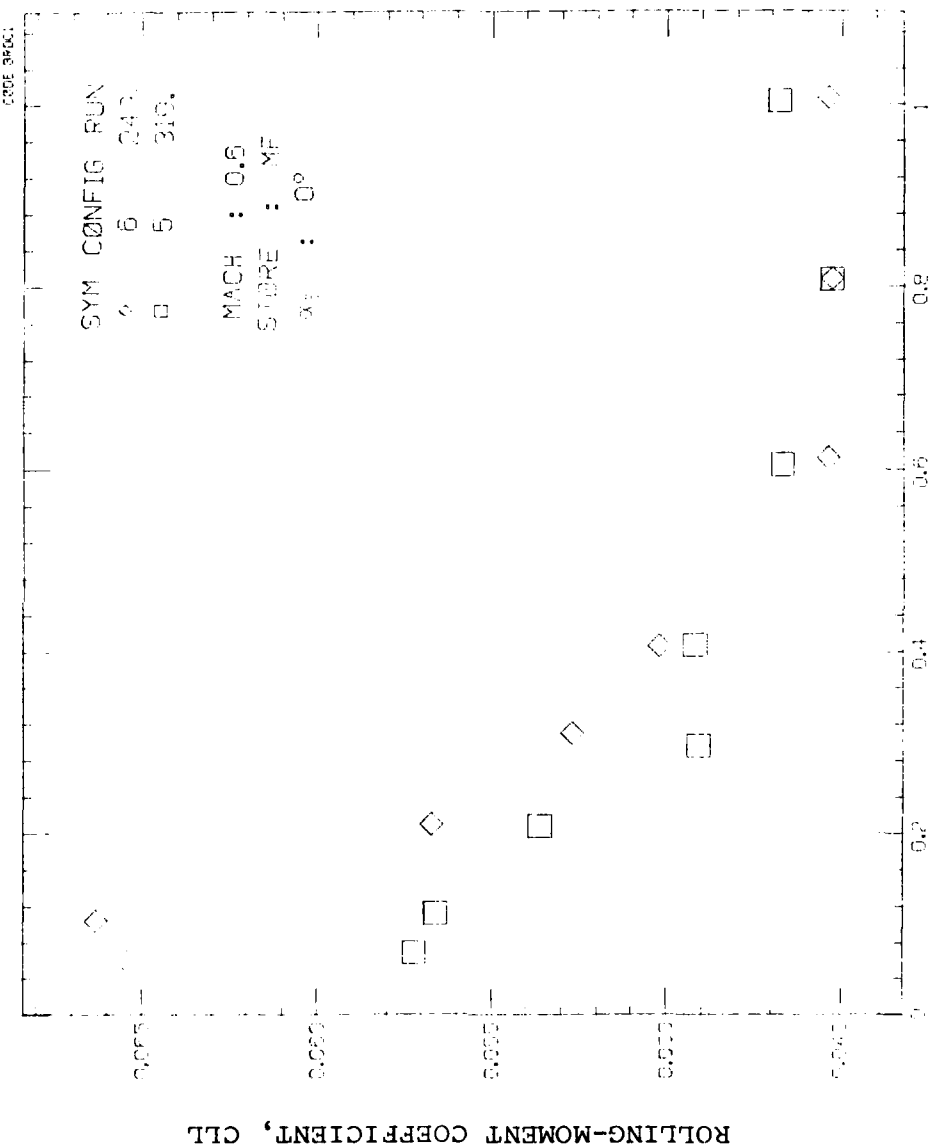

(e) Rolling-moment coefficient.

FIGURE 25. Concluded.

influenced by M_∞ and α_s. The following table gives some results from figures not shown.

$M_\infty = 0.6$	$\alpha_s = 8^\circ$
CN:	.05 in .20
CY:	negligible
CLM:	0.15 in 0.4
CLN:	10%
CLL:	negligible

$M_\infty = 0.95$	$\alpha_s = 0^\circ$
CN:	10%
CY:	.015 in 0.11
CLM:	0.25 in 1.75
CLN:	negligible
CLL:	.008 in .06

$M_\infty = 0.95$	$\alpha_s = 8^\circ$
CN:	negligible
CY:	negligible
CLM:	0.2 out of 0.8
CLN:	.08 out of 0.7
CLL:	negligible

Since the effect of the shoulder store fins is usually greatest for small Z_p/D, it is probable that in a store separation trajectory the effect of those fins can be neglected for many cases. However for accurate attached load calculations they should probably be included.

EFFECT OF SHOULDER STORES

Figure 26 compares the loads on store S_{MF} for configurations 3, 5 and 6. These results show the importance of the shoulder stores on the loads of the bottom store and how far out the shoulder stores affect the loads. For normal-force and pitching-moment coefficients the second store adds an increment about as large as that due to addition of one store, and the interference effects are significant out to 4-6 store diameters. Comparable results are shown for side force and yawing moment except that the interference effects are only significant to 1-2 store diameters. The rolling moment results indicate large effects only for small Z_p/D values, and show a difference of magnitude of .005 for $Z_p/D > 1.0$.

The range of the interference effects of the shoulder stores on the bottom store is judged to be large enough that it can have significant effects on trajectory calculations. Such stores also must be accounted for in determining attached loads.

EFFECT OF SWAY BRACES

Measurements have been made to determine the importance on store grid loads of sway braces such as shown in Figure 5. Measurements, with and without sway braces, are indicated in Table 6. Comparing the grid data for the bottom store of configuration 6 at M_∞ = 0.6, 0.8, 0.9, and 0.95 at $\alpha_s = 0^\circ$ with and without sway braces, we find their effects are generally negligible except in a few cases for close proximity to the attached position for CN and CLM.

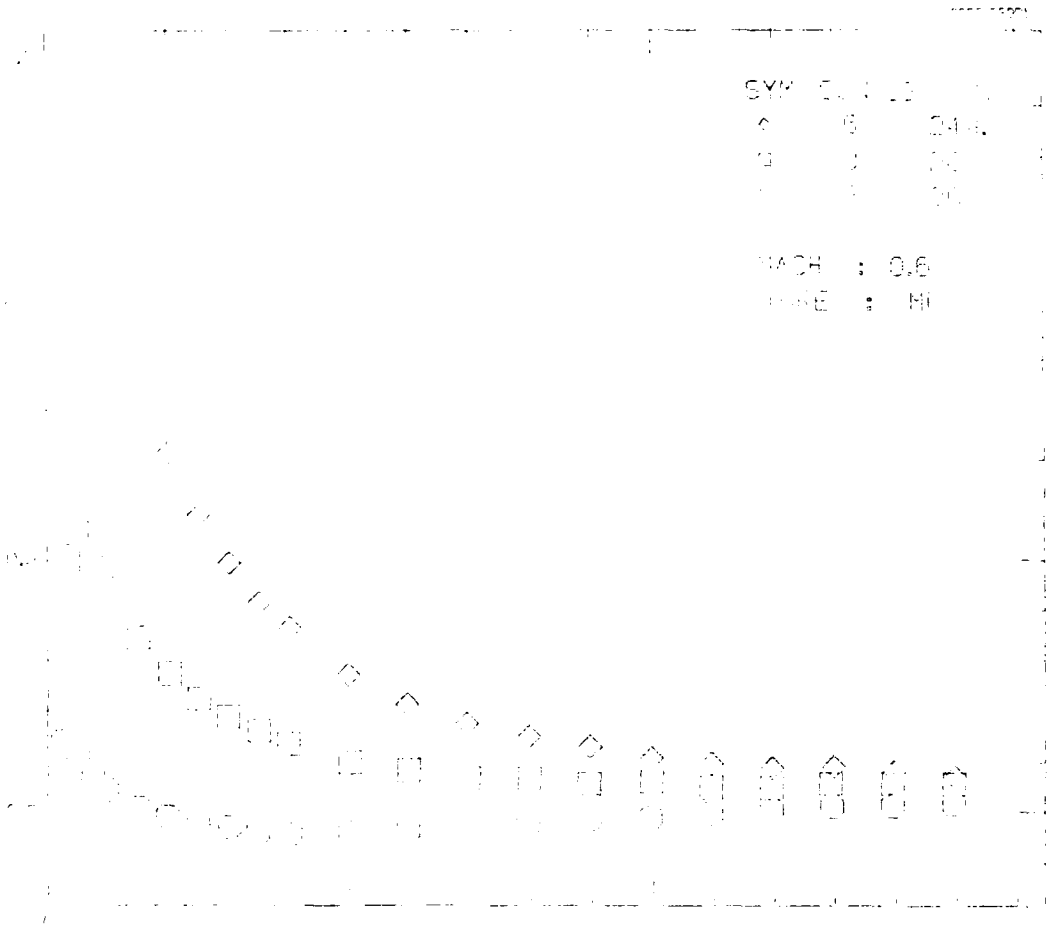

(a) Normal-force coefficient.

FIGURE 26. Grid Loads on Store S_{MF} as Influenced by Number of Shoulder Stores; $M_\infty = 0.6$, $\alpha_s = 0^\circ$.

(b) Side-force coefficient.

FIGURE 26. Continued.

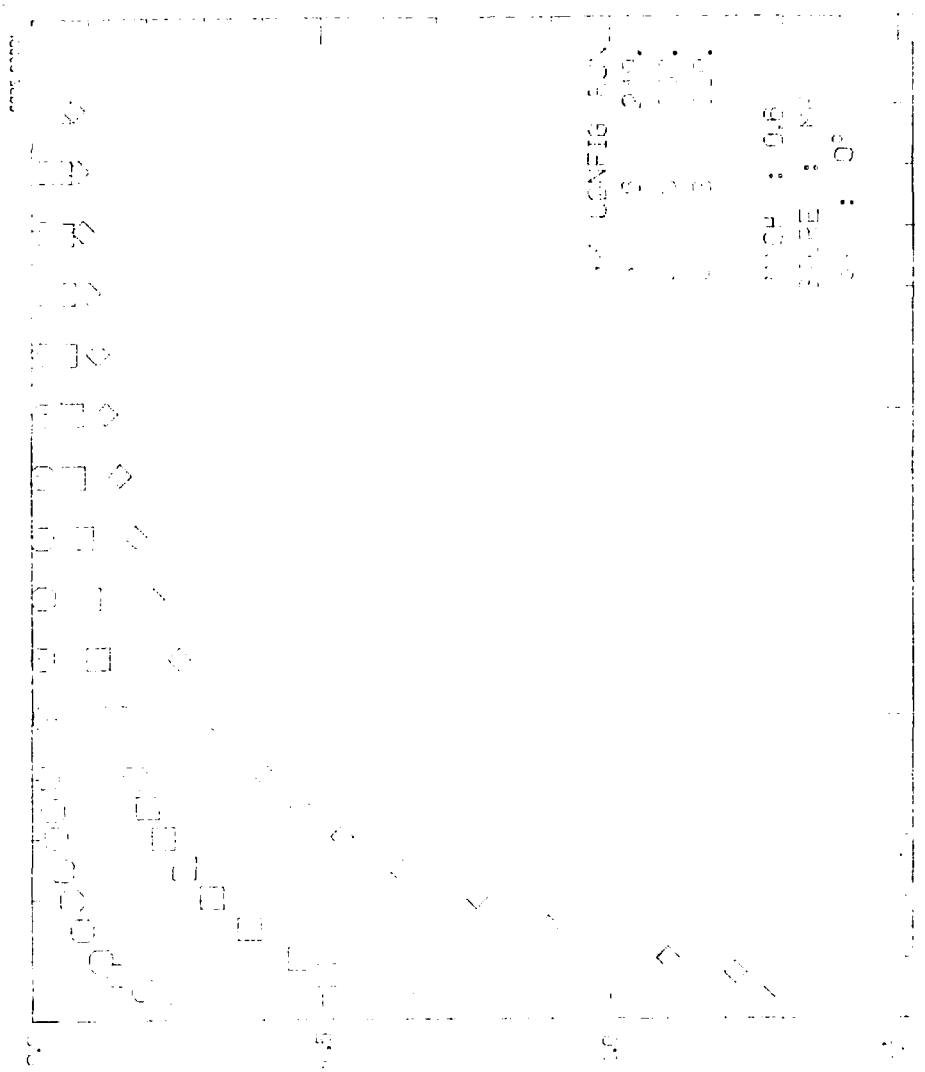

(c) Pitching-moment coefficient.

FIGURE 26. Continued.

STORE VERTICAL POSITION, Z_P/D

(d) Yawing-moment coefficient.

FIGURE 26. Continued.

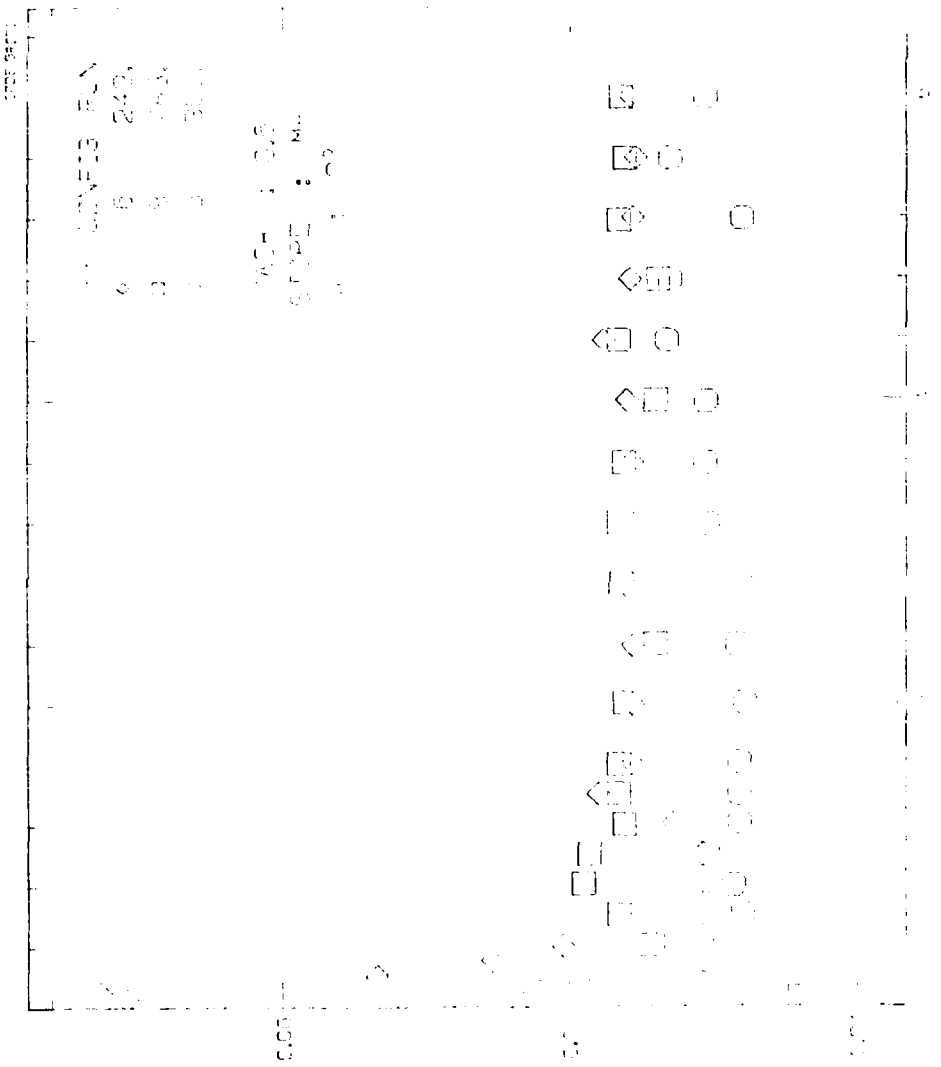

STORE VERTICAL POSITION, Z_p/D

(e) Rolling-moment coefficient.

FIGURE 26. Concluded.

For CN of 0.6, an effect of 0.1 for $Z_p/D < 0.1$ is about the maximum. For a CM of 1.2 a change of 0.1 to 0.2 is a maximum. These changes attenuate to very small values by $Z_p/D = 0.5$. These results are representative of all Mach numbers.

Dix in Reference 6 examined the effects of sway braces on the attached loads for the same configuration. At $\alpha_s = 0^\circ$ his results were the same as described above except for CM. He found increments in CM as high as 0.6.

DISCUSSION OF FLOW FIELD MEASUREMENTS

The nature of the flow field is influenced by the same parameters which affect the store loads. They include vertical position, angle of attack, configuration, Mach number, number of shoulder stores, and addition of fins to the shoulder stores. The quantities shown in the ensuing figures are VZ/V and VY/V, which are, respectively, the upwash and sidewash velocities divided by the free-stream velocity. For the purposes of this report, these quantities can be equated to the upwash and sidewash angles in radians within a few percent in all cases. The angles are measured in the attached store or probe axis system shown in Figure 5.

EFFECT OF VERTICAL POSITION AND ANGLE OF ATTACK

Figure 27 shows measured upwash and sidewash under the rack of configuration 3 at $M_\infty = 0.6$ at Z_p/D of 0 and 1.0 for both 0° and 16° angles of attack. It is noted that the change in upwash between these vertical positions for both angles of attack is not large. The sidewash angle in Figure 27(b) tends to show more variation between positions.

The results which follow are for $Z_p/D = 0$.

EFFECT OF CONFIGURATION

The effects of configuration will first be examined with regards to adding the pylon and then the rack to the clean airplane by comparing data for configurations 1, 2, and 3. The upwash and sidewash for $M_\infty = 0.6$ and $\alpha_s = 0^\circ$ are shown in Figure 28 for these configurations as well as others. Adding the pylon to the clean airplane hardly changes the upwash, but adding the rack causes a significant effect; as much as 2°. The effect of adding the pylon on sidewash has a maximum effect of about 0.5° while adding the rack has about three times this effect.

Examining similar results in Figure 29 for $\alpha_s = 4^\circ$, we note results of about the same magnitude for upwash angle. The results for sidewash in Figure 29(b) are similar to those for $\alpha_s = 0^\circ$ but are of larger magnitude.

It seems desirable to model the pylon and necessary to model the rack.

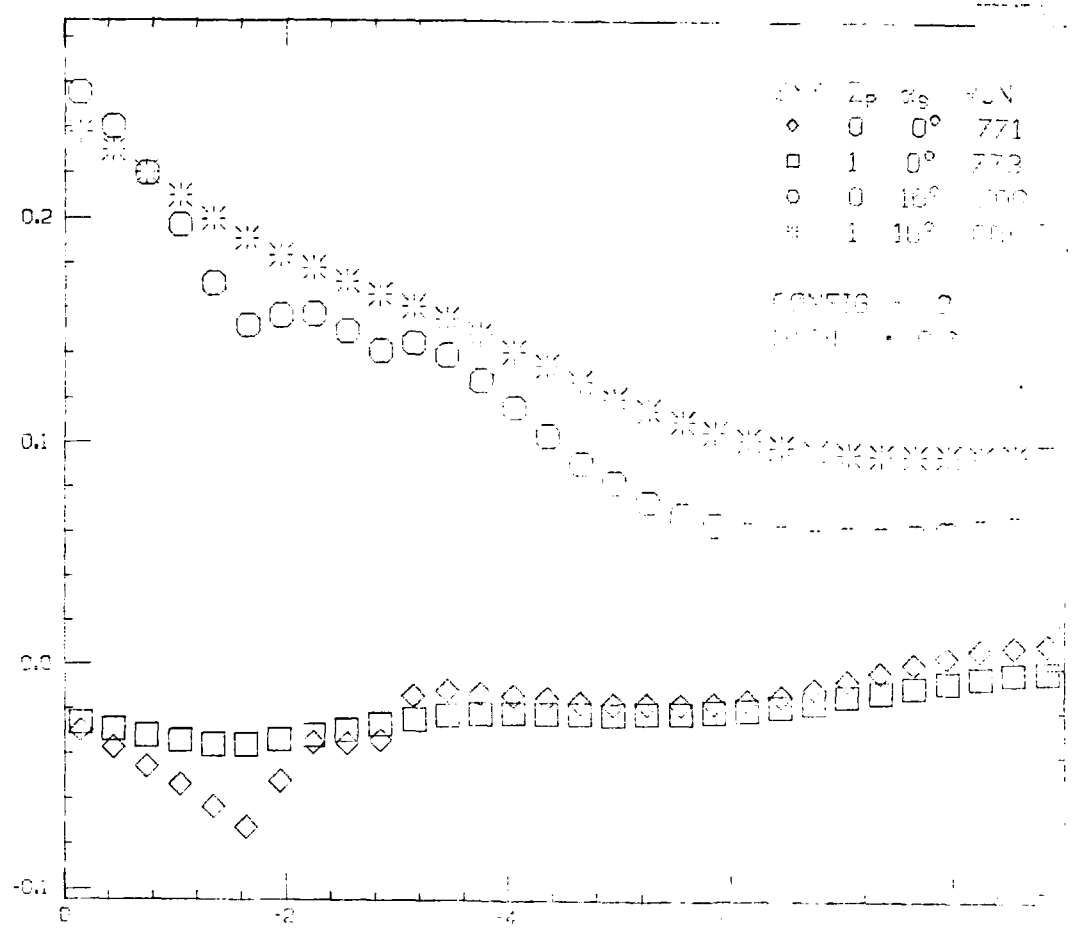

$\frac{VZ}{V}$

PROBE AXIAL POSITION, X_p, IN.

(a) Upwash angle.

FIGURE 27. Upwash and Sidewash Angles Along Position of Store Centerline for Z_p/D = 0 and 1.0; Configuration 3, M_∞ = 0.6.

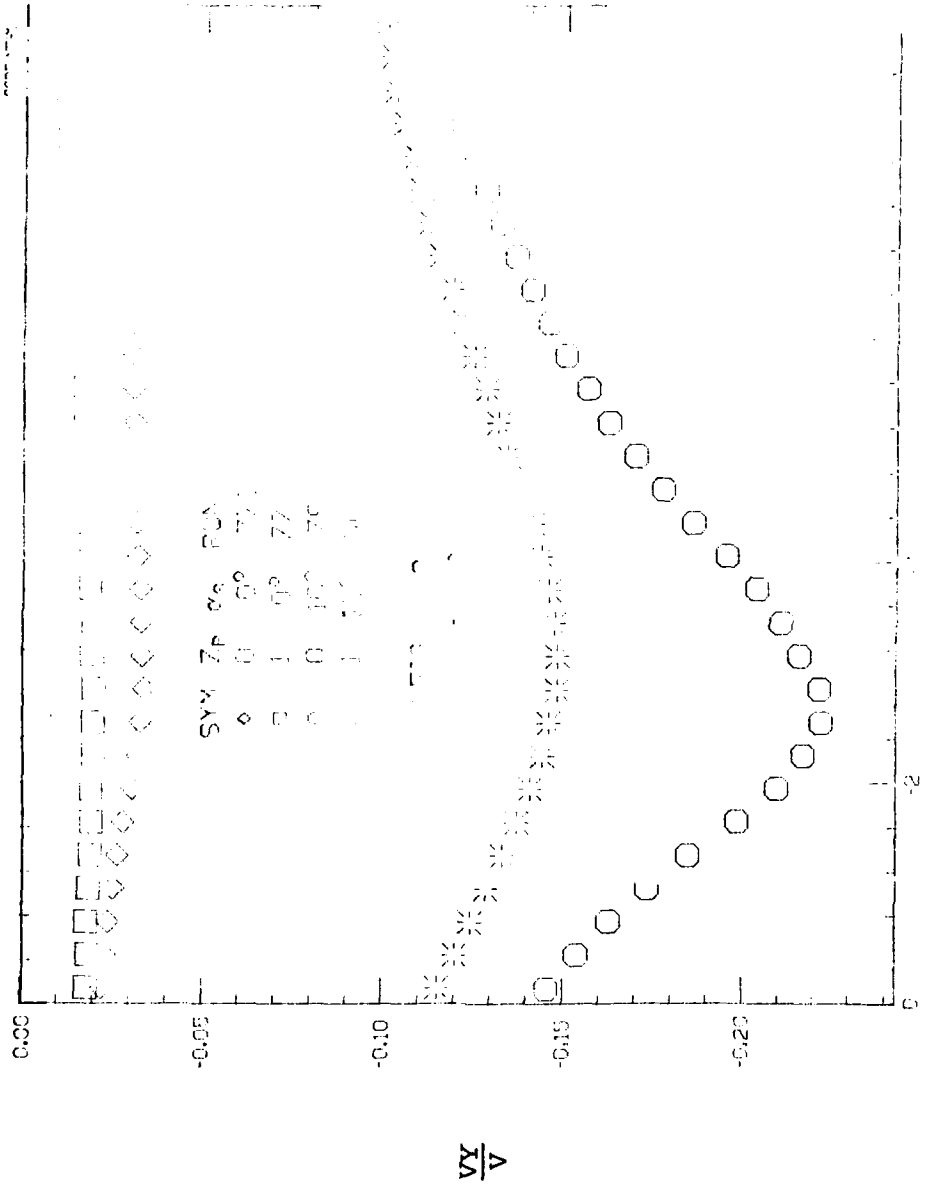

(b) Sidewash angle.

FIGURE 27. Concluded.

(a) Upwash angle.

FIGURE 28. Effect of Configuration on Flow Angles at $Z_P/D = 0$ at $M_\infty = 0.6$; $\alpha_g = 0°$.

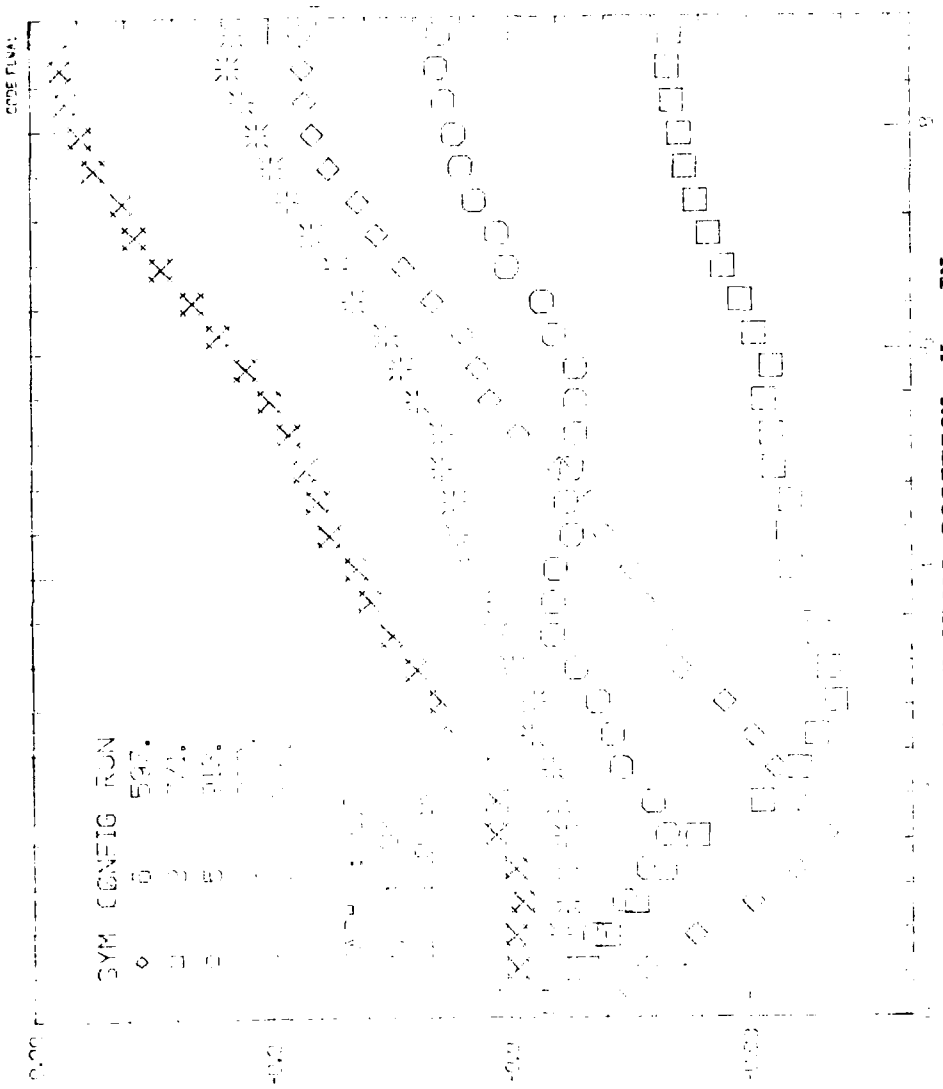

(b) Sidewash angle.

FIGURE 28. Concluded.

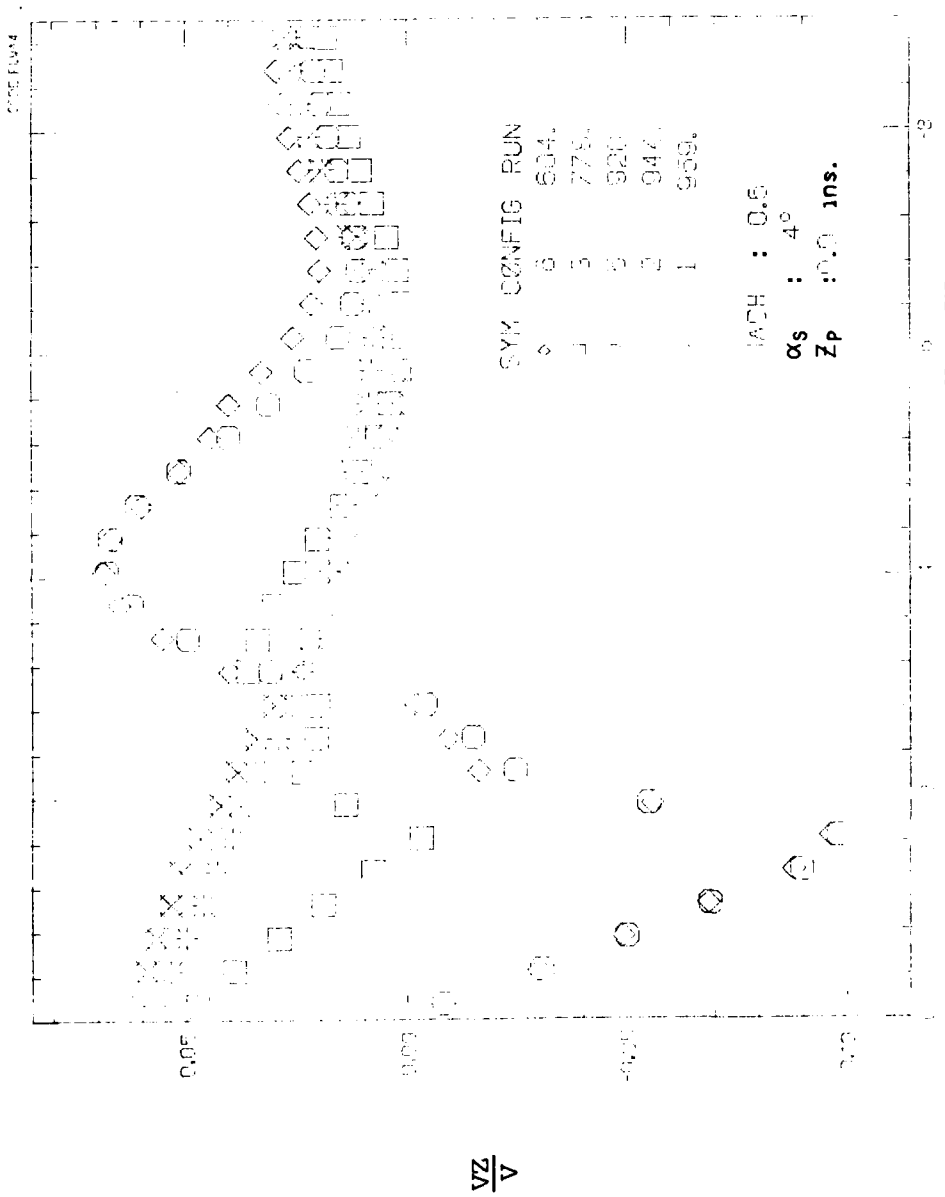

(a) Upwash angle.

FIGURE 29. Effect of Configuration on Flow Angles at $Z_p/D = 0$ at $M_\infty = 0.6$; $\alpha_s = 4°$.

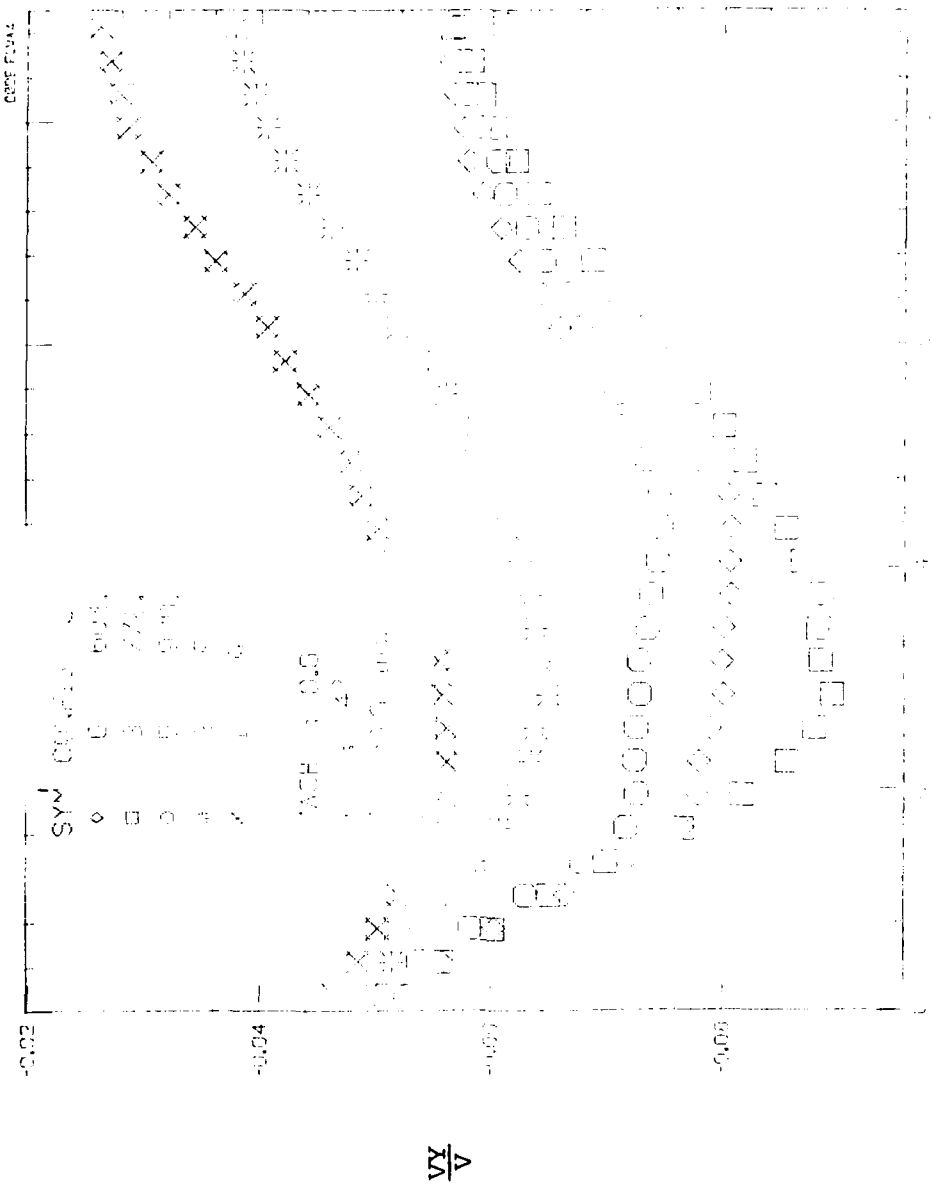

(b) Sidewash angle.

FIGURE 29. Concluded.

The effects of adding shoulder stores to the rack and pylon and fins to the shoulder stores can be seen by comparing configurations 3, 5, and 6 in Figures 28 and 29. It is noted that configurations 5 and 6 cause large changes in upwash from configuration 3 in Figure 28(a) but they have virtually identical upwash for $0 < X_p < -5$. The $X_p = -5$ position is near the fin leading edge, and only behind this point is the upwash field due to the addition of the fins of significance.

Adding the shoulder stores to the rack causes significant increments in sidewash but these are usually less than those caused by adding the rack to the pylon. The further addition of the fins causes small sidewash increments which are felt in front of and behind the fins. At $\alpha_s = 4^o$, the same general conclusion holds for upwash, while the maximum increment in sidewash is about 1.0^o due to adding shoulder stores and another 0.5^o due to addition of fins.

It thus appears that addition of the rack has significant effects on upwash and sidewash. Addition of a pair of shoulder stores also has significant effects on the upwash and sidewash. Addition of fins to the shoulder stores has little effect on upwash, and then only behind the fins. It has a small effect on sidewash in front of and behind the fins.

EFFECT OF MACH NUMBER

The effect of Mach number on the upwash and sidewash at $\alpha_s = 4^o$ is shown for configuration 3 in Figure 30. There is an effect of M_∞ on upwash in the region of large axial

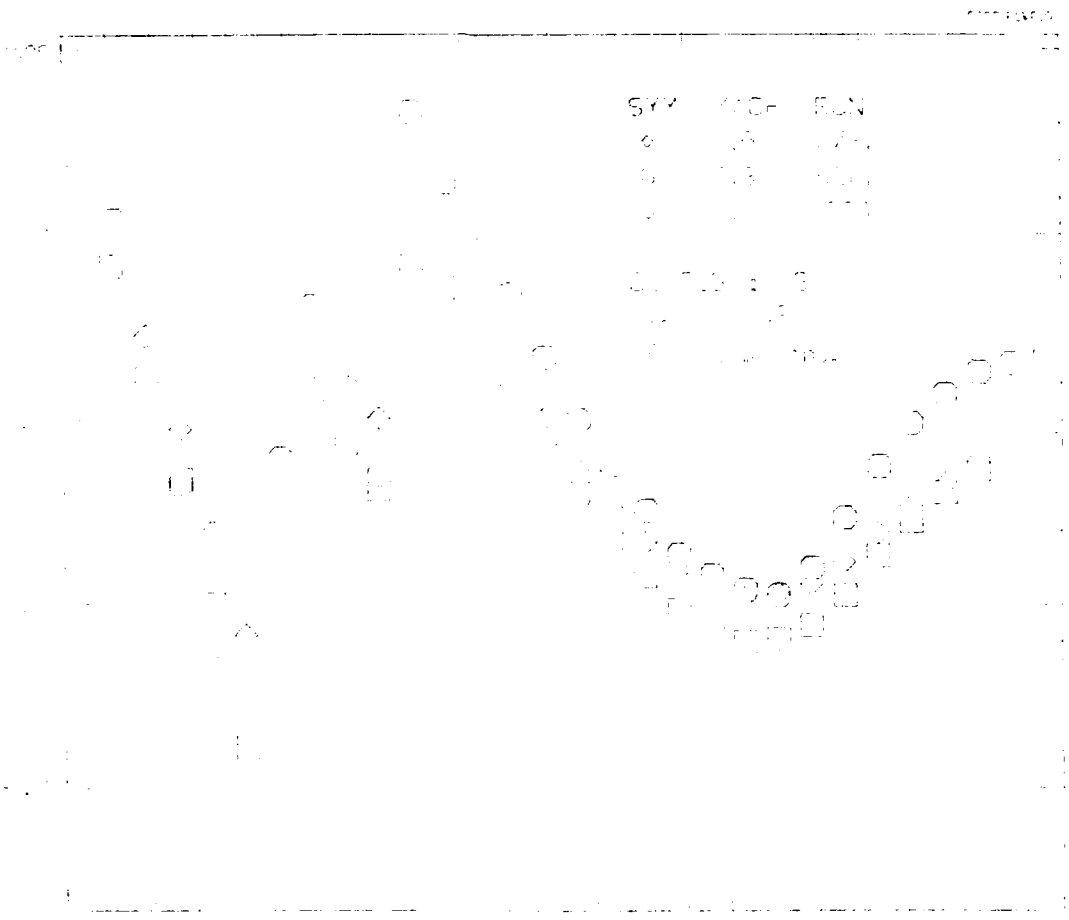

PROBE AXIAL POSITION, X_p, IN.

(a) Upwash angle.

FIGURE 30. Effect of Mach Number on Flow Angles at $Z_p/D = 0$ for $\alpha_s = 4^\circ$; Configuration 3.

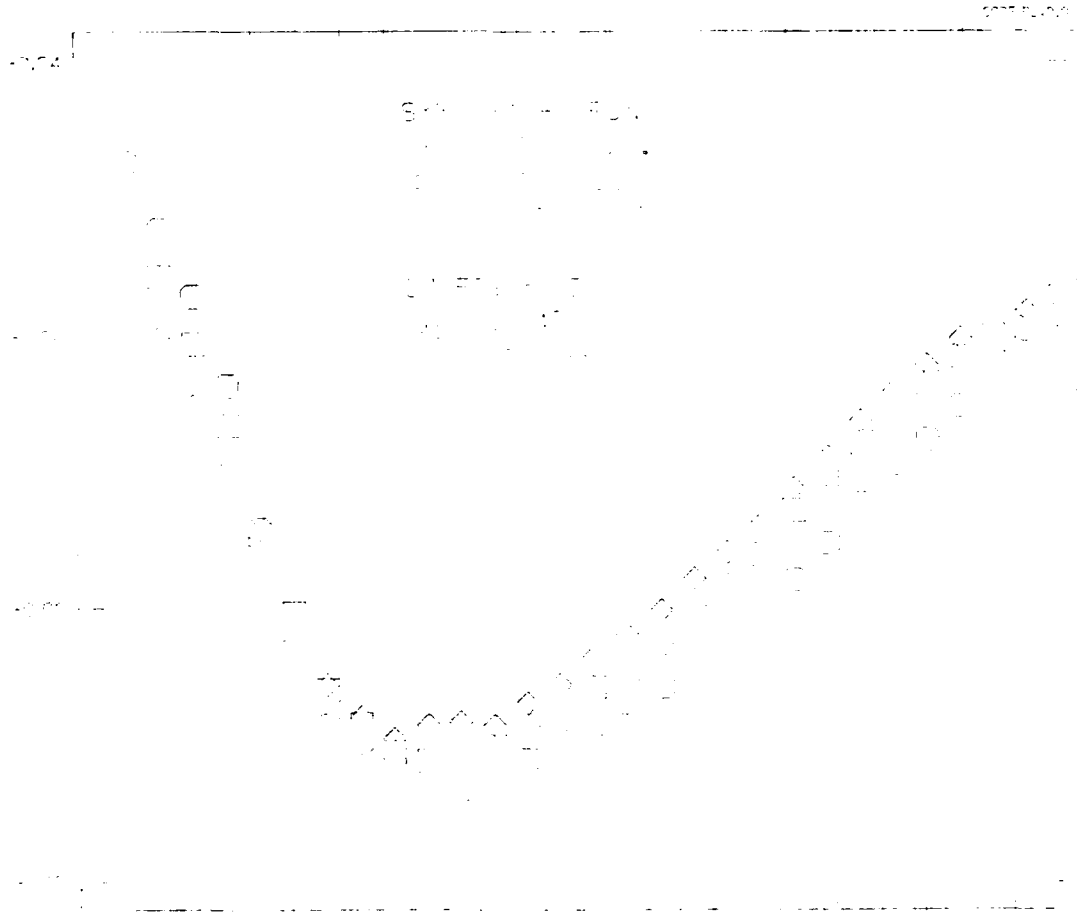

PROBE AXIAL POSITION, X_p, IN.

(b) Sidewash angle.

FIGURE 30. Concluded.

gradients, but there is a small effect on sidewash for the range $0.6 \leq M_\infty \leq 0.95$. Similar data are presented for configuration 6 in Figure 31. There are small effects of M_∞ on upwash and sidewash up to $M_\infty = 0.8$. There is a maximum change in sidewash angle of about 1^o over a small X_p range due to change in M_∞ from 0.8 to 0.95.

EFFECT OF NUMBER OF SHOULDER STORES

The effect of adding the outboard shoulder store (including fins) to the rack is found by comparing configurations 3 and 8, and the effect of adding both shoulder stores (including fins) to the rack is found by comparing configurations 3 and 6. These effects are shown on upwash and sidewash for $Z_p/D = 0$ at $M_\infty = 0.6$ in Figure 32 for $\alpha_s = 0^o$ and in Figure 33 for $\alpha_s = 4^o$. Examining Figure 32(a), we can see that adding both stores causes generally more than twice the effect on upwash of adding one store. The sidewash angles, Figure 32(b), are negative, and for the present measurements under the left wing, the flow is directed outboard. The effect of adding two shoulder stores is not to change the sidewash angle for the first two inches (one-third of the store length), while one shoulder store decreases the sidewash angle substantially. There is a clearcut difference between the effects of adding one or two shoulder stores on the sidewash.

The upwash results for $\alpha_s = 4^o$ in Figure 33(a) show that adding the outboard shoulder store has a greater effect over the forward half of the survey, and that adding the inboard store has the greater effect over the rear half of the survey. With regard to sidewash, the results noted in Figure 32(a)

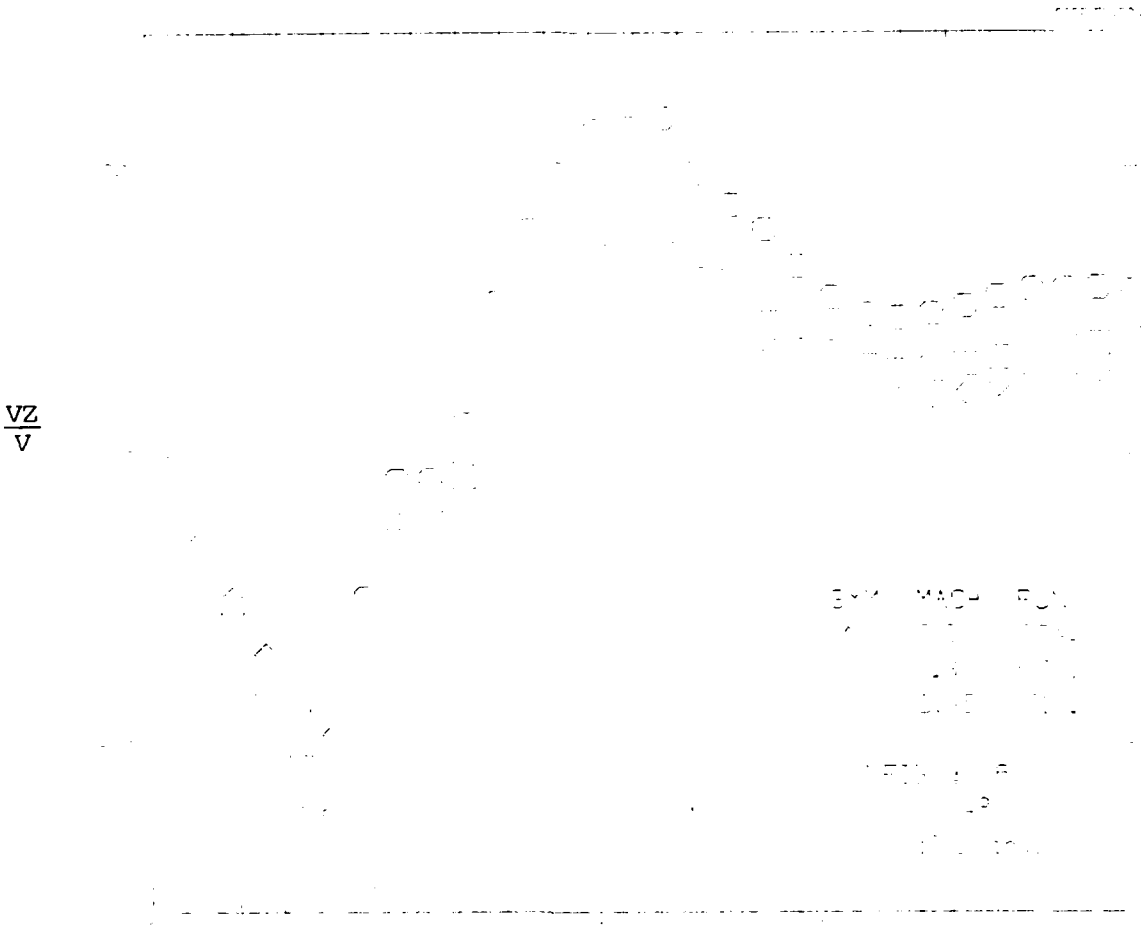

PROBE AXIAL POSITION, X_p, IN.

(a) Upwash angle.

FIGURE 31. Effect of Mach Number on Flow Angles at $Z_p/D = 0$ for $\alpha_s = 4^\circ$; Configuration 6.

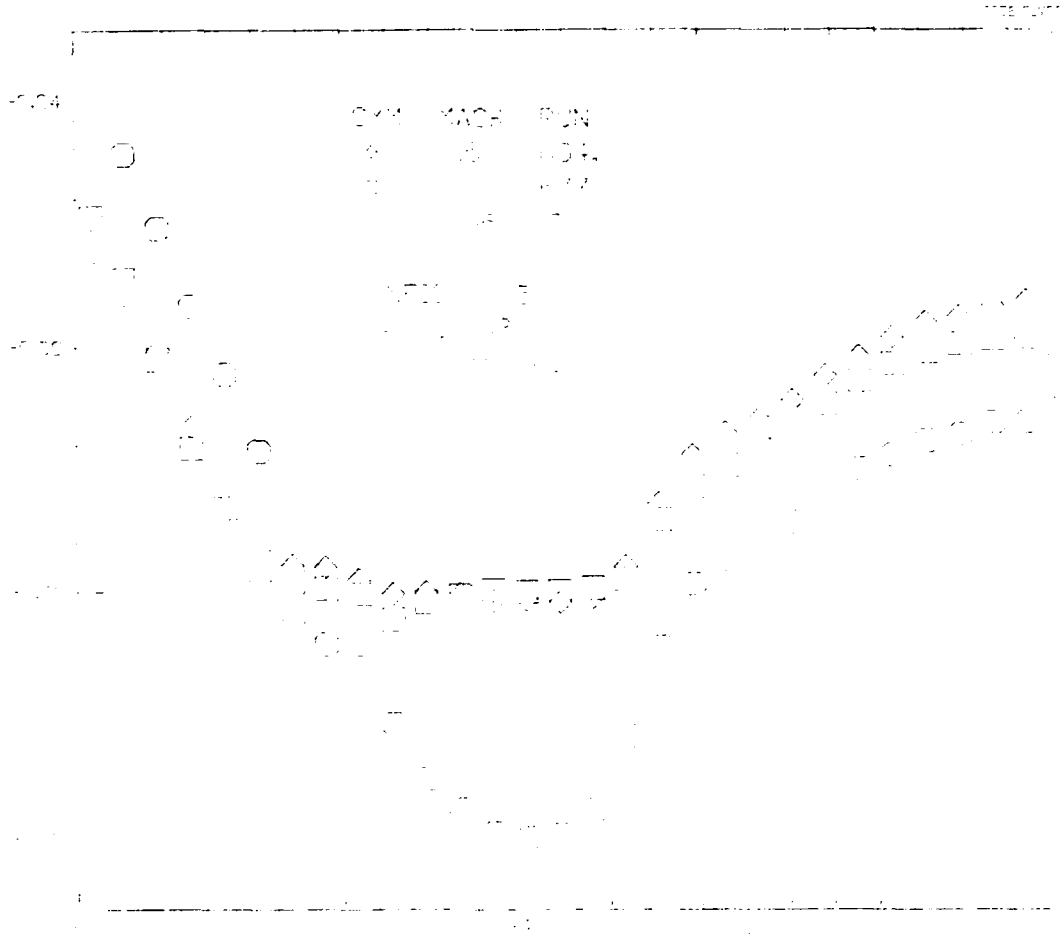

(b) Sidewash angle.

FIGURE 31. Concluded.

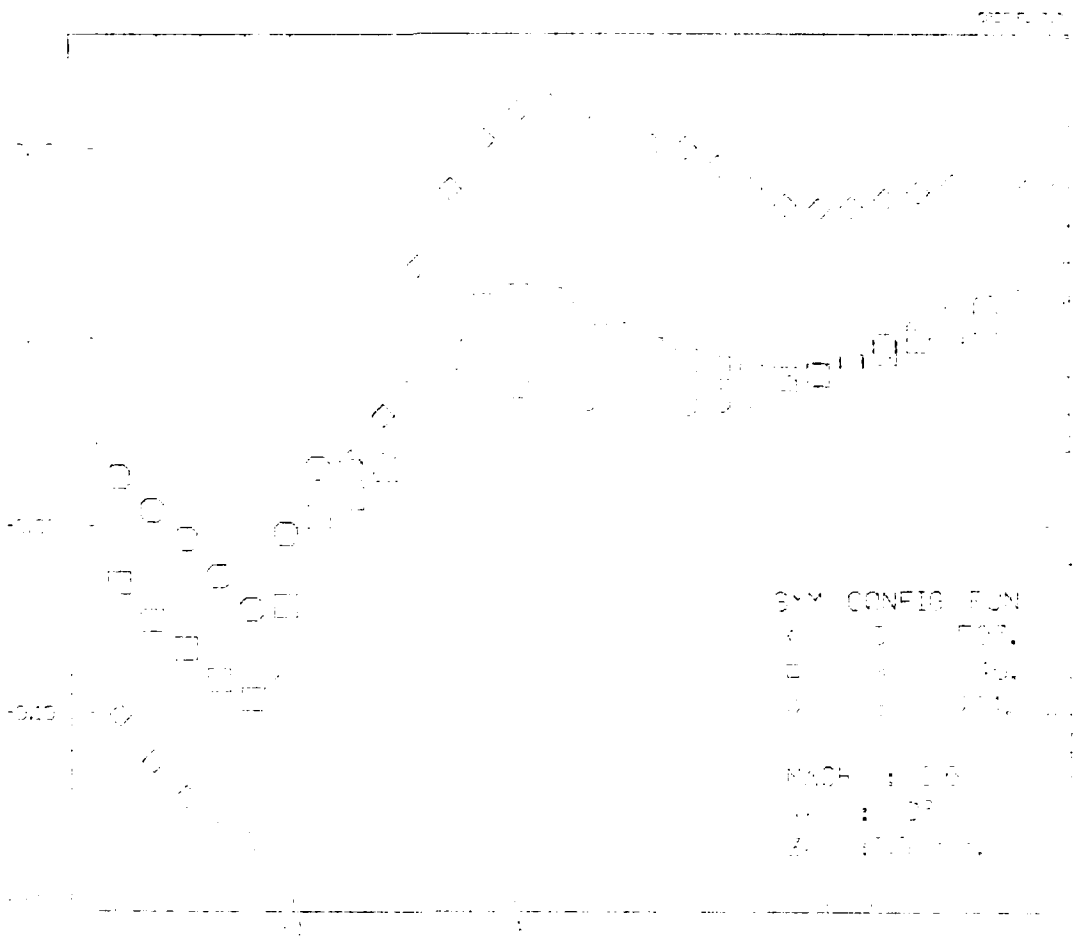

(a) Upwash angle.

FIGURE 32. Effects of Adding Shoulder Stores to Rack and of Adding Fins to Shoulder Stores on Flow Angles at $Z_p/D = 0$ and $M_\infty = 0.6$; $\alpha_s = 0^\circ$.

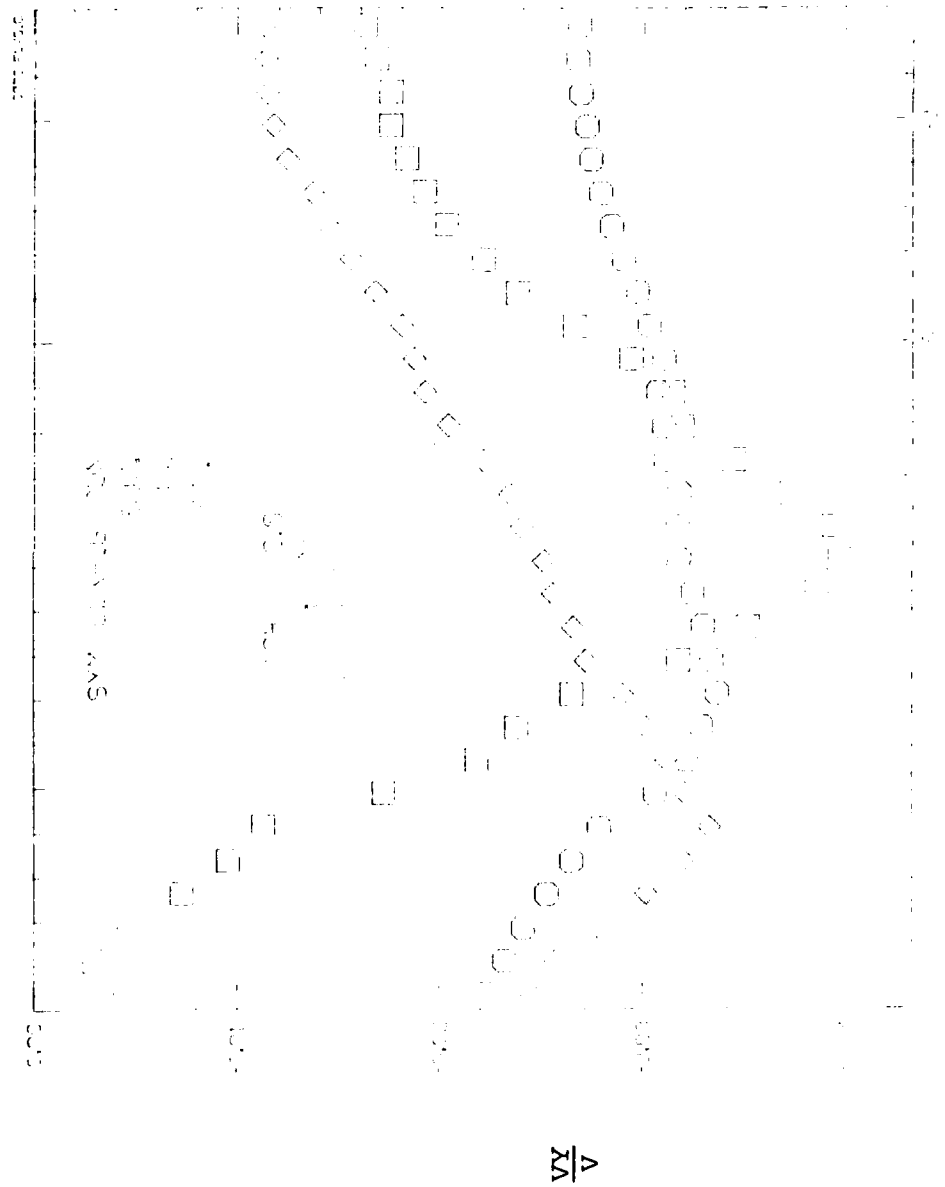

(b) Sidewash angle.

FIGURE 32. Concluded.

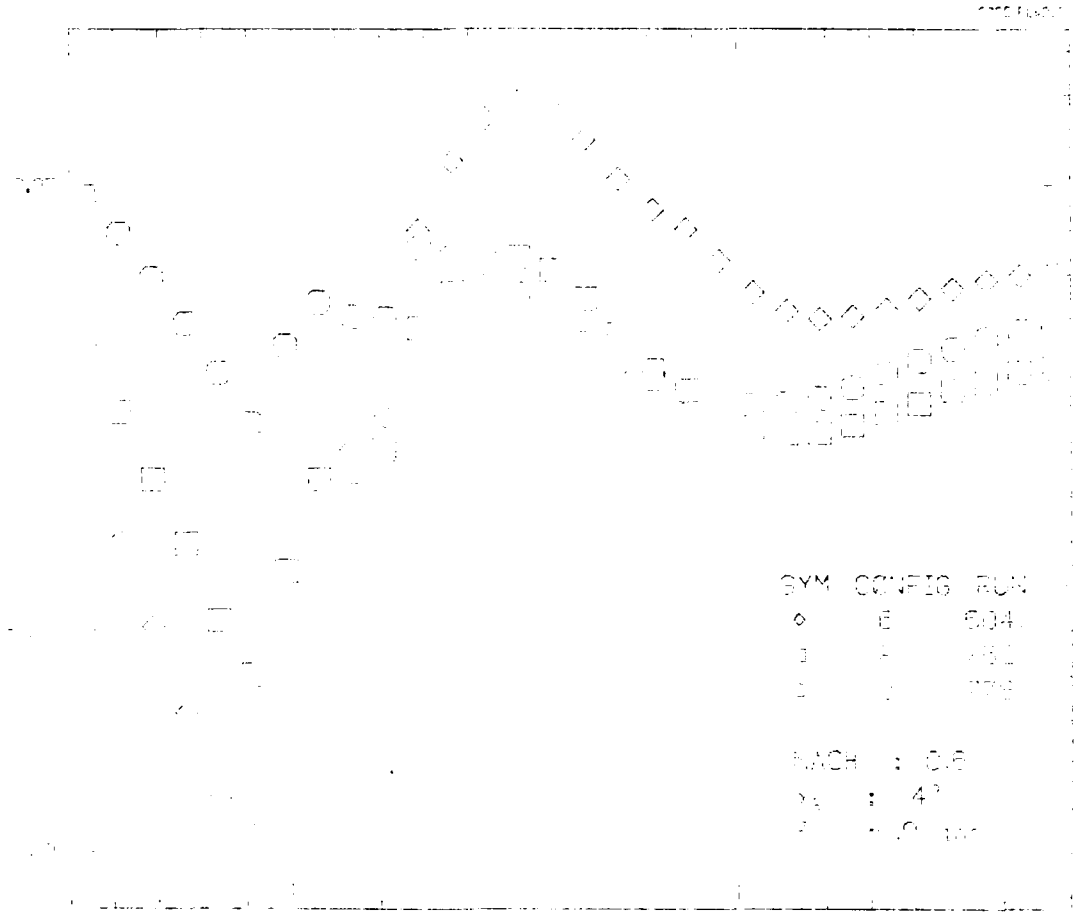

PROBE AXIAL POSITION, X_p, IN.

(a) Upwash angle.

FIGURE 33. Effects of Adding Shoulder Stores to Rack and of Adding Fins to Shoulder Stores on Flow Angles at $Z_p/D = 0$ and $M_\infty = 0.6$; $\alpha_s = 4^\circ$.

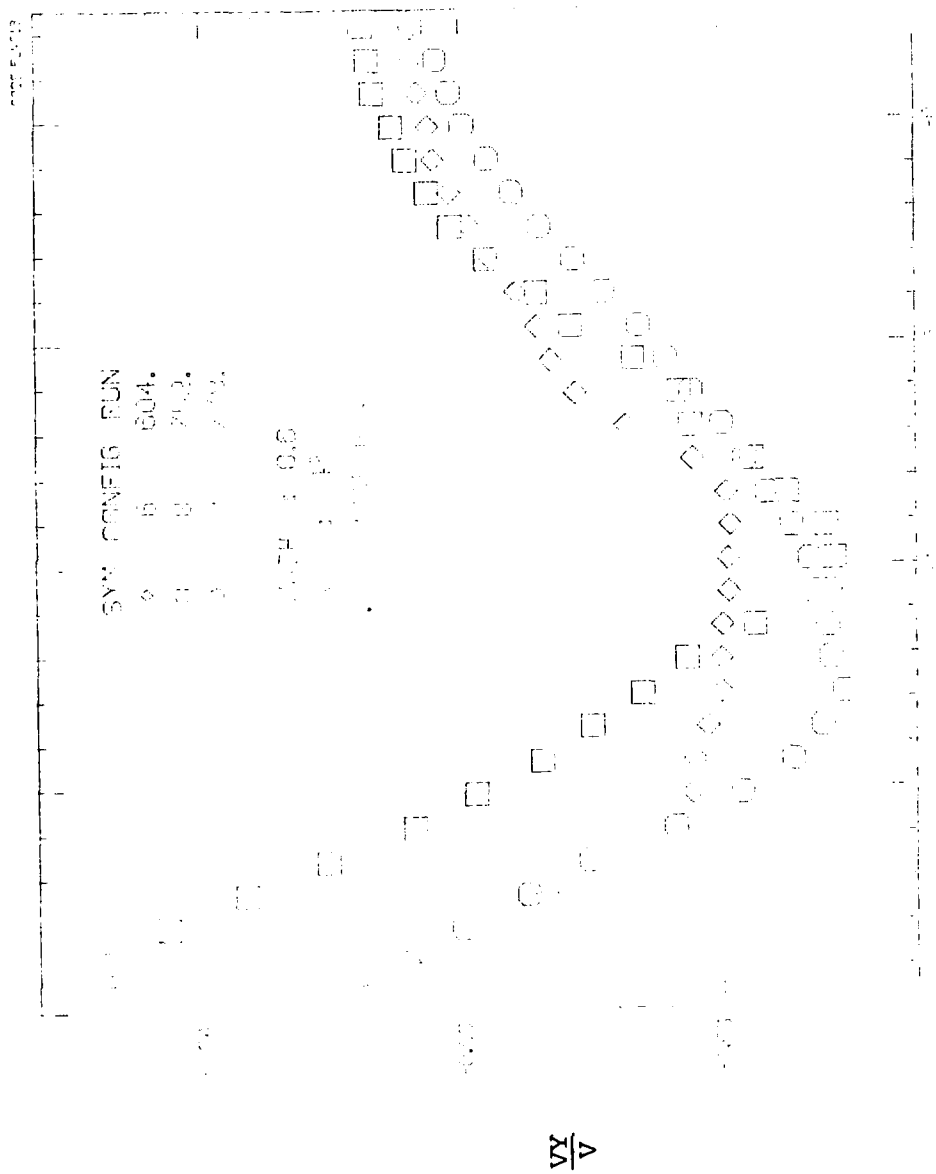

(b) Sidewash angle.

FIGURE 33. Concluded.

for $0 > X_p > -2$ are repeated, but the effect of adding either or both stores on sidewash is small for $X_p < -3$.

EFFECT OF ADDING FINS TO SHOULDER STORES

Comparison of configurations 5 and 6 shows the effect of adding fins to the shoulder stores. These results are given for $M_\infty = 0.6$ in Figure 34 for $\alpha_s = 0^o$ and in Figure 35 for $\alpha_s = 4^o$. With respect to upwash there are no large effects of adding the fins. There is about a 1^o change in upwash at $\alpha_s = 0^o$ behind the fins of the store due to the addition of the fins. The changes in sidewash are small, not exceeding 1/4 to 1/2 degree. At $\alpha_s = 4^o$, there is little change in upwash and about a maximum of 0.4^o in sidewash.

COMPARISON BETWEEN EXPERIMENT AND THEORY

GENERAL APPROACH

The basic objective of the experimental investigation is to provide data for validating the computer program of Reference 1 and for providing insight into methods for upgrading the computer program. Accordingly the comparisons between theory and experiment are directed toward these ends. In order to make such comparisons meaningful, it is of interest to describe the main assumptions that are made in the computer program especially with respect to pylon, rack, and stores and to suggest areas where refinements in the computer program may appear necessary.

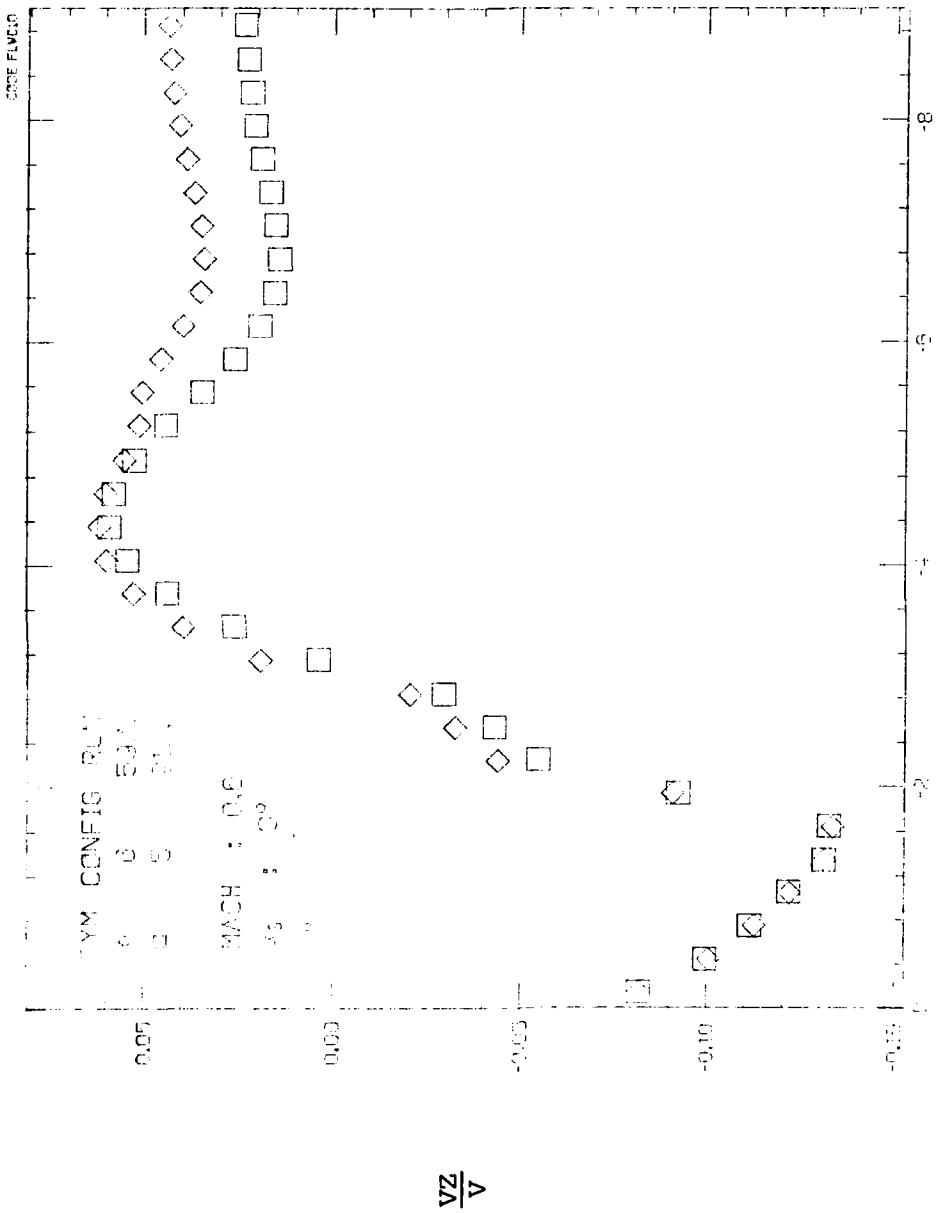

$\frac{\partial \varepsilon}{\partial \alpha}$

PROBE AXIAL POSITION, X_P, IN.

(a) Upwash angle.

FIGURE 34. Effect of Adding Fins to Shoulder Stores on Flow Angles at $Z_P/D = 0$ for $M_\infty = 0.6$; $\alpha_s = 0^o$.

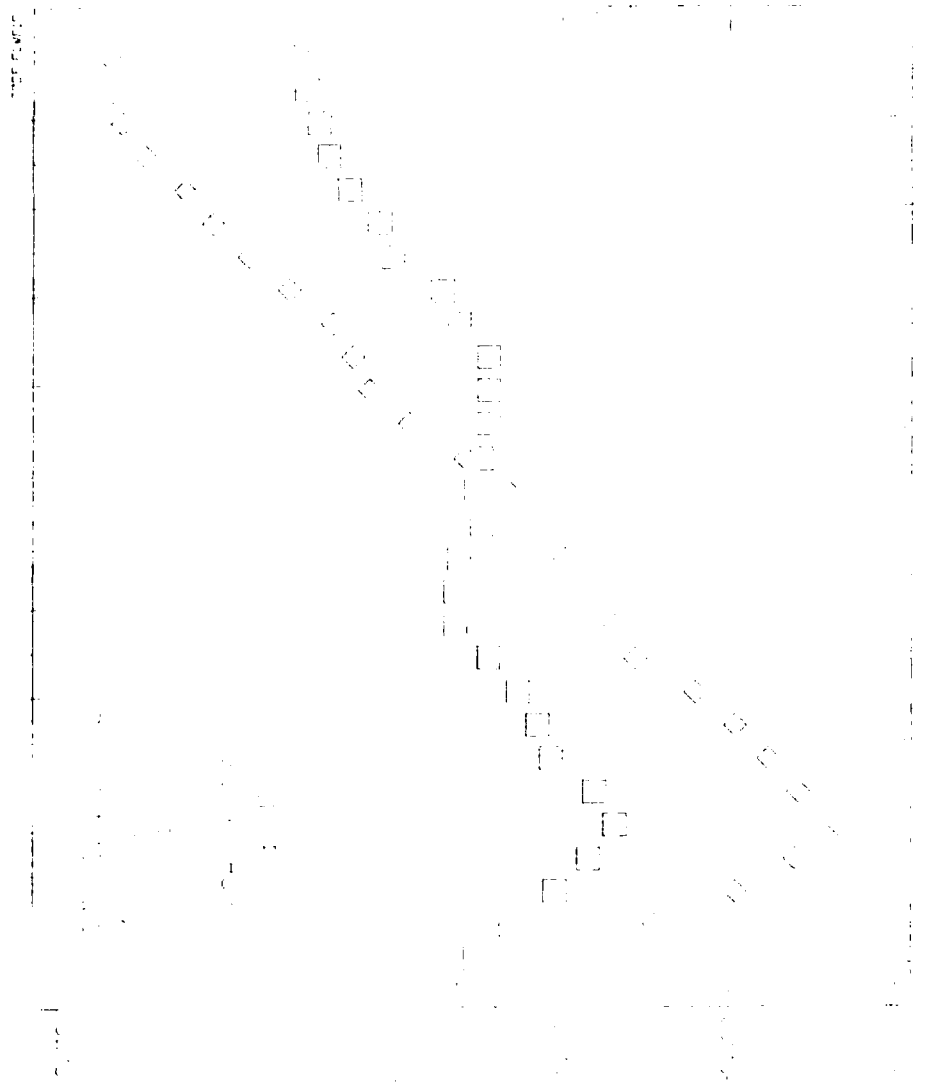

PROBE AXIAL POSITION, X_P, IN.

(b) Sidewash angle.

FIGURE 34. Concluded.

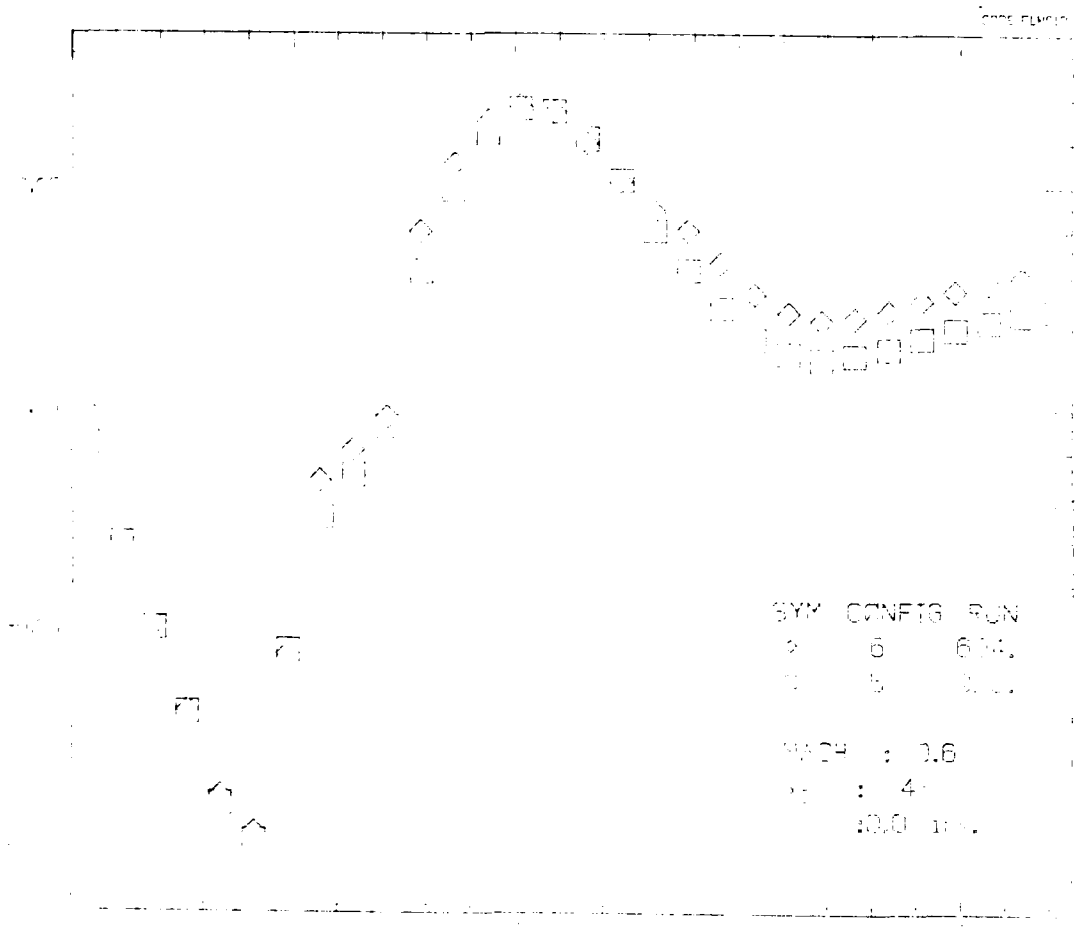

PROBE AXIAL POSITION, X_p, IN.

(a) Upwash angle.

FIGURE 35. Effect of Adding Fins to Shoulder Stores on Flow Angles at $Z_p/D = 0$ for $M_\infty = 0.6$; $\alpha_s = 4^\circ$.

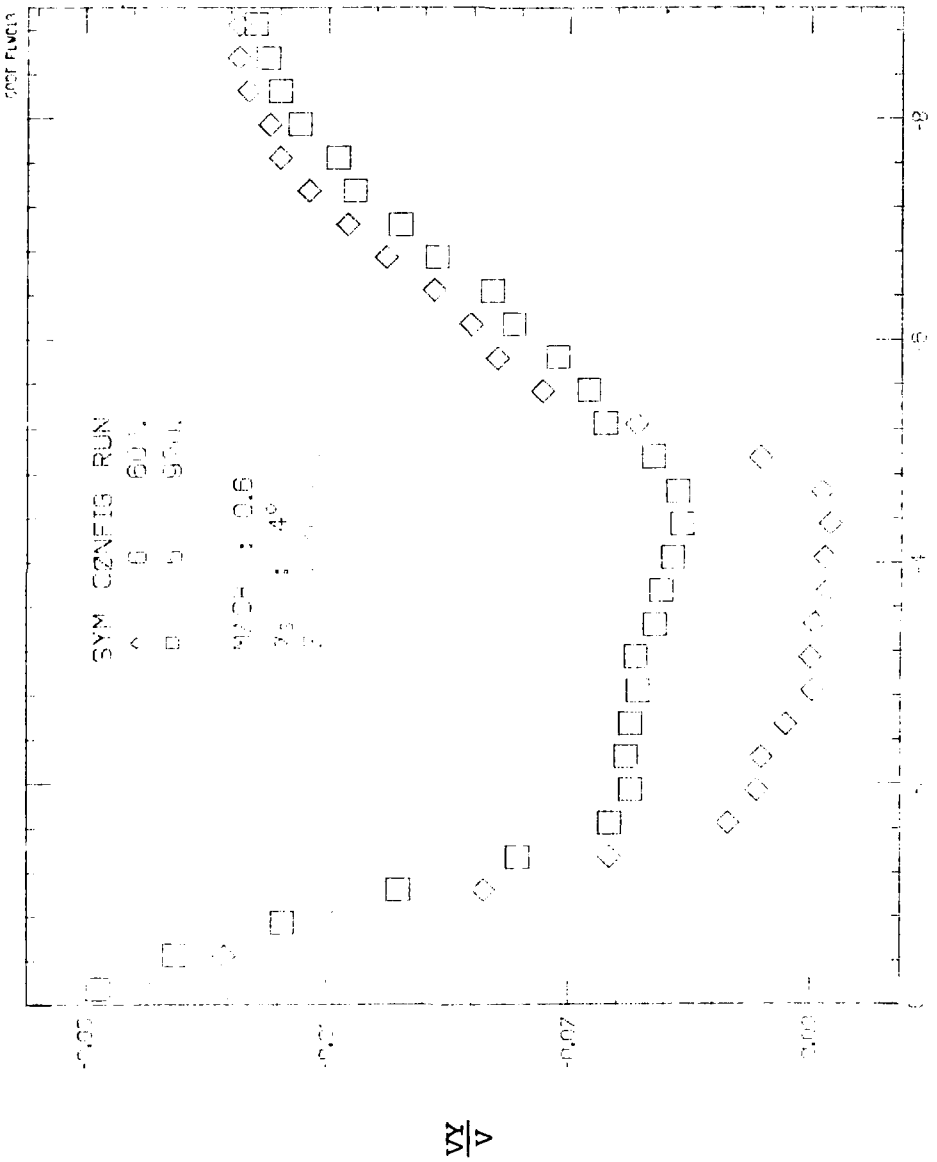

(b) Sidewash angle.

FIGURE 35. Concluded.

ASSUMPTIONS OF THE COMPUTER PROGRAM

The computer program is based on linear theory, Laplace's equation for the flow field with the Glauert-Prandtl theory to account for compressibility. The fuselage, which can be noncircular, is modeled by using sources, doublets, and high-order solutions along the axis of the fuselage to satisfy its boundary conditions, with a vortex-lattice layout on the wing to satisfy the wing boundary conditions. The vortex-lattice system is imaged in the fuselage (assumed circular). Wing thickness is modeled by source panels. Account is taken of airflow through inlets and ducts by changing the effective cross-sectional area distribution of the body.

The pylon is modeled with regard to thickness by source panels and with regard to the normal velocity boundary condition by a vortex-lattice layout.

The rack is modeled for volume by a body of revolution.

The stores are modeled for volume by three-dimensional source distributions along their axes. No mutual interference between stores or between stores and rack is accounted for. No doublets to model store angle of attack distributions are included. The tail fins of the shoulder stores are not modeled.

The forces on the ejected store are calculated by slender-body theory. Both upwash and sidewash distributions are taken into account. Also a loading due to buoyancy is included in the calculation. If the flow separates at some axial station, crossflow drag theory is

used to calculate the loading downstream of separation. The tail fin contributions are determined using the spanwise variation of induced downwash across the tail span together with reverse-flow theorems in a method which has accuracy nearly equivalent to full linear theory.

POSSIBLE SHORTCOMINGS OF COMPUTER PROGRAM

In the ensuing remarks a distinction will be made between the problem of determining the loads on a separating store sufficiently accurately to calculate its separation trajectory and the problem of accurately predicting attached loads. The large changes in loads in the first few tenths of diameter of store downward travel do not need to be accurately predicted for the first problem because the store spends very little of its total time under the influence of the aircraft in this region. With regard to the second problem it should also be borne in mind that the attached aerodynamic loads are also augmented by inertial loads, and therefore represent only part of the maximum loads.

The questions that need examination with respect to the computer program are largely those of whether the airplane, pylon, rack, and stores are individually adequately modeled, and whether their mutual interferences are properly accounted for. Additional questions arise concerning the limits of the computer program because of nonlinear effects of angle of attack and Mach number. Some remarks concerning the pylon-rack-store interference problem should be helpful in the subsequent comparisons between experiment and theory.

With regards to Figure 5, the pylon is a lifting surface which should be modeled fairly accurately by vortex-lattice methods. Its effect on the store is minimized by the fact that the store is fairly far away because of the intervening rack. At angle of attack $\alpha_s = 4^o$, Figure 29(b) shows about 3^o of sidewash at the store position. At the rack, the sidewash would be still higher. The rack is modeled as a body of revolution, and no doublets to account for downwash or sidewash at the rack are included in the model.

Figure 3 shows a detailed model of the TER. The first 0.8 in. of the rack has cross sections similar to the upper half of the cross-sectional shape shown. This part of the rack is probably modeled sufficiently accurately by a body of revolution. From 0.8 in. to about 2.2 in., the rack has the A-A cross section shown. In effect a secondary pylon exists beneath the rack which is in close proximity to the store. This secondary pylon is not properly accounted for by modeling the rack as a body of revolution. The rear part of the rack is hexagonal, and is well modeled by a body of revolution. The rack as a body of revolution is over a rack diameter away from the lower store. Since the flow field of three-dimensional sources drops off with radius as r^{-2} and that due to doublets as r^{-3}, it is to be expected that the source terms due to the rack will dominate the lower store. For the shoulder stores it may not be true that this is the case because of the close proximity of the rack to the shoulder stores.

Consider now the shoulder store modeling. In the computer codes they are modeled only by source distributions with no mutual interference between each other or between rack and lower store. There are upwash and sidewash angles

at the shoulder store locations which should be modeled for attached loads. Also the mutual interference among all stores and the rack should be accounted for.

In determining the loads on the lower store, the flow field induced directly by the rack and shoulder stores is taken into account with no mutual interference between these components. Such mutual interference should probably be accounted for to obtain better estimates of the induced flow field at the bottom store position. When the bottom store is introduced, it produces additional mutual interference between itself and the rack and shoulder stores. This mutual interference arises from bottom store source and doublet distributions. It seems, that as a minimum, mutual interference among the sources should be accounted for, and possibly also doublets near the attached position.

Finally, tail fins on the shoulder stores are not accounted for in the computer program. Modeling them is probably of secondary importance compared to the above shortcomings based on the small differences seen between configurations 5 and 6.

COMPARISON BETWEEN DATA AND THEORY FOR CLEAN AIRPLANE

In the ensuing comparisons, the effects of adding the pylon to the clean airplane, the effect of adding the rack to the pylon, and the effect of adding the shoulder stores to the rack will be isolated and compared with theory. These increments are all to be added to the clean airplane characteristics as a base configuration. It is therefore

of interest to examine the comparison between experiment and theory for the clean airplane.

In Figure 36 the downwash and sidewash angles are shown along the $Z_p/D = 0$ location for $M_\infty = 0.6$ for various angles of attack. It is noted that the experimental upwash angle is predicted fairly well up to about 8° angle of attack although it is consistently less than theory. Significantly large deviations between experiment and theory occur by the time $\alpha_s = 16^\circ$ is reached. The sidewash is predicted well up to $\alpha_s = 8^\circ$. The deviations that do exist at the higher angles could be due to a number of considerations such as departure of the aircraft lift from the range of linearity, imprecise model dimensions, tunnel flow angularity, and mismatch of the engine mass flow ratio between the theoretical model and the wind-tunnel model.

Before comparing the theory and experiment for the forces and moments measured under the conditions of Figure 36, it is of interest to describe the characteristics of store S_{MF} used in the comparison. Test data for the store with and without tail fins in the X configuration were used to determine the increment in normal force due to adding the tail fins to the body. The increment was divided between tail fins and the body in accordance with the K_W and K_B interference factors described in Reference 7. The body alone has a boattail with possible separation. A crossflow drag coefficient was selected for the afterbody based on crossflow Mach number, and an axial position of separation was chosen for the body alone so that the normal force was correctly predicted. The pitching moments of the body alone and body-tail were then predicted from the theory using the theoretical center-of-pressure positions. The resulting theoretical characteristics of the store S_{MF}

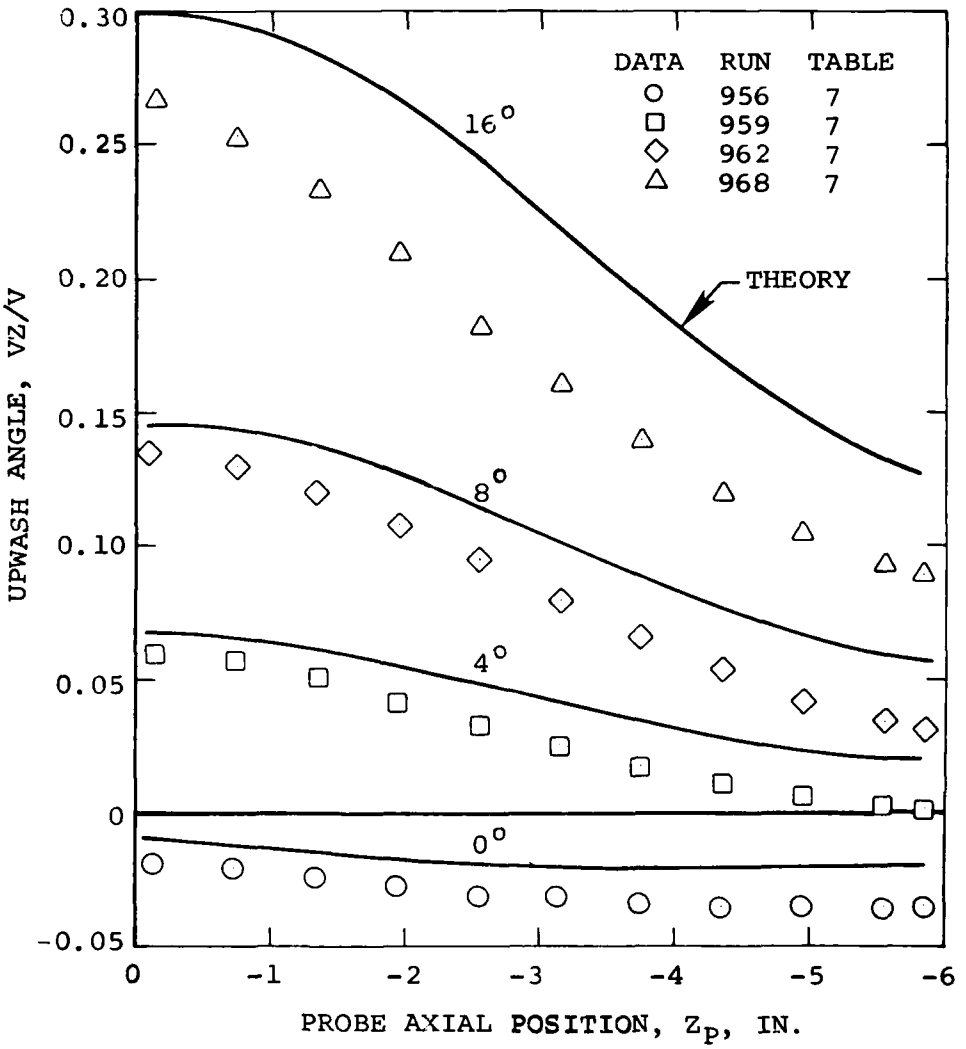

(a) Upwash angle.

FIGURE 36. Flow Field Comparisons for Clean Airplane at M_∞ = 0.6 and Z_p/D = 0 as a Function of Angle of Attack.

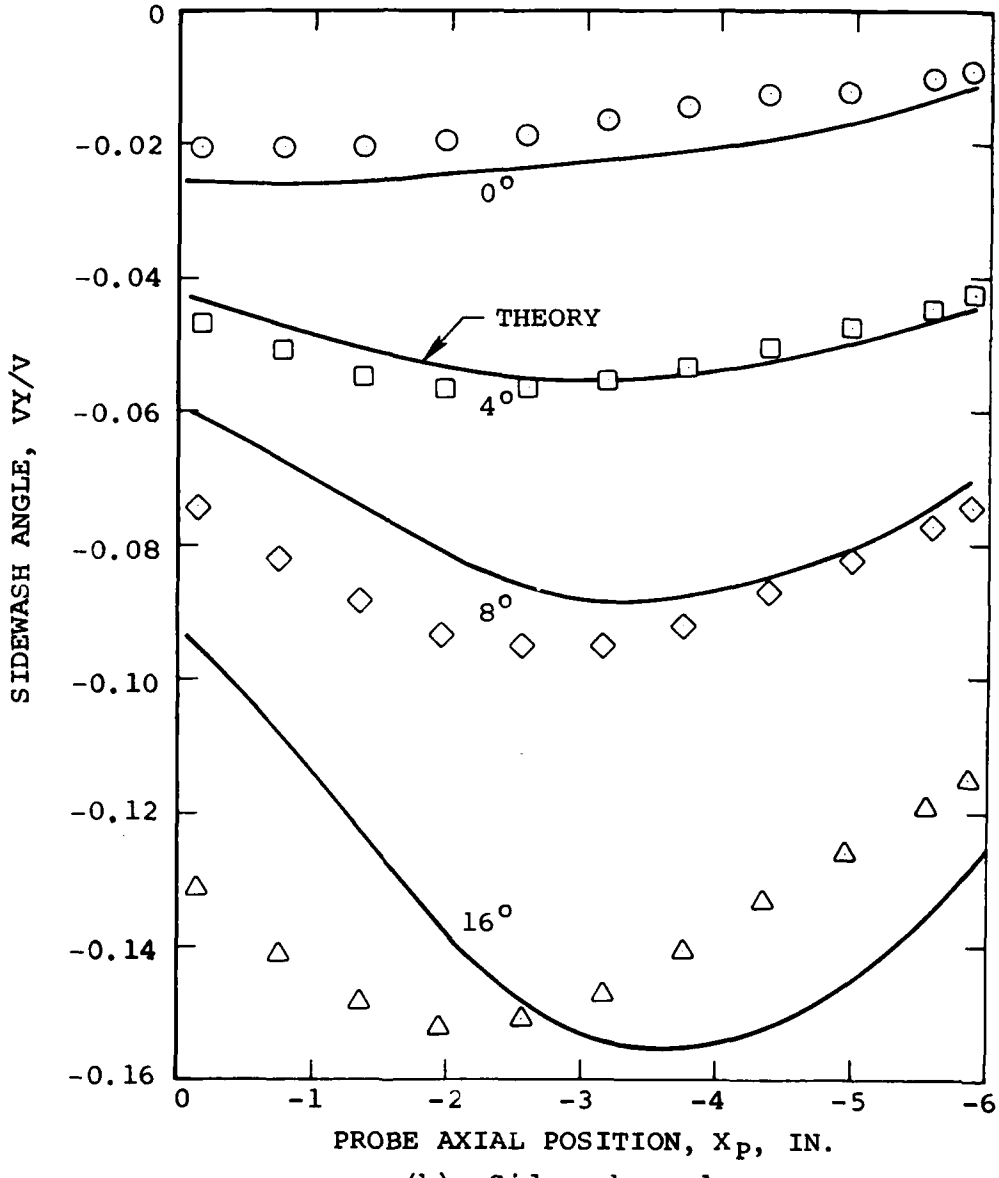

(b) Sidewash angle.

FIGURE 36. Concluded.

are shown in Figure 37 for $M_\infty = 0.6$ together with the measured normal-force, pitching-moment, and rolling-moment characteristics. The rolling moment is associated with 2° of cant of all four tail fins. It is seen that the use of the experimental data in this manner yields good theoretical estimates of the body and body-tail characteristics. The computer program should therefore not give spurious store loads for the various configurations because of inaccuracies in predicting store alone characteristics in a parallel flow.

In Figure 38, the loads on store S_{MF} in combination with the clean airplane at $Z_p/D = 0$ are shown for the angle of attack range from 0° to 16° and compared with the predictions of the computer program. The normal force is predicted well up to about 8°, and is about half of its free-stream value for the same angle of attack. The side force is predicted well up to about 12°. The pitching moments and yawing moments are not well predicted, but they are generally less than those of Figure 37 for the store in the free stream. The center-of-pressure position for yawing moment is in error by as much as 0.5 diameters. In the theory, the separation position on the boattail corresponding to α_s has been used. The results of Figure 36 show that the average angle of attack on the boattail is much less than α_s. Accordingly separation occurs more aft than predicted. This yields more download on the boattail and more nose-up moment. However, the tail will gain upload as a result of decreased separation resulting in a nose-down moment. What we observe is the net effect of those two opposing tendencies. It thus appears that for engineering purposes an improvement to the computer program can be made for boattail bodies by taking account of the local angle of

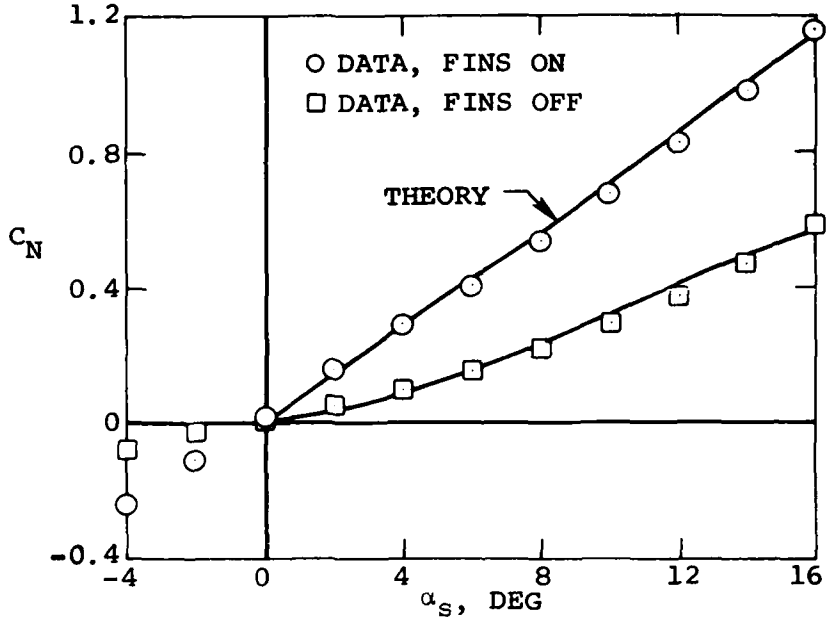

(a) Normal force.

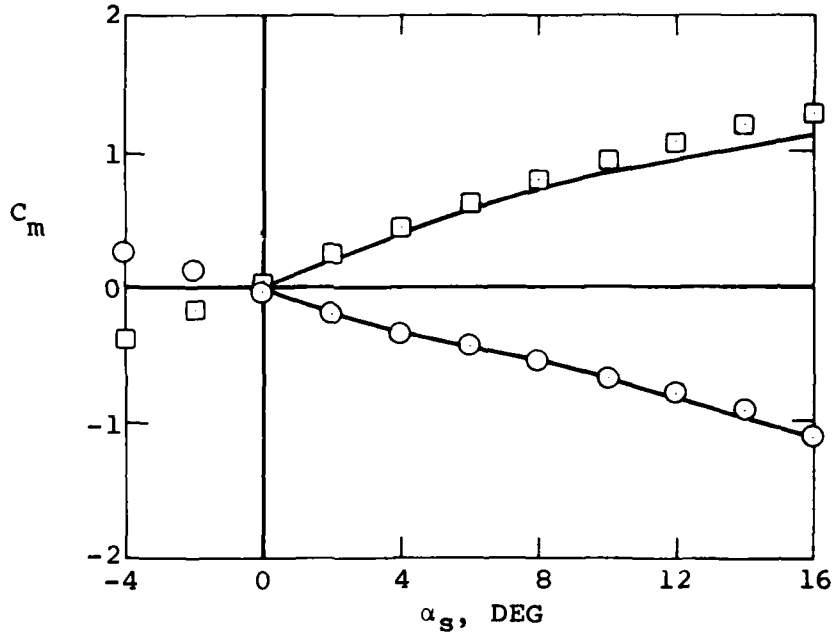

(b) Pitching moment.

FIGURE 37. Comparison Between Experiment and Theory for the Free-Stream Aerodynamics of Store S_{MF} at $M_\infty = 0.6$.

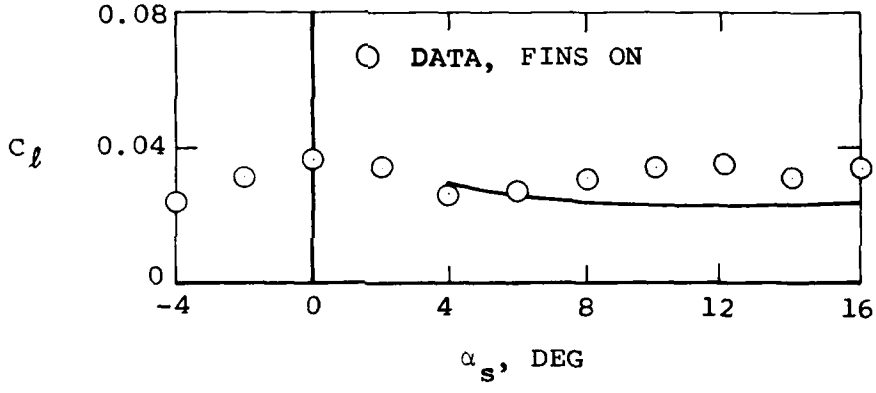

(c) Rolling moment.

FIGURE 37. Concluded.

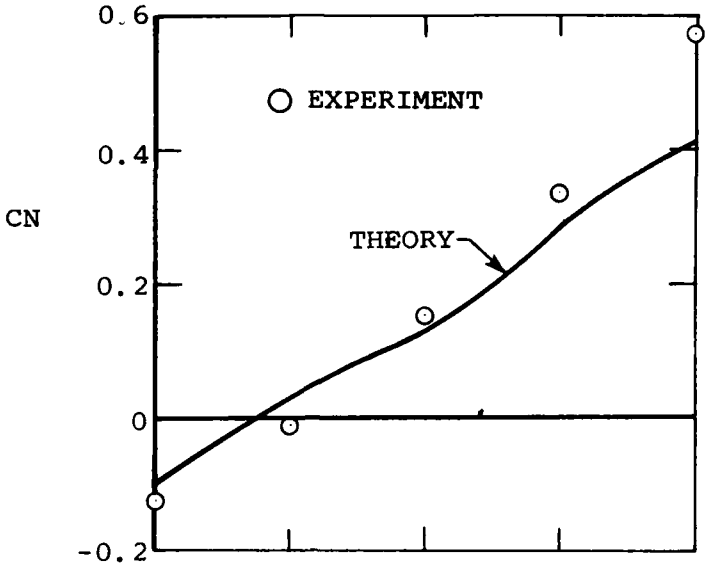

(a) Normal force.

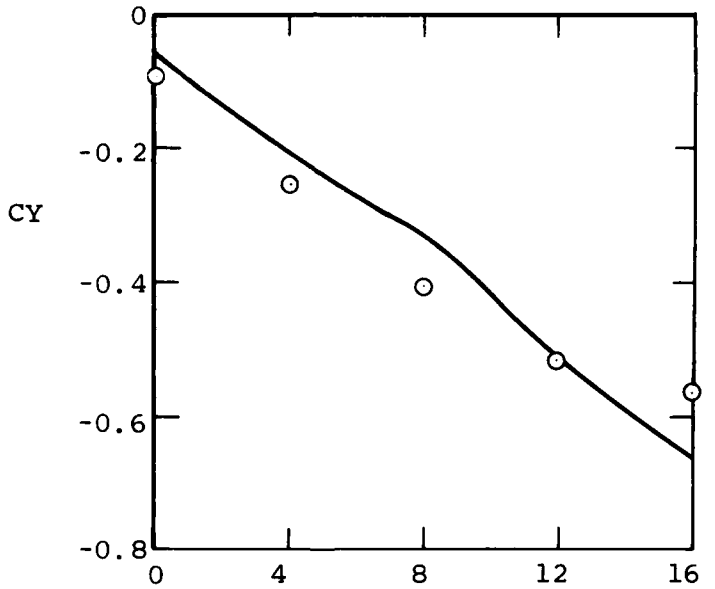

(b) Side force.

FIGURE 38. Loads on Store S_{MF} in Combination with Clean Airplane at $M_\infty = 0.6$; $Z_p/D = 0$.

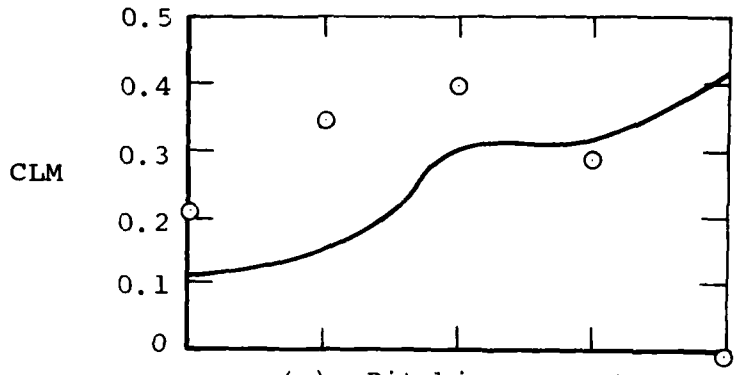

(c) Pitching moment.

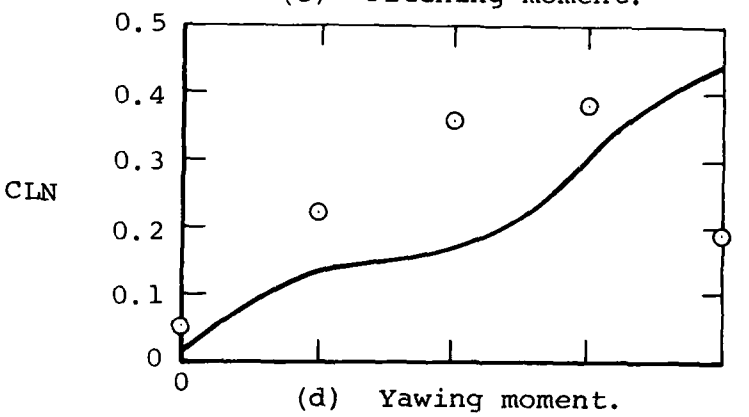

(d) Yawing moment.

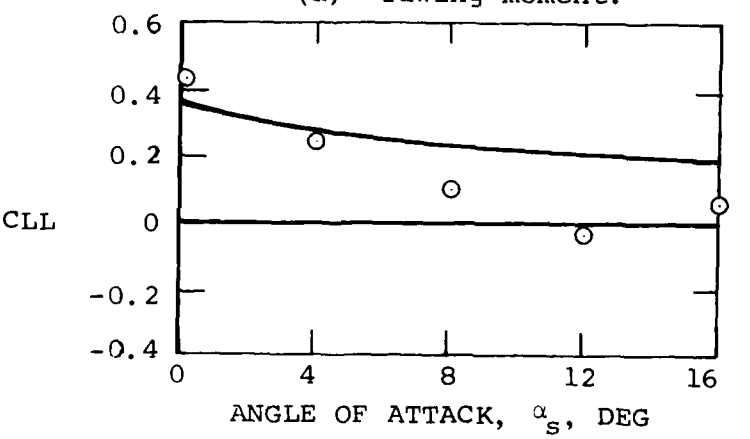

(e) Rolling moment.

FIGURE 38. Concluded.

attack and sidewash on the boattail in specifying the separation location.

The rolling-moment coefficient is small, and is fairly well predicted.

Similar results in Figure 39 for $Z_p/D = 1.0$ exhibit similar results as for $Z_p/D = 0$.

COMPARISON BETWEEN DATA AND THEORY FOR EFFECT OF THE PYLON

The effects on the flow field of adding the pylon to the airplane can be determined by subtracting data for configuration 1 from that for configuration 2. In this way the effects of the pylon can be examined unmasked by configuration 1 effects. The next four figures show the pylon effects on upwash and sidewash at $M_\infty \approx 0.6$ for the four following conditions:

Figure	α_s	Z_p/D
40	0	0
41	0	1
42	4°	0
43	4°	1

It is clear that the pylon effect on the flow field is small and accurately predicted for the conditions shown.

It would be normally assumed that if the flow angles induced by the pylon at the store location are small, that

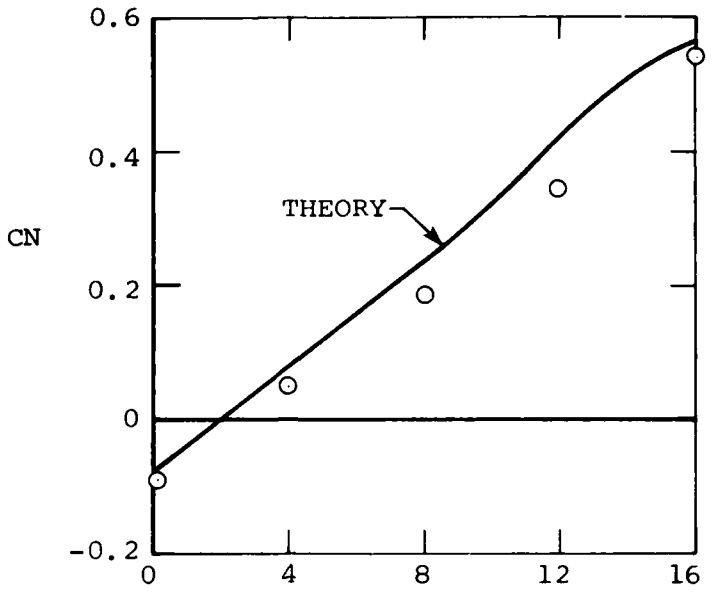

(a) Normal force.

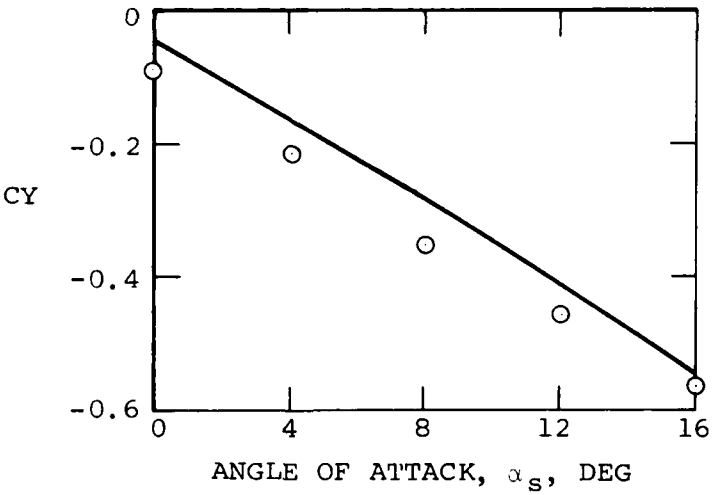

(b) Side force.

FIGURE 39. Loads on Store S_{MF} in Combination with Clean Airplane at $M_\infty = 0.6$; $Z_p/D = 1.0$.

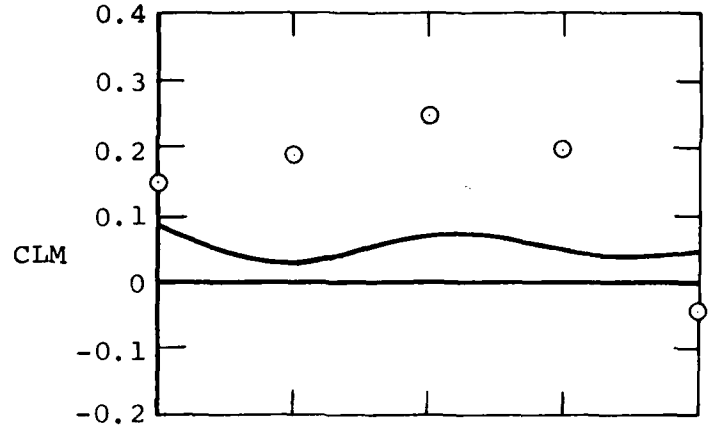

(c) Pitching moment.

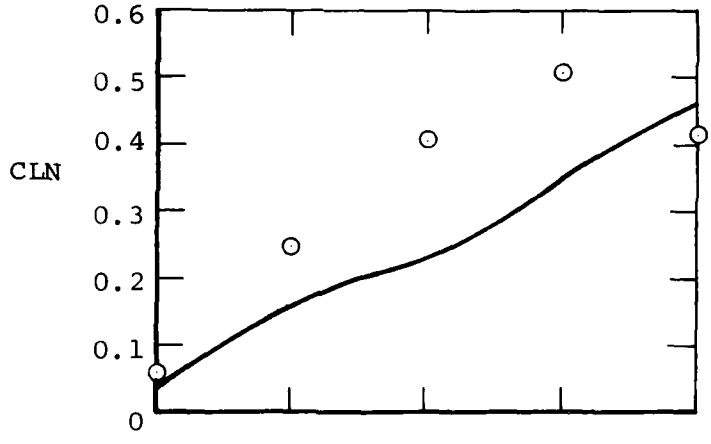

(d) Yawing moment.

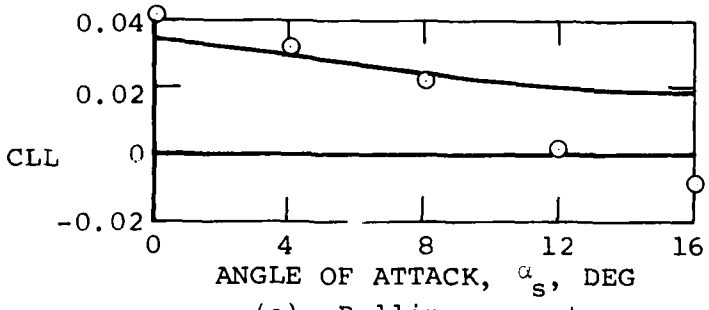

(e) Rolling moment.

FIGURE 39. Concluded.

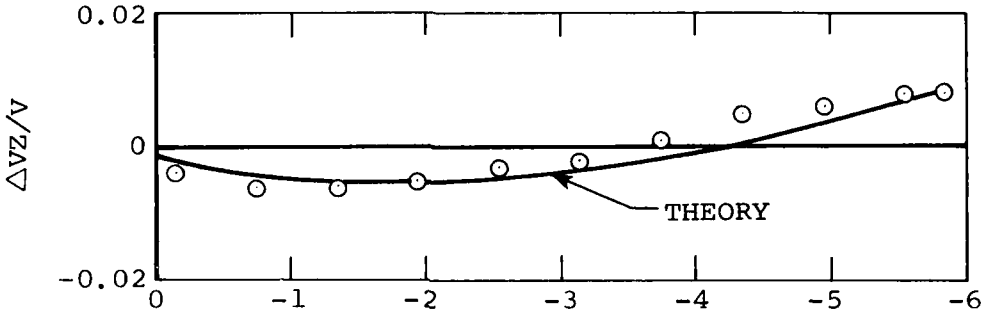

(a) Upwash angle.

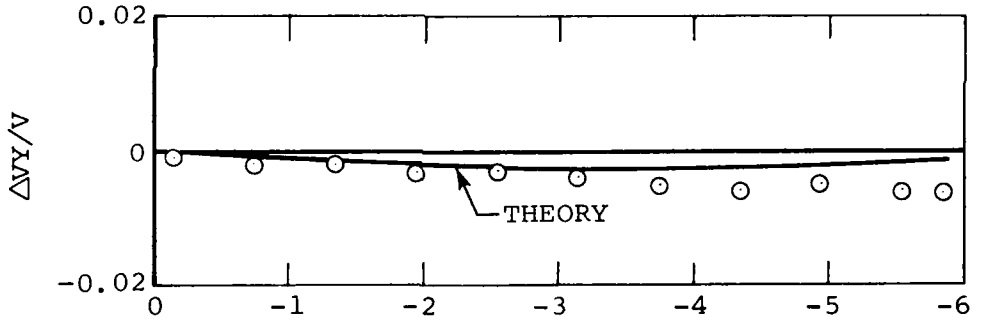

(b) Sidewash angle.

FIGURE 40. Effect of Adding a Pylon to the Clean Airplane on the Flow Angles Along the Centerline Position of the Bottom Store at M_∞ = 0.6; i_s = 0°; Z_p/D = 0.

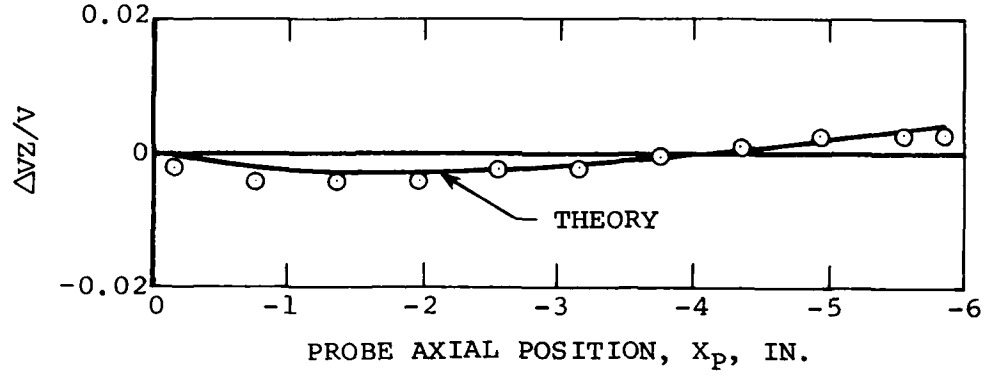

(a) Upwash angle.

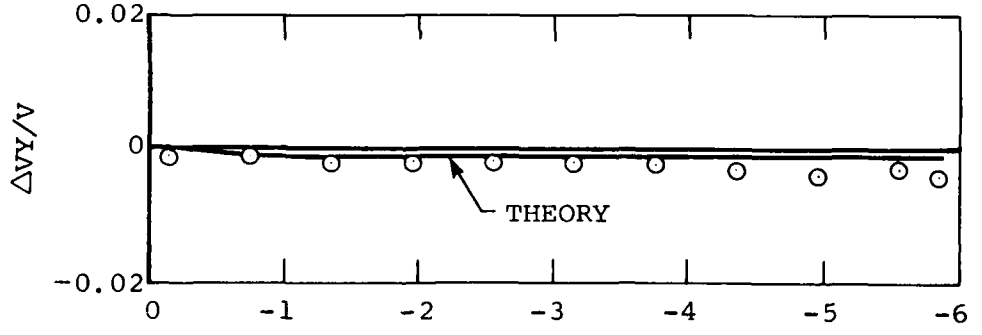

(b) Sidewash angle.

FIGURE 41. Effect of Adding a Pylon to the Clean Airplane on the Flow Angles Along the Centerline Position of the Bottom Store at $M_\infty = 0.6$; $\alpha_s = 0^\circ$; $Z_p/D = 1.0$.

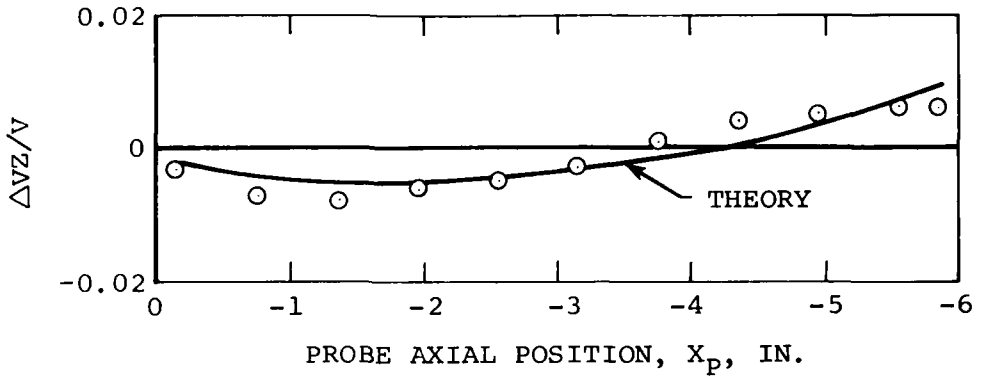

(a) Upwash angle.

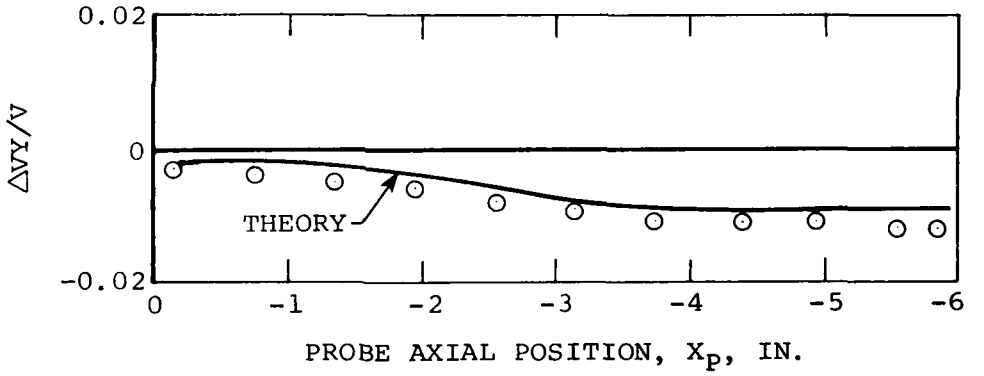

(b) Sidewash angle.

FIGURE 42. Effect of Adding a Pylon to the Clean Airplane on the Flow Angles Along the Centerline Position of the Bottom Store at $M_\infty = 0.6$; $\alpha_s = 4^\circ$; $Z_p/D = 0$.

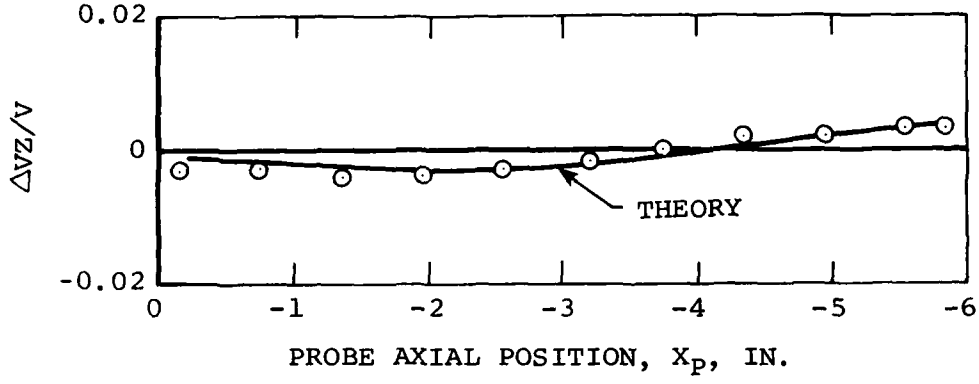

(a) Upwash angle.

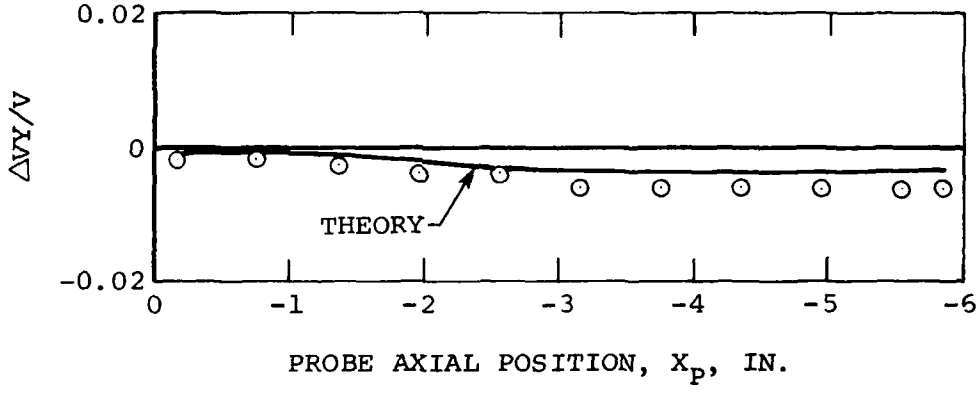

(b) Sidewash angle.

FIGURE 43. Effect of Adding a Pylon to the Clean Airplane on the Flow Angles Along the Centerline Position of the Bottom Store at $M_\infty = 0.6$; $\alpha_s = 4^\circ$; $Z_p/D = 1.0$.

the corresponding loads induced by the pylon on the store would be small. As an example, consider the following table which shows the loads on the S_{MF} stcre for the four above cases due to the addition of the pylon.

TABLE 8. Loads Due to Pylon.

S_{MF}; $M_\infty = 0.6$

	Z_p/D	ΔCN	ΔCY	ΔCLM	ΔCLN	ΔCLL
(a) $\alpha_s = 0°$ $Z_p/D = 0$						
Data	0.07	0.063	-.019	-.206	0.028	0.002
Theory	0	.031	-.010	-.145	.001	0
(b) $\alpha_s = 0°$ $Z_p/D = 1.0$						
Data	1.20	0.030	-.008	-.100	0.012	0.001
Theory	1.00	.016	-.004	-.077	.001	0
(c) $\alpha_s = 4°$ $Z_p/D = 0$						
Data	0.10	0.069	-.061	-.220	0.071	0
Theory	0	.028	-.048	-.138	.051	0.001
(d) $\alpha_s = 4°$ $Z_p/D = 1.0$						
Data	1.24	0.031	-.024	-.096	0.031	-.003
Theory	1.00	.020	-.022	-.072	.029	0

Generally speaking the difference between experiment and theory is not large so that the loads were satisfactorily predicted.

An interpretation of the above loads will now be attempted. The largest change in CN is 0.069 and the largest change in CLM is -.220. Based on the slopes of the CN and CM curves at the origin in Figure 37, those values

correspond to free-stream angles of attack of the store of 1^{o} and 2.2^{o}, respectively. No such large pylon-induced flow angles are to be found in Figures 40-43. The combined effects of flow curvature and mutual interference appear to have the possibility of magnifying the effects over what might be expected on the grounds of induced flow angle alone when the store is in close proximity to the interfering component.

COMPARISON OF DATA AND THEORY FOR THE EFFECT OF ADDING THE TER

The effects on the flow field of adding the rack to the airplane pylon combination are shown in Figures 44-47. These results for both data and theory represent configuration 3 minus configuration 2. The first thing that is clear is that the induced angles of upwash and sidewash are generally several times larger than those due to the pylon at $Z_p/D = 0$. It is also apparent that the effect of the rack attenuates much in going from $Z_p/D = 0$ to $Z_p/D = 1.0$. For instance, the induced upwash maxima fall from about -0.04 to about -0.01 in this distance. It happens that the $Z_p/D = 0$ position is about one diameter below the centerline of the rack and the $Z_p/D = 1.0$ position is about two diameters below the rack centerline. This suggests that the upwash is strongly source dominated. The effect of the rack is modeled solely by sources in the theory. However, the theoretical source effect is too weak, particularly at $Z_p/D = 0$.

Looking at the sidewash angle, the maximum sidewash exists at $Z_p/D = 0$ and attenuates greatly at $Z_p/D = 1$. The theory predicts no sidewash since the rack sources produce none directly below themselves. It is clear that

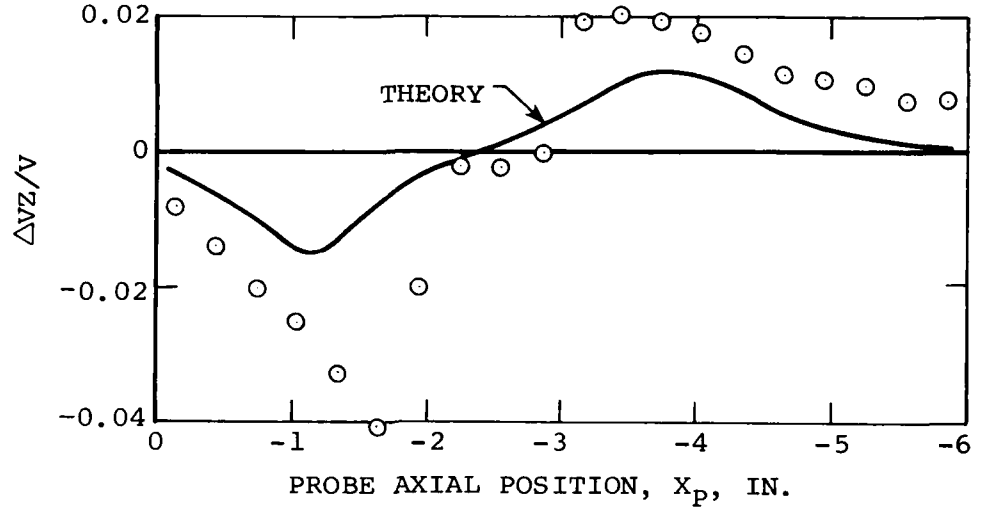

(a) Upwash angle.

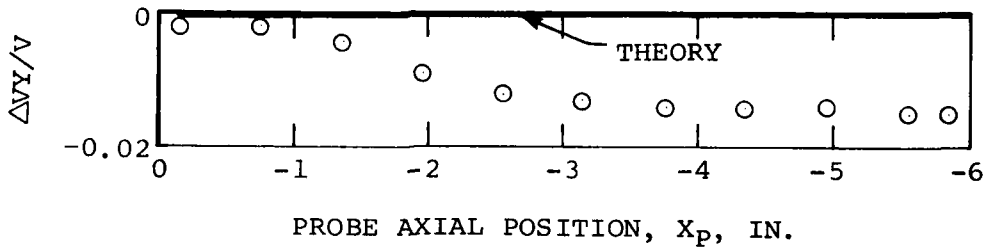

(b) Sidewash angle.

FIGURE 44. Effect of Adding TER to Pylon on the Flow Angles Along the Centerline Position of the Bottom Store at $M_\infty = 0.6$; $\alpha_s = 0°$; $Z_p/D = 0$.

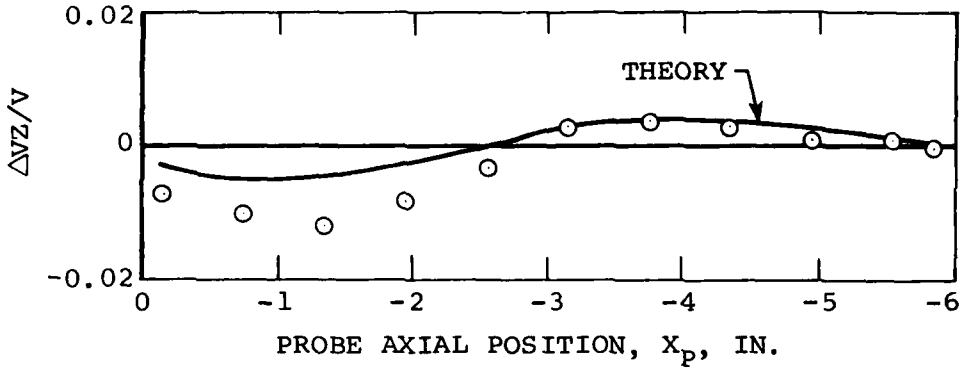

(a) Upwash angle.

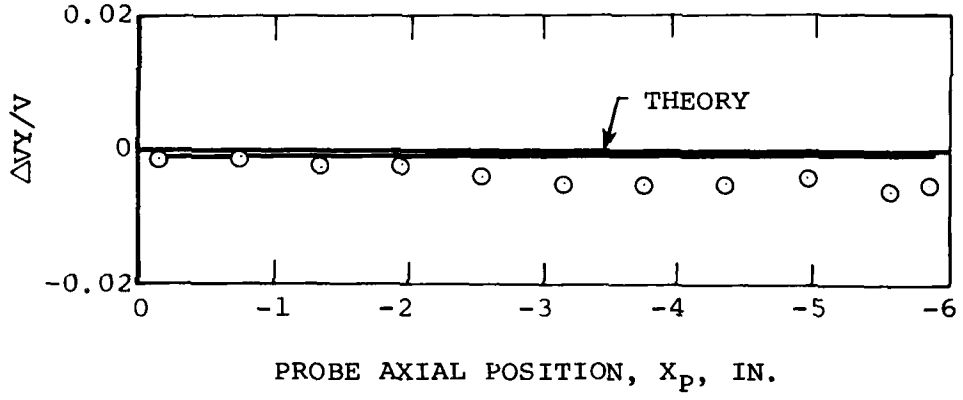

(b) Sidewash angle.

FIGURE 45. Effect of Adding TER to Pylon on the Flow Angles Along the Centerline Position of the Bottom Store at $M_\infty = 0.6$; $\alpha_s = 0°$; $Z_p/D = 1.0$.

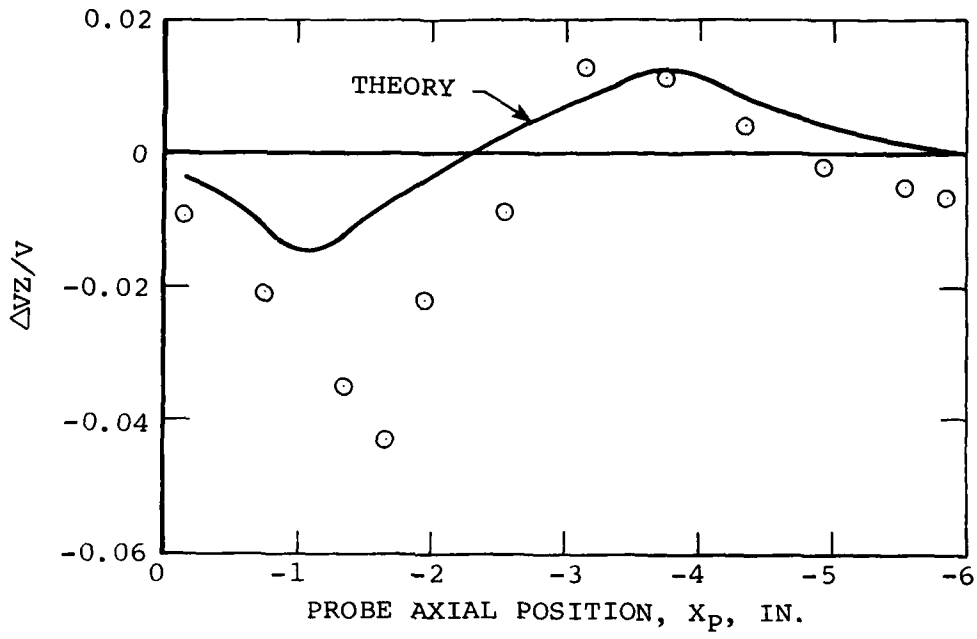

(a) Upwash angle.

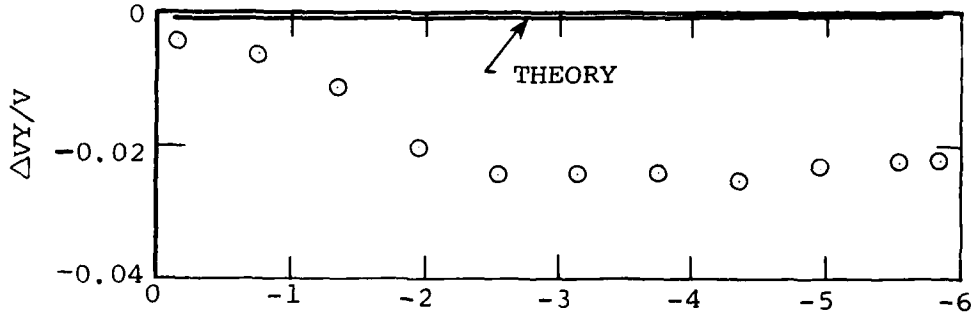

(b) Sidewash angle.

FIGURE 46. Effect of Adding TER to Pylon on the Flow Angles Along the Centerline Position of the Bottom Store at $M_\infty = 0.6$; $\alpha_s = 4^\circ$; $Z_p/D = 0$.

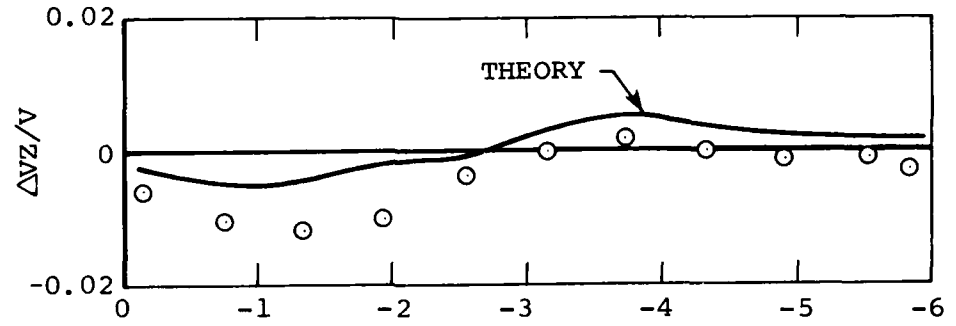

(a) Upwash angle.

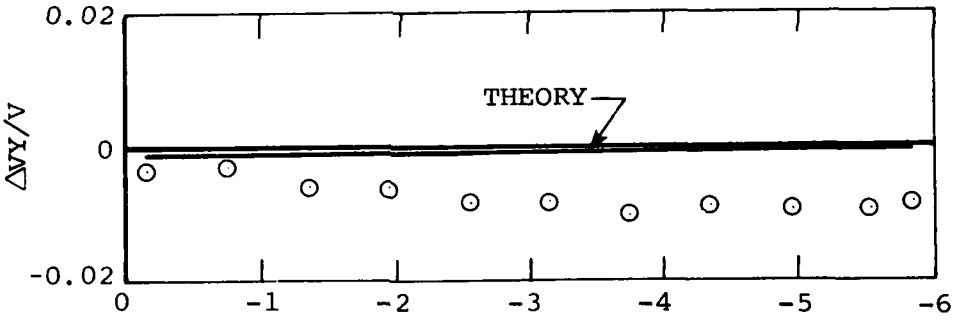

(b) Sidewash angle.

FIGURE 47. Effect of Adding TER to Pylon on the Flow Angles Along the Centerline Position of the Bottom Store at M_∞ = 0.6; α_s = 4°; Z_p/D = 1.0.

mechanisms to produce sidewash due to addition of the rack must be introduced into the computer program.

It might appear that the introduction of doublets to cancel both upwash and sidewash velocities along the rack are called for since they are not used in the computer program. However, it appears probable that doublet effects will attenuate too fast to achieve the desired magnitude of effect. If one compares the effects of the pylon in Figures 40-43 with the effects of the rack in Figures 44-47, one is struck by the similarity between the qualitative behaviors of the two. The rack acts like a pylon not a body of revolution. It thus appears that the small "rack pylon" can be modeled as an extension of the main pylon. The rest of the rack can still be modeled as a body of revolution with volume since it will not change the pylon normal velocity boundary conditions.

It is not to be expected that the loads on store S_{MF} due to addition of the rack to the pylon will be predicted well for $Z_p/D = 0$ since the upwash and sidewash are significant at this location, and the theory underpredicts them. It is of interest to examine the load increments due to the rack in a similar form to that for the pylons.

TABLE 9. Loads Due to Rack.

S_{MF}; $M_\infty = 0.6$

(a) $\alpha_s = 0°$ $Z_p/D = 0$

	Z_p/D	ΔCN	ΔCY	ΔCLM	ΔCLN	ΔCLL
Data	0.07	0.116	-.059	-.222	-.003	0.007
Theory	0	.051	.001	-.035	-.002	0

TABLE 9. (Contd.)

(b) $\alpha_s = 0°$ $Z_p/D = 1.0$

	Z_p/D	ΔCN	ΔCY	ΔCLM	ΔCLN	ΔCLL
Data	1.21	0.037	-.015	-.086	0.045	0.001
Theory	1.00	.024	.001	-.027	-.001	0

(c) $\alpha_s = 4°$ $Z_p/D = 0$

Data	0.07	0.042	-.196	0	-.034	+.039
Theory	0	.050	+.001	0.031	-.001	0

(d) $\alpha_s = 4°$ $Z_p/D = 1.0$

Data	1.23	0.019	-.043	-.063	0.040	0
Theory	1.00	.024	0	-.024	0	0

Examination of the foregoing table immediately shows that the computer program gives no contribution to CY, CLN, and CLL due to addition of the rack. This shortcoming of the method is more important at $\alpha_s = 4^o$ than $\alpha_s = 0^o$ since the sidewash is greater at $\alpha_s = 4^o$. An error of about 0.2 in side-force coefficient occurs and about 0.045 in yawing-moment coefficient. There is a surprising effect on rolling-moment at $\alpha_s = 4^o$ and $Z_p/D = 0$, the value of CLL for configuration 3 being 0.064 and for configuration 2 being 0.025. There is a sidewash gradient between the top and bottom fins of the X arrangement which is, if anything, weaker at $Z_p/D = 0$ than at $Z_p/D = 1.0$. Since the effect does not occur at $Z_p/D = 1.0$, some other phenomenon must be producing this difference which is equivalent to about 2^o of cant of all fins. The phenomenon is believed due to a trailing vortex from the rack pylon.

The magnitudes of the largest measured changes in Tables 8 and 9 are now compared.

	$(\Delta CN)_{max}$	$(\Delta CY)_{max}$	$(\Delta CLM)_{max}$	$(\Delta CLN)_{max}$	$(\Delta CLL)_{max}$
Table 8	0.069	0.061	0.220	0.071	0.001
Table 9	.116	.196	.220	.045	.039

The maximum effect of the rack on forces and rolling moment is much greater than that of the pylon, but its maximum effect on pitching moment is about the same.

The lower store is released with the two shoulder stores in position, but for diagnostic purposes it is interesting to see how theory and experiment compare for the way the store loads vary with Z_p/D when the shoulder stores are not present. This information is shown in Figure 48 for $M_\infty = 0.6$ and $\alpha_s = 4^\circ$. The theory and experiment both show wiggles as Z_p/D approaches zero. However, in the last 0.1 a large change in the data to the attached load is shown. The theory also shows a sharp change but in the opposite direction. The side-force coefficient goes smoothly to $Z_p/D = 0$ in both theory and experiment, although the theory is inaccurate near the rack for reasons already pointed out.

The data for the pitching-moment shows an unexpected and unexplained phenomenon in its oscillation near $Z_p/D = 0$. It was thought that this result might be due to spurious data so comparable results for $M_\infty = 0.8$ are shown on

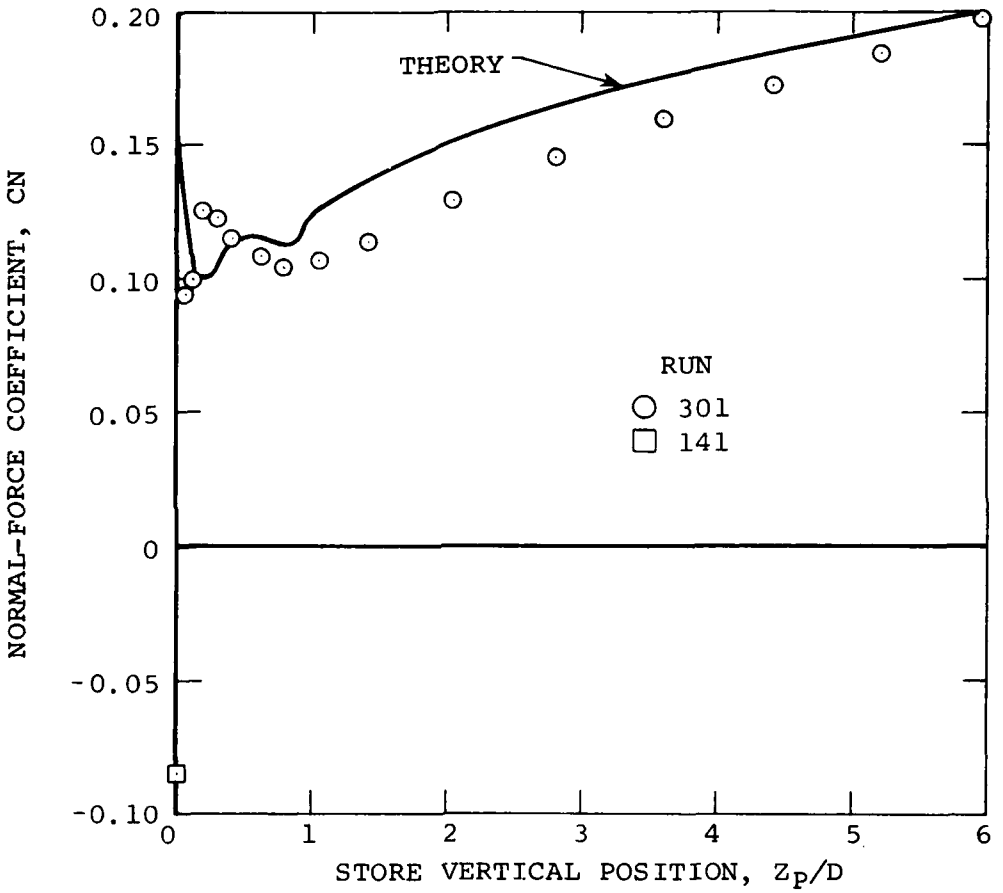

(a) Normal force.

FIGURE 48. Loads on Store S_{MF} Under Configuration 3 at $M_\infty = 0.6$ and $\alpha_s = 4^\circ$.

AD-A094 751 NIELSEN ENGINEERING AND RESEARCH INC MOUNTAIN VIEW CA F/G 1/1
EXPERIMENTAL AND THEORETICAL STUDY OF FLOW FIELDS AND STORE FOR--ETC(U)
SEP 80 F K GOODWIN, J N NIELSEN N60530-79-C-0169
UNCLASSIFIED NEAR-TR-222 NWC-TP-6210 NL

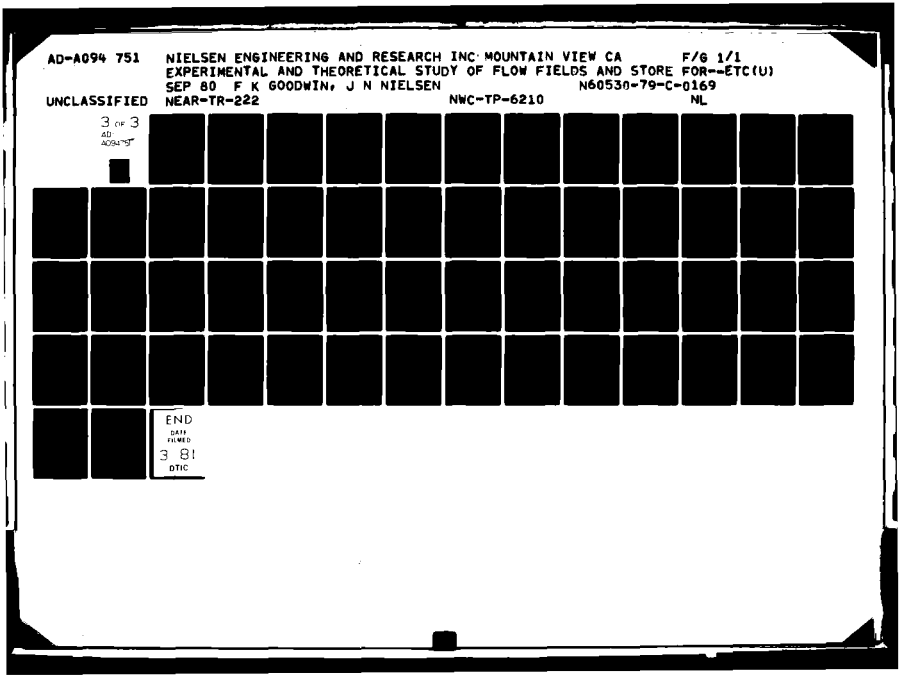

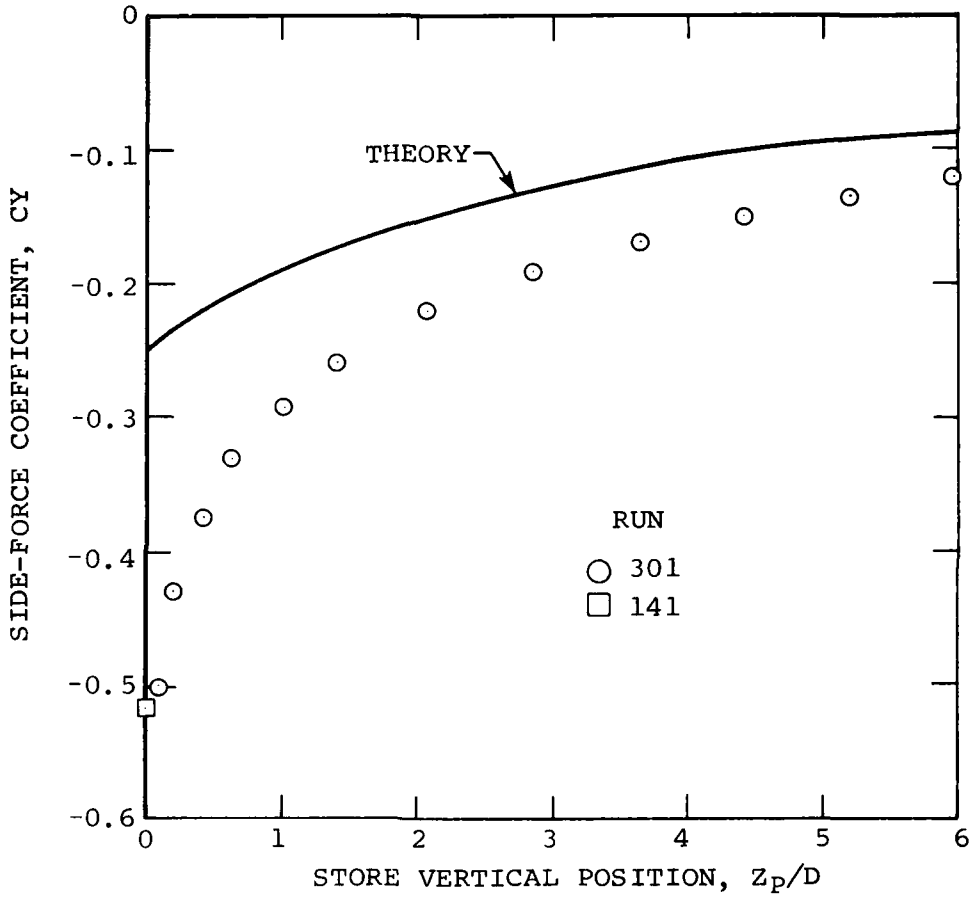

(b) Side force.

FIGURE 48. Continued.

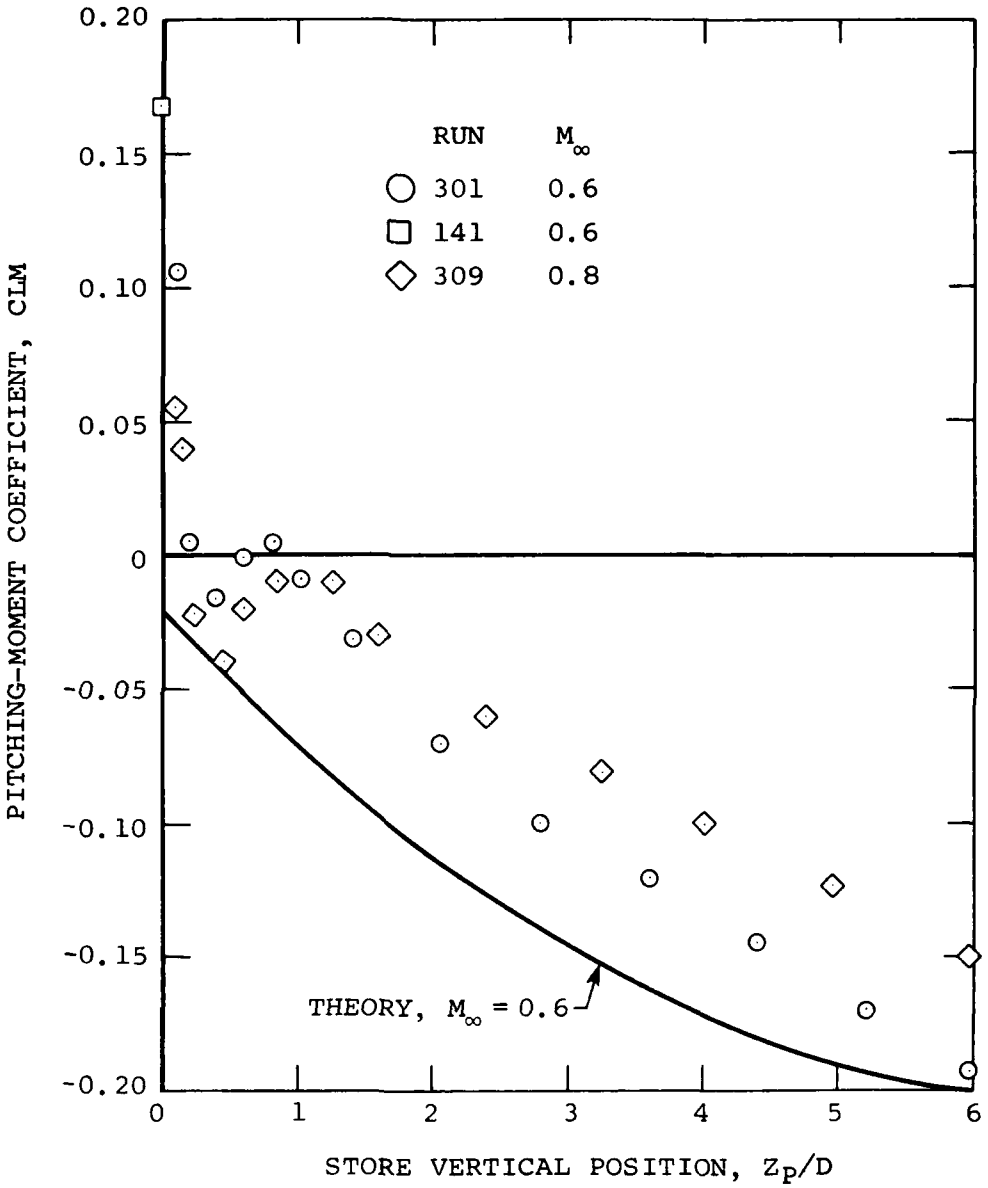

(c) Pitching-moment.

FIGURE 48. Continued.

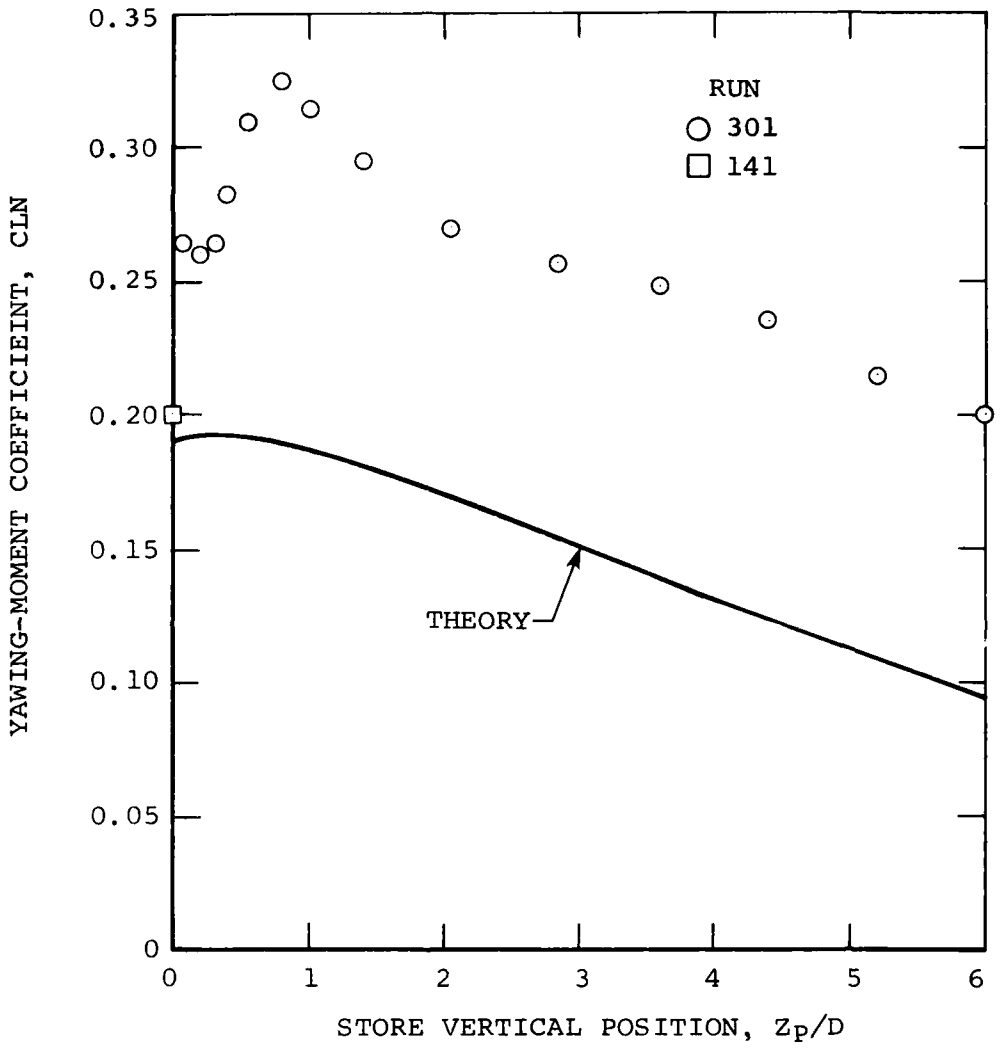

(d) Yawing-moment.

FIGURE 48. Continued.

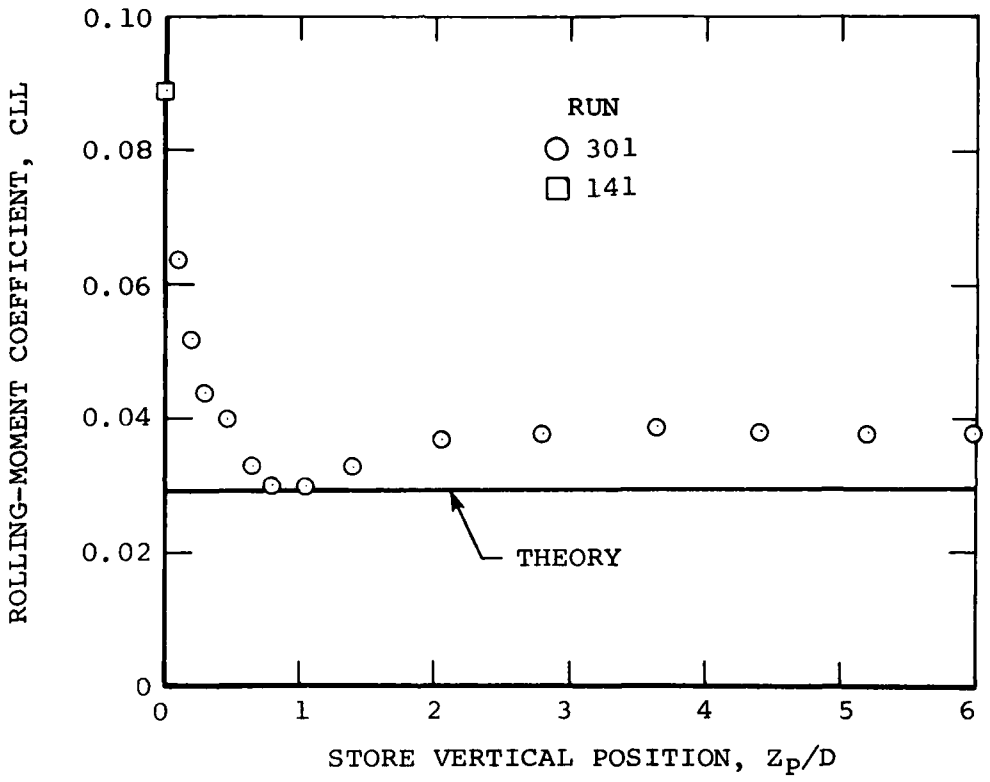

(e) Rolling moment.

FIGURE 48. Concluded.

Figure 48(c). The phenomenon is shown but at a much reduced magnitude. This phenomenon disappears when the shoulder stores are present.

The yawing moment and rolling moment show a change in their trends with Z_p/D for small values of this parameter. For the yawing moment this is readily ascribed to rack-induced sidewash effects neglected in the computer program, but the rolling-moment results are not so easy to explain. Referring to Figure 5, it is seen that the tail fins are well behind the rack and the rack pylon. The possibility of a trailing vortex from the rack pylon seems the only possibility which might induce a rolling-moment coefficient change from 0.04 to 0.09. The rack induced effect is larger than that due to the 2° cant on the fins.

COMPARISON BETWEEN EXPERIMENT AND THEORY FOR EFFECTS OF ADDING THE SHOULDER STORES

The effect of adding the shoulder stores will be determined by taking the difference between the results for configuration 5 and configuration 3. Any effects of the fins of the shoulder stores will not be included by this means. Also, the theory does not include the effect of shoulder store fins, and these have been shown to be small.

Figures 49-52 show the effects on the upwash and sidewash angles along the store axis position for several angles of attack and vertical positions at $M_\infty = 0.6$. Both experiment and theory are shown. The upwash angles get to be nearly as large as -6°, while the sidewash is generally much less

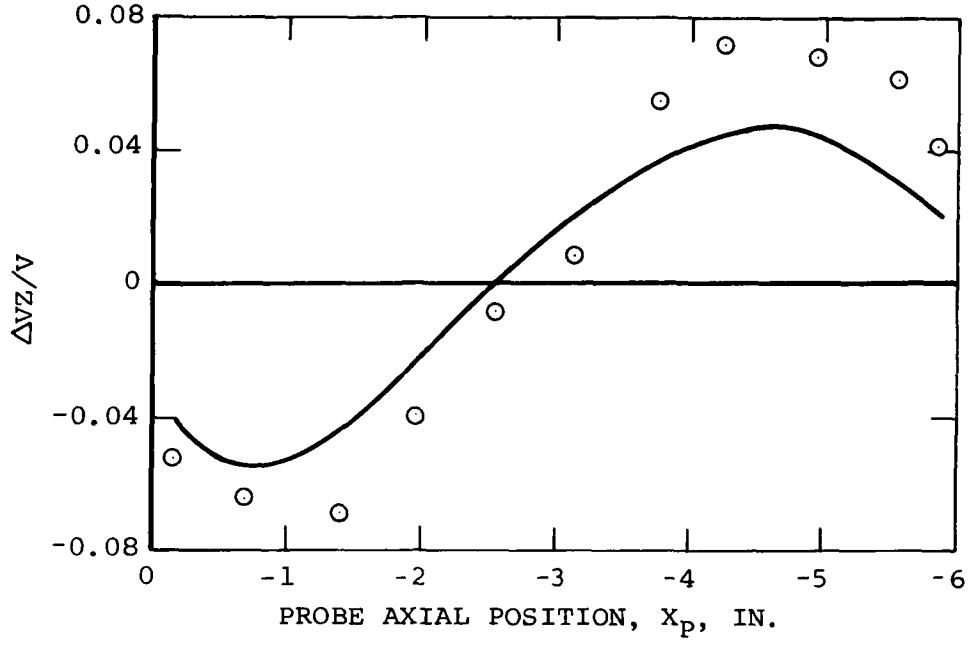

(a) Upwash angle.

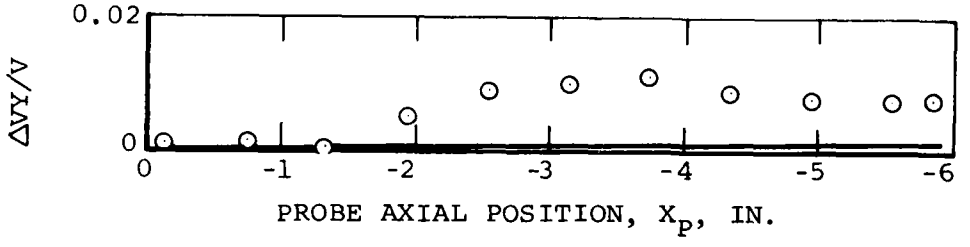

(b) Sidewash angle.

FIGURE 49. Effect of Adding Shoulder Stores to Configuration 3 on the Flow Angles Along the Centerline Position of the Bottom Store; $M_\infty = 0.6$, $\alpha_s = 0^\circ$, $Z_p/D = 0$.

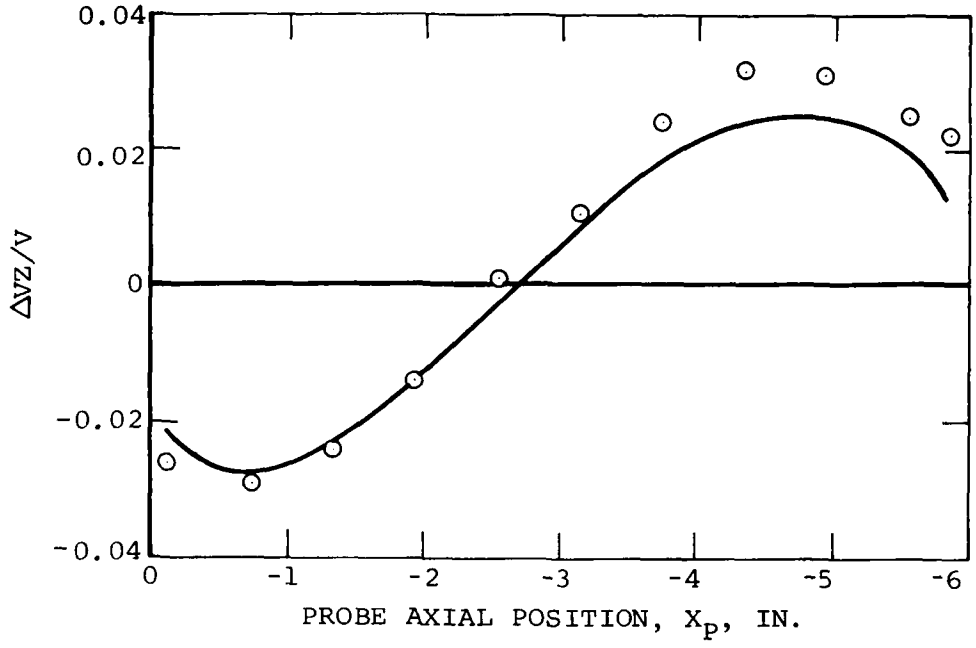

(a) Upwash angle.

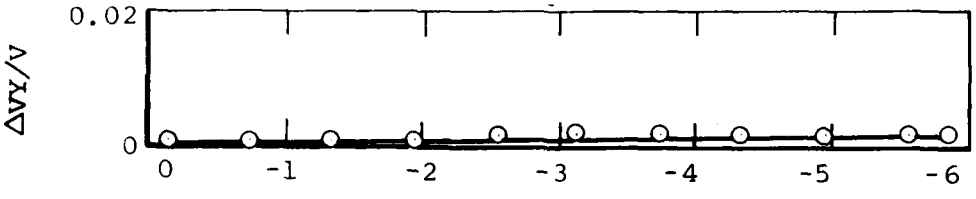

(b) Sidewash angle.

FIGURE 50. Effect of Adding Shoulder Stores to Configuration 3 on the Flow Angles Along the Centerline Position of the Bottom Store; $M_\infty = 0.6$, $\alpha_s = 0°$, $Z_p/D = 1.0$.

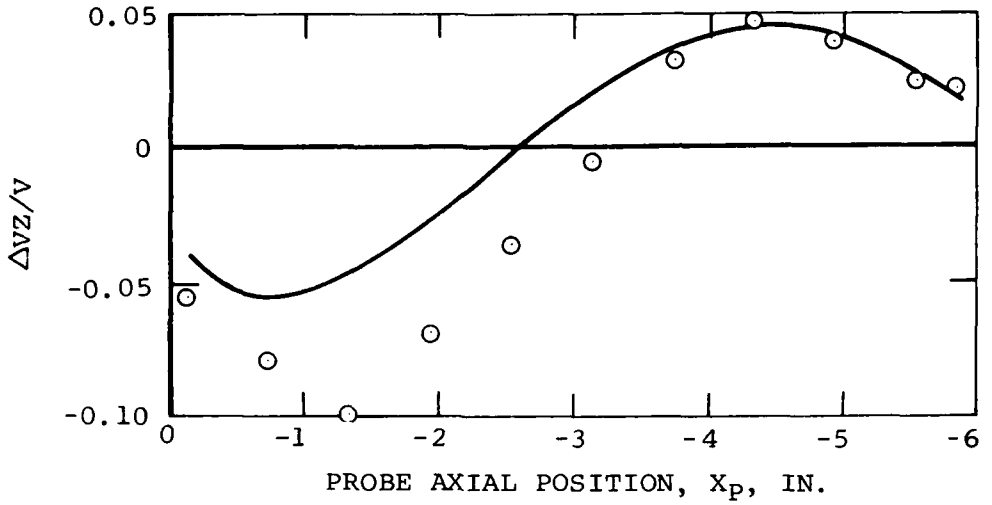

(a) Upwash angle.

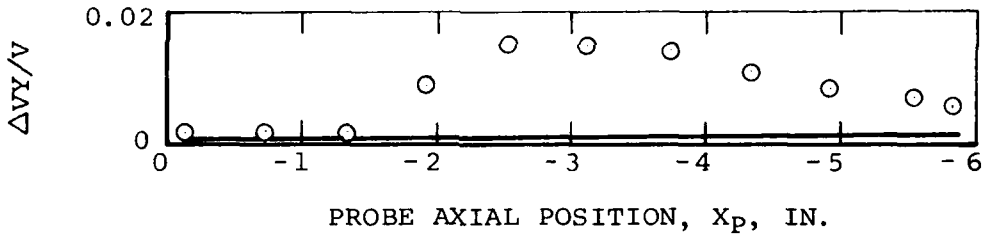

(b) Sidewash angle.

FIGURE 51. Effect of Adding Shoulder Stores to Configuration 3 on the Flow Angles Along the Centerline Position of the Bottom Store; $M_\infty = 0.6$, $\alpha_s = 4^\circ$, $Z_p/D = 0$.

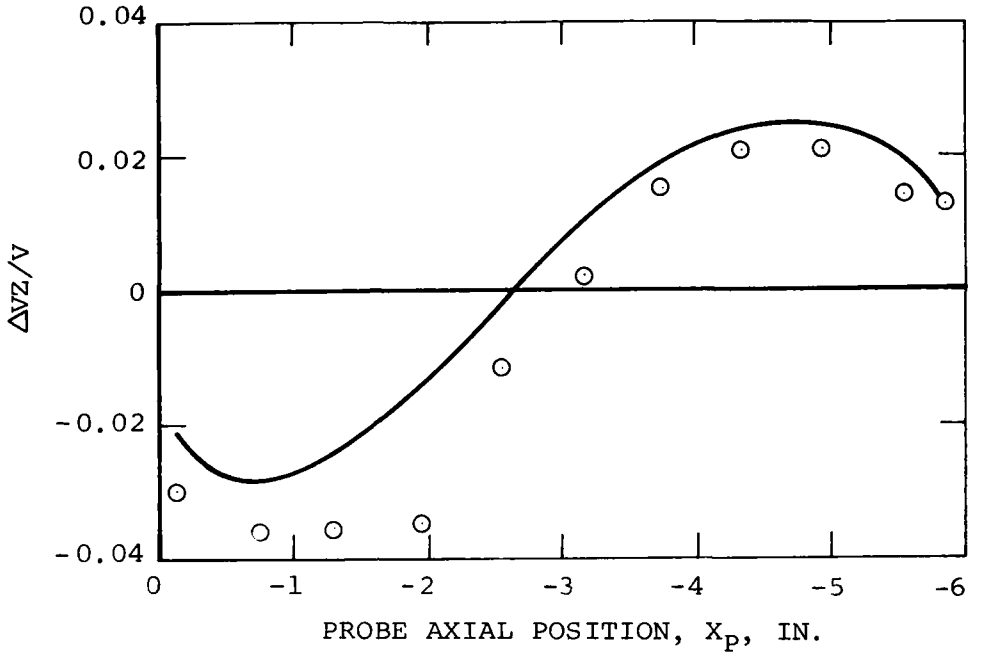

(a) Upwash angle.

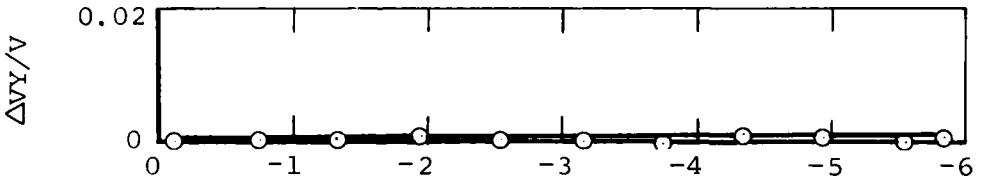

(b) Sidewash angle.

FIGURE 52. Effect of Adding Shoulder Stores to Configuration 3 on the Flow Angles Along the Centerline Position of the Bottom Store; $M_\infty = 0.6$, $\alpha_s = 4^o$, $Z_p/D = 1.0$.

than 1^{o}. The theory in some cases predicts the upwash well, but more often underpredicts it. The degree of agreement is surprising in view of the fact that only the volume effect of the two stores are modeled with no interference between them. Thus the theoretical VZ/V increment due to the shoulder stores at a fixed value of Z_p/D does not vary with α_s. The theoretical sidewash increment, VY/V, is small. By comparison of Figures 49(a) and 51(a) it is clear that some angle-of-attack variation of VZ/V due to the shoulder stores is apparent.

At $Z_p/D = 0$ some sidewash exists but at $Z_p/D = 1$ it is negligible for $\alpha_s = 0^{o}$. At $\alpha_s = 4^{o}$, the sidewash is stronger at $Z_p/D = 0$, but again negligible at $Z_p/D = 1.0$. The rapid decay of this sidewash suggests that some dipole distribution is causing it. The two shoulder stores are subject to sidewash which are not equal. Dipoles to cancel these sidewash boundary conditions will produce differential sidewash under the rack. This represents a possible source of the sidewash. Likewise doublets to cancel the downwash distribution along the shoulder stores would modify the upwash and could account in part for the differences between experiment and theory. Some account of mutual interference between shoulder stores and rack-pylon may be required to get accurate flow fields. The shoulder stores can change the rack-pylon lifting surface boundary condition, the pylon can influence the boundary conditions of the shoulder stores, and the shoulder stores can interfere with each other. These interferences can be evaluated to see which are of sufficient magnitude to influence the flow field. The work of Martin (Reference 8) will be useful in this connection.

It is of interest to see the magnitude of the loads on the bottom store induced by the shoulder stores. The following table presents the resuls for two angles of attack and two vertical positions.

TABLE 10. Loads Due to Shoulder Stores.

S_{MF}; $M_\infty = 0.6$

	Z_p/D	ΔCN	ΔCY	ΔCLM	ΔCLN	ΔCLL
(a) $\alpha_s = 0°$ $Z_p/D = 0$						
Data	0.07	0.456	-.018	-1.049	-.049	0.006
Theory	0	.334	.008	-.605	-0.012	0
(b) $\alpha_s = 0°$ $Z_p/D = 1.0$						
Data	1.2	0.201	-.008	-.452	-.021	0.003
Theory	1.0	.190	.003	-.380	-.010	0
(c) $\alpha_s = 4°$ $Z_p/D = 0$						
Data	0.07	0.237	-.063	-.955	-.022	0.028
Theory	0	.320	.006	-.551	-.008	-.005
(d) $\alpha_s = 4°$ $Z_p/D = 1.0$						
Data	1.23	0.130	0	-.389	-.070	0.013
Theory	1.0	.181	0.005	-.385	-.007	0

The table shows that the addition of shoulder stores has its maximum effects on CN and CLM, and has generally small effects on CY, CLN, and CLL. This result is in general accordance with the flow-field comparisons. It is noted that the changes in CN and CLM are better predicted at $Z_p/D = 1.0$ than at $Z_p/D = 0$, a fact also in agreement with the flow-field results. Some error at

$Z_p/D = 0$ is due to prediction of the flow field. But even with an accurate flow-field prediction, some errors in loads will be predicted at this position. It is probable that mutual interference between all three stores, at least for volume effects, will influence the loads. This could be investigated by the method of Martin (Reference 8).

COMPARISON BETWEEN EXPERIMENT AND THEORY FOR EFFECTS OF MACH NUMBER

In testing the computer program for its ability to predict Mach number effects, we will compare measured and predicted changes in flow angles and store loads between $M_\infty = 0.6$ and $M_\infty = 0.95$. This will be done for the clean airplane configuration so that any problems the computer program may have predicting the interference among pylon, stores, and rack at $M_\infty = 0.6$ will not cloud the comparisons.

The normal-force and pitching-moment curves of store S_{MF} in the free stream at $M_\infty = 0.95$ are input into the computer program for the load comparisons. The method for generating the theoretical characteristics so that they best fit the experimental data has already been described. The fit between experimental and theoretical store-alone characteristics are shown in Figure 53. It is seen that the data for the finned store are matched fairly well except for pitching-moment coefficient at $\alpha_s = 16^\circ$. Hence the body-alone pitching-moment curve is underestimated in the high range of angle of attack. It is not possible to match the data for all four curves precisely with a fixed separation point location even though this was well

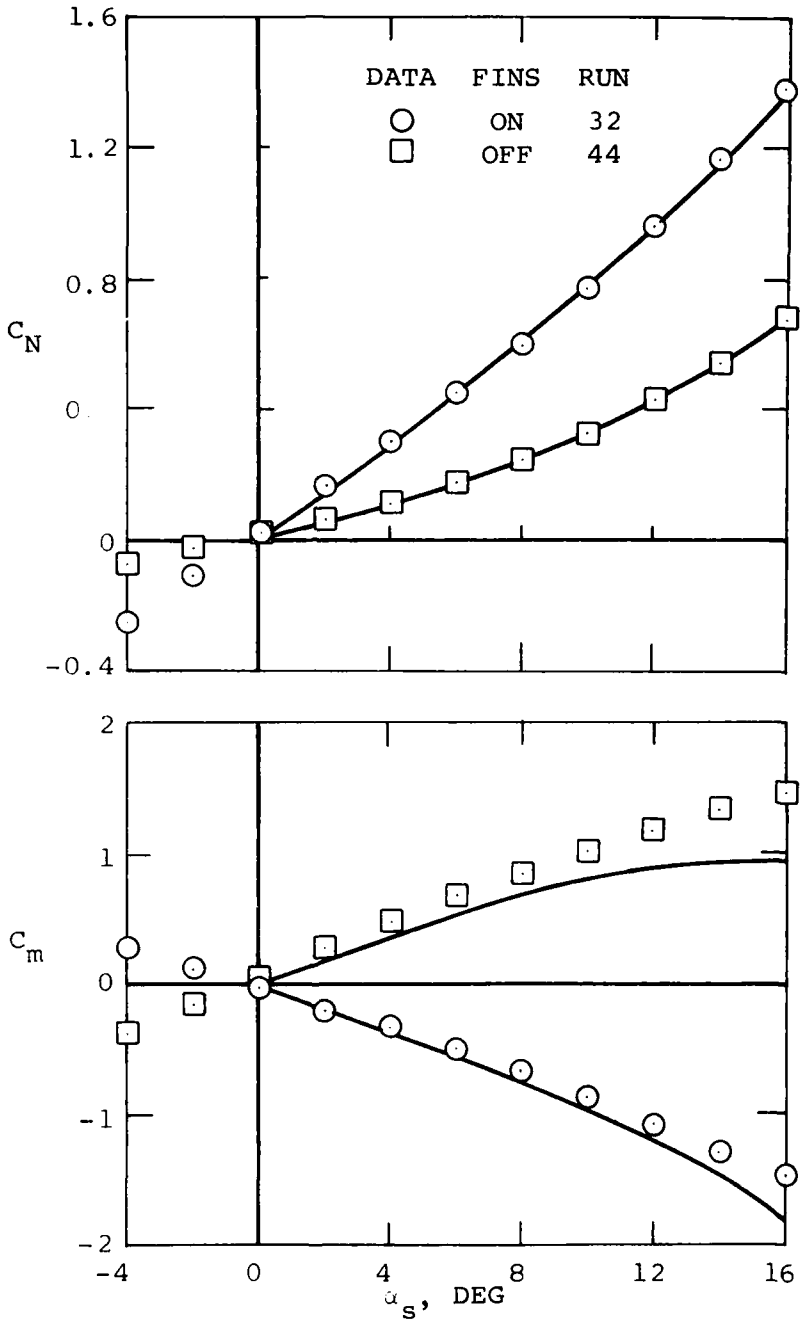

FIGURE 53. Comparison Between Experiment and Theory for the Free-Stream Aerodynamics of Store S_{MF} at $M_\infty = 0.95$.

approximated for the $M_\infty = 0.6$ data in Figure 37. Since we are interested in stores with fins, the emphasis must be placed on fitting the data for this case.

Figure 54 shows the afterbody separation locations used in the computer program. The separation location moves slightly forward with increase in angle of attack. The effect of Mach number is small.

The comparisons between experiment and theory are shown for upwash and sidewash angles in Figure 55 for $\alpha_s = 0^\circ$. In this figure the differences in upwash and sidewash angles between $M_\infty = 0.95$ and $M_\infty = 0.6$ are shown along the centerline position the store would occupy if mounted on the bottom station of the rack on the left inboard pylon. The differences as measured and as predicted for upwash are small up to about $\alpha_s = 12^\circ$ and at $\alpha_s = 16^\circ$ errors of the order of 1° to 1.4° exist in predicting the Mach number effect on the change in upwash angle. The agreement with regards to sidewash angle is good almost to 8° where it is fair, errors of the order of 0.5° to 0.75° occurring here. However, in lieu of data, the predictions can probably be used for estimating the flow angle to $\alpha_s = 16^\circ$ at $M_\infty = 0.95$ for preliminary design purposes since the upwash and sidewash angles with respect to the store are fairly large under this condition.

The differences in the store loads between $M_\infty = 0.95$ and $M_\infty = 0.6$ as measured and as predicted are given in Figure 56 as a function of angle of attack. These loads

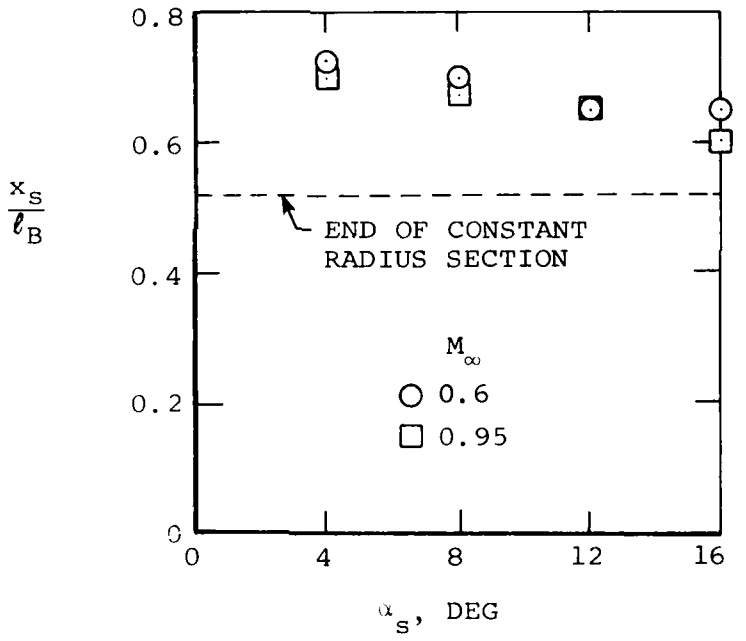

FIGURE 54. Variation of Axial Separation Point on Store S_{MF} with Angle of Attack.

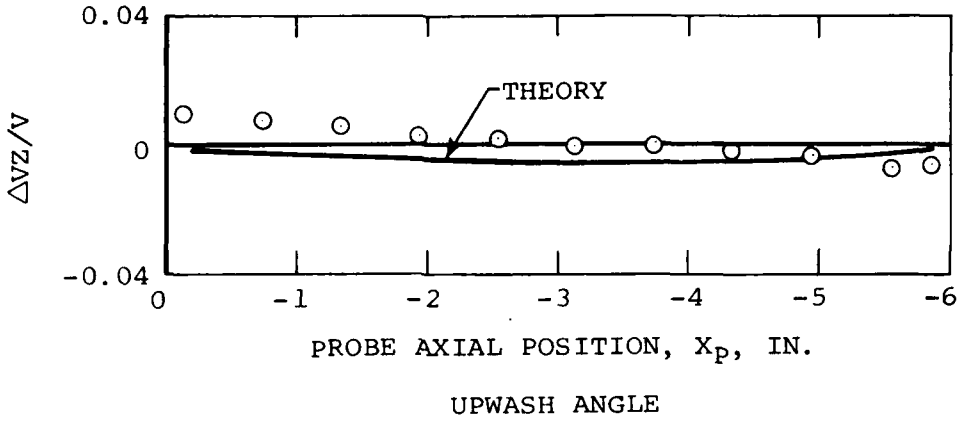

UPWASH ANGLE

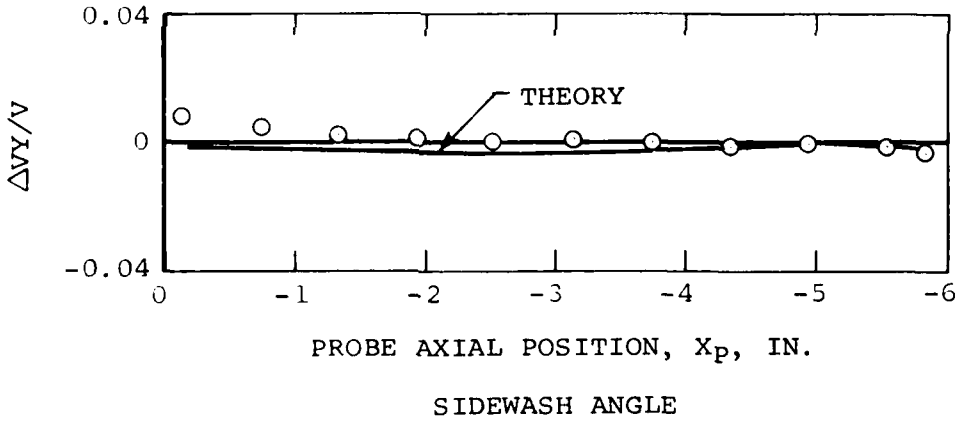

SIDEWASH ANGLE

(a) $\alpha_s = 0^\circ$

FIGURE 55. Differences Between Flow Angles at $M_\infty = 0.95$ and $M_\infty = 0.6$ for Clean Airplane (Configuration 1) at Centerline Position Store Would Have if Mounted on Rack on Inboard Pylon.

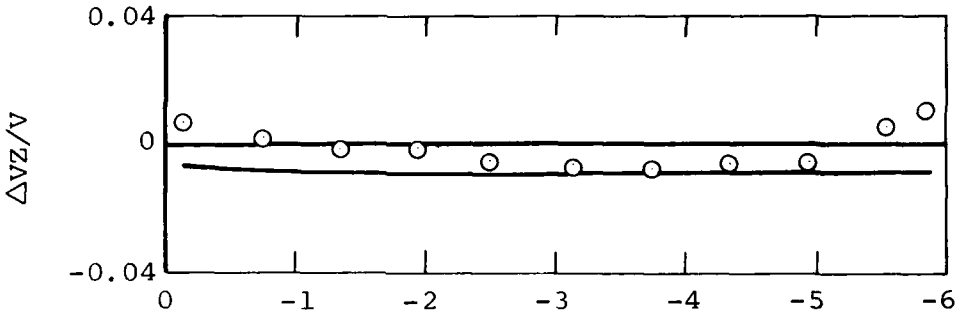

UPWASH ANGLE

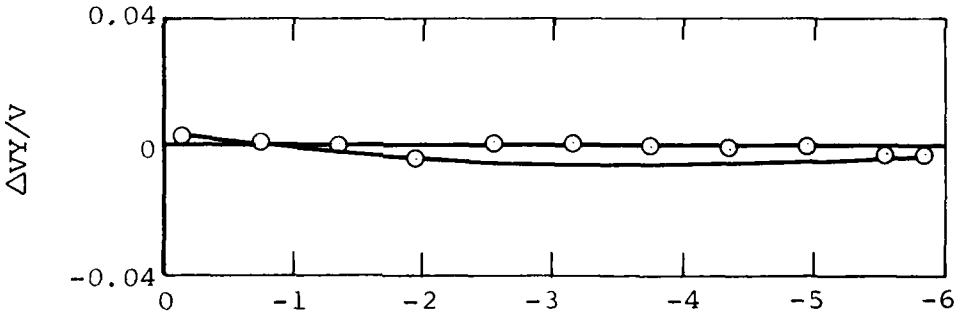

SIDEWASH ANGLE

(b) $\alpha_s = 4^\circ$.

FIGURE 55. Continued.

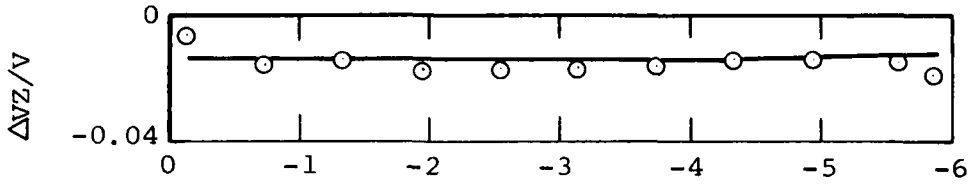

UPWASH ANGLE

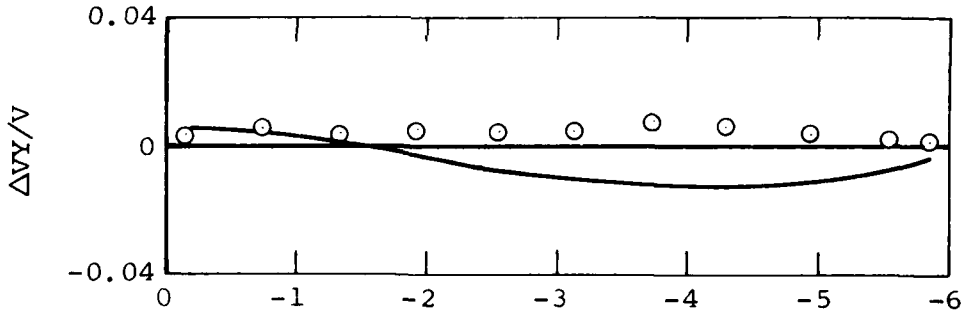

SIDEWASH ANGLE

(c) $\alpha_s = 8^\circ$.

FIGURE 55. Continued.

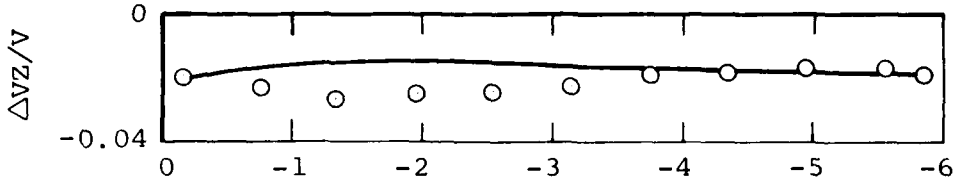

PROBE AXIAL POSITION, X_p, IN.

UPWASH ANGLE

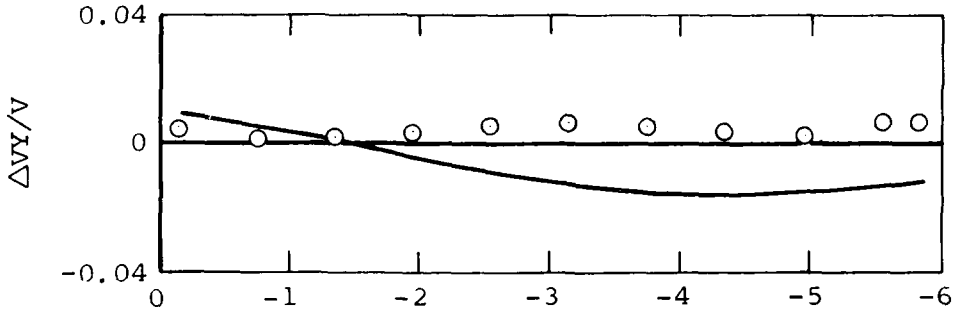

PROBE AXIAL POSITION, X_p, IN.

SIDEWASH ANGLE

(d) $\alpha_s = 12^\circ$.

FIGURE 55. Continued.

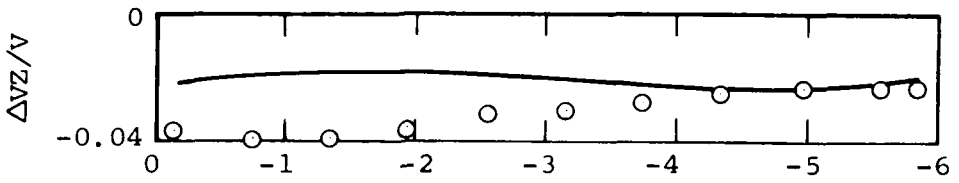

PROBE AXIAL POSITION, X_p, IN.

UPWASH ANGLE

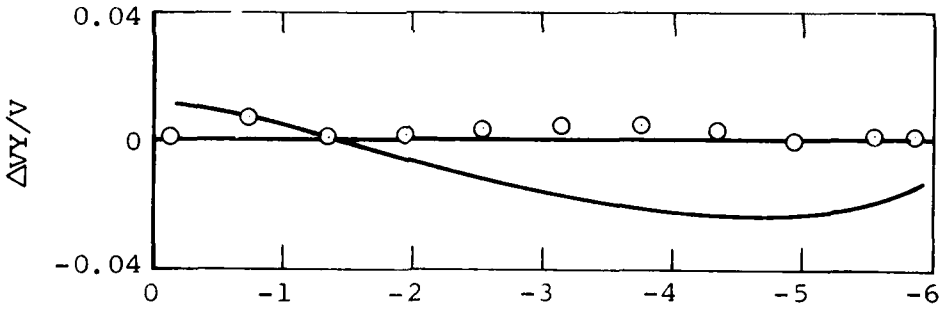

PROBE AXIAL POSITION, X_p, IN.

SIDEWASH ANGLE

(e) $\alpha_s = 16^\circ$.

FIGURE 55. Concluded.

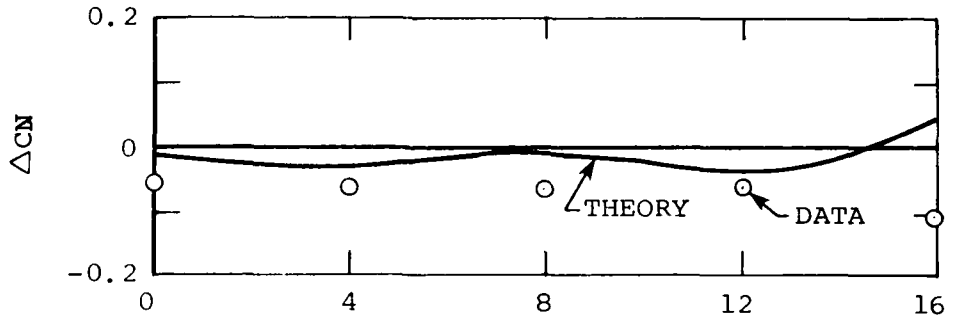

(a) Normal-force coefficient.

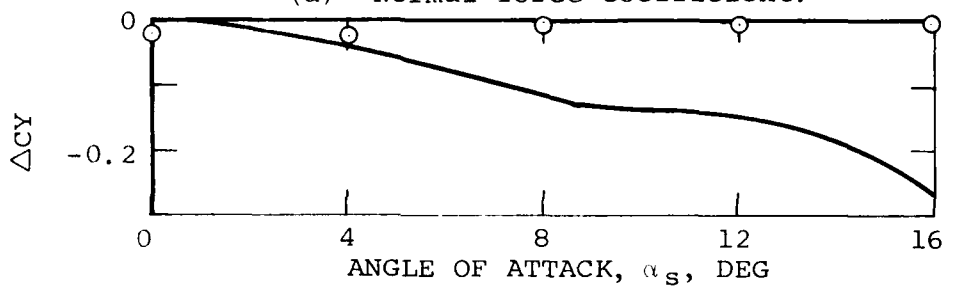

(b) Side-force coefficient.

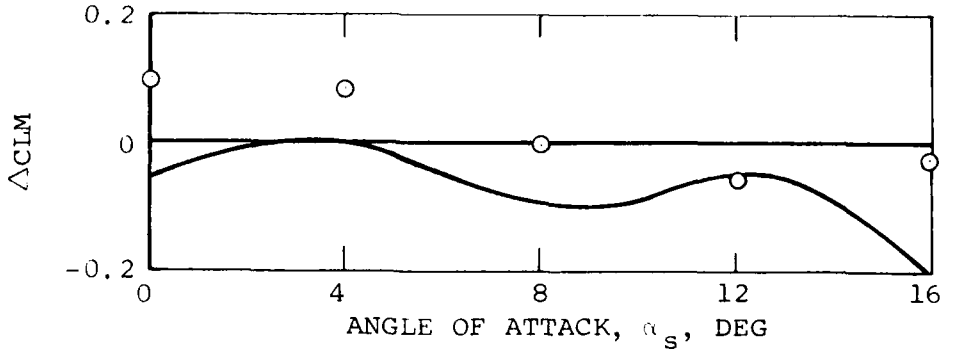

(c) Pitching-moment coefficient.

FIGURE 56. Differences in Loads on Store S_{MF} Between M_∞ = 0.95 and 0.6 as Measured and as Predicted; Configuration 1, Z_p/D = 0.

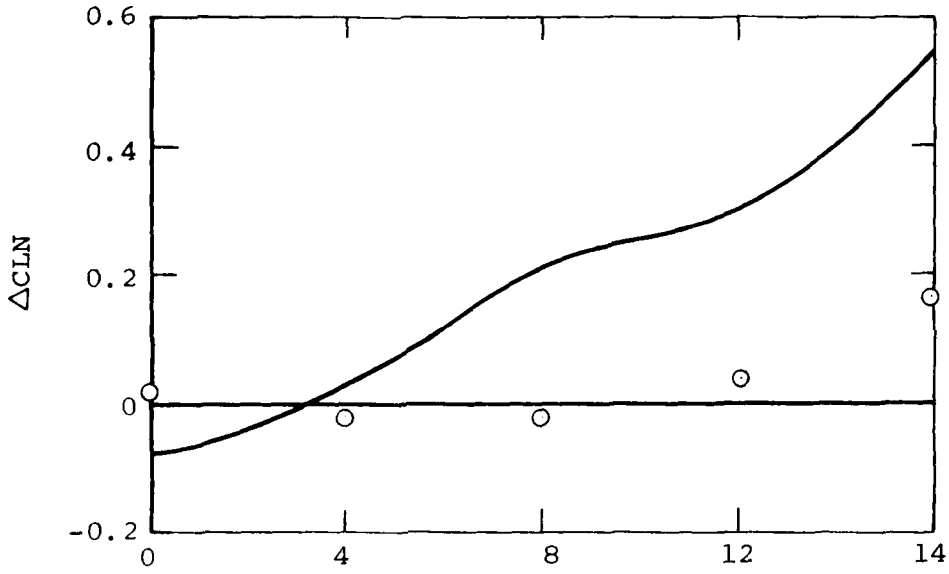

(d) Yawing-moment coefficient.

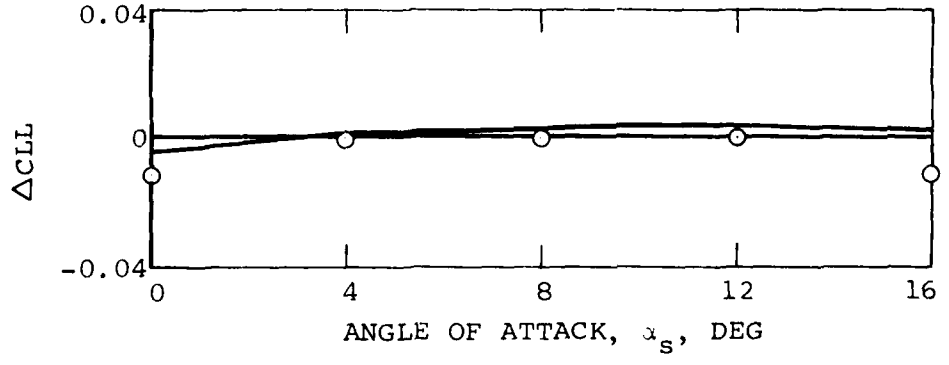

(e) Rolling-moment coefficient.

FIGURE 56. Concluded.

correspond to store S_{MF} at the $Z_p/D = 0$ position. In general the loads, with the exception of yawing moment, do not show much change due to Mach number between $\alpha_s = 0^o$ and 8^o. As the angle of attack increases, the agreement between prediction and data generally becomes worse. It thus appears that the compressibility effects on loads for $\alpha_s > 8^o$ at $M_\infty = 0.95$ are not well predicted by the linear theory. Some of this limitation of linear theory is due to inaccuracies in predicting the flow angles in the high angle-of-attack range as shown in Figure 55.

CONCLUSIONS

ATTACHED VERSUS GRID LOADS

1. The forces and moments on a store in close proximity to a TER can exhibit large changes within the first few tenths of a store diameter from the attached position.

2. It is not generally feasible using present measuring methods to extrapolate loads measured on a CTS supported model to those for the attached position.

3. Strong aerodynamic interference forces act on a store in close proximity to a TER which is only weakly dependent on Mach number in the range $0.6 \leq M_\infty \leq 0.95$.

ATTACHED LOADS

1. Adding the shoulder stores to the rack had the following effects on the attached loads of store S_{AF} at $M_\infty = 0.6$.

(a) The normal forces received a large positive increment due to addition to the rack of the outboard shoulder store in the low angle of attack range, and further increments of comparable magnitude by subsequent addition of inboard shoulder store. At high angles of attack, $\alpha_s > 10^o$, the increments became much smaller.

(b) The changes in side-force coefficient were small.

(c) There were definite changes in the pitching-moment coefficient, but these were greater than those in yawing-moment coefficient.

(d) Rolling-moment coefficient exhibited significant changes.

2. Adding fins to the shoulder stores under the conditions of (1) generally causes small changes in the store loads except at large angles of attack.

3. At $M_\infty = 0.95$ the same quantitative configuration effects described in (1) and (2) were found.

4. The effects of Mach number on the attached loads for store S_{AF} mounted on configuration 6 were small for the range $0.6 < M_\infty < 0.95$ except for normal-force coefficient.

The effect of M_∞ on CN was systematically to reduce it by an amount which increased as the angle of attack reduced from positive (16^o) to negative (-4^o). These results suggest that systematic interference effects were present.

5. At $M_\infty = 0.6$ addition of the fins to the shoulder stores causes negligible effect on the loads of store S_{AF} except for CLM and CLL at large angles of attack.

6. The addition of the inboard shoulder store adds increments to CN, CLM, and CLN which reverse sign with increases in angle of attack. It causes no change in CY and decreases CLL. This behavior is representative of the M_∞ = 0.6 and 0.95 results.

GRID LOADS

1. At $M_\infty = 0.6$ and at $\alpha_s = 0^o$ with store S_{MF} within 1 store diameter of the rack the most important things influencing the bottom store loads are in decreasing order of importance:

(a) Addition of shoulder stores to TER.
(b) Addition of TER to pylon.
(c) Addition of fins to the shoulder stores.

Changing the angle of attack to 8^o does not change the foregoing conclusion.

2. The addition of fins to the shoulder stores for the ranges of M_∞ and α_s of the tests has a generally small effect, and the effect is largest at small values of Z_p/D. It

appears, therefore, that the addition of the fins may be neglected for trajectory purposes but not for accurate attached loads.

3. The effect of Mach number on the loads of store S_{MF} for configuration 6 is evident for all the coefficients. However, its effects on CN, CY, and CLL seems to be smaller than its effects on CLM and CLN. Some qualitative changes in CLN due to Mach number occur at the highest Mach number ($M_\infty = 0.95$) for small Z_p/D.

4. The data indicate that the shoulder stores influence the loads on the bottom store for about 5 store diameters from the rack.

5. Sway braces have negligible effects on the bottom store loads except for CN and CLM in immediate proximity to the rack, where the effects are small.

FLOW FIELD MEASUREMENTS

1. Adding the pylon to the airplane has little effect on the flow field in the position to be occupied by the attached lower store, but adding the rack has a much larger effect.

2. Adding a pair of shoulder stores to the rack causes large changes in upwash, but the changes in sidewash angle are moderate.

3. Addition of the fins to the shoulder stores has a small effect on upwash behind the fins, and a small effect on sidewash in front of and behind the fins.

4. Mach number causes minor changes in sidewash and upwash between M_∞ = 0.6 to 0.95 in the low angle of attack range. A maximum change in sidewash of 1° at M_∞ = 0.95 was found over a small range of X_p.

5. The effects of adding one and then another shoulder store were to increase upwash in both cases, but the effects on sidewash were not clearcut. The effects of adding each store were not equal.

COMPARISON BETWEEN EXPERIMENT AND THEORY

1. By using some experimental data in the computer input quantities for the store-alone characteristics in the free stream, satisfactory agreement between data and the computer program were obtained for the normal-force, pitching-moment, and rolling-moment curves of the store with tail fins in the X roll orientation.

2. For the clean airplane, the upwash and sidewash angles near the store location at the inboard pylon are predicted adequately for preliminary design purposes to $\alpha_s = 8^\circ$ but not up to $\alpha_s = 16^\circ$.

3. For store S_{MF} in combination with the clean airplane near the attached inboard position, the normal force, side force, and rolling moment are well predicted by the computer program up to $\alpha_s = 8^\circ$. However, the pitching

moment and yawing moment are not predicted well probably as a result of movement of the separation position on the boattail afterbody due to the nonuniform flow field and its resulting effects on afterbody and tail normal forces.

4. Adding the pylon to the clean airplane produced downwash and sidewash changes near the location of the attached store on the inboard pylon which were usually less than 0.5° and which were accurately predicted by the computer program.

5. The loads on store S_{MF} at $Z_p/D = 0$ and 1 due to the addition of the pylon were predicted satisfactorily. In magnitude they correspond in some cases to a change in angle of attack of the store in the free stream of 1° to 2°.

6. Adding the TER to the airplane-pylon combination caused changes in downwash angle and sidewash angle at the attached store position. They are several times greater than those due to the addition of the pylon, and the theory generally underpredicts these changes. In fact the theory predicts no sidewash changes since the rack is modeled by a body of revolutions with volume only (sources and sinks).

7. The upwash and sidewash increments due to the rack are qualitatively similar to those for adding the pylon. It appears that a "rack pylon" will account for the observed effects. It can be modeled as an extension of the wing pylon, and the body-of-revolution model of the rack still retained.

8. Generally the computer program predicts zero yawing-moment, side-force, and rolling-moment contributions due to addition of the rack since no sidewash is predicted. The normal-force and pitching-moment increments are fairly well predicted.

9. The load increments due to the addition of the rack can be several times greater than those due to the addition of the pylon.

10. As store S_{MF} moves toward the attached inboard position from below, the normal force, side force, yawing moment, and rolling moment as measured show rapid changes within the last 0.5 diameters of travel. These rapid changes are not predicted by the computer program. The proposed addition of a rack pylon model will change the predicted loads in this interval. Better account of mutual interference between rack, pylon, and store may also be required to predict accurate attached store loads.

11. The sudden increase in rolling moment as Z_p/D approaches zero is thought to be the result of a tip vortex from the rack pylon.

12. The pitching moment exhibits an unexplained non-linearity as $Z_p/D \to 0$ since it suddenly goes negative and then reverses to its positive value for the attached position.

13. The upwash distribution due to adding the shoulder stores to the rack is predicted fairly well at $Z_p/D = 1.0$ but is underestimated at $Z_p/D = 0$. The use of doublets to cancel the upwash acting on the shoulder stores could be

one source of upwash not included in the theory. Another source could be mutual interference between shoulder stores and rack pylon.

14. Theory predicts no sidewash under the pylon due to the shoulder stores, but a small amount exists at $Z_p/D = 0$ which varies with α_s. It is thought that doublets to cancel the sidewash on the shoulder stores might account for this small sidewash which goes away at $Z_p/D = 1.0$.

15. With regards to the effect of the shoulder stores on the loads on the bottom store, large changes are evident in CN and CM but generally small changes in CY, CLN, and CLL.

16. The changes in CN and CLM at $Z_p/D = 1.0$ due to the shoulder stores are well predicted, but at $Z_p/D = 0$ they are not well predicted. While improving the predictions of the flow fields at $Z_p/D = 0$ should improve this situation, it may require accounting for mutual interference among all three stores and the rack to estimate loads accurately in the attached position and its proximity.

RECOMMENDATION FOR IMPROVEMENTS TO COMPUTER PROGRAM

Based on systematic comparisons between experiment and theory for the flow field and forces and moments acting on a modified Mk-83 bomb tested in conjunction with a TER mounted on the inboard wing pylon of an F-4C airplane, a number of ways have been found of improving the computer

program based on the theory. The suggestions are aimed principally at determining the loads on the bottom store in its attached position or close to the rack. In solving this problem mutual interference between rack and shoulder stores is to be included. Thus after the bottom store is dropped, the loads on the shoulder stores should be more accurately predicted.

The determination of the loads on the bottom store under the conditions of interest requires that the flow field at the position to be occupied by the bottom store be accurately calculated with the two shoulder stores present. Certain improvements in the model are needed to achieve this objective. The second requirement appears to be that the full mutual interference among all three stores and the rack be taken into account in determining the loads on the bottom store. Let us take up these two requirements serially.

The present rack model does not give accurate flow fields because it does not account for the rack pylon. It is suggested that the rack pylon be modeled as an extension of the wing pylon passing through the rack. At the same time that part of the rack which does not include the rack pylon, can still be modeled by a body of revolution. If these changes do not give the desired accuracy, then rack doublet distributions to offset the downwash and sidewash at the rack centerline can be introduced.

The present modeling of the shoulder stores by source distributions does not give accurate downwash just under the rack. It is suggested that mutual interference between these source distributions be taken account of as well as with that of the rack. This three-body problem can be

handled by the method of Martin, Reference 8. The three bodies already have a vertical plane of symmetry so that the pylon boundary conditions are met. If this does not give a sufficiently accurate flow field, the next degree of approximation, which should be included, is to consider the doublet distributions for the attached stores due to upwash and sidewash.

The second requirement, when the flow-field calculation is accurate enough, is to take account of mutual interference among all three stores and the rack in determining the loads on the bottom store. This is first of all a four-body problem in sources which can be approximately attacked by the method of Martin, Reference 8. Then the problem should be done again for the doublet distributions by the same general method.

In addition to these suggestions, certain others have arisen as being useful under certain circumstances. It would be useful if the experimental data for the store alone in the free stream were used in the computer program to improve its accuracy. (An attempt in this direction has been previously described herein.) If a boattail afterbody occurs on the external store with separated flow, increased accuracy can be obtained by accounting for movement of the separation location based on the local angle of attack at the afterbody position. In case rolling moments are important, account should be taken of the rack pylon trailing vortex as it might induce rolling moments on the tail fins of the stores.

A final requirement would be to include the effect of shoulder store tail fins on the loads acting on the bottom store.

REFERENCES

1. Goodwin, F.K. and Dillenius, M.F.E.: Extension of the Method for Predicting Six-Degree-of-Freedom Store Separation Trajectories at Speeds Up to the Critical Speed to Include a Fuselage with Noncircular Cross Section. Vol. II - Users Manual for the Computer Program. Technical Report AFFDL-TR-74-130, Vol. II, Nov. 1974.

2. Maddox, A.R., Dix, R.E. and Mattasits, G.R.: In-Flight Measurements of Captive Loads on a Store as Compared with Wind Tunnel and Mathematical Simulation. NWC TP 6026, April 1978.

3. Hesketh, A.A.: A Wind Tunnel Test to Study the Mutual Interference of Multiple Bodies in the Flow Field of the F-4C Aircraft in the Transonic Speed Range. AEDC-TSR-79-P79, December 1979.

4. Test Facilities Handbook (Eleventh Edition). "Propulsion Wind Tunnel Facility, Vol. 4" Arnold Engineering Development Center, June 1979.

5. Dix, R.E.: Comparison of Two Methods Used to Measure Aerodynamic Loads Acting on Captive Store Models in Wind-Tunnel Tests. AEDC-TR-76-122, September 1976.

6. Dix, R. E.; Influences of Sway Braces and Mounting Gaps on the Static Aerodynamic Loading of External Stores. AEDC-TR-77-112, February 1978.

7. Nielsen, Jack N.: "Missile Aerodynamics", McGraw-Hill Book Co., Inc., 1960, pp. 118-121.

8. Martin, F. W.: Image System Solutions for Mutual Aerodynamic Interference. Auburn University, School of Engineering. No date.

Appendix A

CAPTIVE LOADS DATA RETRIEVAL PROGRAM

```
      PROGRAM RETCAP (INPUT,OUTPUT,TAPE5=INPUT,TAPE6=OUTPUT,TAPE10)
C     PROGRAM TO RETRIEVE RANDOM RUN NUMBERS FROM THE
C     CAPTIVE LOADS TAPE
C
C
      DIMENSION  R(26),IHDR(25),IPTR(100),ITITLE(3),RUNNO(100)
      DIMENSION ICONF(7),ISTORE(3)
C
      DATA ICARD /4HCAPT/, ITAPE /4H CAP/
C
C
C     READ TAPE TITLE AND RUN NOS.
C
      READ (5,1000, ITITLE
      IF (ITITLE(1) .EQ. ICARD) GO TO 20
        WRITE (6,2000) (ITITLE(I),I=1,3)
        STOP
   20 CONTINUE
      READ (10,1010) IHDR
      IF (IHDR(2) .EQ. ITAPE) GO TO 40
        WRITE (6,2010) (IHDR(I),I=1,25)
        STOP
   40 CONTINUE
      READ (5,1020) N
      READ (5,1030) (RUNNO(I),I=1,N)
      WRITE (6,2020) (I,RUNNO(I),I=1,N)
C
C     SORT THE RUN NOS. AND THE POINTERS TO THE RUN NOS.
C
      DO 60 I= 1,N
        IPTR(I)= I
   60 CONTINUE
      IF (N .LE. 1) GO TO 85
        N1= N-1
        DO 80 I=1,N1
          I1= I+1
          DO 80 J= I1,N
            IF (RUNNO(IPTR(I)) .LE. RUNNO(IPTR(J))) GO TO 80
              ITEMP= IPTR(I)
              IPTR(I)= IPTR(J)
              IPTR(J)= ITEMP
   80   CONTINUE
   85 CONTINUE
C
C     SEARCH TAPE FOR SORTED RUN NOS.
C
      READ (10,1040) (R(I),I=1,25)
      OLDRUN= 0.0
      DO 160 I= 1,N
C
C       DO WHILE DESIRED RUN NO. GREATER THAN TAPE RUN NO.
C
  100   CONTINUE
        IF (RUNNO(IPTR(I)) .LT. R(1)) GO TO 160
          IF (R(1) .NE. RUNNO(IPTR(I))) GO TO 140
            IF (R(1) .EQ. OLDRUN) GO TO 120
C
C             WRITE HEADING FOR NEW RUN NO.
C
              CALL CONFIG (R(10),   ICONF,ISTORE)
              WRITE (6,2030) (IHDR(J),J=1,25)
              IRUN= R(1)
              WRITE (6,2040) IRUN,(ICONF(J),J=1,7),(ISTORE(J),J=1,3)
              WRITE (6,2050) (R(J),J=2,4),(R(J),J=6,8),R(5),R(9)
```

```
              WRITE (6,2060)                                              65.
              OLDRUN= R(1)                                                66.
  120       CONTINUE                                                      67.
C                                                                         68.
C           WRITE DATA                                                    69.
C                                                                         70.
            WRITE (6,2070) R(21),(R(J),J=11,20),(R(J),J=22,25)            71.
  140     CONTINUE                                                        72.
        READ (10,1040) (R(J),J=1,25)
          IF (EOF(10)) 200,100
        GO TO 100                                                         74.
  160 CONTINUE                                                            75.
C                                                                         76.
C     END OF FILE OR ALL DESIRED RUN NOS. FOUND                           77.
C                                                                         78.
  200 CONTINUE                                                            79.
      REWIND 10                                                           80.
C                                                                         81.
C                                                                         82.
C     * * READ FORMATS                                                   83.
C                                                                         84.
 1000 FORMAT (3A4)                                                        85.
 1010 FORMAT (25A4)                                                       86.
 1020 FORMAT (I5)                                                         87.
 1030 FORMAT (8F10.0)                                                     88.
 1040 FORMAT (1P10F12.5)                                                  89.
C                                                                         90.
C     * * WRITE FORMATS                                                  91.
C                                                                         92.
 2000 FORMAT (1H0,5X,17H* * * ERROR * * *,                                93.
     1 46HINPUT CARD DOES NOT SPECIFY CAPTIVE LOADS DATA /                94.
     2 5X, 11HCARD TITLE=, 3A4)                                           95.
 2010 FORMAT (1H0, 5X,17H* * * ERROR * * *,                               96.
     1 46HTAPE TITLE DOES NOT SPECIFY CAPTIVE LOADS DATA /
     2 5X,11HTAPE TITLE=, 25A4)                                           98.
*2020 FORMAT (1H1,17HINPUT RUN NUMBERS /                                  99.
     1 2X,1HI,3X,7HRUN NO. / (1X,I2,F10.2))                              100.
 2030 FORMAT (1H1,1X,25A4)                                               101.
 2040 FORMAT (1H0,3X,7HRUN NO.,7X,20HPARENT CONFIGURATION,               102.
     1 15X,5HSTORE, /                                                    103.
     2 5X,I3,8X,7A4,7X,3A4)                                              104.
 2050 FORMAT (1H0,17X,34H***** FREE-STREAM CONDITIONS *****, /           105.
     1 4X,4HMACH,4X,2HPT,6X,2HTT,7X,1HP,7X,1HT,7X,1HV,7X,                106.
     2 1HQ,7X,5HRE/FT, /                                                 107.
     3 5X,2HNO,4X,4HPSFA,3X,6HDEG(R),3X,4HPSFA,3X,                       108.
     4 6HDEG(R),2X,6HFT/SEC,4X,3HPSF,6X,6HFT(-1) /                       109.
     5 2X,F6.3,6F8.1,F7.2,6H*10**6)                                      110.
 2060 FORMAT (1H0,50X,22H***** MODEL DATA ***** /                        111.
     1 4X,5HALPHA,3X,5HALPHA,3X,4HBETA /                                 112.
     2 5X,3HPAR,4X,5HSTORE,3X,5HSTORE,4X,2HCN,6X,2HCY,6X,                113.
     3 3HCAT,5X,3HCLM,5X,3HCLN,5X,3HCLL,6X,3HNCP,6X,                     114.
     4 3HYCP,4X,3HMNF,3X,5HMDOTN,3X,2HCR,5X,2HVR /                       115.
     5 5X, 3HDEG,5X,3HDEG,5X,3HDEG,53X,5HDIAMS,4X,5HDIAMS,               116.
     6 8X, 7HLBM/SEC )                                                   117.
 2070 FORMAT (1X,3(2X,F6.2),6(2X,F6.3),2(2X,F7.3),4F7.3)                 118.
C                                                                        119.
C                                                                        120.
      STOP                                                               121.
      END                                                                122.
```

```
      SUBROUTINE CONFIG (B,   ICONF,ISTORE)                              200.
C                                                                        201.
C     DECIPHER THE CONFIGURATION CODE AND SET UP AN ALPHABETIC           202.
C     ARRAY FOR THE CONFIGURATION AND THE STORE                          203.
C                                                                        204.
C                                                                        205.
      DIMENSION IC(18),ICONF(7),IS(7),ISTORE(3)                          206.
      DATA IC /4HF-4C, 4H,PI,, 4HT,(S, 4H2)U,, 4H2)F,,                   207.
     1 4H,PI , 4HT   , 4H2)U , 4H(S3), 4HU   , 4HF   ,                   208.
     2 4H,PCL, 4HF,PO, 4H2)F , 4HTM,(, 4HS2)F, 4H,(S3,                   209.
     3 4H)F   /                                                          210.
      DATA IS /4HMK-A, 4H3,MF, 4H3,MU, 4H3,AF, 4H3,AU,                   211.
     1 4HPROR, 4HE   /                                                   212.
      DATA IBLANK /4H    /                                               213.
C                                                                        214.
      IF (B .EQ. 610.0) B= 91.0                                          215.
      MB= B                                                              216.
      MY= MOD(MB,10)                                                     217.
      MX= MB/10                                                          218.
C                                                                        219.
C     CASE CONFIGURATION                                                 220.
C                                                                        221.
C     CASE X=0                                                           222.
C                                                                        223.
      IF (MX .NE. 0) GO TO 50                                            224.
        DO 40 I=1,7                                                      225.
          ICONF(I)= IBLANK                                               226.
   40   CONTINUE                                                         227.
        GO TO 150                                                        228.
C                                                                        229.
   50 GO TO (60,70,80,90,100,110,120,130,140),MX                         230.
C                                                                        231.
C     CASE X=1                                                           232.
C                                                                        233.
   60 CONTINUE                                                           234.
        ICONF(1)= IC(1)                                                  235.
        DO 65 I= 2,7                                                     236.
          ICONF(I)= IBLANK                                               237.
   65   CONTINUE                                                         238.
        GO TO 150                                                        239.
C                                                                        240.
C     CASE X=2                                                           241.
C                                                                        242.
   70 CONTINUE                                                           243.
        ICONF(1)= IC(1)                                                  244.
        ICONF(2)= IC(A)                                                  245.
        DO 75 I= 3,7                                                     246.
          ICONF(I)= IBLANK                                               247.
   75   CONTINUE                                                         248.
        GO TO 150                                                        249.
C                                                                        250.
C     CASE X=3                                                           251.
C                                                                        252.
   80 CONTINUE                                                           253.
        ICONF(1)= IC(1)                                                  254.
        ICONF(2)= IC(1)                                                  255.
        ICONF(3)= IC(2)                                                  256.
        DO 85 I=4,7                                                      257.
          ICONF(I)= IBLANK                                               258.
   85   CONTINUE                                                         259.
        GO TO 150                                                        260.
C                                                                        261.
C     CASE X=4                                                           262.
C                                                                        263.
   90 CONTINUE                                                           264.
        DO 95 I=1,3                                                      265.
```

```
            ICONF(I)= IC(I)                                          266.
   95     CONTINUE                                                   267.
          ICONF(4)= IC(8)                                            268.
          DO 96 I= 5,7                                               269.
            ICONF(I)= IBLANK                                         270.
   96     CONTINUE                                                   271.
          GO TO 150                                                  272.
C                                                                    273.
C       CASE X=5                                                     274.
C                                                                    275.
  100   CONTINUE                                                     276.
          DO 105 I= 1,4                                              277.
            ICONF(I)= IC(I)                                          278.
  105     CONTINUE                                                   279.
          ICONF(5)= IC(9)                                            280.
          ICONF(6)= IC(10)                                           281.
          ICONF(7)= IBLANK                                           282.
          GO TO 150                                                  283.
C                                                                    284.
C       CASE X=6                                                     285.
C                                                                    286.
  110   CONTINUE                                                     287.
          DO 115 I= 1,3                                              288.
            ICONF(I)=IC(I)                                           289.
  115     CONTINUE                                                   290.
          ICONF(4)= IC(5)                                            291.
          ICONF(5)= IC(9)                                            292.
          ICONF(6)= IC(11)                                           293.
          ICONF(7)= IBLANK                                           294.
          GO TO 150                                                  295.
C                                                                    296.
C       CASE X=7                                                     297.
C                                                                    298.
  120   CONTINUE                                                     299.
          ICONF(1)= IC(1)                                            300.
          ICONF(2)= IC(12)                                           301.
          ICONF(3)= IC(2)                                            302.
          ICONF(4)= IC(3)                                            303.
          ICONF(5)= IC(5)                                            304.
          ICONF(6)= IC(9)                                            305.
          ICONF(7)= IC(13)                                           306.
          GO TO 150                                                  307.
C                                                                    308.
C       CASE X=8                                                     309.
C                                                                    310.
  130   CONTINUE                                                     311.
          DO 135 I= 1,3                                              312.
            ICONF(I)= IC(I)                                          313.
  135     CONTINUE                                                   314.
          ICONF(4)= IC(14)                                           315.
          DO 136 I= 5,7                                              316.
            ICONF(I)= IBLANK                                         317.
  136     CONTINUE                                                   318.
          GO TO 150                                                  319.
C                                                                    320.
C       CASE X=9                                                     321.
C                                                                    322.
  140   CONTINUE                                                     323.
          ICONF(1)= IC(1)                                            324.
          ICONF(2)= IC(2)                                            325.
          ICONF(3)= IC(15)                                           326.
```

```
      ICONF(4) = IC(16)                                                 327.
      ICONF(5) = IC(17)                                                 328.
      ICONF(6) = IC(18)                                                 329.
      ICONF(7) = IBLANK                                                 330.
C                                                                       331.
C     END CASE CONFIGURATION                                            332.
  150 CONTINUE                                                          333.
C                                                                       334.
C                                                                       335.
C     CASE STORE                                                        336.
C                                                                       337.
      ISTORE(1) = IS(1)                                                 338.
      ISTORE(3) = IBLANK                                                339.
      GO TO (170,180,190,200,210,220,230), MY                           340.
C                                                                       341.
C     CASE Y=1                                                          342.
C                                                                       343.
  170 CONTINUE                                                          344.
        ISTORE(2) = IS(2)                                               345.
        GO TO 240                                                       346.
C                                                                       347.
C     CASE Y=2                                                          348.
C                                                                       349.
  180 CONTINUE                                                          350.
        ISTORE(2) = IS(3)                                               351.
        GO TO 240                                                       352.
C                                                                       353.
C     CASE Y=3                                                          354.
C                                                                       355.
  190 CONTINUE                                                          356.
        ISTORE(2) = IS(4)                                               357.
        GO TO 240                                                       358.
C                                                                       359.
C     CASE Y=4                                                          360.
C                                                                       361.
  200 CONTINUE                                                          362.
        ISTORE(2) = IS(5)                                               363.
        GO TO 240                                                       364.
C                                                                       365.
C     CASE Y=5                                                          366.
C                                                                       367.
  210 CONTINUE                                                          368.
        ISTORE(1) = IS(6)                                               369.
        ISTORE(2) = IS(7)                                               370.
        GO TO 240                                                       371.
C                                                                       372.
C     CASE Y= 6                                                         373.
  220 CONTINUE                                                          374.
        ISTORE(2) = IS(2)                                               375.
        GO TO 240                                                       376.
C                                                                       377.
C     CASE Y=7                                                          378.
  230 CONTINUE                                                          379.
        ISTORE(2) = IS(3)                                               380.
C                                                                       381.
C     END CASE STORE                                                    382.
C                                                                       383.
  240 CONTINUE                                                          384.
C                                                                       385.
      RETURN                                                            386.
      END                                                               387.
```

Appendix B

GRID FORCE AND MOMENT DATA RETRIEVAL PROGRAM

```
      PROGRAM RETGRD (INPUT,OUTPUT,TAPE5=INPUT,TAPE6=OUTPUT,TAPE10)
C     PROGRAM TO RETRIEVE RANDOM RUN NUMBERS FROM THE                    2.
C     GRID TAPE
C                                                                        4.
C                                                                        5.
      DIMENSION  R(26),IHDR(25),IPTR(100),ITITLE(3),RUNNO(100)           6.
      DIMENSION ICONF(7),ISTORE(3)                                       7.
C                                                                        8.
      DATA ICARD /4HGRID/, ITAPE /4H GRI/                                9.
C                                                                       10.
C                                                                       11.
C     READ TAPE TITLE AND RUN NOS.                                      12.
C                                                                       13.
      READ (5,1000) ITITLE                                              14.
      IF (ITITLE(1) .EQ. ICARD) GO TO 20                                15.
        WRITE (6,2000) (ITITLE(I),I=1,3)                                16.
        STOP                                                            17.
   20 CONTINUE                                                          18.
      READ (10,1010) IHDR                                               19.
      IF (IHDR(2) .EQ. ITAPE) GO TO 40                                  20.
        WRITE (6,2010) (IHDR(I),I=1,25)                                 21.
        STOP                                                            22.
   40 CONTINUE                                                          23.
      READ (5,1020) N                                                   24.
      READ (5,1030) (RUNNO(I),I=1,N)                                    25.
      WRITE (6,2020) (I,RUNNO(I),I=1,N)                                 26.
C                                                                       27.
C     SORT THE RUN NOS. AND THE POINTERS TO THE RUN NOS.                28.
C                                                                       29.
      DO 60 I= 1,N                                                      30.
        IPTR(I)= I                                                      31.
   60 CONTINUE                                                          32.
      IF (N .LE. 1) GO TO 85                                            33.
        N1= N-1                                                         34.
        DO 80 I=1,N1                                                    35.
          I1= I+1                                                       36.
          DO 80 J= I1,N                                                 37.
            IF (RUNNO(IPTR(I)) .LE. RUNNO(IPTR(J))) GO TO 80            38.
              ITEMP= IPTR(I)                                            39.
              IPTR(I)= IPTR(J)                                          40.
              IPTR(J)= ITEMP                                            41.
   80   CONTINUE                                                        42.
   85 CONTINUE                                                          43.
C                                                                       44.
C     SEARCH TAPE FOR SORTED RUN NOS.                                   45.
C                                                                       46.
      READ (10,1040) (R(I),I=1,26)                                      47.
      OLDRUN= 0.0                                                       48.
      DO 160 I= 1,N                                                     49.
C                                                                       50.
C       DO WHILE DESIRED RUN NO. GREATER THAN TAPE RUN NO.              51.
C                                                                       52.
  100   CONTINUE                                                        53.
        IF (RUNNO(IPTR(I)) .LT. R(1)) GO TO 160                         54.
          IF (R(1) .NE. RUNNO(IPTR(I))) GO TO 140                       55.
            IF (R(1) .EQ. OLDRUN) GO TO 120                             56.
C                                                                       57.
C             WRITE HEADING FOR NEW RUN NO.                             58.
C                                                                       59.
              CALL CONFIG (R(10),   ICONF,ISTORE)                       60.
              WRITE (6,2030) (IHDR(J),J=1,25)                           61.
              IRUN= R(1)                                                62.
              WRITE (6,2040) IRUN,(ICONF(J),J=1,7),(ISTORE(J),J=1,3)    63.
              WRITE (6,2050) (J,R(J),J=2,9),(R(J),J=11,18),R(25),R(26)  64.
```

```
                WRITE (6,2060)                                          65.
                OLDRUN= B(1)                                            66.
  120         CONTINUE                                                  67.
C                                                                       68.
C             WRITE DATA                                                69.
C                                                                       70.
              WRITE (6,2070) B(1),B(17),B(18),B(15),B(16),              71.
     1        (B(J),J=12,14),(B(J),J=21,26),B(19),B(20)                 72.
  140       CONTINUE                                                    73.
          READ (10,1040) (B(J),J=1,26)
            IF (EOF(10)) 200,100
  160 CONTINUE                                                          76.
C                                                                       77.
C     END OF FILE OR ALL DESIRED RUN NOS. FOUND                         78.
C                                                                       79.
  200 CONTINUE                                                          80.
      REWIND 10                                                         81.
C                                                                       82.
C                                                                       83.
C     * * READ FORMATS                                                 84.
C                                                                       85.
 1000 FORMAT (3A4)                                                      86.
 1010 FORMAT (25A4)                                                     87.
 1020 FORMAT (I5)                                                       88.
 1030 FORMAT (8F10.0)                                                   89.
 1040 FORMAT (1P10E12.5)                                                90.
C                                                                       91.
C     * * WRITE FORMATS                                                92.
C                                                                       93.
 2000 FORMAT (1H0,5X,17H* * * ERROR * * *,                              94.
     1 37HINPUT CARD DOES NOT SPECIFY GRID DATA /                       95.
     2 5X, 11HCARD TITLE=, 3A4)                                        96.
 2010 FORMAT (1H0, 5X,17H* * * ERROR * * *,                             97.
     1 37HTAPE TITLE DOES NOT SPECIFY GRID DATA /
     2 5X,11HTAPE TITLE=, 25A4)                                        99.
 2020 FORMAT (1H1,17HINPUT RUN NUMBERS /                               100.
     1 2X,1HI,3X,7HRUN NO. / (1X,I2,F10.2))                            101.
 2030 FORMAT (1H1,1X,25A4)                                             102.
 2040 FORMAT (1H0,3X,7HRUN NO.,7X,20HPARENT CONFIGURATION,             103.
     1 15X,5HSTORE, /                                                  104.
     2 5X,I3,8X,7A4,7X,3A4)                                            105.
 2050 FORMAT (1H0,17X,34H***** FREE-STREAM CONDITIONS *****, /         106.
     1 4X,4HMACH,4X,2HPT,6X,2HTT,7X,1HP,7X,1HT,7X,1HV,7X,              107.
     2 1H0,7X,5HRE/FT, /                                               108.
     3 5X,2HNO,4X,4HPSFA,3X,5HDEG(R),3X,4HPSFA,3X,                     109.
     4 6HDEG(R),2X,6HFT/SEC,4X,3HPSF,6X,6HFT(-1) /                     110.
     5 2X,F6.3,6FA.1,F7.2,6H*10**6)                                    111.
 2060 FORMAT (1H0,50X,22H***** MODEL DATA ***** /                      112.
     1 4X,5HALPHA,3X,5HALPHA,3X,4HBETA,4X,4HDIHA,4X,4HDPHI /           113.
     2 5X,3HPAR,4X,5HSTORE,3X,5HSTORE,3X,5HSTORE,3X,5HSTORE,           114.
     3 4X,2HXP,5X,2HYP,4X,4HZPZD,4X,2HCN,6X,2HCY,6X,3HCAT,             115.
     4 5X,3HCLM,5X,3HCLN,5X,3HCLL,6X,3HCNP,6X,3HYCP /                  116.
     5 5X, 3HDEG,5X,3HDEG,5X,3HDEG,5X,3HDEG,5X,3HDEG,5X,               117.
     6 2HIN,5X,2HIN,6X,5HDIAMS,4X,5HDIAMS )                            118.
 2070 FORMAT (1X,5(2X,F6.2),3(2X,F5.2),5(2X,F6.3),2(2X,F7.3))          119.
C                                                                      120.
C                                                                      121.
      STOP                                                             122.
      END                                                              123.
```

```
      SUBROUTINE CONFIG (B,   ICONF,ISTORE)                              200.
C                                                                        201.
C     DECIPHER THE CONFIGURATION CODE AND SET UP AN ALPHABETIC           202.
C     ARRAY FOR THE CONFIGURATION AND THE STORE                          203.
C                                                                        204.
C                                                                        205.
      DIMENSION IC(10),ICONF(7),IS(7),ISTORE(3)                          206.
      DATA IC /4HF-4C, 4H-PI, 4HT-(S, 4H2)U, 4H2)F,                      207.
     1 4H-PI , 4HT   , 4H2)U , 4H(S3), 4HU   , 4HF   ,                   208.
     2 4H-PCL, 4HF-PD, 4H2)F , 4HTM,( , 4HS2)F, 4H-(S3,                  209.
     3 4H)F  , 4HNONE /                                                 210.
      DATA IS /4HMK-R, 4H3-MF, 4H3-MU, 4H3-AF, 4H3-AU,                   211.
     1 4HPROR, 4HE   /                                                  212.
      DATA IBLANK /4H    /                                             213.
C                                                                        214.
      IF (B .EQ. 610.0) B= 91.0                                          215.
      MB= B                                                              216.
      MY= MOD(MB,10)                                                     217.
      MX= MB/10                                                          218.
C                                                                        219.
C     CASE CONFIGURATION                                                 220.
C                                                                        221.
C     CASE X=0                                                           222.
C                                                                        223.
      IF (MX .NE. 0) GO TO 50                                            224.
        ICONF(1)= IC(10)                                                 225.
        DO 40 I=2,7                                                      226.
          ICONF(I)= IBLANK                                               227.
   40   CONTINUE                                                         228.
        GO TO 150                                                        229.
C                                                                        230.
   50 GO TO (60,70,80,90,100,110,120,130,140),MX                         231.
C                                                                        232.
C     CASE X=1                                                           233.
C                                                                        234.
   60 CONTINUE                                                           235.
        ICONF(1)= IC(1)                                                  236.
        DO 65 I= 2,7                                                     237.
          ICONF(I)= IBLANK                                               238.
   65   CONTINUE                                                         239.
        GO TO 150                                                        240.
C                                                                        241.
C     CASE X=2                                                           242.
C                                                                        243.
   70 CONTINUE                                                           244.
        ICONF(1)= IC(1)                                                  245.
        ICONF(2)= IC(6)                                                  246.
        DO 75 I= 3,7                                                     247.
          ICONF(I)= IBLANK                                               248.
   75   CONTINUE                                                         249.
        GO TO 150                                                        250.
C                                                                        251.
C     CASE X=3                                                           252.
C                                                                        253.
   80 CONTINUE                                                           254.
        ICONF(1)= IC(1)                                                  255.
        ICONF(2)= IC(2)                                                  256.
        ICONF(3)= IC(7)                                                  257.
        DO 85 I=4,7                                                      258.
          ICONF(I)= IBLANK                                               259.
   85   CONTINUE                                                         260.
        GO TO 150                                                        261.
C                                                                        262.
```

```
C      CASE X=4                                                          263.
C                                                                        264.
   90 CONTINUE                                                           265.
        DO 95 I=1,3                                                      266.
          ICONF(I)= IC(I)                                                267.
   95   CONTINUE                                                         268.
        ICONF(4)= IC(8)                                                  269.
        DO 96 I= 5,7                                                     270.
          ICONF(I)= IBLANK                                               271.
   96   CONTINUE                                                         272.
        GO TO 150                                                        273.
C                                                                        274.
C      CASE X=5                                                          275.
C                                                                        276.
  100 CONTINUE                                                           277.
        DO 105 I= 1,4                                                    278.
          ICONF(I)= IC(I)                                                279.
  105   CONTINUE                                                         280.
        ICONF(5)= IC(9)                                                  281.
        ICONF(6)= IC(10)                                                 282.
        ICONF(7)= IBLANK                                                 283.
        GO TO 150                                                        284.
C                                                                        285.
C      CASE X=6                                                          286.
C                                                                        287.
  110 CONTINUE                                                           288.
        DO 115 I= 1,3                                                    289.
          ICONF(I)=IC(I)                                                 290.
  115   CONTINUE                                                         291.
        ICONF(4)= IC(5)                                                  292.
        ICONF(5)= IC(9)                                                  293.
        ICONF(6)= IC(11)                                                 294.
        ICONF(7)= IBLANK                                                 295.
        GO TO 150                                                        296.
C                                                                        297.
C      CASE X=7                                                          298.
C                                                                        299.
  120 CONTINUE                                                           300.
        ICONF(1)= IC(1)                                                  301.
        ICONF(2)= IC(12)                                                 302.
        ICONF(3)= IC(2)                                                  303.
        ICONF(4)= IC(3)                                                  304.
        ICONF(5)= IC(5)                                                  305.
        ICONF(6)= IC(9)                                                  306.
        ICONF(7)= IC(13)                                                 307.
        GO TO 150                                                        308.
C                                                                        309.
C      CASE X=8                                                          310.
C                                                                        311.
  130 CONTINUE                                                           312.
        DO 135 I= 1,3                                                    313.
          ICONF(I)= IC(I)                                                314.
  135   CONTINUE                                                         315.
        ICONF(4)= IC(14)                                                 316.
        DO 136 I= 5,7                                                    317.
          ICONF(I)= IBLANK                                               318.
  136   CONTINUE                                                         319.
        GO TO 150                                                        320.
C                                                                        321.
C      CASE X=9                                                          322.
C                                                                        323.
  140 CONTINUE                                                           324.
        ICONF(1)= IC(1)                                                  325.
```

```
        ICONF(2)= IC(2)                                                 326.
        ICONF(3)= IC(15)                                                327.
        ICONF(4)= IC(16)                                                328.
        ICONF(5)= IC(17)                                                329.
        ICONF(6)= IC(18)                                                330.
        ICONF(6)= IC(18)                                                331.
        ICONF(7)= IBLANK                                                332.
C                                                                       333.
C     END CASE CONFIGURATION                                            334.
  150 CONTINUE                                                          335.
C                                                                       336.
C                                                                       337.
C     CASE STORE                                                        338.
C                                                                       339.
      ISTORE(1)= IS(1)                                                  340.
      ISTORE(3)= IBLANK                                                 341.
      GO TO (170,180,190,200,210,220,230), MY                           342.
C                                                                       343.
C     CASE Y=1                                                          344.
C                                                                       345.
  170 CONTINUE                                                          346.
        ISTORE(2)= IS(2)                                                347.
        GO TO 240                                                       348.
C                                                                       349.
C     CASE Y=2                                                          350.
C                                                                       351.
  180 CONTINUE                                                          352.
        ISTORE(2)= IS(3)                                                353.
        GO TO 240                                                       354.
C                                                                       355.
C     CASE Y=3                                                          356.
C                                                                       357.
  190 CONTINUE                                                          358.
        ISTORE(2)= IS(4)                                                359.
        GO TO 240                                                       360.
C                                                                       361.
C     CASE Y=4                                                          362.
C                                                                       363.
  200 CONTINUE                                                          364.
        ISTORE(2)= IS(5)                                                365.
        GO TO 240                                                       366.
C                                                                       367.
C     CASE Y=5                                                          368.
C                                                                       369.
  210 CONTINUE                                                          370.
        ISTORE(1)= IS(6)                                                371.
        ISTORE(2)= IS(7)                                                372.
        GO TO 240                                                       373.
C                                                                       374.
C     CASE Y= 6                                                         375.
  220 CONTINUE                                                          376.
        ISTORE(2)= IS(2)                                                377.
        GO TO 240                                                       378.
C                                                                       379.
C     CASE Y=7                                                          380.
  230 CONTINUE                                                          381.
        ISTORE(2)= IS(3)                                                382.
C                                                                       383.
C     END CASE STORE                                                    384.
C                                                                       385.
  240 CONTINUE                                                          386.
C                                                                       387.
      RETURN                                                            388.
      END
```

Appendix C

FLOW FIELD DATA RETRIEVAL PROGRAM

```
      PROGRAM RETFLO (INPUT,OUTPUT,TAPE5=INPUT,TAPE6=OUTPUT,TAPE10)
C     PROGRAM TO RETRIEVE RANDOM RUN NUMBERS FROM THE                    2.
C     FLOW FIELD SURVEY TAPE                                             3.
C                                                                        4.
C                                                                        5.
      DIMENSION  R(26),IHDR(25),IPTR(100),ITITLE(3),RUNNO(100)           6.
      DIMENSION ICONF(7),ISTORE(3)                                       7.
C                                                                        8.
      DATA ICARD /4HFLOW/, ITAPE /4H FLO/                                9.
C                                                                        10.
C                                                                        11.
C     READ TAPE TITLE AND RUN NOS.                                       12.
C                                                                        13.
      READ (5,1000) ITITLE                                               14.
      IF (ITITLE(1) .EQ. ICARD) GO TO 20                                 15.
        WRITE (6,2000) (ITITLE(I),I=1,3)                                 16.
        STOP                                                             17.
   20 CONTINUE                                                           18.
      READ (10,1010) IHDR                                                19.
      IF (IHDR(2) .EQ. ITAPE) GO TO 40                                   20.
        WRITE (6,2010) (IHDR(I),I=1,25)                                  21.
        STOP                                                             22.
   40 CONTINUE                                                           23.
      READ (5,1020) N                                                    24.
      READ (5,1030) (RUNNO(I),I=1,N)                                     25.
      WRITE (6,2020) (I,RUNNO(I),I=1,N)                                  26.
C                                                                        27.
C     SORT THE RUN NOS. AND THE POINTERS TO THE RUN NOS.                 28.
C                                                                        29.
      DO 60 I= 1,N                                                       30.
        IPTR(I)= I                                                       31.
   60 CONTINUE                                                           32.
      IF (N .LE. 1) GO TO 85                                             33.
        N1= N-1                                                          34.
        DO 80 I=1,N1                                                     35.
          I1= I+1                                                        36.
          DO 80 J= I1,N                                                  37.
            IF (RUNNO(IPTR(I)) .LE. RUNNO(IPTR(J))) GO TO 80             38.
              ITEMP= IPTR(I)                                             39.
              IPTR(I)= IPTR(J)                                           40.
              IPTR(J)= ITEMP                                             41.
   80   CONTINUE                                                         42.
   85 CONTINUE                                                           43.
C                                                                        44.
C     SEARCH TAPE FOR SORTED RUN NOS.                                    45.
C                                                                        46.
      READ (10,1040) (R(I),I=1,26)                                       47.
      OLDRUN= 0.0                                                        48.
      DO 160 I= 1,N                                                      49.
C                                                                        50.
C       DO WHILE DESIRED RUN NO. GREATER THAN TAPE RUN NO.               51.
C                                                                        52.
  100   CONTINUE                                                         53.
        IF (RUNNO(IPTR(I)) .LT. R(1)) GO TO 160                          54.
          IF (R(1) .NE. RUNNO(IPTR(I))) GO TO 140                        55.
            IF (R(1) .EQ. OLDRUN) GO TO 120                              56.
C                                                                        57.
C             WRITE HEADING FOR NEW RUN NO.                              58.
C                                                                        59.
              CALL CONFIG (R(10),   ICONF,ISTORE)                        60.
              WRITE (6,2030) (IHDR(J),J=1,25)                            61.
              IRUN= R(1)                                                 62.
              WRITE (6,2040) IRUN,(ICONF(J),J=1,7)                       63.
              WRITE (6,2050) (R(J),J=2,4),(R(J),J=6,8),R(5),R(9)         64.
```

```
            WRITE (6,2080) R(11),R(26)                                    65.
            WRITE (6,2060)                                                66.
            OLDRUN= R(1)                                                  67.
  120       CONTINUE                                                      68.
C                                                                         69.
C           WRITE DATA                                                    70.
C                                                                         71.
            WRITE (6,2070) (R(J),J=12,14),R(16),R(15),R(25),              72.
     1      (R(J),J=17,20),R(23),R(24),R(22),R(21)                        73.
  140     CONTINUE                                                        74.
        READ (10,1040) (R(J),J=1,26)
          IF (EOF(10)) 200,100
  160 CONTINUE                                                            77.
C                                                                         78.
C     END OF FILE OR ALL DESIRED RUN NOS. FOUND                           79.
C                                                                         80.
  200 CONTINUE                                                            81.
      REWIND 10                                                           82.
C                                                                         83.
C                                                                         84.
C     * * READ FORMATS                                                   85.
C                                                                         86.
 1000 FORMAT (3A4)                                                        87.
 1010 FORMAT (25A4)                                                       88.
 1020 FORMAT (I5)                                                         89.
 1030 FORMAT (8F10.0)                                                     90.
 1040 FORMAT (1P10E12.5)                                                  91.
C                                                                         92.
C     * * WRITE FORMATS                                                  93.
C                                                                         94.
 2000 FORMAT (1H0,5X,17H* * * ERROR * * *,                                95.
     1 50HINPUT CARD DOES NOT SPECIFY FLOW FIELD SURVEY DATA /             96.
     2 5X, 11HCARD TITLE=, 3A4)                                           97.
 2010 FORMAT (1H0, 5X,17H* * * ERROR * * *,                               98.
     1 50HTAPE TITLE DOES NOT SPECIFY FLOW FIELD SURVEY DATA /
     2 5X,11HTAPE TITLE=, 25A4)                                           100.
 2020 FORMAT (1H1,17HINPUT RUN NUMBERS /                                  101.
     1 2X,1HI,3X,7HRUN NO. / (1X,I2,F10.2))                               102.
 2030 FORMAT (1H1,1X,25A4)                                                103.
 2040 FORMAT (1H0, // 3X,7HRUN NO.,7X,20HPARENT CONFIGURATION, /          104.
     1 5X,I3,8X,7A4)                                                      105.
 2050 FORMAT (1H0,17X,34H***** FREE-STREAM CONDITIONS *****, /            106.
     1 4X,4HMACH,4X,2HPT,6X,2HTT,7X,1HP,7X,1HT,7X,1HV,7X,                 107.
     2 1H0,7X,5HRE/FT, /                                                  108.
     3 5X,2HNO,4X,4HPSFA,3X,6HDEG(R),3X,4HPSFA,3X,                        109.
     4 6HDEG(R),2X,6HFT/SEC,4X,3HPSF,6X,6HFT(-1) /                        110.
     5 2X,F6.3,6F8.1,F7.2,6H*10**6)                                       111.
 2060 FORMAT (1H0,43X,27H***** FLOW FIELD DATA ***** /                    112.
     1 6X,2HXP,5X,2HYP,5X,2HZP,5X,3HALP,5X,3HSIG,                         113.
     2 5X,4HALPT,5X,3HPHI,4X,4HVX/V,4X,4HVY/V,4X,                         114.
     3 4HVZ/V,4X,4HVI /V,5X,2HML,5X,4HQL/Q,4X,6HPTP/PT,                   115.
     4 / 6X,2HIN,5X,2HIN,5X,2HIN,5X,3HDEG,5X,3HDEG,5X,                    116.
     5 3HDEG,6X,3HDEG)                                                    117.
 2070 FORMAT (3X,F6.2,2(2X,F5.2),3(2X,F6.2),2X,F7.2,7(2X,F6.3))           118.
 2080 FORMAT (1H0,3X,12HALPHA  ALPHA / 5X,11HPAR   PROBE /                119.
     1 5X,10HDEG    DEG, / 4X,F5.2,2X,F5.2)                               120.
C                                                                         121.
C                                                                         122.
      STOP                                                                123.
      END                                                                 124.
```

```
      SUBROUTINE CONFIG (R,   ICONF,ISTORE)                              200.
C                                                                        201.
C     DECIPHER THE CONFIGURATION CODE AND SET UP AN ALPHABETIC           202.
C     ARRAY FOR THE CONFIGURATION AND THE STORE                          203.
C                                                                        204.
C                                                                        205.
      DIMENSION IC(18),ICONF(7),IS(7),ISTORE(3)                          206.
      DATA IC /4HF-4C, 4H,PI,, 4HT,(S, 4H2)U,, 4H2)F,,                   207.
     1 4H,PT , 4HT    , 4H2)U , 4H(S3), 4HU    , 4HF    ,                208.
     2 4H,PCL, 4HF,P0, 4H2)F , 4HTM,(, 4HS2)F, 4H,(S3,                   209.
     3 4H)F   /                                                          210.
      DATA IS /4HMK-R, 4H3,MF, 4H3,MU, 4H3,AF, 4H3,AU,                   211.
     1 4HPROB, 4HF    /                                                 212.
      DATA IBLANK /4H    /                                               213.
C                                                                        214.
      IF (R .EQ. 610.0) R= 91.0                                          215.
      MR= R                                                              216.
      MY= MOD(MR,10)                                                     217.
      MX= MR/10                                                          218.
C                                                                        219.
C     CASE CONFIGURATION                                                 220.
C                                                                        221.
C     CASE X=0                                                           222.
C                                                                        223.
      IF (MX .NE. 0) GO TO 50                                            224.
        DO 40 I=1,7                                                      225.
          ICONF(I)= IBLANK                                               226.
   40   CONTINUE                                                         227.
        GO TO 150                                                        228.
C                                                                        229.
   50 GO TO (60,70,80,90,100,110,120,130,140),MX                         230.
C                                                                        231.
C     CASE X=1                                                           232.
C                                                                        233.
   60 CONTINUE                                                           234.
        ICONF(1)= IC(1)                                                  235.
        DO 65 I= 2,7                                                     236.
          ICONF(I)= IBLANK                                               237.
   65   CONTINUE                                                         238.
        GO TO 150                                                        239.
C                                                                        240.
C     CASE X=2                                                           241.
C                                                                        242.
   70 CONTINUE                                                           243.
        ICONF(1)= IC(1)                                                  244.
        ICONF(2)= IC(6)                                                  245.
        DO 75 I= 3,7                                                     246.
          ICONF(I)= IBLANK                                               247.
   75   CONTINUE                                                         248.
        GO TO 150                                                        249.
C                                                                        250.
C     CASE X=3                                                           251.
C                                                                        252.
   80 CONTINUE                                                           253.
        ICONF(1)= IC(1)                                                  254.
        ICONF(2)= IC(2)                                                  255.
        ICONF(3)= IC(7)                                                  256.
        DO 85 I=4,7                                                      257.
          ICONF(I)= IBLANK                                               258.
   85   CONTINUE                                                         259.
        GO TO 150                                                        260.
C                                                                        261.
C     CASE X=4                                                           262.
C                                                                        263.
   90 CONTINUE                                                           264.
        DO 95 I=1,3                                                      265.
```

```
            ICONF(I)= IC(I)                                          266.
   95     CONTINUE                                                   267.
          ICONF(4)= IC(8)                                            268.
          DO 96 I= 5,7                                               269.
            ICONF(I)= IBLANK                                         270.
   96     CONTINUE                                                   271.
          GO TO 150                                                  272.
C                                                                    273.
C       CASE X=5                                                     274.
C                                                                    275.
  100 CONTINUE                                                       276.
          DO 105 I= 1,4                                              277.
            ICONF(I)= IC(I)                                          278.
  105     CONTINUE                                                   279.
          ICONF(5)= IC(9)                                            280.
          ICONF(6)= IC(10)                                           281.
          ICONF(7)= IBLANK                                           282.
          GO TO 150                                                  283.
C                                                                    284.
C       CASE X=6                                                     285.
C                                                                    286.
  110 CONTINUE                                                       287.
          DO 115 I= 1,3                                              288.
            ICONF(I)=IC(I)                                           289.
  115     CONTINUE                                                   290.
          ICONF(4)= IC(5)                                            291.
          ICONF(5)= IC(9)                                            292.
          ICONF(6)= IC(11)                                           293.
          ICONF(7)= IBLANK                                           294.
          GO TO 150                                                  295.
C                                                                    296.
C       CASE X=7                                                     297.
C                                                                    298.
  120 CONTINUE                                                       299.
          ICONF(1)= IC(1)                                            300.
          ICONF(2)= IC(12)                                           301.
          ICONF(3)= IC(2)                                            302.
          ICONF(4)= IC(3)                                            303.
          ICONF(5)= IC(5)                                            304.
          ICONF(6)= IC(9)                                            305.
          ICONF(7)= IC(13)                                           306.
          GO TO 150                                                  307.
C                                                                    308.
C       CASE X=8                                                     309.
C                                                                    310.
  130 CONTINUE                                                       311.
          DO 135 I= 1,3                                              312.
            ICONF(I)= IC(I)                                          313.
  135     CONTINUE                                                   314.
          ICONF(4)= IC(14)                                           315.
          DO 136 I= 5,7                                              316.
            ICONF(I)= IBLANK                                         317.
  136     CONTINUE                                                   318.
          GO TO 150                                                  319.
C                                                                    320.
C       CASE X=9                                                     321.
C                                                                    322.
  140 CONTINUE                                                       323.
          ICONF(1)= IC(1)                                            324.
          ICONF(2)= IC(2)                                            325.
          ICONF(3)= IC(15)                                           326.
```

```
      ICONF(4)= IC(16)                                                  327.
      ICONF(5)= IC(17)                                                  328.
      ICONF(6)= IC(18)                                                  329.
      ICONF(7)= IBLANK                                                  330.
C                                                                       331.
C     END CASE CONFIGURATION                                            332.
  150 CONTINUE                                                          333.
C                                                                       334.
C                                                                       335.
C     CASE STORE                                                        336.
C                                                                       337.
      ISTORE(1)= IS(1)                                                  338.
      ISTORE(3)= IBLANK                                                 339.
      GO TO (170,180,190,200,210,220,230), MY                           340.
C                                                                       341.
C     CASE Y=1                                                          342.
C                                                                       343.
  170 CONTINUE                                                          344.
        ISTORE(2)= IS(2)                                                345.
        GO TO 240                                                       346.
C                                                                       347.
C     CASE Y=2                                                          348.
C                                                                       349.
  180 CONTINUE                                                          350.
        ISTORE(2)= IS(3)                                                351.
        GO TO 240                                                       352.
C                                                                       353.
C     CASE Y=3                                                          354.
C                                                                       355.
  190 CONTINUE                                                          356.
        ISTORE(2)= IS(4)                                                357.
        GO TO 240                                                       358.
C                                                                       359.
C     CASE Y=4                                                          360.
C                                                                       361.
  200 CONTINUE                                                          362.
        ISTORE(2)= IS(5)                                                363.
        GO TO 240                                                       364.
C                                                                       365.
C     CASE Y=5                                                          366.
C                                                                       367.
  210 CONTINUE                                                          368.
        ISTORE(1)= IS(6)                                                369.
        ISTORE(2)= IS(7)                                                370.
        GO TO 240                                                       371.
C                                                                       372.
C     CASE Y= 6                                                         373.
  220 CONTINUE                                                          374.
        ISTORE(2)= IS(2)                                                375.
        GO TO 240                                                       376.
C                                                                       377.
C     CASE Y=7                                                          378.
  230 CONTINUE                                                          379.
        ISTORE(2)= IS(3)                                                380.
C                                                                       381.
C     END CASE STORE                                                    382.
C                                                                       383.
  240 CONTINUE                                                          384.
C                                                                       385.
      RETURN                                                            386.
      END                                                               387.
```

NOMENCLATURE

The following list contains the nomenclature used in the report except for that used in the model component designation and in the data tabulations. That nomenclature is defined in lists in the text of the report.

A_e	Engine exhaust exit area, 7.4662×10^{-3} square feet, model scale
A_i	Engine inlet area used in data reduction, 1.705×10^{-2} square feet model scale
c_R	Capture ratio calculated using Equation (3)
C_A	Axial-force coefficient, axial force/$q_\infty S$
C_ℓ, CLL	Store rolling-moment coefficient, rolling moment/$q_\infty Sd$
C_m, CLM	Store pitching-moment coefficient, pitching moment/$q_\infty Sd$
C_n, CLN	Store yawing-moment coefficient, yawing moment/$q_\infty Sd$
C_N, CN	Store normal-force coefficient, normal force/$q_\infty S$
C_Y, CY	Store side-force coefficient, side force/$q_\infty S$
d, D	Store diameter, 0.7 inch model scale
ℓ_B	Length of modified afterbody store, 5.723 inches model scale
M_e	Engine exhaust Mach number
M_∞	Free-stream Mach number
$\dot{m}_e$	Engine exhaust mass flow rate calculated using Equation (2), lbm/sec
P_{t_∞}	Free-stream total pressure, psfa
$\bar{P}$	Average static pressure in engine exhaust, psfa

NOMENCLATURE (Contd.)

$\bar{P}_t$	Average total pressure in engine exhaust, psfa
q_∞	Free-stream dynamic pressure, psf
Re_∞	Free-stream Reynolds number per foot, ft^{-1}
r	Radial distance, in
S	Reference area which is store frontal area, 0.385 square inches model scale
T_{t_∞}	Free-stream total temperature, °R
V_e	Engine exit velocity calculated using Equation (4), ft/sec
V_∞	Free-stream velocity, ft/sec
VY/V	Local Y_P velocity component, positive in the positive Y_P direction, divided by the free-stream velocity; also termed sidewash angle, rad
VZ/V	Local Z_P velocity component, positive in the negative Z_P direction, divided by the free-stream velocity; also termed upwash angle, rad
X_P, Y_P, Z_P	Coordinate system in which probe static pressure taps are located; origin shown in Figure 5
X_s, Y_s, Z_s	Coordinate system in which store nose is located; origin shown in Figure 5
x_s	Assumed flow separation location on store body measured from nose, in
Z_f/D	Store vertical position relative to attached, or carriage, position; equal to Z_s/D
α_p	Angle of attack of the probe, deg
α_s	Angle of attack of the store, deg
ϕ_s	Store rolling angle, positive clockwise looking upstream and measured relative to fins 45 degrees from the vertical and horizontal, deg

INITIAL DISTRIBUTION

14 Naval Air Systems Command
- AIR-03A (1)
- AIR-03B (1)
- AIR-03E (1)
- AIR-03P2 (1)
- AIR-30212 (2)
- AIR-320 (1)
- AIR-320B (1)
- AIR-320C (1)
- AIR-5108 (1)
- AIR-5323 (1)
- AIR-53242 (1)
- AIR-950D (2)

1 Chief of Naval Operations

6 Naval Sea Systems Command
- SEA-033 (1)
- SEA-03513 (1)
- SEA-62R41 (1)
- SEA-6543 (1)
- SEA-99612 (2)

1 Chief of Naval Research, Arlington (ONR-461)

3 David Taylor Naval Ship Research and Development Center, Bethesda
- Code 1606 (1)
- Code 166 (1)
- Code 167 (1)

2 Naval Air Development Center, Johnsville, Warminster
- Code 01A (1)
- Technical Library (1)

1 Naval Air Engineering Center, Lakehurst

1 Naval Air Test Center (CT-176), Patuxent River (Aeronautical Publications Library)

1 Naval Avionics Center, Indianapolis (Technical Library)

1 Naval Ocean Systems Center, San Diego (Code 1311)

1 Naval Ordnance Station, Indian Head

1 Naval Postgraduate School, Monterey

1 Naval Research Laboratory (Code 2021)

9 Naval Surface Weapons Center Detachment, White Oak Laboratory, Silver Spring
- G-41 (1)
- K-04 (1)
- K-21 (1)
- K-80 (1)
- K-81 (1)
- K-82 (1)
- R-44 (1)
- Technical Library (2)

1 Operational Test & Evaluation Force, Norfolk

3 Pacific Missile Test Center, Point Mugu
Code 0101 (1)
Code 3132 (1)
Technical Library (1)
3 Army Missile Research and Development Command, Redstone Arsenal (Redstone Scientific Information Center)
4 Aberdeen Proving Ground
Dr. B. Karpov (2)
Development and Proof Services (2)
2 Army Ballistic Research Laboratories, Aberdeen Proving Ground
DRDAR-TSB-S (STINFO) (1)
1 Tactical Air Command, Langley Air Force Base (TPL-RQD-M)
1 Air University Library, Maxwell Air Force Base
2 Armament Development & Test Center, Eglin Air Force Base
AFATL/ADLA (1)
Directorate of Ballistics, A. S. Galbraith (1)
12 Defense Technical Information Center
1 Weapons Systems Evaluation Group
1 Lewis Research Center, NASA, Cleveland
1 Applied Physics Laboratory, JHU, Laurel, MD (Document Library)
1 Chemical Propulsion Information Agency, APL, Laurel, MD
1 Jet Propulsion Laboratory, CIT, Pasadena, CA (Technical Library)
1 Massachusetts Institute of Technology, Aerophysics Laboratory, Cambridge, MA
1 The Rand Corporation, Santa Monica, CA (Aero-Astronautics Dept.)

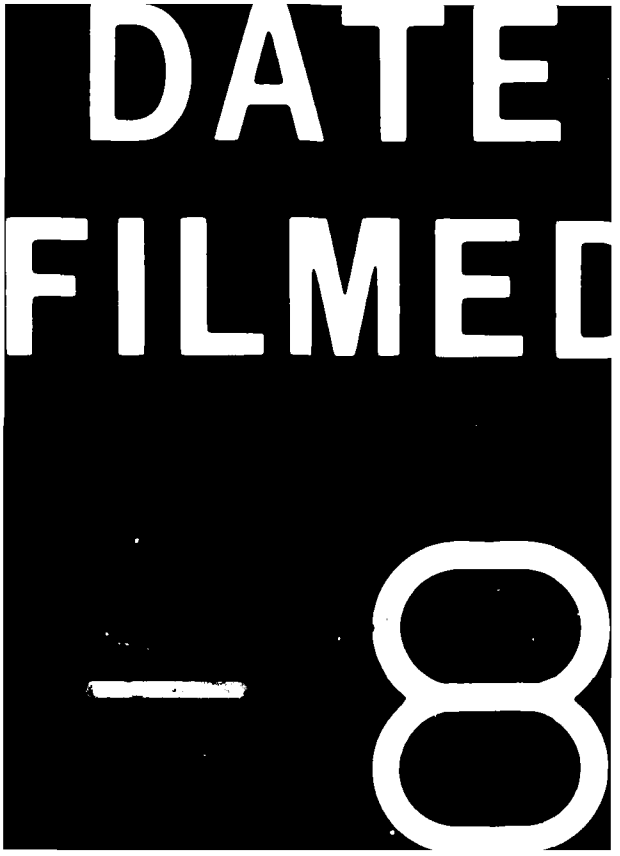
DATE
FILMED
8